

**The author(s) shown below used Federal funds provided by the U.S. Department of Justice and prepared the following final report:**

**Document Title:           Developing Guidelines for the Application of  
Multivariate Statistical Analysis to Forensic  
Evidence**

**Author(s):                 Ruth Waddell Smith, David R. Foran, Victoria L.  
McGuffin**

**Document No.:           248566**

**Date Received:          January 2015**

**Award Number:         2011-DN-BX-K560**

**This report has not been published by the U.S. Department of Justice. To provide better customer service, NCJRS has made this Federally-funded grant report available electronically.**

**Opinions or points of view expressed are those  
of the author(s) and do not necessarily reflect  
the official position or policies of the U.S.  
Department of Justice.**

Developing Guidelines for the Application of Multivariate Statistical Analysis  
to Forensic Evidence

Final Technical Report

Ruth Waddell Smith<sup>1</sup>, David R. Foran<sup>1</sup>, and Victoria L. McGuffin<sup>2</sup>

<sup>1</sup>Forensic Science Program and <sup>2</sup>Department of Chemistry

Michigan State University

East Lansing, MI 48824

Award Number: 2011-DN-BX-K560

Office of Justice Programs

National Institute of Justice

Department of Justice

This project was supported by Award No. 2011-DN-BX-K560 awarded by the National Institute of Justice, Office of Justice Programs, U.S. Department of Justice. The opinions, findings, and conclusions or recommendations expressed are those of the authors and do not necessarily reflect those of the Department of Justice.

## Abstract

Recommendation 3 in the 2009 National Academy of Sciences' National Research Council report "Strengthening Forensic Science in the United States: A Path Forward" highlighted the lack of statistical comparison of forensic evidence. Multivariate statistical procedures have potential as a means to overcome this deficiency by providing an additional tool for analysts to use in such comparisons. However, these procedures are not widely implemented in forensic laboratories. The purpose of this research was to investigate and demonstrate application of multivariate statistical procedures to forensically relevant data and highlight the advantages and limitations that must be considered for these procedures to be used in forensic investigations.

To be as realistic and as practical as possible, three separate and diverse data sets were generated. The first contained chromatographic data of ignitable liquid reference standards and simulated fire debris samples, the second contained spectral data of controlled substance reference standards and simulated street samples, and the third contained ribosomal RNA gene sequence data of bacteria in soil samples from different habitats. For each data set, statistical procedures were used to associate or classify samples to the corresponding reference standard.

The chromatographic and spectral data sets were initially probed using principal components analysis (PCA) and hierarchical cluster analysis (HCA). These two procedures are exploratory in nature and are used to identify patterns in the data, enabling association of similar samples with distinction from different samples. Both procedures are based on the principle of distance measurements in multidimensional space and hence, in theory, the same association and differentiation of samples within a data set will be achieved irrespective of procedure used. However, PCA reduces the dimensionality of the data set, retaining the most important information while in HCA, all dimensions are retained and expressed. While there are advantages and disadvantages for each procedure, in this particular application, greater success in associating the simulated sample to the appropriate reference standard was achieved using HCA.

The same two data sets were further probed using two classification procedures: soft independent modeling of class analogy (SIMCA) and  $k$ -nearest neighbors ( $k$ -NN). SIMCA has theoretical advantages in using statistical models for the classification and not forcing classification. However, for this particular application, the development of representative models

was challenging and limited the success of SIMCA. In contrast, the  $k$ -NN procedure is based on the proximity of samples to reference standards in multidimensional space rather than statistical models. Although  $k$ -NN forces classification, the simulated samples were more successfully classified according to appropriate reference standard using this procedure rather than SIMCA.

The sequencing data were analyzed with PCA and nonmetric multidimensional scaling (NMDS). While both procedures are based on similar principles, NMDS is better suited to nonparametric data. Similar to PCA, NMDS reduces the dimensions of the data set for easier interpretation. Differentiation among the habitats was possible based on the gene sequence data; however, NMDS was able to cluster replicate samples of each soil within standard error whereas, only mild association of replicates was possible using PCA.

Aspects of this research have been disseminated to the wider forensic community through poster and oral presentations, which have been given by both graduate students in the Forensic Science Program at Michigan State University and the PIs. Three manuscripts are in preparation (one for each data type) and tutorials outlining the application, interpretation, and considerations for these data analysis procedures are currently being developed.

## Table of Contents

Abstract.....	i
Executive Summary .....	1
1. Introduction.....	9
2. Theory .....	14
2.1 Data Pretreatment Procedures .....	14
2.2 Exploratory Procedures .....	19
2.3 Classification Procedures .....	35
3. Materials and Methods.....	39
3.1 Chromatographic Data .....	39
3.2 Spectral Data .....	42
3.3 Gene Sequence Data.....	44
4. Results and Discussion .....	49
4.1 Chromatographic Data .....	49
4.2 Spectral Data .....	120
4.3 Gene Sequence Data.....	145
5. Conclusions.....	158
6. References.....	164
7. Dissemination of Results .....	169

## Executive Summary

The 2009 National Academy of Sciences' National Research Council report "Strengthening Forensic Science in the United States: A Path Forward" was instrumental in highlighting current deficiencies in the practice of forensic science across the country. Among the thirteen recommendations made in the report, one in particular identified the limitations in forensic evidence comparisons and called for "the development and establishment of quantifiable measures of the reliability and accuracy of forensic analyses" and the "development of quantifiable measures of uncertainty in the conclusions of forensic analyses."<sup>1</sup> Throughout the report, the current methods for nuclear DNA analysis were highlighted as the gold standard. With this type of evidence, DNA profiles from a questioned source are generated using advanced analytical instrumentation, and then compared to a known sample or database of DNA profiles. This comparison can provide the likelihood that the particular DNA profile occurred by random chance, which in turn can be used to express an error rate associated with the comparison.

Similar statistical procedures are not currently employed for other evidence comparisons. In trace evidence and controlled substance analysis, submitted samples are analyzed using gas chromatography-mass spectrometry and infrared spectroscopy, among other techniques. The data generated by these instruments are complex, containing hundreds, even thousands of variables. Despite the complexity, comparisons of the resulting chromatograms and spectra between a questioned sample and a reference standard are currently based on visual assessment, which naturally introduces some subjectivity. In an effort to minimize such subjectivity, a more statistical-based comparison is necessary. The complex chromatographic and spectral data are ideal candidates for multivariate statistical procedures. These procedures compare all variables simultaneously to identify patterns in the data that can be used to associate similar samples and discriminate different samples.

Forensic analysis of soil samples is typically based on a physical and chemical assessment of the soil, which are class characteristics. However, analysis of the microbial population of the soil has the potential to create a 'microbial fingerprint' to associate soils from similar habitats while discriminating those from different habitats. In the microbial genomics field, soils are analyzed using next generation sequencing, which routinely generates over 100,000 sequences. Again, this type of data lends itself to analysis using multivariate statistical procedures.

The purpose of the proposed research was to investigate the applicability of a selection of multivariate statistical procedures for the analysis and comparison of forensically relevant data. The selected procedures are widely used and reported in other scientific fields such as analytical chemistry or microbial studies, but are not yet tried and tested specifically for forensic evidence applications. Therefore, a second intention of the research was to highlight considerations and current limitations with regard to the implementation of these procedures. Finally, the third intention was to produce a document that describes the theory, application, and interpretation of results for these procedures using forensically relevant evidence as the model data. This document could serve as a resource for forensic laboratories considering implementation of such statistical procedures.

The first step in the research was to generate suitable data sets for statistical analysis. Three distinct data sets that represented different types of data encountered in forensic analyses were generated. The first data set contained chromatographic data of ignitable liquid reference standards and simulated fire debris samples. The second set contained spectral data of controlled substance reference standards and simulated street samples, and the third set contained ribosomal RNA gene sequence data of bacteria in soil samples collected from different habitats.

Although all three data sets contained thousands of variables, there were distinct differences between the chemical data (*i.e.*, the chromatographic and spectral data) and the biological (*i.e.*, gene sequencing) data. First, the chromatographic and spectral data consisted of continuous variables while the gene sequencing data contained discrete variables. Second, the former data sets were assumed to follow a normal distribution while the gene sequencing data were nonparametric in nature. As a result, different statistical procedures were applied according to the distribution of the data, thus for clarity, the chromatographic and spectral data sets are discussed separately from the gene sequence data throughout this report.

Similar procedures were applied to the chromatographic and spectral data sets to investigate association of the simulated samples to the appropriate reference standard, and distinction of the simulated samples from all other reference standards in the data set. Although both data sets contained approximately 3,500 variables, the chromatographic data were more complex and hence, much of the investigative aspect of the research focused on this particular set to provide a test of the robustness of the procedures applied.

While the focus of the research was the application of statistical procedures, data pretreatment prior to analysis is an important consideration for data collected using instrumental techniques and over a prolonged time period. Variance that is non-chemical in nature can exist in such data as a result of random fluctuations in noise, differences in the mass or volume of sample analyzed, and fluctuations in the parameters used for the analysis (*e.g.*, carrier gas flow rate or variations in oven temperature in gas chromatography). When present in a data set, these non-chemical sources of variance can be identified by the statistical procedures as chemical differences among the samples. As such, it is important to minimize or eliminate non-chemical variance to ensure data analysis results are meaningful.

To address this consideration, various pretreatment procedures were applied to the data and the effect of each was assessed. For the chromatographic data, retention time alignment, normalization, and scaling were investigated. Two different alignment algorithms were considered (peak-match and correlation optimized warping) and for each algorithm, various user-defined parameters were compared. For this particular data set, alignment was not necessary, primarily because reference standards and simulated samples were analyzed using the same instrument and column and over a relatively short time period. However, this will not always be true in forensic laboratories and hence, it is important to visually assess the data to determine the need for retention time alignment.

Three normalization procedures were investigated (constant sum, constant maximum, and constant vector length) for this data set. Normalization was necessary to improve precision of replicates; however, no one procedure offered improvement for all standards in the data set. This was primarily due to both the complexity of the data and the chemical diversity among the reference standards. Hence, it was necessary to reach a compromise in which all data were subjected to constant sum normalization prior to data analysis. Scaling procedures (autoscaling and Pareto scaling) were also investigated. For this pretreatment, there was no improvement in replicate precision compared to the unscaled data as all the data were of similar magnitude.

Pretreatment for the spectral data set focused on normalization to take into account variation among samples as a result of day-to-day instrument variation. Again, three different normalization procedures (constant sum, constant vector length, and standard normal variate) were assessed based on the improvement in precision of replicate spectra. For these data, the standard normal variate procedure proved optimal and was used for all subsequent analyses.

Following the investigation of data pretreatment procedures, two different types of statistical procedures (exploratory and classification) were investigated for the chromatographic and spectral data sets. Exploratory procedures identify patterns in the data with no prior knowledge of the identity of any samples or even standards in the data set. Three exploratory procedures (Pearson product-moment correlation, principal components analysis, and hierarchical cluster analysis) were initially applied to investigate association of the simulated samples to the appropriate reference standard with distinction from all other standards.

Pearson product-moment correlation (PPMC) offers a pairwise comparison of samples (in this case, simulated sample compared to reference standard) resulting in a single number (the correlation coefficient) that indicates the degree of similarity between the two. However, through analysis of the chromatographic data set, a number of limitations for this particular application were highlighted. Firstly, the coefficient is calculated on a point-by-point basis between the two samples. Chromatograms of the simulated samples contained interference compounds (*e.g.*, interference compounds from debris substrates or cutting agents in street samples) that were not present in the reference standards. These additional peaks lowered the coefficient, resulting in only weak to moderate correlation between the simulated samples and the corresponding reference standard. Further, while the comparison of a sample and standard can be represented by a single number, the number of coefficients calculated for a given data set increases with the square of the number of samples. Comparison of a single sample with each standard in a reference collection can generate a large number of coefficients, which makes comparison and investigation of the coefficients particularly time consuming. Hence, PPMC coefficients were not investigated further beyond the chromatographic data set due to these limitations.

The chromatographic and spectral data sets were separately subjected to principal components analysis (PCA). This procedure reduces the dimensionality of the data set by identifying and maintaining the major sources of variance. Complex data can be represented in a smaller number of dimensions without losing discriminatory information. Results from PCA are most commonly displayed in the form of scores and loadings plots. The scores plot is a scatter plot that represents the similarities and differences within the data set; that is, samples that are chemically similar are positioned closely in the scores plot and separately from those that are chemically distinct. Loadings plots are used to identify those variables that contribute to the

variance described by each principal component and can be useful in explaining the positioning of samples on the scores plot.

For each data set, PCA was initially performed on the reference standards alone, generating scores and loadings plots. Scores were calculated for the simulated samples using the eigenvectors for the standards and then projected onto the original scores plot. Performing PCA in this manner has the advantage of minimizing or eliminating contributions from sample interference compounds (*e.g.*, debris substrates or cutting agents) as only those compounds present in the reference standards contribute to the scores calculated for the samples. Further, association and discrimination in the scores plot was assessed using two additional metrics (Euclidean distance and PPMC coefficients) to provide a more objective method to interpret the scores plot.

Association of simulated samples to the corresponding reference standard using PCA was of limited success for both data sets. For the chromatographic data, simulated fire debris samples containing liquids that were chemically distinct from other reference standards were appropriately associated. However, for the remaining samples, clear association to one reference standard was not possible. Additionally, the success of association was dependent on the nature of the substrate interference compounds. For the spectral data, simulated samples were successfully associated to the corresponding reference standard in the presence of low levels of cutting agent. However, as the percentage of cutting agent present increased, successful association became limited, with fewer samples associated successfully.

The final exploratory procedure considered was hierarchical cluster analysis (HCA). This procedure is often considered complementary to PCA; that is, HCA assesses similarity among samples in a data set while PCA identifies differences in the form of variance among samples. The output from HCA is a dendrogram which displays clusters of similar samples, along with the similarity level at which the clusters form, with higher similarity level indicating greater similarity.

Cluster analysis was performed separately on each data set to again assess association of simulated samples to the appropriate reference standard. While the actual similarity level at which the simulated samples clustered with the reference standards varied, the simulated samples clustered first with the corresponding reference standard before clustering to any other standard. This was true for both the chromatographic and spectral data sets. Further, in most cases,

exclusive clusters were formed; that is, the cluster contained the simulated sample and the appropriate reference standards only. There were some exceptions to this in the chromatographic data set in which certain simulated fire debris samples formed clusters with a group containing more than one reference standard. However, this overlap in clustering was due to the high degree of chemical similarity among these particular reference standards.

This research indicated that HCA had greater potential than PCA for these applications. Despite apparent differences in mode of operation (HCA is based on similarity while PCA is based on variance), both procedures are founded on the same basis; that is, the distance between samples and reference standards in multidimensional space. Hence, both procedures should theoretically yield similar results in terms of association and discrimination. However, probing these results is considerably simpler using HCA as all dimensions are retained and accounted for in the resulting dendrogram. In contrast, typically only the first few principal components (dimensions) are retained and assessed in the PCA scores and loadings plots. To achieve the same association and discrimination as HCA, all principal components must be considered. However, this is no small undertaking as  $n-1$  principal components are calculated, where  $n$  is the number of samples or variables, whichever is smaller. Further, as only two or three dimensions can be readily visualized, probing additional principal components would require plotting numerous scores plots. Not only would this be extremely time consuming, but subsequent interpretation and comparison of all the resulting plots would become arduous.

While exploratory procedures have the advantage of not requiring any knowledge of the data set, the limitation is that only association (or differentiation) of samples is possible based on patterns in the data. In contrast, classification procedures require knowledge of pre-defined groups within the data set. Samples are subsequently classified according to one of the previously defined groups. Two classification procedures (soft independent modeling of class analogy and  $k$ -nearest neighbors) were used to investigate classification of simulated samples to the appropriate reference standard with distinction from all other standards.

The soft independent modeling of class analogy (SIMCA) approach develops statistical models for the pre-defined groups in the data set and then uses these models to classify the 'new' samples (in this case, the simulated samples). Models are developed using PCA and hence, SIMCA can be considered an extension of PCA. Through this investigation for both the chromatographic and spectral data sets, multiple iterations of model development were

conducted. Initial models that contained only the reference standards were not sufficiently representative of the data to be classified and hence, no classification was possible.

The greatest success in classification using SIMCA was achieved with models that included not only the reference standards but also the burned substrate or cutting agent (for the chromatographic and spectral data, respectively), as well as replicates of the simulated samples. For both data sets, the most successful classification was achieved at the 99.9% confidence level; however, it should be noted that higher confidence levels are least rigorous when association is considered, as is the case here. Not all simulated samples were classified and in each case, the lack of classification was attributed to differences in abundance between the simulated samples to be classified and those included in the model. Hence, despite being more representative of the data to be classified, the models were too specific, to the extent that differences in abundance prevented classification.

In contrast to SIMCA, the *k*-nearest neighbors (*k*-NN) approach to classification requires no model building; instead, known groups and ‘new’ samples are considered at the same time, with the ‘new’ sample being classified according to the group to which it is positioned most closely in the multidimensional space. As a result, *k*-NN can be considered an extension of HCA in that sample distances are calculated and groupings are based on close proximity. Using this procedure, classification of the simulated samples was considerably more successful. Further, samples previously misclassified using SIMCA were correctly classified using *k*-NN.

For the classification procedures, *k*-NN was deemed to be more promising for this application than the SIMCA approach. Despite being a ‘hard’ procedure that forces classification, greater success in classification was achieved using *k*-NN. In contrast, SIMCA is based on the development of representative PCA models. Classification success improved with the inclusion of the substrate (for chromatographic data) or cutting agent (for spectral data) in the models; however, this is a practical limitation in forensic laboratories as the substrate or cutting agent may not be readily known. Thus, the development of suitable models that are representative of the data without being too specific is challenging and a major limitation particularly in forensic applications of this nature.

The gene sequence data set included over 100,000 sequences for ten soil samples that were collected from three different habitats (marsh, woodlot, and yard). Extensive data processing was necessary before statistical analysis. Processing was performed using the mothur

open source software, which is designed to facilitate sequence processing from next generation sequencing platforms. As errors in sequencing are possible, much of the pretreatment involved the removal of possibly erroneous sequences. In addition, repetitive sequences were removed to reduce the dataset and allow for faster processing.

Unlike the spectral and chromatographic data, this data set was not assumed to be normally distributed and hence, along with PCA, nonmetric multidimensional scaling (NMDS) was also investigated. This procedure makes no assumptions regarding the distribution of the data and is commonly used for the analysis and interpretation of gene sequence data. The gene sequence data were analyzed using both procedures and the results from each were compared.

Biological replicates were associated and samples from different habitats were distinguished using both PCA and NMDS. However, between the two procedures, there was a difference in the ability to cluster replicate samples. Using PCA, there was more spread among replicates, which would indicate that the replicates were not as similar biologically as anticipated. However, PCA is a parametric procedure, making an assumption that the data are normally distributed. Because of this assumption, the relationships in the data can be misrepresented. In contrast, NMDS makes no assumptions regarding the distribution of the data and using this procedure, replicate samples were more closely clustered (within standard error), revealing the close nature of the replicate samples and the differences among the habitats. As a result, NMDS was more suitable for the analysis of the gene sequence data.

While preliminary in nature and despite using relatively small data sets, this research has highlighted some important considerations and limitations for the application of multivariate statistical procedures in forensic evidence comparisons. Overall, HCA and  $k$ -NN were deemed to be more appropriate for these types of data. However, it must be emphasized that these procedures should only be considered as a supplemental tool to aid analysts in their comparison and interpretation of evidence. This research is considered only a very initial step in the investigation of multivariate statistical procedures in forensic evidence comparisons and future research using larger, more representative data sets (*e.g.*, through collaboration with forensic laboratories to access case samples), as well as investigating additional procedures, is warranted.

This research has been disseminated through poster and oral presentations at regional and national forensic science conferences, as well as at national analytical chemistry conferences. Three graduate students conducted different aspects of this research in partial fulfillment of the

requirements for the Master's degree in Forensic Science. Additionally, three initial manuscripts are in preparation (one for each data type) for journal submission, with another two manuscripts planned focusing on the relationship between the two exploratory procedures and the two classification procedures, respectively. Further dissemination of this research is currently underway, with the development of a series of tutorials that demonstrate application of these procedures to forensically relevant data. The first in the series focuses on data pretreatment and exploratory procedures, using the chromatographic and spectral data sets to illustrate application of the procedures and interpretation of the results obtained. The second planned tutorial will focus on classification procedures and, according to the success of these, a third will be considered that focuses on statistical procedures for discrete data.

## 1. Introduction

### 1.1 Statement of the Problem

The 2009 report of the National Academy of Sciences' National Research Council (NRC) entitled *Strengthening Forensic Science in the United States: a Path Forward*", highlighted various deficiencies in the current state of forensic science in this country.<sup>1</sup> Thirteen recommendations were made to address these deficiencies among which the "development of quantifiable measures of uncertainty in the conclusions of forensic analyses" was one. This was illustrated using mass spectra of controlled substances as an example. The report stated that such comparisons are based on "identification of peaks on a spectrum that appear at frequencies consistent with the controlled substance and that stand out above background noise." Despite using an objective method for analysis (commonly gas chromatography-mass spectrometry), interpretation of the resulting data is subjective, based on visual assessment of the complex spectral patterns. It is cases such as this where a statistical evaluation of the comparison between a questioned and known sample is necessary, but is currently lacking in routine forensic laboratory analyses.

Although the data generated in many forensic analyses (*e.g.*, chromatograms, infrared spectra, mass spectra, etc.) is complex, such data can still be assessed, using multivariate statistical procedures to assess the significance of a 'match' between a questioned sample and a known reference standard. These procedures are either based on, or are extensions of, univariate statistical tests such as F-tests and Student's t-tests. The difference is the simultaneous

comparison of multiple variables, an approach that is ideally suited for the statistical evaluation of data containing thousands of variables, as is typically the case with chromatographic and spectral data.

Multivariate statistical procedures have been used in many different branches of science; hence, they are widely accepted and have been peer-reviewed and published, meeting important requirements of the *Daubert* ruling<sup>\*</sup>. Despite this, such procedures are not routinely utilized or embraced in forensic science<sup>2</sup>, although they certainly have the potential to meet the recommendation in the NRC report that called for “quantifiable measures of uncertainty in the conclusions of forensic analyses.”

## 1.2 Literature Review

Multivariate statistical procedures are widely used in analytical chemistry for the comparison of complex data, and the same procedures are directly applicable to data generated from the analysis of forensic evidence.<sup>3,4</sup> Although the NRC report highlighted a lack of statistical evaluation of forensic data in routine casework, these procedures have actually been applied in forensic research, although not in a systematic and comparative manner on different types of data.

The potential of multivariate statistical procedures in fire debris analysis to address the issues of liquid evaporation and substrate contributions has been demonstrated. Sandercock and DuPasquier analyzed 35 gasoline samples obtained from 24 different service stations using gas chromatography.<sup>5</sup> Using principal components analysis (PCA) and linear discriminant analysis based on the C<sub>0</sub>-C<sub>2</sub> naphthalene range in the chromatogram, the gasoline samples were classified into 32 groups. Using the same statistical procedures, the authors later reported association of evaporated gasoline (4 different evaporation levels) to the unevaporated counterpart.<sup>6</sup> Tan *et al.* used both PCA and a soft independent modeling of class analogy (SIMCA) approach to successfully classify 51 ignitable liquids according to chemical class.<sup>7</sup> Baerncopf *et al.* conducted a study in which correlation coefficients and PCA were used to associate a liquid extracted from simulated fire debris samples to the original liquid, despite evaporation of the liquid and the presence of substrate contributions.<sup>8</sup> Continuing this work with the consideration of a different substrate, Prather *et al.* also included hierarchical cluster analysis (HCA), as well as

---

<sup>\*</sup> Daubert et al. v. Merrell Dow Pharmaceuticals (509 US 579 (1993))

PCA and correlation coefficients to investigate association of fire debris samples to the appropriate reference standard.<sup>9</sup> Turner and Goodpaster investigated the effect of microbial degradation on the identification of ignitable liquid residues in soil samples, using PCA to identify degradation trends over time.<sup>10</sup> Waddell *et al.* reported a method to identify and classify ignitable liquids in fire debris using a combination of PCA, linear discriminant analysis, and quadratic discriminant analysis, with all statistical analyses performed on total ion spectra rather than chromatographic data.<sup>11</sup>

Multivariate statistical procedures have also been reported in the controlled substances discipline, particularly for profiling purposes. Klemenc demonstrated association of heroin samples according to production batch using a combination of HCA, PCA, and *k*-nearest neighbors (*k*-NN).<sup>12</sup> Chan *et al.* assessed trace elements present in street samples of heroin, using PCA to identify links among samples based on the elements present.<sup>13</sup> Weyermann *et al.* used correlation procedures to successfully associate MDMA (‘ecstasy’) samples from the same production batch with discrimination from samples produced in different batches.<sup>14</sup> Bodnar Willard *et al.* demonstrated the use of both PCA and HCA to differentiate the plant material, *Salvia divinorum*, from other *Salvia* species based on the presence of the hallucinogenic compound, salvinorin A.<sup>15</sup> The statistical procedures were subsequently used to associate different plant samples adulterated with salvinorin A to *S. divinorum*.<sup>16</sup> Further applications of similar statistical procedures in the analysis of controlled substances were reviewed by NicDaéid and Waddell.<sup>17</sup>

For DNA analysis, statistical methods for estimating a likelihood ratio (the odds that the evidence originated from the suspect over the odds that it originated from someone else) are well established. However, DNA data without population statistics are a different matter. Multivariate statistical procedures have been proposed for complex data sets such as those produced in high throughput sequencing<sup>18</sup> and terminal restriction fragment length polymorphism.<sup>19</sup> Lenz and Foran used similar methods for analysis of mock forensic soil samples.<sup>20</sup> Hedman *et al.* examined the information garnered from multiple characteristics of DNA electropherograms (*e.g.*, peak height, peak balance) from different DNA polymerases using a PCA approach.<sup>21</sup> In general however, multivariate statistical measures have not been widely used by forensic biologists, although their use has been proposed.<sup>22</sup>

A variety of statistical procedures have been applied to DNA analysis of the microbial content of soil. Such studies have often focused on analyzing the 16S rRNA gene via various assays (*e.g.*, denaturing gradient gel electrophoresis, terminal restriction fragment length polymorphism analysis, or next generation sequencing). The types of statistical procedures employed range from ordination methods like canonical correspondence analysis<sup>23, 24</sup> to cluster analysis methods, including HCA.<sup>25, 26</sup> Each method has its own advantages and disadvantages<sup>27</sup> with the mode of analysis chosen usually corresponding to the type of data being analyzed.

Among the exploratory methods commonly used for soil microbe analysis are PCA and multidimensional scaling (MDS). Dollhopf *et al.*, Girvan *et al.*, and McCaig *et al.* utilized PCA in conjunction to analyze bacterial community structure of environmental soil samples.<sup>28-30</sup> All incorporated additional statistical procedures including Kohonen self-organizing maps, HCA, and canonical variate analysis, respectively. Additionally, each group applied these statistical measures to different types of data (*e.g.*, Dollhopf *et al.* and Girvan *et al.* conducted terminal restriction fragment length polymorphism analysis, while McCaig *et al.* sequenced 16S rRNA clones that were analyzed using denaturing gradient gel electrophoresis).<sup>28-30</sup>

The majority of researchers who used MDS analyzed their data with nonmetric multidimensional scaling (NMDS). Fierer *et al.*, Nagy *et al.*, and Phillippot *et al.* used this procedure to understand the populations of bacteria in the habitats being studied.<sup>31-33</sup> Like the PCA examples, the laboratories used different experimental techniques, and had additional statistical analyses accompanying their NMDS results. Further occurrences of PCA and NMDS, as well as other ordinal or cluster analyses, are common in the literature for the statistical analysis of soil bacterial communities.<sup>34-39</sup>

A substantial body of research has been conducted in the Forensic Biology Laboratory at Michigan State University studying the bacterial composition of soil in a forensic context. Spatiotemporal factors influencing bacterial populations have been investigated using terminal restriction fragment length polymorphism analysis of all bacteria coupled with analysis of variance (ANOVA) and MANOVA, which is the multivariate version of ANOVA.<sup>40</sup> The heterogeneity as well as temporal changes of bacterial populations were analyzed within five habitats. Lenz *et al.* took a different approach for the spatiotemporal profiling of bacterial populations of the same five locations.<sup>20</sup> While terminal restriction fragment length polymorphism analysis was still employed; the rhizobial *recA* gene was targeted rather than all

bacterial populations. The resulting profiles were analyzed using NMDS in an attempt to differentiate the habitats.

Although various pretreatment and statistical procedures have been reported in the literature for the association and classification of different forensic evidence types, including footwear impressions,<sup>41, 42</sup> toolmarks,<sup>43, 44</sup> ballistics,<sup>45</sup> and questioned documents,<sup>46-48</sup> as well as the others discussed above, there exists no systematic evaluation of such procedures for the different types of data. In many cases, these procedures are conducted on pre-selected variables (*e.g.*, specific impurities in controlled substance samples), which could result in a loss of potentially discriminating variables. A variety of different pretreatment procedures are applied to the same data types, but with no comparison of the effects of different pretreatments on subsequent association and discrimination. To become more widely used in forensic science, these procedures must be demonstrated, evaluated, and documented, providing an essential resource for forensic laboratories. The principal aim of the research presented here was to meet this need.

### 1.3 Rationale for Research

The purpose of the research detailed here was to investigate the utility of multivariate statistical procedures to address Recommendation 3 in the NRC report, with specific application to forensically relevant data. Three diverse data sets were generated, each containing reference standards and simulated samples. All data sets were probed using both exploratory and classification procedures. Exploratory procedures were used to assess association of samples to the corresponding reference standard, with no prior knowledge of the data set. Classification procedures were used to classify the samples to the known reference standards. Tutorials were developed that document the application of each procedure, along with the advantages, limitations, and other considerations. These tutorials are intended as a resource for forensic laboratories interested in implementing statistical procedures as an additional tool for the comparison of evidence.

## 2. Theory

### 2.1 Data Pretreatment Procedures

#### 2.1.1 Chromatographic Data

For chromatographic data, pretreatment procedures are necessary to remove instrumental sources of variance among samples. In gas chromatography, non-chemical sources of variance can result from differences in injection volume (particularly when samples are injected manually rather than by using an autosampler), fluctuations in mobile phase flow rate and oven temperature, as well as degradation of the stationary phase that occurs over time. All of these parameters vary with each injection, leading to differences in chromatograms that are not chemical in nature.

Data pretreatment essentially minimizes or eliminates these non-chemical differences to ensure that in subsequent data analysis, differences identified among samples are chemical in nature and not artifacts of the analytical system or methodology. Numerous pretreatment procedures are available but, for chromatographic data, the more commonly applied procedures include background correction, smoothing, retention time alignment, and normalization. Background correction can be used to minimize low frequency noise originating from drift in the background signal, as well as to subtract, or remove, peaks present in the background. Smoothing is used to minimize noise in the chromatograms, thereby improving peak shape and increasing the signal-to-noise ratio. Retention time alignment may be necessary to account for shifts in retention time of the same compound that are due to instrumental drift. Finally, normalization procedures are used to account for small differences in peak abundance among samples that are a result of differences in the volume of sample injected/mass of sample analyzed.

##### 2.1.1.1 Background Subtraction and Smoothing

As the eventual aim of this research is to provide data analysis methods that can be incorporated into forensic laboratories, the data pretreatment procedures ideally should use software that is already available or easily accessible to laboratories. The operating software for the instrument used in this research (Agilent ChemStation, version E.01.00.237) incorporates a

background subtraction and a smoothing algorithm that require minimal user input and hence, both were used in this research.

The background subtraction function in the operating software subtracts the mass spectrum of a selected compound or region in the chromatogram from all scans in the total ion chromatogram (TIC). Caution should be exercised when performing this function to ensure that chemically relevant ions are not removed from the TIC. In such cases, the abundance of the ions in the sample compound would be reduced, resulting in a spectrum that is not truly representative of the compound.

The smoothing function in the instrument software applies a Savitzky-Golay algorithm to the TIC. This algorithm applies a least-squares polynomial fit to sections (windows) of the chromatogram containing a specified number of data points.<sup>49</sup> Second- or third-order polynomial functions are typically used as the shape of these functions most closely resembles the ideal Gaussian shape of chromatographic peaks. It should be noted that the even-numbered polynomial order and the next highest odd-numbered order will yield the same results; that is, applying a second or third order polynomial will result in the same degree of smoothing.<sup>50</sup>

The number of data points within each window should be less than the number of data points across a peak for smoothing to be effective. Beginning at the start of the chromatogram, the polynomial is fit to the specified number of data points. The central data point in the window is replaced with the value predicted by solving the polynomial. The algorithm moves forward by one data point and the process is repeated, replacing the value of the new central point with the value predicted by the polynomial. After smoothing, the resulting chromatograms should be visually inspected to ensure an appropriate degree of smoothing has been applied. It should be noted that the first few and last few data points in a chromatogram will not be smoothed as these points will never be in the center of a window. However, modifications to the algorithm are available that enable smoothing of all data points in the chromatogram.<sup>51</sup> The Savitzky-Golay algorithm is also susceptible to over-smoothing, which can result in a lower signal-to-noise ratio and a loss of peak resolution.

#### 2.1.1.2 Retention Time Alignment

Retention time alignment is often necessary for chromatographic data to correct for small shifts in retention time that occur over time as a result of mobile phase flow rate fluctuation,

oven temperature fluctuation, and stationary phase degradation, among others. Chromatographic data should therefore be assessed to determine the extent of retention time drift and the need for alignment. In this research, two different retention time algorithms were investigated: a peak-match algorithm<sup>52</sup> and a correlation optimized warping algorithm.<sup>53, 54</sup>

Both algorithms align chromatograms to a user-selected target chromatogram. Options for the target chromatogram include randomly selecting a chromatogram from the data set, or generating either an average chromatogram or a consensus chromatogram. As the target chromatogram should ideally contain all compounds in the data set to be aligned, the random target is only suitable for data sets that contain samples of the same type. An average target chromatogram can be generated by averaging the abundance of each variable across all samples in the data set. The resulting chromatogram contains all peaks in the sample set; however, mathematically averaging in this manner can lead to artificial peak broadening. A consensus target can be generated by combining aliquots of each sample into a single solution that is then analyzed under the same conditions as all samples in the data set. However, depending on the sample set in question, the consensus solution may be so complex that baseline resolution is not achieved thus compromising the ability to appropriately align chromatographic peaks.

The peak-match algorithm investigated in this research aligns peak maxima in the sample and target chromatograms.<sup>52</sup> Prior to alignment, a baseline correction is performed by subtracting a baseline offset from each chromatogram. The offset is estimated for each chromatogram by linear regression of the last few points of the chromatogram, which only account for noise. The next step is the identification of peaks in each sample chromatogram. To do this, the first derivative of the chromatogram is estimated and the difference in abundance between consecutive data points is determined. The leading edge of a peak is identified when the difference in abundance exceeds the peak identification threshold, which in this research, is set as five times the standard deviation of the baseline noise. On identifying a leading edge, the algorithm then searches for a zero crossing, which indicates the tailing edge of the peak. Through interpolation, the retention time at which this zero crossing occurs is determined, rounded to the next nearest integer, and added to a table of retention times being generated for that chromatogram. This is done for all chromatograms, including the target, generating a list of retention times at which peaks occur in each chromatogram.

Each sample chromatogram in turn is then compared to the target chromatogram, assessing where peak maxima occur. To do this, a user-defined window is defined and peaks present in this window in both the sample and target chromatograms are considered a match. The retention time axis is then interpolated to include or exclude data points so that the apex of the peak in the sample chromatogram occurs at the same retention time as the apex of the corresponding peak in the target chromatogram. In cases where a peak is identified in the sample chromatogram but is not present in the target, or vice versa, there is no interpolation of the retention time axis. As a result, this algorithm can align chromatograms that contain a different number of peaks. When using this algorithm, caution must be exercised in the choice of window size: if the window is too small, there will be difficulty in aligning peaks but if the window size is too large, there is the danger of aligning peaks in the sample to a neighboring, rather than the corresponding, peak in the target.

The correlation optimized warping algorithm aligns sections of a sample chromatogram to corresponding sections in the target chromatogram.<sup>53, 54</sup> In this case, the optimal alignment parameters are determined by calculating correlation coefficients between the corresponding sections of the sample and target chromatograms. There are two user-defined variables that must be specified in this algorithm. The first is the segment size ( $s$ ) which determines the number of sections the chromatograms will be divided into for alignment. It should be noted that the definition of segment size can vary depending on the software used for the alignment. In some software programs, the segment size is the number of data points per section while in others, the segment size is the actual number of segments that the chromatogram is divided into. The second user-defined variable is the warp ( $w$ ) which corresponds to the number of data points by which a segment in the sample chromatogram can be stretched or compressed to align with the appropriate section in the target chromatogram.

To perform the alignment, the algorithm begins by assessing the last segments in the sample and target chromatograms and applying warps from  $-w$  to  $+w$ . As an example, with a warp of 1, there are three possibilities for alignment: 1 data point is subtracted from the segment (equivalent to  $-w$ ), no data points are added or subtracted, or 1 data point is added to the segment (equivalent to  $+w$ ). Thus, for a segment containing 75 data points, applying a warp of 1 results in three segments: one segment contains 74 data points, one contains 75, and the third contains 76 data points. In the first and last cases, where the segment is compressed or stretched, data points

are interpolated so that the number of data points in the segment remains the same as the number in the corresponding section in the target chromatogram. Local correlation coefficients are then calculated to assess the effect of each warp on alignment of the section to the target chromatogram. Although all coefficients are stored, the warp that offers the highest correlation is retained and the algorithm moves onto the next segment in the chromatogram.

The whole process is repeated for the remaining segments, working from the end of the chromatogram to the beginning and, in each case, calculating local correlation coefficients for each warp and segment combination. A global correlation coefficient is then calculated from the sum of the local correlation coefficients. This is done for all combinations of local correlation coefficients and the combination resulting in the highest global correlation is deemed the optimal warp and segment size for alignment.

#### 2.1.1.3 Normalization and Scaling

Normalization procedures are applied to all variables in a sample and are used to eliminate variation due to differences in signal intensity as a result of differences in the volume or mass of sample analyzed, as well as differences in instrument response. A variety of normalization procedures are available according to the nature of the data under investigation. For the chromatographic data in this research, three normalization procedures were investigated: constant sum, constant maximum, and constant vector length.<sup>55</sup>

For the constant sum normalization procedure, the value of all variables in the chromatogram is summed and then the value of each variable is divided by that sum. Following this normalization, the sum of all variables in a given sample equals one. For the constant maximum normalization procedure, all variables in the chromatogram are divided by the abundance of the maximum variable in the chromatogram. This is analogous to mass spectral data in which each ion is expressed as a proportion of the base peak. Following this normalization, the maximum value in each chromatogram equals one and the values of all other variables ranges from zero to one.<sup>56</sup> For the constant vector length normalization procedure, the value of each variable is divided by the square root of the sum of the squares of all variables in the chromatogram.<sup>10</sup>

In addition to normalization, the effect of scaling was also investigated. Whereas normalization procedures are applied to all variables in a sample, scaling procedures are applied

to individual variables across all samples in the data set. Two scaling procedures were investigated: autoscaling and Pareto scaling. For both scaling procedures, the first step is to mean center the data by subtracting the mean of each variable across the data set from the corresponding variable in each sample. To autoscale, each mean-centered variable is divided by the standard deviation of the variable across the data set while to Pareto scale, each mean-centered variable is divided by the square root of the standard deviation. As the mean of an autoscaled data set is zero, with a standard deviation equal to one, all variables have similar variance and hence, are more equally weighted for comparison. However, autoscaling tends to increase the importance of noise. This problem is somewhat overcome in Pareto scaling, in which the scaled data more closely resemble the original data.<sup>57</sup> Scaling is not always necessary but does offer advantages for data sets in which sample responses are of different magnitudes.

## 2.1.2 Spectral Data

### 2.1.2.1 Normalization

The spectral data were subjected to three normalization procedures: constant sum, constant vector length, and the standard normal variate (SNV) normalization. Both constant sum and constant vector length normalization procedures were discussed previously with reference to the chromatographic data and were applied to the spectral data in a similar manner. The SNV procedure is commonly applied to spectral data to eliminate or minimize variance as a result of differences in effective path length. Such differences can originate from differences in the particle size or thickness of the sample analyzed, as well as differences in the instrument optics.<sup>58</sup> The SNV procedure is similar to autoscaling although is applied to all variables in a sample, rather than across all variables in the data set as is the case in autoscaling. Thus, the mean value of all variables in the sample is subtracted from the value of each individual variable, then divided by the standard deviation of all variables. SNV is termed a “weighted normalization” as not all variables have equal contribution. Instead, those variables that show greater deviation from the mean of the sample have greater weighting.

## 2.2 Exploratory Procedures

Exploratory procedures are statistical procedures in which no prior knowledge about the data set is necessary. As such, exploratory procedures can be a useful first step in the analysis of

complex data containing hundreds of variables, such as the chromatographic and spectral data considered in this research. Exploratory procedures have great utility in a forensic setting as they allow differences among complex data to be more easily visualized. Three different exploratory procedures were investigated in this research: Pearson product-moment correlation, cluster analysis, and principal components analysis. The first two procedures assess similarity among samples while the latter identifies the sources of greatest variance among samples.

### 2.2.1 Pearson Product-Moment Correlation Coefficients

Pearson product-moment correlation (PPMC) coefficients provide a method to compare samples in a pairwise manner to assess the correlation, or similarity. As such, coefficients can be calculated between two chromatograms or spectra (*e.g.*, reference standard and questioned sample) to assess the correlation between the two. In this case, each data point is a variable and the two chromatograms or spectra are compared on a point-by-point basis, using Equation 1.

$$r_{x,y} = \frac{\sum_{i=1}^n (x_i - \bar{x})(y_i - \bar{y})}{\sqrt{\sum_{i=1}^n (x_i - \bar{x})^2 \sum_{i=1}^n (y_i - \bar{y})^2}} \quad (1)$$

where  $r_{x,y}$  is the correlation coefficient between chromatogram (or spectrum)  $x$  and  $y$ ,  $x_i$  and  $y_i$  represent the abundance of variable  $i$  in chromatogram (or spectrum)  $x$  and  $y$ , respectively, while  $\bar{x}$  and  $\bar{y}$  represent the average abundance of all variables in the chromatogram (or spectrum) of  $x$  and  $y$ , respectively.

Correlation coefficients range in value from -1.00 to +1.00. Coefficients of  $\pm 1.00$  indicate perfect similarity between the two samples being compared, with the sign indicating positive or negative correlation. Coefficients in the range  $\pm 0.80$ - $0.99$  represent strong correlation between the two samples, coefficients from  $\pm 0.50$ - $0.79$  represent moderate correlation, coefficients less than  $\pm 0.49$  represent weak correlation, and coefficients close to 0.00 indicate no correlation.<sup>59</sup>

### 2.2.2 Principal Components Analysis

Principal component analysis (PCA) is a procedure used to highlight relationships among samples that may otherwise be difficult to observe due to the complexity of the data.<sup>3</sup> Using PCA, a complex data set (such as chromatographic or spectral data) is reduced to a few principal components that represent the greatest contributions to variance among the samples. As a result, the most discriminatory variables are identified and maintained whereas those that are uninformative are eliminated. This reduction in the dimensionality of the data set is useful as it allows patterns in the complex data to be more readily observed.

In PCA, the data set is represented in  $n$ -dimensional space, where  $n$  is the number of variables. For example, the chromatograms generated in this research each contain approximately 3,600 data points—each of these data points is a variable. In PCA, latent axes, known as principal components (PCs), are defined and the samples are projected onto the new axes. The first principal component (PC1) is the axis that maximizes the variance of the projected samples. This projected value is known as the score and hence, PC1 maximizes the variance of the scores. The second principal component (PC2) is positioned orthogonally to PC1 and accounts for the next greatest variance of the scores. Subsequent PCs follow this rule; that is, each is orthogonal to the preceding PC and accounts for next greatest source of variance.

The first step in PCA is to calculate a covariance matrix for the data set. Covariance is a measure of the correlation between two random variables and is calculated using Equation 2:

$$Cov(x, y) = \frac{\sum_{i=1}^n (x_i - \bar{x})(y_i - \bar{y})}{n-1} \quad (2)$$

For chromatographic or spectral data,  $x_i$  and  $y_i$  in Equation 2 represent the abundance of variable  $i$  in chromatogram (or spectrum)  $x$  and  $y$ , respectively,  $\bar{x}$  and  $\bar{y}$  represent the average abundance of all variables in the chromatogram (or spectrum) of  $x$  and  $y$ , respectively, and  $n$  is the number of dimensions (or variables). Note that the data are mean-centered during the process of calculating the covariance.

A matrix is then generated showing the covariance of all pairwise combinations in the data set. As an example, a data set with three dimensions ( $x$ ,  $y$ , and  $z$ ) would result in the following 3 x 3 covariance matrix:

$$\begin{bmatrix} \text{cov}(x, x) & \text{cov}(x, y) & \text{cov}(x, z) \\ \text{cov}(y, x) & \text{cov}(y, y) & \text{cov}(y, z) \\ \text{cov}(z, x) & \text{cov}(z, y) & \text{cov}(z, z) \end{bmatrix}$$

The covariance matrix shown above is symmetrical about the main diagonal as  $\text{cov}(x, y)$  is equivalent to  $\text{cov}(y, x)$ . For PCA, this covariance matrix should be square: if this condition is not met, additional zeros must be added to generate such a matrix.

Eigenanalysis of the covariance matrix is then performed to generate eigenvectors and corresponding eigenvalues. An eigenvector is a unit vector that can be multiplied by the data matrix to yield a vector that is a multiple of the original unit vector. The corresponding eigenvalue is the factor by which the eigenvector differs from the original matrix. For a data set containing  $n$  dimensions,  $n$  eigenvectors are defined and each has an associated eigenvalue that corresponds to the amount of variance described by that eigenvector. The eigenvectors are ranked in order of highest to lowest eigenvalues. The eigenvector with the largest associated eigenvalue is the first principal component (PC1) which, by definition, accounts for the maximum variance in the scores of the data. The eigenvector with the next greatest eigenvalue is the second principal component (PC2) and accounts for the next greatest variance in the data set. Theoretically, the maximum number of PCs that can be calculated for a given data set is equal to  $n-1$  where  $n$  is the number of samples or the number of data points, whichever is smaller. A plot of the variance accounted for against principal component (known as a Scree plot) can be used to determine the number of principal components that are necessary to adequately describe the data. Ideally, the first few principal components should account for 80-90% of the total variance, indicating that the structure of the data is represented adequately. Thus, a data set of  $n$  dimensions can be described in substantially fewer PCs, while still retaining the underlying patterns in the data.

The two outputs from PCA that are typically used for data interpretation are scores and loadings plots. The score for each sample on PC1 is calculated by multiplying the mean-centered data for the sample by the eigenvector for PC1 and summing the product. Scores for the samples on additional PCs are calculated in a similar manner, multiplying by the corresponding eigenvector. The scores for each sample on two (or three) PCs can then be plotted to generate a scores plot. Samples that are chemically similar have similar scores and, therefore, are positioned

closely in the scores plot. In contrast, chemically different samples have dissimilar scores and such samples are positioned distinctly in the scores plot.

Loadings plots are used to identify the variables contributing to the variance described by the PCs and are obtained by plotting the relevant eigenvectors. For chromatographic data, the eigenvectors for each principal component can be plotted against retention time while for spectral data, the eigenvectors can be plotted against wavenumber. In this way, each of the variables contributing to the variance can be identified. These variables are those that are responsible for the association and discrimination of the samples and hence, positioning of samples in the scores plot can be explained with reference to the appropriate loadings plots.

While the scores plot provides a graphical representation of association and discrimination among samples in the data set, the interpretation can be somewhat subjective, based on visual assessment of sample positioning in the plot. In this research, Euclidean distance and PPMC coefficients were subsequently employed where necessary to provide a quantitative assessment of the scores plot.

The Euclidian distance was calculated for pairwise comparisons of samples to reference standards. The distance was calculated based on the mean scores of the sample and standard on the first four principal components (Equation 3) and hence, the calculated distance represents the numerical distance between the sample and standard on the scores plot.

$$d(Sam, Std) = \sqrt{(PC1_{SAM} - PC1_{STD})^2 + (PC2_{SAM} - PC2_{STD})^2 + (PC3_{SAM} - PC3_{STD})^2 + (PC4_{SAM} - PC4_{STD})^2} \quad (3)$$

where  $d(Sam, Std)$  is the Euclidean distance between the sample and reference standard,  $PC1_{SAM}$ ,  $PC2_{SAM}$ ,  $PC3_{SAM}$ , and  $PC4_{SAM}$ , are the average scores of the sample on PC1, PC2, PC3, and PC4, respectively and  $PC1_{STD}$ ,  $PC2_{STD}$ ,  $PC3_{STD}$ , and  $PC4_{STD}$  are the average scores of the reference standard on PC1, PC2, PC3, and PC4, respectively. Association between a sample and standard is represented by a short Euclidean distance whereas, longer distances indicate no association between the sample and standard. However, the point at which two sample distances are short enough to be considered associated or long enough to be considered distinct from one another is not statistically defined.

Pearson product-moment correlation coefficients were also used to assess association of samples and standards based on the PCA scores. For this purpose, coefficients were calculated

using the loadings of the sample and standard (*i.e.*, the product of the mean-centered data and the eigenvector for the appropriate PC). By calculating coefficients in this manner, the sample and standard can be compared based on the variance described by the relevant PC.

### 2.2.3 Hierarchical Cluster Analysis

Cluster analysis also assesses similarity of samples, similar to PPMC coefficients; however, cluster analysis is not limited to pairwise comparisons of data. In agglomerative hierarchical cluster analysis (HCA), all samples are initially considered as individual groups, each containing one sample.<sup>60, 61</sup> Distances between samples are measured using one of many available distance measurements, although the Euclidean distance (Equation 4) is commonly used.

$$d_{AB} = \sqrt{\sum_{i=1}^n (x_{Ai} - x_{Bi})^2} \quad (4)$$

where  $d_{AB}$  is the Euclidean distance between samples A and B,  $x_{Ai}$  and  $x_{Bi}$  are the coordinates of samples A and B, respectively in dimension  $i$ , and  $n$  is the total number of dimensions.

After calculating distances between pairs of samples, the two samples separated by the shortest distance are linked to form a new group. The process of calculating distances among samples is repeated; however, from this stage on, the distance of the sample to groups containing more than one sample must be calculated. Different linkage methods are available to do this. In the single linkage method, the distance between the sample and the nearest sample within each group is calculated (Figure 1A). In the complete linkage method, the distance between the sample and the farthest sample within each group is calculated (Figure 1B) while in the average linkage method, the distance between the sample and the average point in each group is calculated (Figure 1C). In each case, the sample joins the group to which the calculated distance

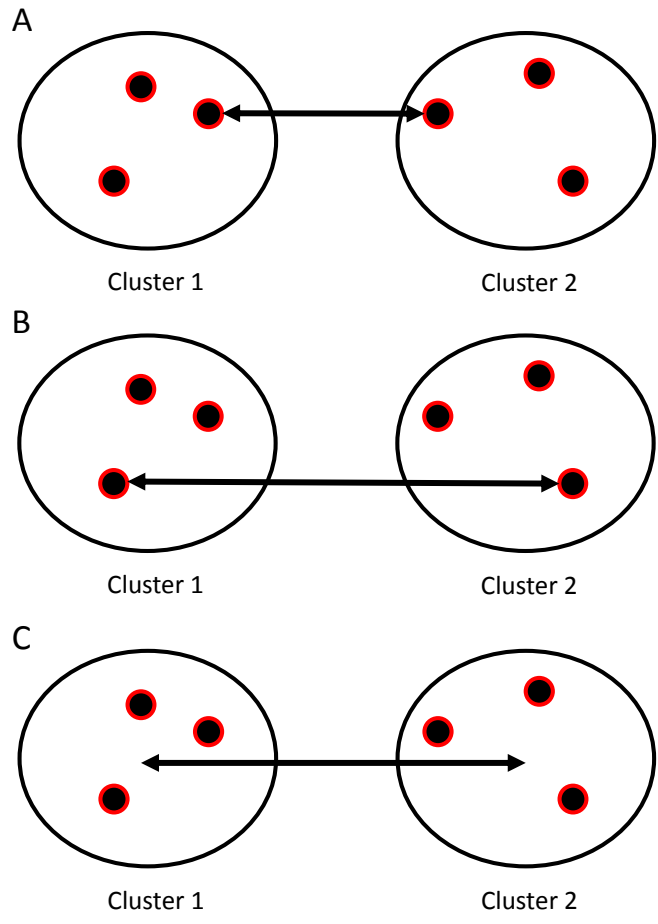


**Figure 1.** Linkage methods in hierarchical cluster analysis (A) single linkage, (B) complete linkage, and (C) average linkage. Euclidean distance is calculated between members of each cluster as shown.

is shortest. It should be noted that if the data set contains distinct groups of samples, then choice of linkage method should not change the groupings observed.

The process of calculating distances and linking groups continues until all samples are members of a single groups. The grouping of samples is commonly displayed as a dendrogram in which the horizontal axis represents the similarity among samples. This similarity is based on the distance measured between two samples compared to the maximum distance between any two samples in the data set (Equation 5).

$$S_{AB} = 1 - \frac{d_{AB}}{d_{max}} \quad (5)$$

where  $S_{AB}$  and  $d_{AB}$  are the similarity and Euclidean distance, respectively, between samples A and B, and  $d_{max}$  is the maximum Euclidean distance between any two samples in the data set. Thus, a similarity of 1 indicates identical samples while a similarity of 0 indicates dissimilar samples.

Dendrograms from HCA provide a method in which similarities among samples can be readily visualized (an advantage over PPMC coefficients), while also providing a metric to compare the degree of similarity among samples. However the similarity index is relative to the population being tested; that is, the two least similar samples in the data set will have a similarity index of 0 and the similarity index of all other samples will be calculated relative to this. As a result, even if two samples have some degree of similarity, the similarity index between the two may be 0 if all other samples in the set are more similar. Furthermore, while similarities among samples are highlighted in HCA, no information is given regarding the variables that are most similar among the samples. Thus, it is often useful to perform another exploratory procedure, namely principal components analysis.

#### 2.2.4 Multidimensional Scaling

Similar to PCA and HCA, multidimensional scaling (MDS) is an exploratory procedure used to understand and visualize the patterns or structure of complex data sets. The goal of MDS is to orient data in a low-dimensional multidimensional space where each data point represents a single sample and the spread of the data represents, as closely as possible, the originally imputed (dis)similarities, also referred to as proximities.<sup>62, 63</sup> Data inputted into MDS takes the form of a

square symmetric matrix of (dis)similarities. The final configuration of the data points, or MDS plot (solution), illustrates the correlations among the data (*e.g.*, closer data points are more highly correlated). In MDS, all data points are randomly plotted in a given number of dimensions. Those points are then systematically adjusted in relation to each other to reduce the amount of stress, which is a measure of how accurately the plot is representing the data. When the global minimum stress is achieved further iterations are discontinued. Figure 2 illustrates a global minimum where, point Y has the lowest stress. Point X is similar to point Y and is considered a local minimum. Depending on the power of the computer being used for analysis and the complexity of the data, a local minimum can be found instead of the global minimum, causing the stress to be higher and a less accurate MDS solution to be developed. The analysis of additional plots (*e.g.*, Scree or Shepard plots) can be used to identify the reliability of the final configuration.

A stress diagram, or Scree plot, is a measure of the badness-of-fit of the MDS configuration to the data.<sup>62</sup> The lower the stress the better the model is fitting the data. For ordinal MDS, as dimensionality increases, stress ( $\sigma$ ) decreases until the number of dimensions ( $m$ ) is equal to the number of samples ( $n$ ) minus two ( $m = n - 2$ ). However, as the number of dimensions increases, the interpretability of the MDS plot decreases. An adequate number of dimensions needs to be identified so that the stress is low and the plot is understandable; generally two dimensions are used. There is no globally accepted level of stress for a MDS plot and thus, acceptance is at the discretion of the analyst, although Kruskal introduced the idea that a final configuration can be chosen where an increase in  $m$  does not greatly reduce stress.<sup>64</sup> This is often referred to as the ‘elbow’ in the stress diagram. Figure 3 indicates a typical stress plot with the ‘elbow’ clearly noticeable at two dimensions.

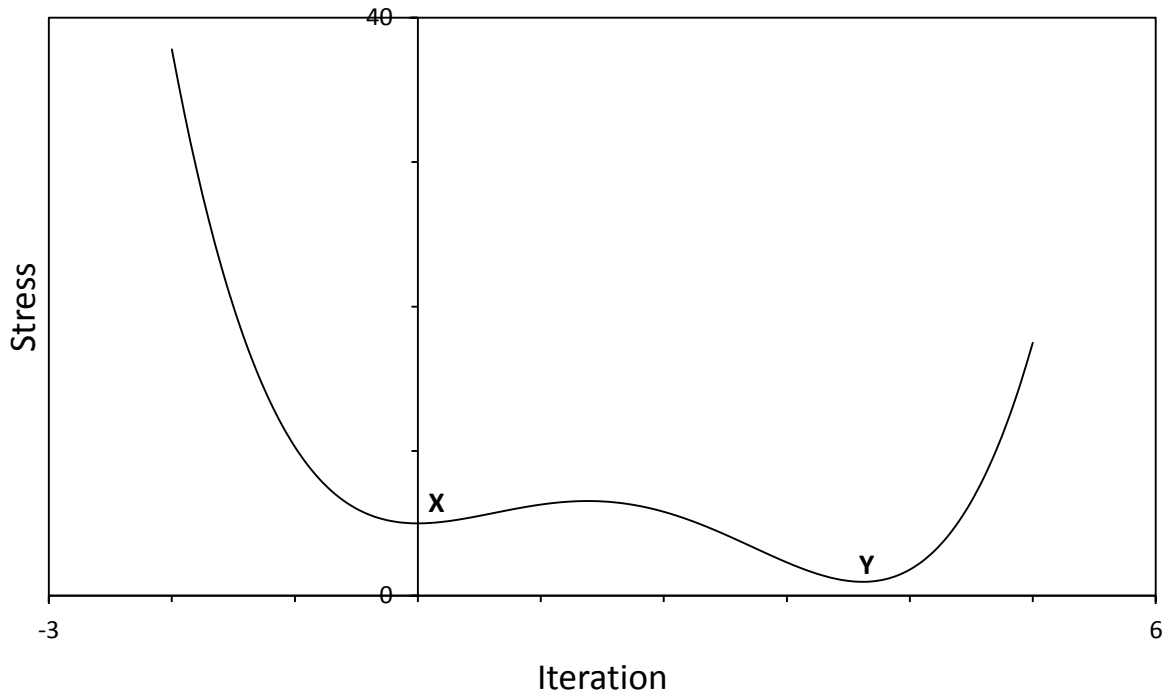


**Figure 2.** Graph illustrating the concept of local and global minimum with regards to stress. Position Y indicates the global minimum having the lowest stress for the entire graph. Position X is similar to Y and is considered a local minimum. Multidimensional scaling aims to attain the global minimum when plotting the data.

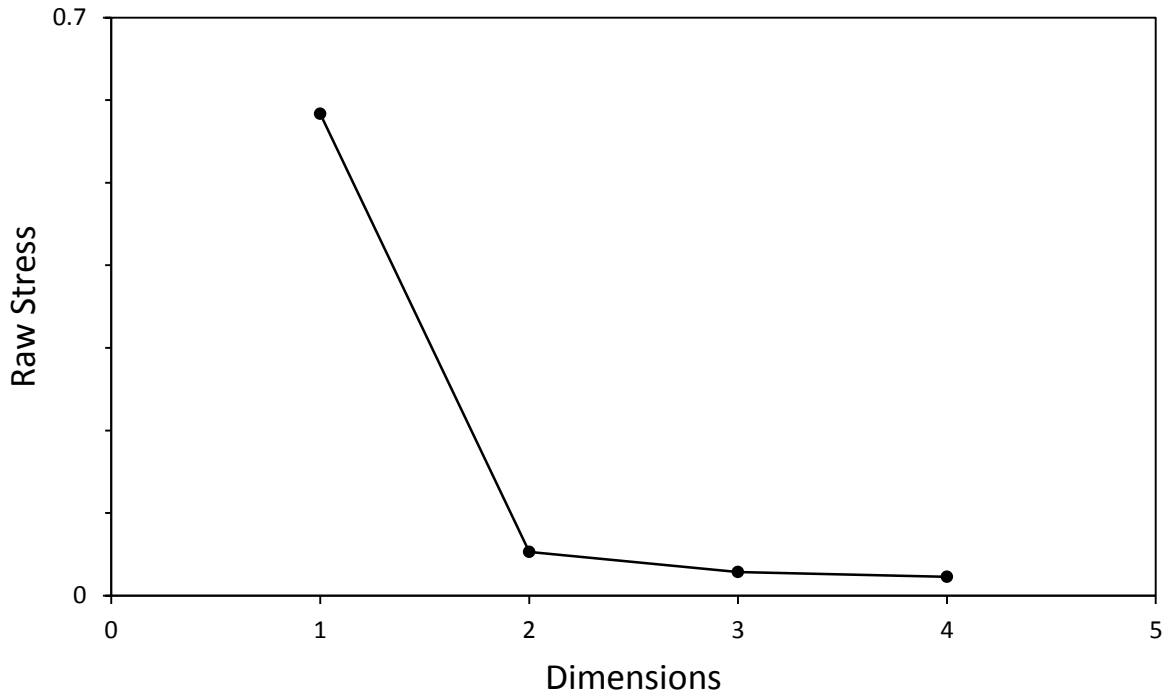


**Figure 3.** Typical stress plot. Stress is high in one dimension followed by a large decrease at two dimensions. Stress continues to decrease into higher dimensionality, though not appreciably, creating the elbow, after which little additional information is gained.

In this research, Kruskal's Stress-1 was calculated for all plots using Equation 6,

$$\text{Stress-1} = \sigma_1 = \sqrt{\frac{\sum [f(p_{ij}) - d_{ij}(\mathbf{X})]^2}{\sum d_{ij}^2(\mathbf{X})}} \quad (6)$$

where  $f$  is a representation function that establishes the MDS model,  $p_{ij}$  is the proximity for point  $i, j$ , and  $d_{ij}(\mathbf{X})$  is the corresponding distance in the MDS solution  $\mathbf{X}$ .<sup>62</sup> The stress is expected to decrease as the number of dimensions increases. Any deviation from this expectation would indicate errors in the way MDS is plotting the data. Figure 4 is an example of such a stress plot. The raw stress is extremely low for all dimensions; however, the increase in stress from one to three dimensions would call the final configuration into question. Logically this should not happen and the MDS plot can be disregarded as being erroneous.

Another test for the acceptability of stress at a given dimension was described by Spence, who proposed that random stress, or stress produced by random data for a given number of samples and dimensions, could be approximated using Equation 7,<sup>65</sup>

$$\sigma_1 = 0.001[a_0 + a_1m + a_2n + a_3 \ln(m) + a_4 \sqrt{\ln(n)}] \quad (7)$$

where  $a_0 = -524.25$ ,  $a_1 = 33.8$ ,  $a_2 = -2.54$ ,  $a_3 = -307.26$ , and  $a_4 = 588.35$ . This estimation of random stress is accurate for the range  $n = 10 - 60$  and  $m = 1 - 15$ . Random stress can be used as a null hypothesis for the acceptance of the MDS plot with relation to its associated stress diagram.

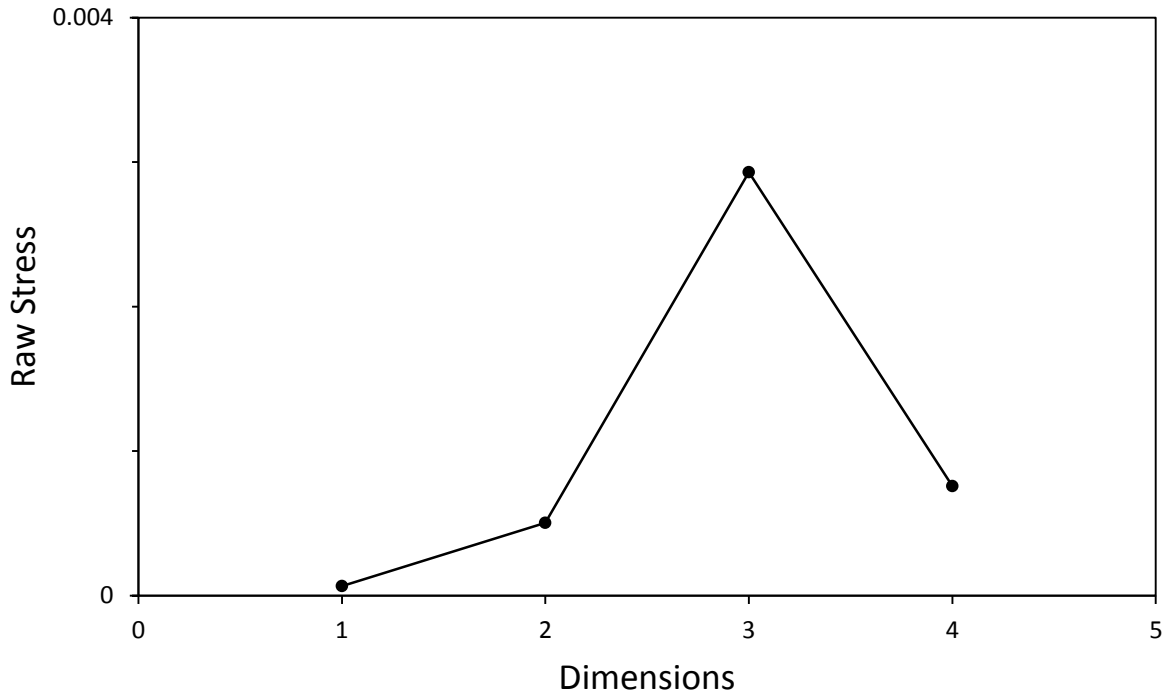


**Figure 4.** Erroneous stress plot. Unlike Figure 3 above, this stress plot exhibits non-normal stress changes with increasing dimensionality. In one dimension, the stress is lowest, with an increase to three dimensions followed by a decrease into four. This does not follow the expected relationship observed in Figure 3 and would indicate that the multidimensional scaling configurations associated with the plot could be misrepresenting the data.

A Shepard diagram (Figure 5) plots proximities or dissimilarities on the X-axis against the disparities (open circles) and approximated distances (filled circles) on the Y-axis.<sup>62</sup> Proximities fall on a monotonic regression that varies depending on the model being used. A plot with a perfect stress of zero would have disparities and distances sitting atop each other. In cases where stress is nonzero, the vertical distance between each disparity and distance is the error of representation for that pair. The comparison of these points allows for the identification of outliers and possible sources of high stress. The larger the deviations of distances from disparities the worse MDS is at explaining the data and the larger the stress. Similar to stress diagrams, Shepard diagrams are an indicator of the badness-of-fit for the final configuration of the data.

### 2.2.5 Beta-Diversity Indices

Beta ( $\beta$ )-diversity was defined by Whittaker as “the extent of change of community composition, or degree of community differentiation, in relation to a complex-gradient of environment, or a pattern of environments.”<sup>66</sup> Two commonly used  $\beta$ -diversity indices, the Bray-Curtis dissimilarity index (BCDI)<sup>67</sup>, and Sørensen-Dice coefficient (SDC; described independently by Sørensen<sup>68</sup> and Dice<sup>69</sup>), were utilized to investigate the diversity in bacterial populations among the three habitats sampled in this study. The pairwise distances developed by each index were the input for NMDS.

The BCDI is a popular method for calculating quantitative measurements of ecological data. The BCDI allows count data to be transformed into dissimilarity measurements between two samples, including large data sets, by comparing the structure, or in this case bacterial membership, of the samples. Equation 8 shows the dissimilarity equation as used in the mothur software ([www.mothur.org](http://www.mothur.org)).

$$D_{Bray-Curtis} = 1 - 2 \frac{\sum \min(S_{A,i}, S_{B,i})}{\sum S_{A,i} + \sum S_{B,i}} \quad (8)$$

This equation outputs dissimilarity data by subtracting the sum of the minimum number of DNA sequences seen in a single operational taxonomic unit (OTU) between two samples ( $S_A$  and  $S_B$ ) divided by the sum of the total number of sequences for each sample multiplied by two.

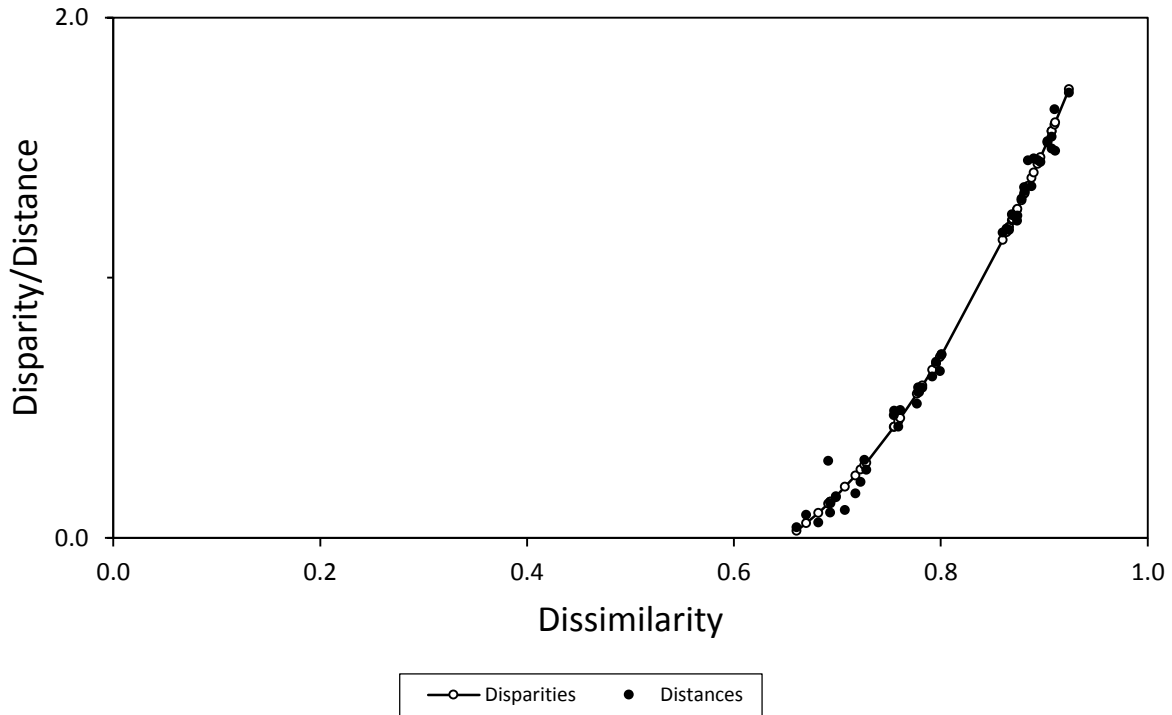


**Figure 5.** A sample Shepard diagram with low stress and good association of disparities and distances. The closer the association of the filled circles (representing approximated distances) and open circles (representing disparities) the better multidimensional scaling is representing these data. This Shepard diagram shows very close relationship between the two using a polynomial monotonic function.

This process is conducted for each pair of samples until all pairwise comparisons have been made. Note that comparing A to B and B to A will result in the same dissimilarity measurement, so the final matrix is square symmetric.

The SDC is similar to the BCDI; however, the SDC compares the dissimilarity between two samples through community membership. Equation 9 shows the dissimilarity calculation as used in the mothur software.

$$D_{Sørensen} = 1 - \frac{2S_{AB}}{S_A + S_B} \quad (9)$$

This equation outputs dissimilarity data by subtracting double the number of shared OTUs between the samples ( $S_{AB}$ ) divided by the sum of the total number of OTUs in each sample. Unlike the BCDI, the SDC only considers the number of OTUs in common, not the number of sequences in each shared OTU, making it possible to obtain different measures of dissimilarity between the two. The final result from SDC analysis will also be a square symmetric matrix.

## 2.3 Classification Procedures

Classification procedures are supervised statistical procedures that are used to assign unclassified (*e.g.*, questioned) samples to previously defined groups (*e.g.*, reference standards). Typically, these procedures require prior knowledge of the data set (*e.g.*, identities of reference standards); however, when this is not the case, exploratory procedures such as those described in the previous section can be used to identify natural groups of samples in the data set. These clusters then constitute the pre-defined groups for classification. Two classification procedures were investigated in this research: soft independent modeling of class analogy (SIMCA) and  $k$ -nearest neighbors ( $k$ -NN).

Both the SIMCA and  $k$ -NN approaches to classification are based on similarity; that is, questioned samples are members of the class to which they lie closest to in the measurement space. In both procedures, known samples (*e.g.*, reference standards) in the data set are used to develop and optimize the classification model. This model is subsequently used to classify questioned samples. The  $k$ -NN approach is an example of a ‘hard’ classification procedure, meaning that classification is forced such that all questioned samples will be classified to one of the known classes. In contrast, SIMCA is a ‘soft’ classification procedure which means that classification is not forced. As a result, a questioned sample may be considered a member of one class, more than one class, or no classes at all.

### 2.3.1 Soft Independent Modeling of Class Analogy

In the SIMCA approach to classification, PCA is used to develop independent models for each of the assigned classes and the optimal number of PCs is maintained in the model.<sup>55, 61, 70, 71</sup> A cross-validation procedure can be used to determine the appropriate number of principal components to retain in each model. To do this, the data set is firstly divided into a training set and a test set, ensuring that the test set contains samples from each of the known classes in the training set. The optimal number of principal components is initially set to 1 and using this model, an appropriate sample in the test set is fit to the corresponding model. The residuals are calculated for the fit of the sample to the model. The procedure is repeated, this time setting the optimal number of principal components to 2. As before, appropriate samples are fit to the relevant model and residuals are calculated. The procedure is repeated, and the number of principal components that minimizes the residuals is the optimal number of principal

components that should be retained in the model. It should be noted that due to the independent nature of the modeling, the optimal number of PCs will not necessarily be the same for all classes.

Once PCA models have been developed for each class, questioned samples can be classified. Scores for the questioned sample are calculated and projected onto the PCA model for the first class to assess the goodness-of-fit. The variance of the residuals for the questioned sample when fit using this model is calculated using Equation 10, along with the variance of the residuals for members of the class, which is calculated using Equation 11.

$$s_{fit}^2 = \sum_{j=1}^P \frac{(e_{ij})^2}{P-F} \quad (10)$$

$$s_{class}^2 = \sum_{i=1}^N \sum_{j=1}^P \frac{(e_{ij})^2}{(P-F)(N-F-1)} \quad (11)$$

where  $s_{fit}^2$  is the residual variance of the sample fit to the class,  $s_{class}^2$  is the residual variance of the model class,  $e_{ij}$  are the calculated residuals,  $P$  is the dimensionality of the data,  $F$  is the number of principal components retained in the model, and  $N$  is the number of samples in the class.

An F-test is then used to compare the variance of the residuals. In cases where  $s_{fit}^2$  is significantly different from  $s_{class}^2$ , the questioned sample is not well described by the model and is not considered a member of that class. In contrast, where  $s_{fit}^2$  and  $s_{class}^2$  are not significantly different, then the model adequately describes the questioned sample and the sample is considered a member of the class. This procedure is repeated for each of the pre-defined classes, assessing the fit of the questioned sample in each case. It should also be noted that as the F-test can be conducted at different confidence levels, the probability of class membership at different confidence levels can also be assigned.

### 2.3.2 $k$ -Nearest Neighbors

In the  $k$ -NN procedure, classification is based on the proximity of a questioned sample to its nearest neighbors in the measurement space.<sup>55, 61, 71</sup> Samples in the training set are firstly

assigned to known classes and the Euclidean distance between all pairs of samples is calculated according to Equation 12.

$$d_{xy} = \left[ \sum_{j=1}^m (x_j - y_j)^2 \right]^{1/2} \quad (12)$$

where  $d_{xy}$  is the Euclidean distance between data vectors  $x$  and  $y$ ,  $x_j$  and  $y_j$  are the values of the variable  $j$  in data vectors  $x$  and  $y$ , respectively, and  $m$  is the number of variables in the data set.

The  $k$  samples that are closest (*i.e.*, have the shortest Euclidean distance) to the questioned sample are considered the nearest neighbors, where  $k$  is a user-defined integer. The questioned sample is considered a member of the class to which the majority of the  $k$ -nearest neighbors belong. The optimal number of neighbors to consider in the classification is determined during the model development phase. To do this, classification of known samples in the training set is assessed using different  $k$  values for the classification. The optimal  $k$  value occurs where there is correct classification and no misclassifications of the known samples. However, as  $k$  increases, the  $k$ th nearest neighbor is not necessarily close to the known sample in the measurement space.

To prevent ambiguity in classification,  $k$  is typically an odd number. However, where this is not the case and the questioned sample has an equal number of nearest neighbors to two or more classes, the accumulated Euclidean distances can be considered. The questioned sample is subsequently considered a member of the class to which there is the lowest accumulated distance.

As  $k$ -NN is a ‘hard’ classification procedure, all samples will be classified to one class only. However, as the classification is forced, the sample may not actually be a good fit for that class or group. To assess the goodness-of-fit, the distance of the sample to the nearest neighbor in the class is calculated and then compared to the spread or variance of that class. To estimate the spread of the class, the distance among all pairs of samples in the class is firstly determined, then the average of the smallest distance of each sample to all others is calculated. The goodness-of-fit,  $G$ , of a new sample is then calculated using Equation 13.

$$G_i = \frac{d_i - \bar{d}_q}{s(d_q)} \quad (13)$$

where  $d_i$  is the distance of sample  $i$  to the nearest neighbor in the group,  $\bar{d}_q$  is a vector of the smallest distance of each sample in the group to all others, and  $s(d_q)$  is the standard deviation of the vector.

The goodness-of-fit is calculated for all samples to all groups and compared to a threshold value at a given confidence level. Goodness-of-fit values close to the threshold level of a class can indicate that the sample is not truly likely to be a member of that class.<sup>71</sup>

## 3. Materials and Methods

### 3.1 Chromatographic Data

#### 3.1.1 Reference Standards and Simulated Fire Debris Samples

Reference standards from four classes defined by ASTM International were selected (Table 1) and diluted 1:10 (v/v) in methylene chloride<sup>72</sup>. Diluted liquids were spiked onto separate kimwipes (approximately 4 cm x 4 cm), placed in nylon bags that contained one-fourth of an activated carbon strip, and subjected to a passive headspace extraction for 4 hours at 80 °C. Following extraction, the carbon strips were eluted with 200 µL methylene chloride and analyzed by GC-MS using the instrument parameters shown in Table 2. Three extracts were prepared for each reference standard and each extract was analyzed in triplicate to give a total of nine chromatograms for each standard.

**Table 1.** Ignitable liquid reference standards.

ASTM class	Definition	Representative liquids	Abbreviation *	Representative chromatogram
<b>Gasoline</b>	C <sub>3</sub> - and C <sub>4</sub> -alkylbenzenes and various aliphatic compounds	Gasoline 3 (Meijer) Gasoline 4 (Marathon) Gasoline 5 (BP)	GS3 GS4 GS5	Appendix 1A Appendix 1B Appendix 1C
<b>Isoparaffinic products</b>	Branched chain; cyclic alkanes and n-alkanes insignificant or absent	Paint thinner Upholstery & fabric protector	PTH UFP	Appendix 1D Appendix 1E
<b>Naphthenic paraffinic products</b>	Branched chain and cyclic alkanes; n-alkanes insignificant or absent	Marine fuel stabilizer	MFS	Appendix 1F
<b>Petroleum distillate products</b>	Homologous series of n-alkanes in Gaussian distribution; less significant isoparaffinic, cycloparaffinic, and aromatic compounds	Lamp oil Torch fuel Charcoal lighter Diesel Kerosene	LMP TFL CHL DSL KER	Appendix 1G Appendix 1H Appendix 1I Appendix 1J Appendix 1K

\* These abbreviations are used throughout the remainder of the report.

**Table 2.** GC-MS instrument parameters.

<b>Injection</b>	250 °C 1 µL Pulsed splitless (15 psi for 0.25 s)
<b>Carrier gas</b>	Ultra-high purity helium, 1 mL/min
<b>Column</b>	5% diphenyl-95% dimethyl polysiloxane 30 m x 0.25 mm i.d. x 0.25 µm
<b>Oven temperature program</b>	40 °C, hold for 3 min 10 °C/min to 280 °C, hold for 4 min
<b>Transfer line temperature</b>	280 °C
<b>Ionization mode</b>	Electron, 70 eV
<b>Scan range</b>	50-550 Da
<b>Scan rate</b>	2.91 scans/s

Two sets of simulated fire debris samples were prepared. The first set (Set 1) contained eight liquids (paint thinner, upholstery protector, marine fuel stabilizer, lamp oil, torch fuel, charcoal lighter, diesel, and kerosene) spiked onto a carpet and carpet padding substrate. Due to the diverse chemical nature, Set 1 was used to investigate the potential of each of the statistical procedures. The second set (Set 2) contained four liquids (each from different ASTM classes) spiked onto an oil-finished red oak hardwood flooring substrate.

To prepare the fire debris samples, separate samples of each substrate were spiked with the appropriate diluted ignitable liquid reference standard (spike volumes ranged from 100-175 µL for the carpet and carpet padding substrate and from 50-125 µL for the oil-finished wood substrate). For the carpet and carpet padding substrate, a propane blowtorch was applied to the sample for 30 s and the sample was allowed to burn for a further 90 s before being extinguished using an overturned beaker. For the oil-finished wood substrate, the torch was applied for 30 s before the sample was extinguished in a similar manner. Each sample was extracted using the passive-headspace procedure and then analyzed by GC-MS following the same procedures as for the reference standards. For each substrate/reference standard combination, three samples were prepared in this manner and each extract was analyzed in triplicate, yielding a total of 9 chromatograms for each simulated fire debris sample.

### 3.1.2 Chromatographic Data Pretreatment

Standard operating procedures for the data pretreatment procedures are included in Appendix 2 and a summary of each procedure is given below.

Because the reference standards and fire debris samples were extracted in nylon bags, a major compound in the bags (caprolactam) was present at varying abundance in the resulting total ion chromatograms (TICs). The background subtraction function in the instrument operating software (Agilent ChemStation version E.01.00.237, Agilent Technologies) was used to remove the caprolactam peak from each chromatogram, before the smoothing function in the operating software was applied.

A target chromatogram for retention time alignment was generated from the TICs of the reference standards. The random number function in Microsoft Excel was used to randomly select three TICs per reference standard and the average abundance of each variable in the selected TICs was calculated to generate the target. The peak-match algorithm was performed in Matlab (version R2010b, The Mathworks Inc., Natick MA) following the procedure described by Johnson *et al.*, investigating window sizes of 3, 5, and 7<sup>52</sup>. A correlation optimized warping algorithm was performed in The Unscrambler X (version 10.2, Camo Software Inc., Woodbridge NJ), investigating segment sizes of 120, 80, 60, and 40 with warp sizes of 2 and 4 data points. Following alignment, a total of eleven aligned data sets were generated and each was visually inspected to assess the need for retention time alignment.

Total ion chromatograms were then subjected to three separate normalization procedures: constant sum normalization, constant maximum normalization, and constant vector length normalization. The normalized data sets were subsequently autoscaled and Pareto scaled. Principal components analysis was then performed separately on each data set (including the non-normalized data) and the resulting scores plots were used to assess association of replicates of each reference standard as well as discrimination of chemically different reference standards.

### 3.1.3 Chromatographic Data Analysis

Standard operating procedures for the data analysis procedures are included in Appendix 2 and a summary of each procedure is given below.

After preliminary assessment of the data, the appropriate pretreatment procedures were applied to the full data set (reference standards and simulated fire debris samples in Set 1). PPMC coefficients were calculated for pairwise comparisons of the standards, as well as for comparisons of the simulated fire debris to the corresponding standard. Coefficients were calculated using the data analysis add-in in Microsoft Excel. Principal components analysis was

performed in Matlab (version R2010b, The Mathworks Inc., Natick MA) while HCA was performed in Pirouette (version 4.0, Infometrix Inc., Bothell, WA). Both exploratory procedures were used to investigate association of reference standards in the same ASTM class, differentiation of standards in chemically different classes, and association of the simulated fire debris samples to the corresponding reference standard.

Classification procedures were also performed to investigate the ability to successfully classify the ignitable liquid present in each of the simulated fire debris samples. SIMCA was performed in The Unscrambler X (Camo Software Inc.), using a random cross-validation procedure to validate the models, and *k*-NN was performed in Pirouette (Infometrix Inc.). For both procedures, the reference standards were used as the initial training set and classification of the simulated fire debris samples according to ignitable liquid present was investigated.

## 3.2 Spectral Data

### 3.2.1 Reference Standards and Simulated Street Samples

Reference standards of d-amphetamine sulfate, d-methamphetamine hydrochloride, codeine, morphine sulfate, barbital sodium salt, and phenobarbital were purchased from Sigma-Aldrich (St. Louis, MO) and used as purchased. Reference standards of N-methyl-3,4-methylenedioxamphetamine (MDMA) hydrochloride, (+)-N-ethyl-3,4-methylenedioxyamphetamine (MDEA) hydrochloride, and heroin were purchased from Cerilliant Corporation (Round Rock, TX) and also used as received. The data set of reference standards is summarized in Table 3. All standards were individually homogenized in a mortar and pestle prior to analysis by infrared spectroscopy.

Selected reference standards were mixed with caffeine to prepare simulated street samples. Specifically, amphetamine, methamphetamine, MDMA, MDEA, codeine, and barbital were mixed with caffeine (Eastman Kodak Co., Rochester, NY) to give controlled substance/caffeine ratios of 80/20 and 50/50, by mass. Throughout the remainder of this report, these simulated samples are referred to as “80/20” and “50/50”, respectively, to indicate the composition of the sample mixture. The simulated samples were individually homogenized in a mortar and pestle prior to analysis.

**Table 3.** Controlled substance reference standards.

<b>Controlled substance class</b>	<b>Representative substances</b>	<b>Abbreviation</b>	<b>Representative spectrum</b>
<b>Amphetamines</b>	Amphetamine	AMPH	Appendix 3A
	MDEA	MDEA	Appendix 3B
	MDMA	MDMA	Appendix 3C
	Methamphetamine	METH	Appendix 3D
<b>Barbiturates</b>	Barbital	BARB	Appendix 3E
	Phenobarbital	PHEN	Appendix 3F
<b>Opiates</b>	Codeine	CODE	Appendix 3G
	Heroin	HERO	Appendix 3H
	Morphine	MORP	Appendix 3I

Reference standards and simulated samples were analyzed using a Perkin Elmer Spectrum One Fourier-transform infrared (FTIR) spectrometer, equipped with an attenuated total reflectance (ATR) sampling accessory. On each day of analysis, the zinc-selenide crystal was initially cleaned with acetone and a contamination check was performed and a background spectrum was collected. A portion of the relevant standard or sample mixture was placed on the crystal and approximately 80-85 units of pressure were applied. Four scans were collected for each spectrum over the wavenumber range 4000-650  $\text{cm}^{-1}$ , with a resolution of 4  $\text{cm}^{-1}$ . The crystal and pressure anvil were cleaned again with acetone between samples and a new background was collected after every six samples.

The set of standards and samples was analyzed in a similar manner a total of nine times. Spectra were background corrected and smoothed using the automated functions in the instrument software (Spectrum version 5.0.1, Perkin Elmer), then exported as .ascii files into Microsoft Excel. For each data collection day, the average of the three spectra collected for each standard or sample mixture was generated and used in subsequent data analysis.

### 3.2.2 Spectral Data Pretreatment

Standard operating procedures for the data pretreatment procedures are included in Appendix 2 and a summary of each procedure is given below.

The spectra generated and exported into Excel were in transmittance mode and prior to data analysis, the spectra were transformed into absorbance mode. Following transformation, spectra of the reference standards were subjected to three normalization procedures: constant sum normalization, constant maximum normalization, and SNV normalization. All calculations

for the normalization procedures were performed in Microsoft Excel. To assess the effect of normalization, PCA (Matlab, The Mathworks) was performed separately on the non-normalized data and each normalized data set. The resulting scores plots were used to assess association of replicates of each reference standard, as well as discrimination of the chemically different reference standards.

### 3.2.3 Spectral Data Analysis

Standard operating procedures for the data pretreatment procedures are included in Appendix 2 and a summary of each procedure is given below.

The normalized spectra of the reference standards were then subjected to PCA (Matlab, The Mathworks) and HCA (Pirouette, Infometrix Inc.) as initial exploratory data analysis procedures. The resulting scores plot and dendrogram were used to assess association of standards of the same controlled substance class and differentiation of the classes. Both statistical procedures were repeated, this time including the simulated street samples in the data set. The resulting plots were used to investigate association of each simulated sample to the corresponding reference standard and controlled substance class.

Both SIMCA (The Unscrambler, Camo Software Inc.) and *k*-NN (Pirouette Infometrix Inc.) were performed, using the reference standards as the initial training set and investigating classification of the simulated street samples according to the appropriate controlled substance.

## 3.3 Gene Sequence Data

### 3.3.1 Sample Collection and Preparation

#### 3.3.1.1 Sample Collection

Soil samples were collected from three locations in the Fenner Nature Center in Lansing, MI (Table 4). The sampling locations represent three distinct habitats: a yard, a marsh, and a wooded area. GPS coordinates were taken for each site. Soil was collected using a gardening spade, which was washed with water between collections, and the collected soil was stored in a freezer at -20°C within an hour of collection. Three soil samples less than a meter apart were collected from each site and were used as biological replicates and labeled 1 – 3. A mixture (1:1:1) of the yard samples (Ymix) was also processed.

**Table 4.** Sampling sites and corresponding GPS coordinates

Site name	Abbreviation	GPS coordinates
Fenner Nature Center, Yard	Y	N 42° 42.65' W 84° 30.92'
Fenner Nature Center, Marsh	M	N 42° 42.00' W 84° 31.15'
Fenner Nature Center, Soil	S	N 42° 42.43' W 84° 30.59'

### 3.3.1.2 DNA Extraction

Micropipette tips and tubes were UV irradiated in a Spectrolinker XL-1500 UV Crosslinker (Spectronic Corporation Lincoln, NE) for 5 min (~ 2.5 J/cm<sup>2</sup>). DNA was extracted from soil samples using a PowerSoil® DNA Isolation Kit (MoBio Carlsbad, CA) with two minor modifications: an additional wash was conducted after step 16 by adding 500 µL of 70% ethanol and centrifuged for 30 s at 10,000 x g, and DNA was eluted using 100 µL of solution C6 that had been heated to 55°C. Reagent blanks were processed with every extraction.

### 3.3.1.3 PCR Amplification of 16S Hypervariable Regions 4-6

Reagents suitable for UV irradiation and all micropipette tips and tubes were UV irradiated for two or more rounds of 5 min. Hypervariable regions 4 – 6 of bacterial 16S rRNA genes were amplified with universal bacterial primers (Table 5). A PCR master mix was generated, with final concentrations of 1X AmpliTaq Gold buffer (Life Technologies Carlsbad, CA) 2.5 mM MgCl<sub>2</sub>, 0.2 mM nucleotide triphosphates, 1.2 µL of the 10 µM forward primer, 0.4 µg/µL bovine serum albumin, and 3U AmpliTaq Gold (Life Technologies). Master mix was aliquoted into ten PCR tubes to a final volume of 51.6 µL per tube. Six microliters of each soil DNA extract was added to an aliquot, along with 1.2 µL of one of the 10 µM reverse primers (each reverse primer, while identical in binding region, had a unique DNA barcode that was used for downstream analysis). Each 60 µL reactions was mixed, then equally aliquoted into three PCR tubes, with a goal of avoiding stochastic sampling of template DNA. DNAs were amplified on an 2720 thermocycler (Life Technologies) under the conditions noted in Table 6, for 30 cycles. Identical 20 µL reactions were combined into a 60 µL pool and 5 µL was electrophoresed on a 1% agarose gel with ethidium bromide visualization.

**Table 5.** Primer sequences.

<b>Forward or reverse</b>	<b>Adaptor sequence</b>	<b>Barcode</b>	<b>Binding sequence</b>
Forward	CCTATCCCCTGTGTGCCTTGGCAGTCTCAG		CCAGCAGCYGCGGTAAN
Reverse A1	CCATCTCATCCCTGCGTGTCTCCGACTCAG	AATGGTAC	CGACRRCCATGCANCACCT
Reverse A2	CCATCTCATCCCTGCGTGTCTCCGACTCAG	TCTCCGTC	CGACRRCCATGCANCACCT
Reverse A3	CCATCTCATCCCTGCGTGTCTCCGACTCAG	AACCTGGC	CGACRRCCATGCANCACCT
Reverse A4	CCATCTCATCCCTGCGTGTCTCCGACTCAG	ACGAAGTC	CGACRRCCATGCANCACCT
Reverse A5	CCATCTCATCCCTGCGTGTCTCCGACTCAG	TTCGTGGC	CGACRRCCATGCANCACCT
Reverse A6	CCATCTCATCCCTGCGTGTCTCCGACTCAG	AACACAAC	CGACRRCCATGCANCACCT
Reverse A7	CCATCTCATCCCTGCGTGTCTCCGACTCAG	TTCTTGAC	CGACRRCCATGCANCACCT
Reverse A8	CCATCTCATCCCTGCGTGTCTCCGACTCAG	TCCAAGTC	CGACRRCCATGCANCACCT
Reverse A9	CCATCTCATCCCTGCGTGTCTCCGACTCAG	TTCGCGAC	CGACRRCCATGCANCACCT
Reverse A10	CCATCTCATCCCTGCGTGTCTCCGACTCAG	CCGGTCGC	CGACRRCCATGCANCACCT

**Table 6.** PCR cycling parameters

<b>PCR step</b>	<b>Temperature (°C)</b>	<b>Time (s)</b>
Initial Heating	94	600
Denaturation	94	30
Annealing	60	45
Extension	72	60
Final Extension	72	120

### 3.3.1.4 PCR Product Purification

Forty microliters of the remaining pooled amplification reactions was purified using Agencourt® AMPure® XP (Beckman Coulter Brea, CA). The bottle containing the beads was vortexed briefly and 30 µL was aliquoted into a 1.5 ml micro-centrifuge tube. DNA was added and the mixture was vortexed and incubated at room temperature for 15 min. The beads were bound to a MagnaRack™ (Life Technologies) for a minimum of five min. The supernatant was aspirated from the beads and discarded. Undisturbed beads were washed with 500 µL 70% ethanol for 30 s. The supernatant was again aspirated and the beads were washed an additional time. Beads were then dried on the magnet for 30 min at 37°C. DNA was eluted by adding 100 µL of 10 mM Tris, pH 8 and vortexing the tubes for at least 10 s. The tubes were returned to the

magnet and beads were bound for at least five min. Supernatant was aspirated away from the pellet and saved in a 1.5 mL micro-centrifuge tube.

#### 3.3.1.5 PCR Quantification and Equimolar Pooling

Purified PCR product was quantified using a Quant-iT™ dsDNA High-Sensitivity Assay Kit (Life Technologies) following the manufacturer's protocol. The ten quantified samples were pooled so that 25 ng of DNA from each was in the final pool and brought to a final concentration of 1 ng/μL.

#### 3.3.1.6 Sequencing Purified PCR Product

The pooled DNAs were sequenced on a Roche GS Junior 454 Sequencer following the manufacturer's protocols using a titanium emPCR kit (Lib-L), sequencing kit, and PicoTiter plate kit (Roche, San Francisco, CA).

#### 3.3.2 Gene Sequence Data Pretreatment

Sequencing data output for the 454 sequencer was processed using open-source mothur software.<sup>73</sup> The program input codes and explanations for processing sequence data, along with a sample file, are given in Appendix 4A. Bacterial sequences were also classified using the SILVA bacterial reference alignment provided on the mothur website with input codes given in Appendix 4B.

#### 3.3.3 Gene Sequence Data Analysis

Two statistical procedures were used to analyze the biological data: PCA and nonmetric MDS. The OTU's data used for PCA are described at the end of Appendix 4A. PCA was performed using Matlab (version R2010b, The Mathworks).

Pairwise comparisons used for NMDS are described in Appendix 4C. Square dissimilarity matrices developed from BCDI and SDC were input into Addinsoft XLSTAT Pro expansion for Microsoft Excel. NMDS was run, using the Scaling by Majorizing a Complicated Function (SMACOF) algorithm, for four dimensions with 500 iterations, each stopping at a convergence of 0.00001. Two dimensional MDS plots were analyzed along with Shepard diagrams and stress plots, the latter of which were compared against the null hypothesis random

stress plot described by Spence (1979). If the Kruskal's stress was less than random stress, the MDS plots were accepted at that dimension. MDS plots were further accepted with Kruskal's stress for two dimensions lower than 0.1. Finally, standard error bars were applied to all MDS plots.

## 4. Results and Discussion

### 4.1 Chromatographic Data

Exemplar chromatograms of the ignitable liquid reference standards and simulated fire debris samples are included in Appendix 1.

#### 4.1.1 Retention Time Alignment

The aligned data sets were visually compared to assess the alignment of replicates of each reference standard. No single algorithm or alignment parameters improved alignment for all standards in the data set; however, in general, the correlation optimized warping algorithm improved alignment compared to the peak-match algorithm. This is primarily due to differences in the operation of the algorithms. The peak-match algorithm aligns the apex of the peaks but, as a result, the leading and tailing edges of the peaks can be misaligned as the algorithm shifts the peak to align the apex (Figure 6). The extent of misalignment of the edges of the peak is therefore dependent on the window size used in the algorithm. In contrast, the correlation optimized warping algorithm aligns the leading edge or tailing edge of the peak with the result that the apexes may not be well-aligned. For the data set of reference standards, there were more instances of misaligned peaks with the peak-match algorithm than with the correlation optimized warping algorithm.

However, when compared to the unaligned reference standards, neither algorithm offered substantial improvements. The reference standards were analyzed over a relatively short time period during which there was no major instrument maintenance. Consequently, there was little instrument drift with the result that the TICs were generally aligned and further retention time alignment of the reference standards was not deemed necessary.

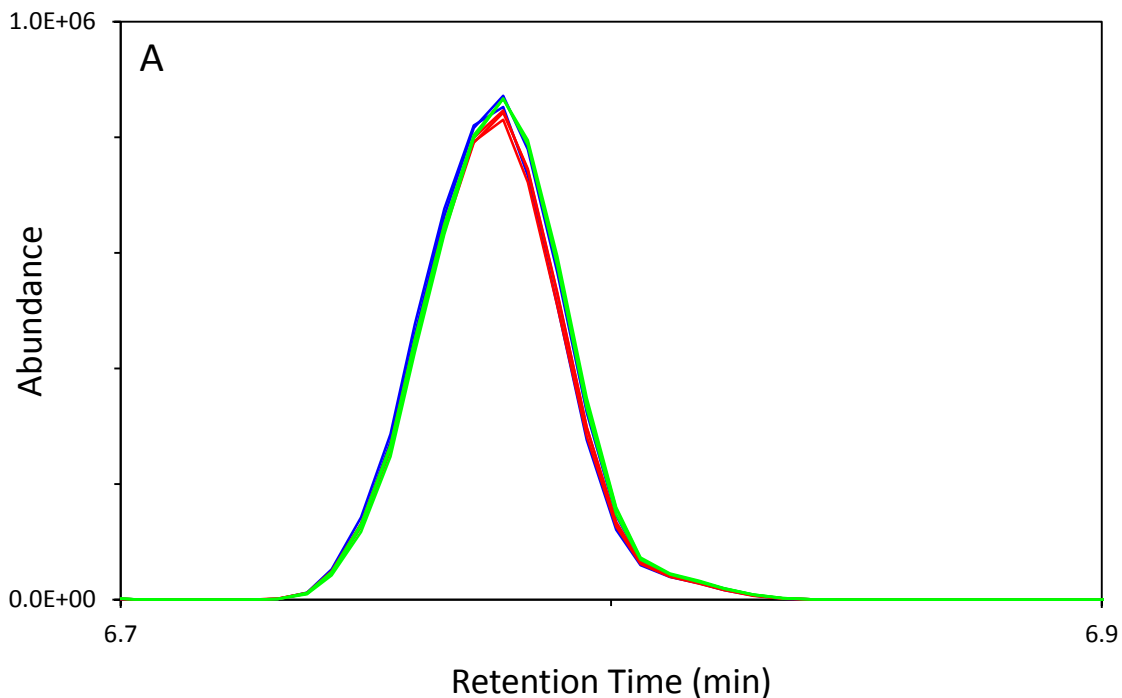


**Figure 6.** Retention time alignment of the m-/p-xylene peak in Gasoline 3 (A) before alignment, (B) after retention time alignment using peak-match algorithm with a window size of 5 data points, and (C) after retention time alignment using the correlation optimized warping algorithm with a warp of 2 data points and a segment size of 120. It should be noted that in (B), a deliberately large window size is shown to demonstrate the potential of worsening the data.

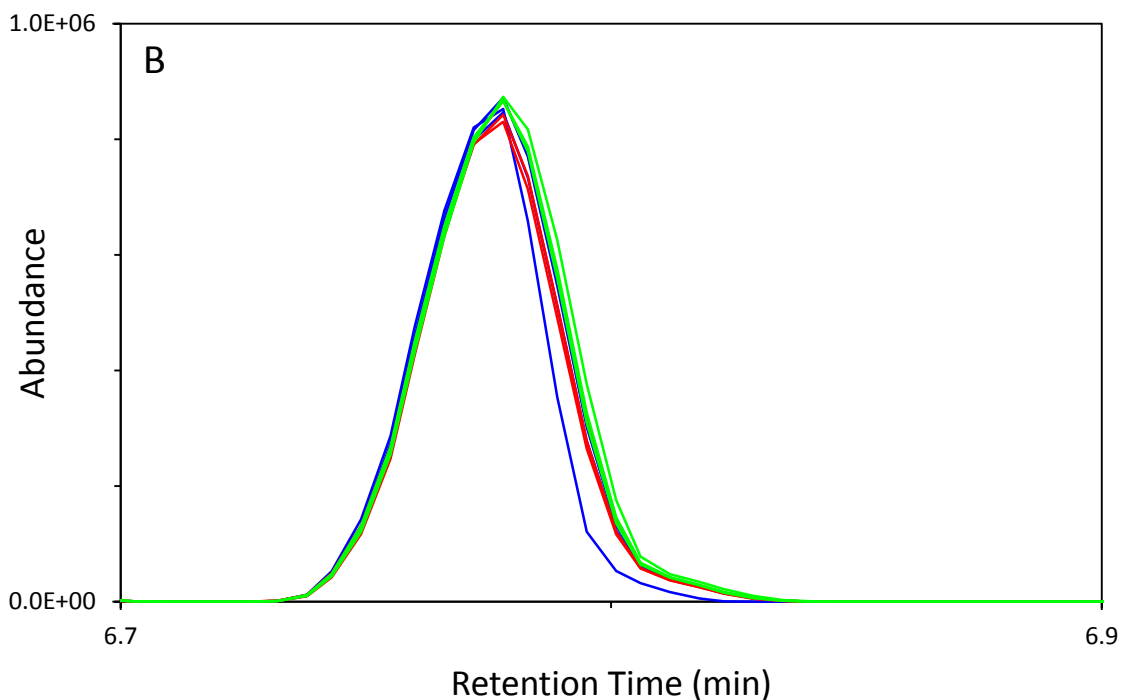


**Figure 6 contd.** Retention time alignment of the m-/p-xylene peak in Gasoline 3 (A) before alignment, (B) after retention time alignment using peak-match algorithm with a window size of 5 data points, and (C) after retention time alignment using the correlation optimized warping algorithm with a warp of 2 data points and a segment size of 120. It should be noted that in (B), a deliberately large window size is shown to demonstrate the potential of worsening the data.

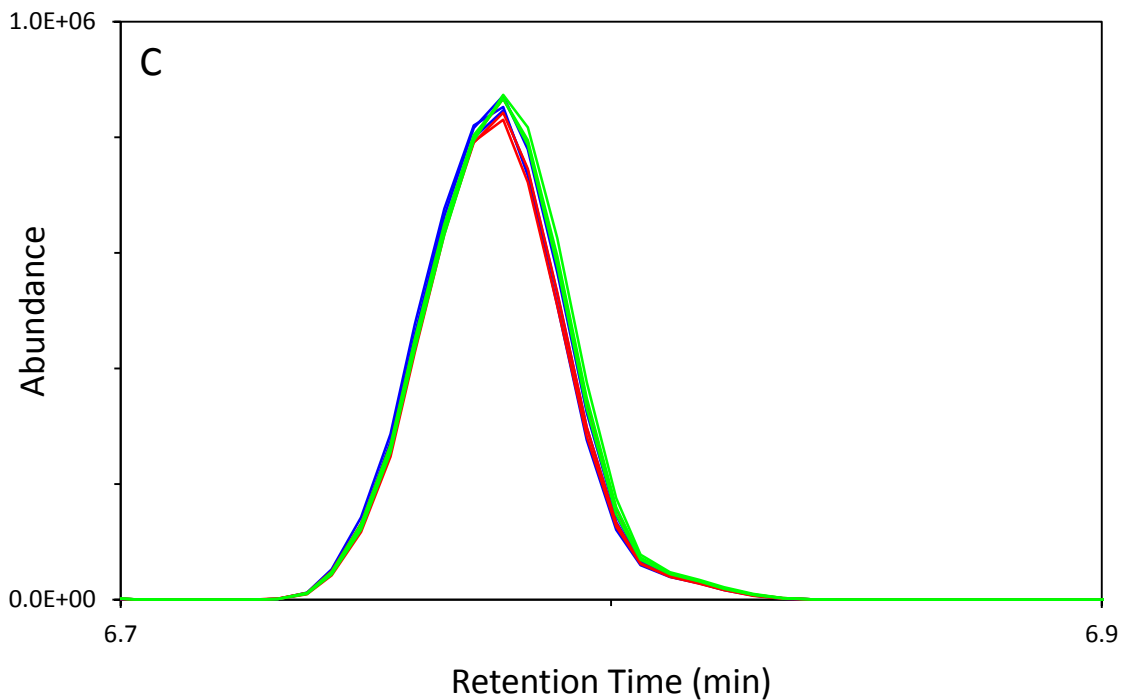


**Figure 6 contd.** Retention time alignment of the m-/p-xylene peak in Gasoline 3 (A) before alignment, (B) after retention time alignment using peak-match algorithm with a window size of 5 data points, and (C) after retention time alignment using the correlation optimized warping algorithm with a warp of 2 data points and a segment size of 120. It should be noted that in (B), a deliberately large window size is shown to demonstrate the potential of worsening the data.

Sets 1 and 2 of the simulated fire debris samples were collected over a longer time period (approximately 12 months). Replicates of each sample were well aligned and were also well aligned to the reference standards, despite the time duration between collection of the standards and samples. As a result, no retention time alignment was actually necessary for these data sets.

The need for retention time alignment will depend on the time period over which the data are collected as well as the state of the instrument during that time. Thus, for each data set, a visual assessment should initially be conducted to assess the need for retention time alignment.

#### 4.1.2 Normalization and Scaling

The non-aligned reference standards were subsequently normalized using three normalization procedures (constant sum, constant maximum, and constant vector length normalization), which were applied to each sample chromatogram.

Figure 7 illustrates the general effects of normalization, focusing on the C<sub>12</sub> peak in replicate chromatograms of the kerosene standard. With no normalization (Figure 7A), there is spread among the replicates in both the baseline and the peak maxima. Following constant sum normalization, there is less spread in the abundance of the baseline; however, spread in the peak maxima remains (Figure 7B). Following constant maximum normalization, there is less spread in the peak maxima but spread remains in the baseline (Figure 7C). Constant vector length normalization is similar to constant sum normalization in that there is spread in the peak maxima but an improvement in the baseline spread (Figure 7D).

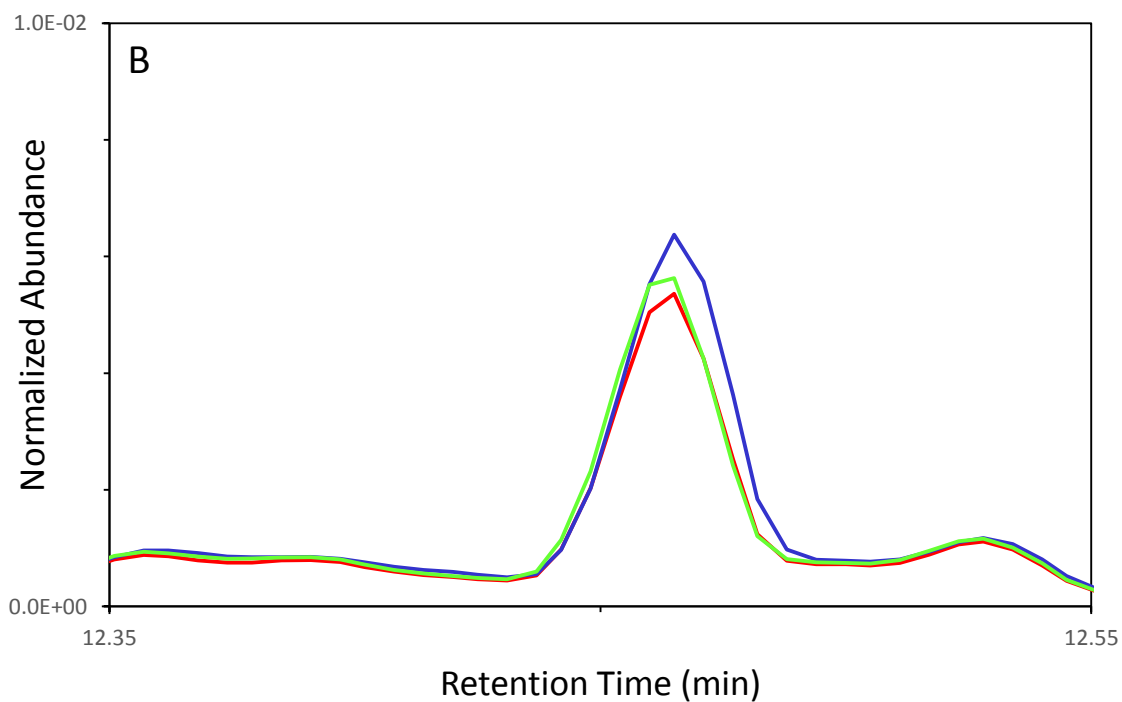
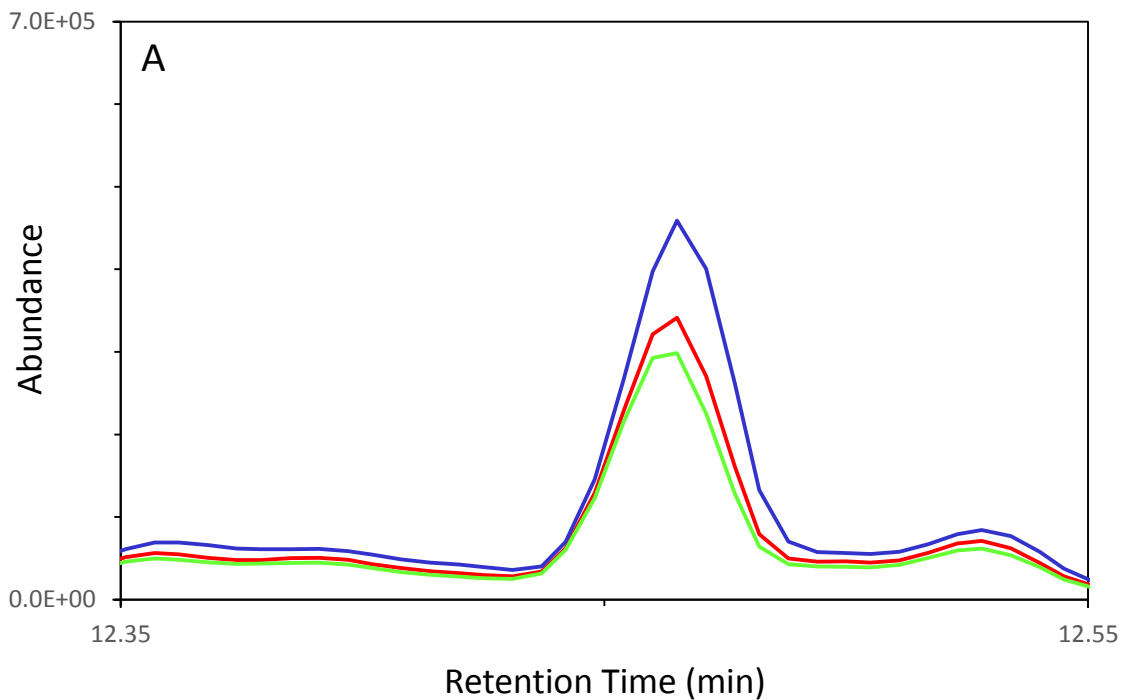


**Figure 7.** Section of chromatogram for kerosene replicates corresponding to  $C_{12}$  peak after (A) no normalization, (B) constant sum normalization, (C) constant maximum normalization, and (D) constant vector length normalization.

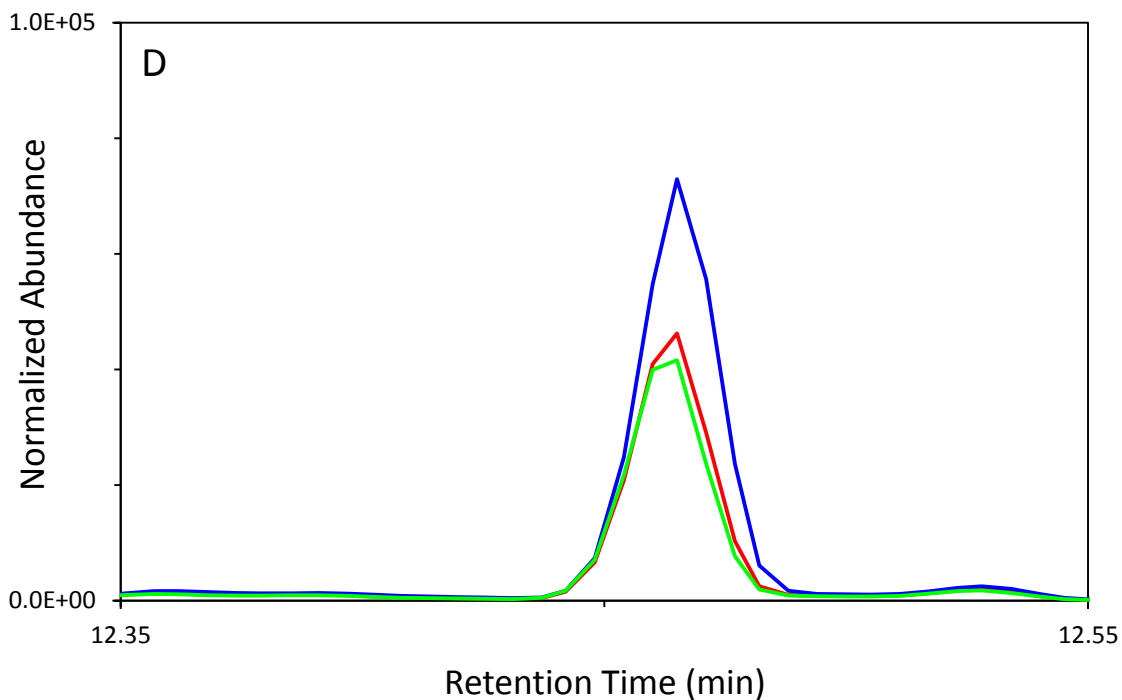
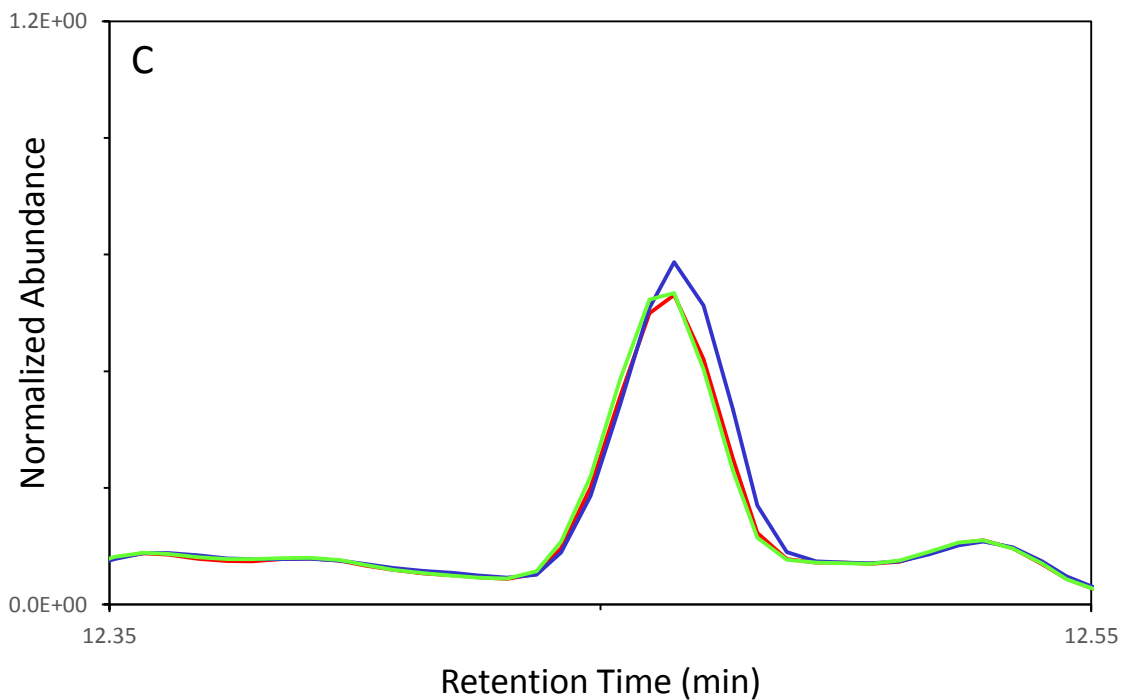


**Figure 7 contd.** Section of chromatogram for kerosene replicates corresponding to C<sub>12</sub> peak after (A) no normalization, (B) constant sum normalization, (C) constant maximum normalization, and (D) constant vector length normalization.

The normalization procedures were further assessed using PCA and the resulting scores plots were assessed (Figure 8). The first two principal components account for approximately 50-60% of the variance in the data set, depending on the normalization procedure used. However, with no normalization (Figure 8A), there is substantial spread among replicates of each standard, which is sufficient to prevent adequate differentiation of four of the standards: upholstery protector and paint thinner (both isoparaffinic class) and charcoal lighter and lamp oil (both petroleum distillate class). There is an improvement in the close positioning of replicates following normalization, although this improvement is greater for the constant sum and constant maximum normalization procedures compared to constant vector length (Figures 8B and C compared to D). To quantify this improvement, the relative standard deviation in the scores of replicates of each standard in the first two principal components was calculated (Tables 7 and 8).

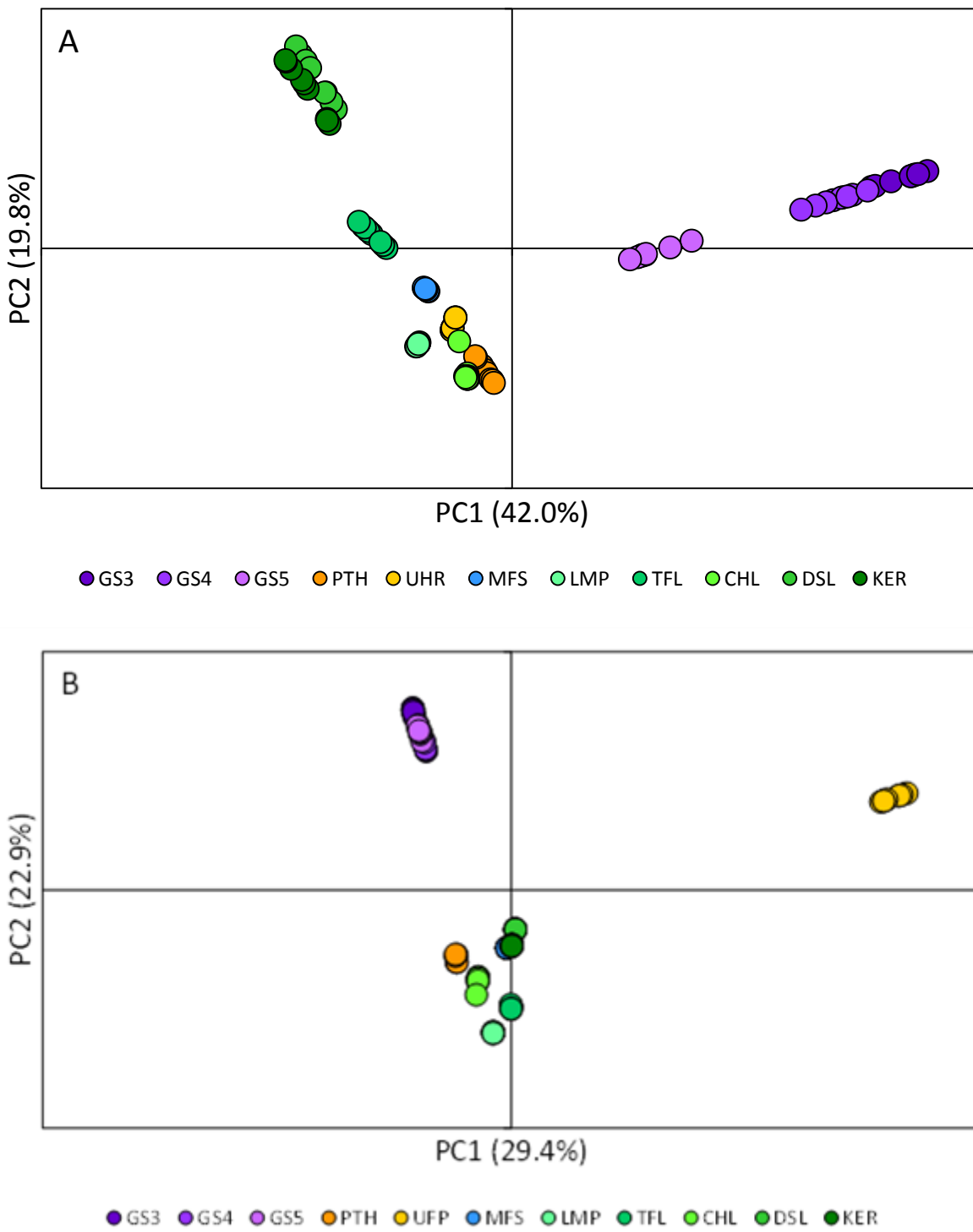


**Figure 8.** Scores plots for ignitable liquid reference standards (A) no normalization, (B) constant sum normalization, (C) constant maximum normalization, and (D) constant vector length normalization. Abbreviations for each standard are defined in Table 1.

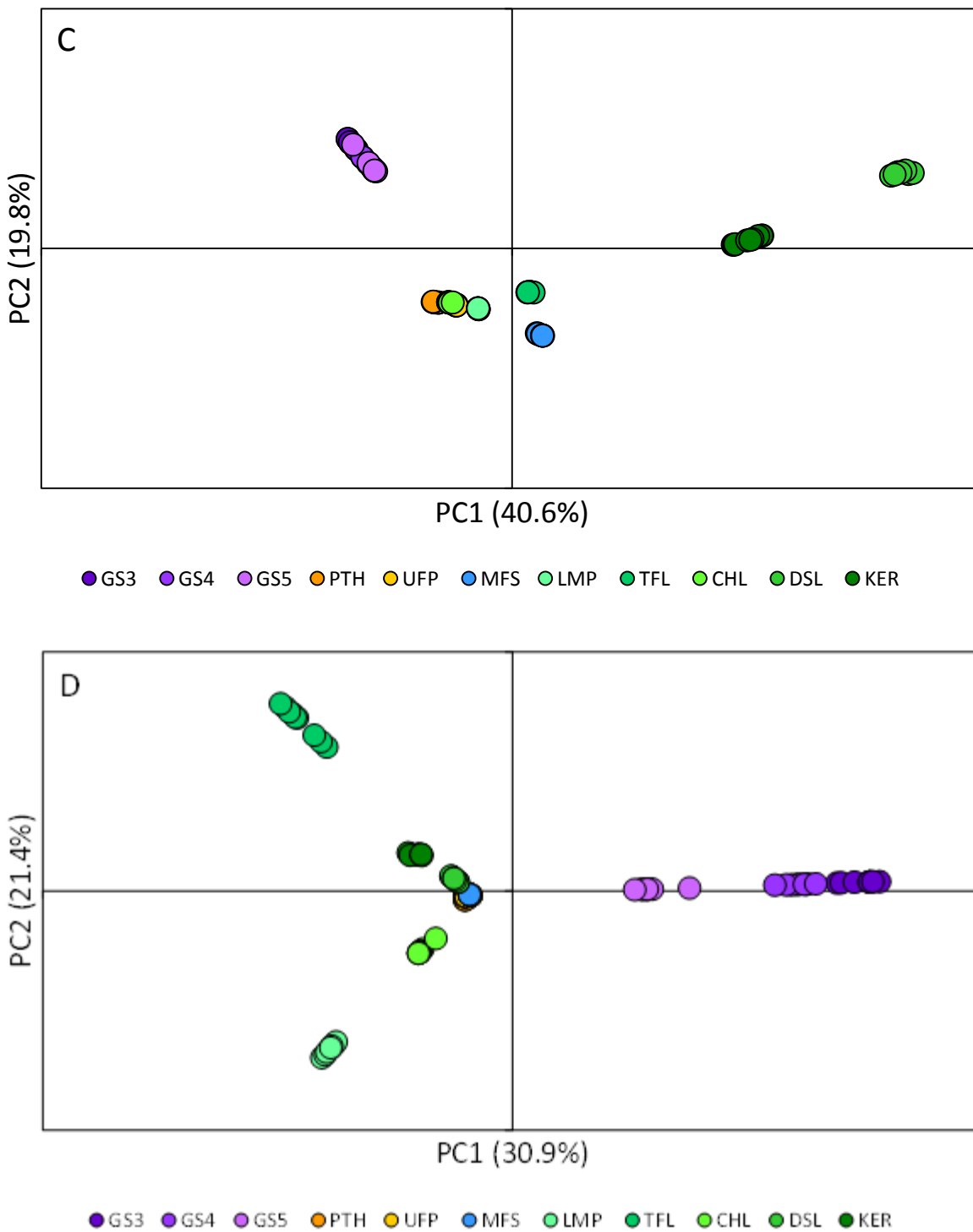


**Figure 8 contd.** Scores plots for ignitable liquid reference standards (A) no normalization, (B) constant sum normalization, (C) constant maximum normalization, and (D) constant vector length normalization Abbreviations for each standard are defined in Table 1.

**Table 7.** Relative standard deviation of scores on the first principal component (PC1) for non-normalized and normalized ignitable liquid reference standards.

Reference standard	Relative standard deviation on PC1			
	Non-normalized	Constant sum	Constant maximum	Constant vector length
GS3	5.0	0.8	2.4	4.2
GS4	6.2	1.3	3.4	4.4
GS5	13.9	1.5	5.0	11.3
PTH	26.7	1.1	3.1	1.8
UFP	2.9	2.5	0.3	6.6
MFS	1.9	2.2	7.9	0.5
LMP	1.2	0.9	0.8	2.5
TFL	6.8	61.8	11.3	7.7
CHL	6.1	1.8	2.2	6.1
DSL	7.3	1.9	2.0	5.0
KER	8.6	53.8	5.0	5.5

Abbreviations for each reference standard are listed in Table 1.

**Table 8.** Relative standard deviation of scores on the second principal component (PC2) for non-normalized and normalized ignitable liquid reference standards.

Reference standard	Relative standard deviation on PC2			
	Non-normalized	Constant sum	Constant maximum	Constant vector length
GS3	7.7	2.0	4.4	5.0
GS4	11.8	2.9	6.6	6.7
GS5	115.9	3.0	10.2	27.2
PTH	8.8	4.7	0.7	9.7
UFP	7.5	3.4	0.7	9.6
MFS	3.2	0.2	1.1	1.6
LMP	1.4	0.4	0.6	3.2
TFL	62.8	1.4	0.3	9.2
CHL	9.6	6.2	0.4	8.0
DSL	13.2	1.4	1.9	20.0
KER	16.1	1.5	45.9	1.9

Abbreviations for each reference standard are listed in Table 1.

Normalization improves association of replicates compared to the non-normalized data, as indicated by the generally lower relative standard deviations in the normalized data. However, due to the chemical diversity of the reference standards in this data set, no single normalization procedure is optimal for all standards; rather, the optimal procedure depends on the chemical complexity of the standard. Constant maximum normalization favors standards that are relatively simple, with no areas of unresolved compounds (*e.g.*, paint thinner and upholstery & fabric protector). In contrast, constant sum normalization favors more complex standards that contain unresolved compounds (*e.g.*, diesel and kerosene). When compared to these two normalization procedures, the constant vector length normalization procedure offers no additional advantages.

The effect of normalization on subsequent data analysis is apparent in the PCA scores plots shown in Figure 8. There is clear improvement in the association of replicates of each standard after normalization; however, the positioning of the reference standards on the scores plots varies according to the normalization procedure. In constant sum normalization, the upholstery protector is distinguished from the other reference standards on PC1 (Figure 8B). This is a relatively simple standard with few compounds but following this normalization, the abundance of each of these compounds is substantially increased such that they dominate the data set. As a result, the compounds are weighted heavily in the loadings plot for the first principal component, meaning that they are the most influential in the positioning of the standards in the scores plot (Figure 9A).

In contrast, with constant maximum normalization, the diesel and kerosene reference standards are distinguished from the other standards. Diesel and kerosene are the most complex standards in the data set and both contain substantial areas of unresolved compounds. Following constant maximum normalization, the lower abundance normal alkanes in these liquids become more dominant and, as the later-eluting alkanes are only present in diesel and kerosene, it is these alkanes that dominate the data set, as indicated in the PC1 loadings plot (Figure 9B).

Following constant vector length normalization, there is distinction of the gasoline standards, as well as two of the petroleum distillate standards (torch fuel and lamp oil) on PC1. The corresponding loadings plot (Fig 9C) is dominated by compounds from gasoline, torch fuel, and lamp oil. As a result, there is little distinction of the remaining standards that includes isoparaffinic and naphthenic paraffinic standards, as well as petroleum distillates, which form a group positioned close to zero on both PC1 and PC2.

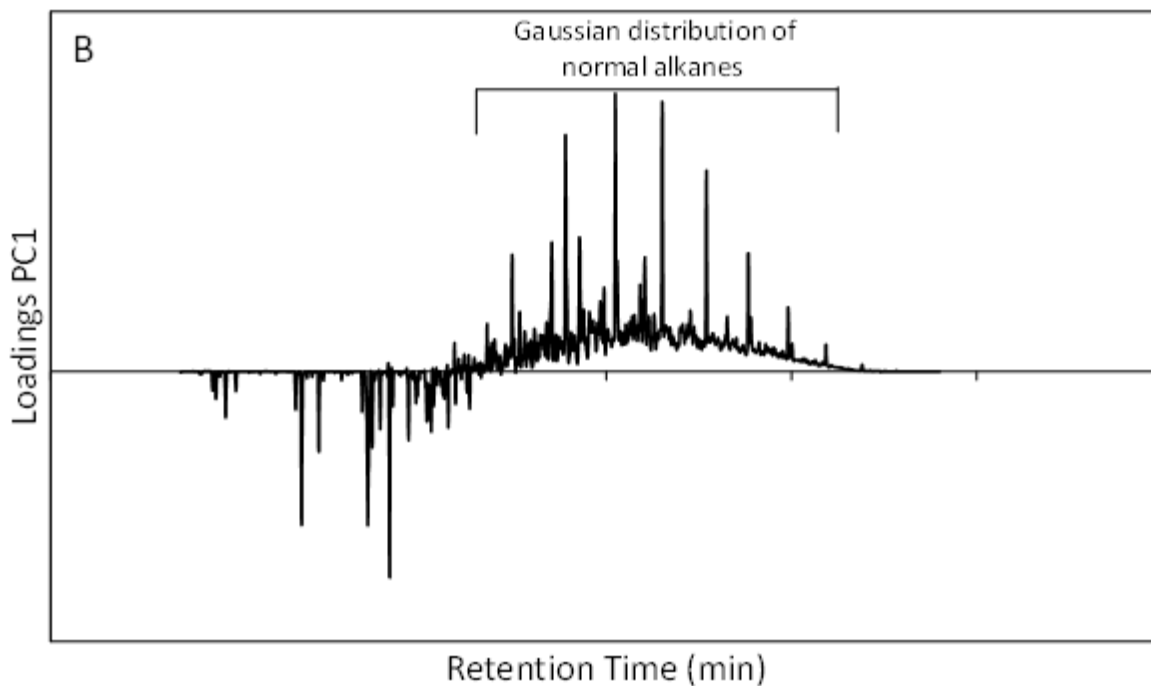
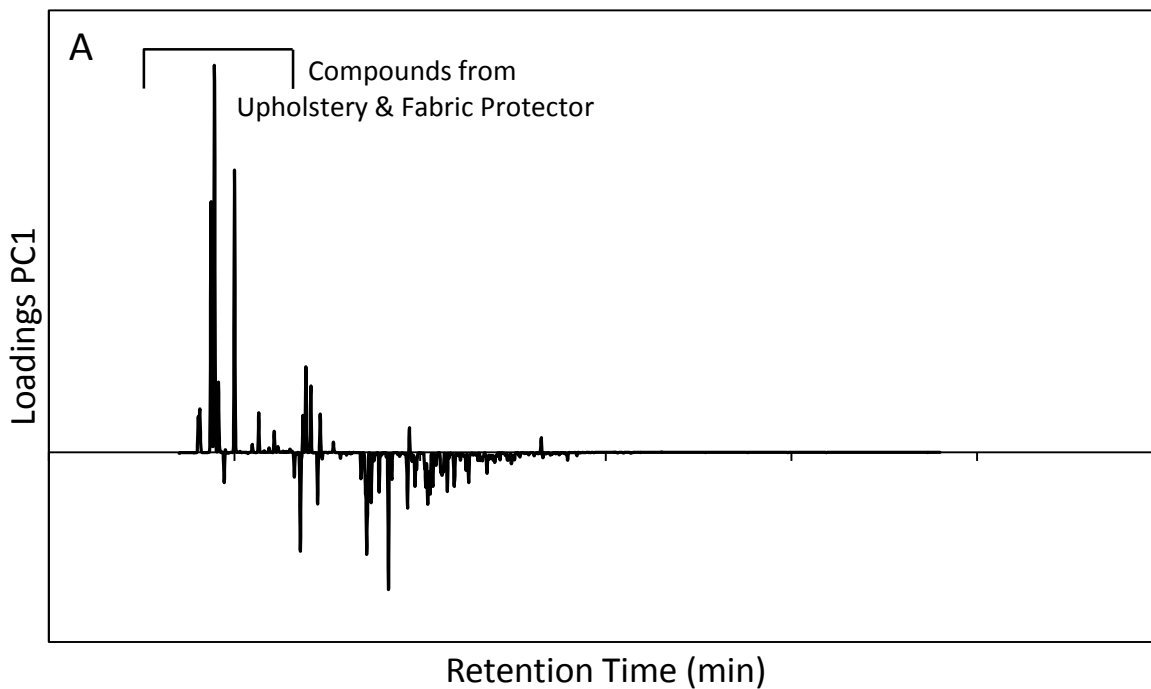


**Figure 9.** Loadings plot of PC1 after (A) constant sum normalization, (B) constant maximum normalization, and (C) constant vector length normalization.

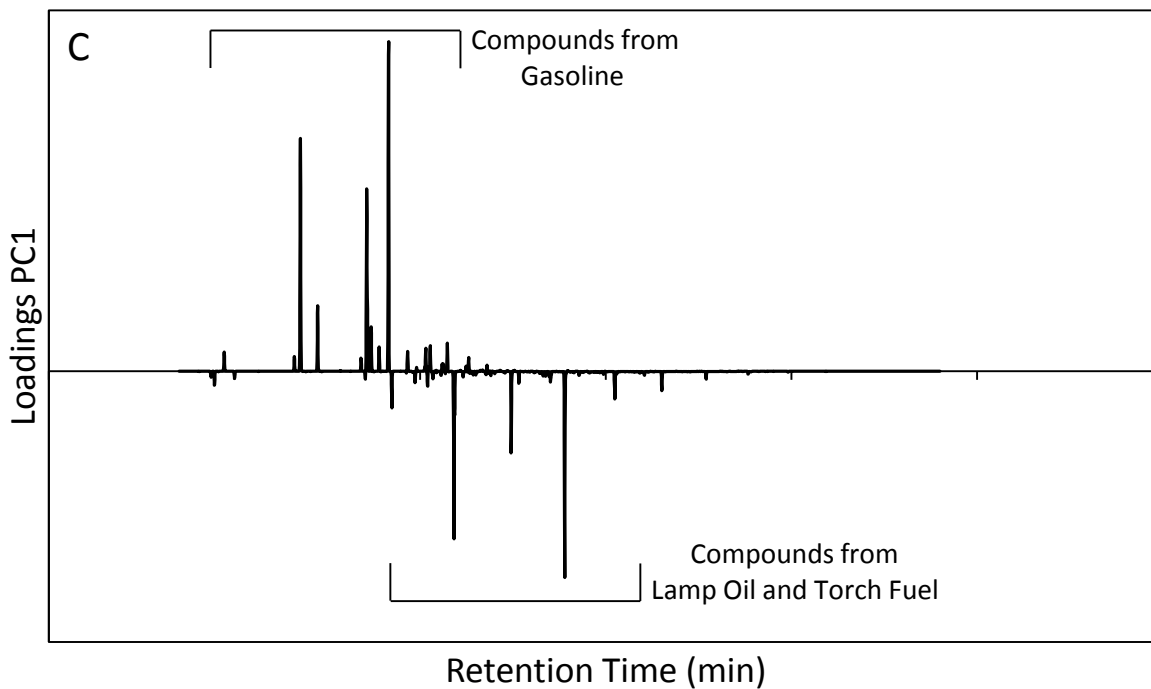


**Figure 9 contd.** Loadings plot of PC1 after (A) constant sum normalization, (B) constant maximum normalization, and (C) constant vector length normalization.

While these results indicate the need for normalization, the actual procedure selected will vary depending on the chemical nature of the data set. The effects of normalization can be evaluated using the procedures demonstrated here (*i.e.*, visual assessment of chromatograms, PCA scores plots, and relative standard deviation of scores for sets of replicates on each PC). In constant sum normalization, an assumption is made that a given volume of sample has the same instrument response, irrespective of the sample identity. However, this means that for samples containing relatively few compounds, constant sum normalization will substantially increase the abundance and hence, the contribution, of these compounds. Constant maximum normalization can also skew the relative abundance of compounds that otherwise would be a factor in distinguishing the samples. As indicated above, the diverse nature of this data set does not lend itself to a single normalization procedure; however, constant sum normalization yielded improvements in the relative standard deviation of scores for sets of replicates for the majority of the reference standards and hence, was selected for subsequent investigation.

The constant sum normalized data set was scaled, using both autoscaling and Pareto scaling. The scaled data sets were then subjected to PCA and the resulting scores plots were assessed (Figure 10 and Table 9) in a similar manner as described above.

Similar to normalization, no single scaling procedure is optimal for all standards. In fact, while Pareto scaling improves the close positioning of replicates on both PCs compared to autoscaling, the improvement is not as great as that observed for the non-scaled data. For these data, scaling is not necessary as the abundance of each chromatogram is similar in magnitude. In cases where the data set contains samples collected using different techniques such that the instrument responses are on different scales, then scaling will become more important. Hence, for this diverse and complex data set, scaling does not offer further advantages. As a result, all subsequent data analysis procedures were conducted using constant sum normalized, non-scaled data.

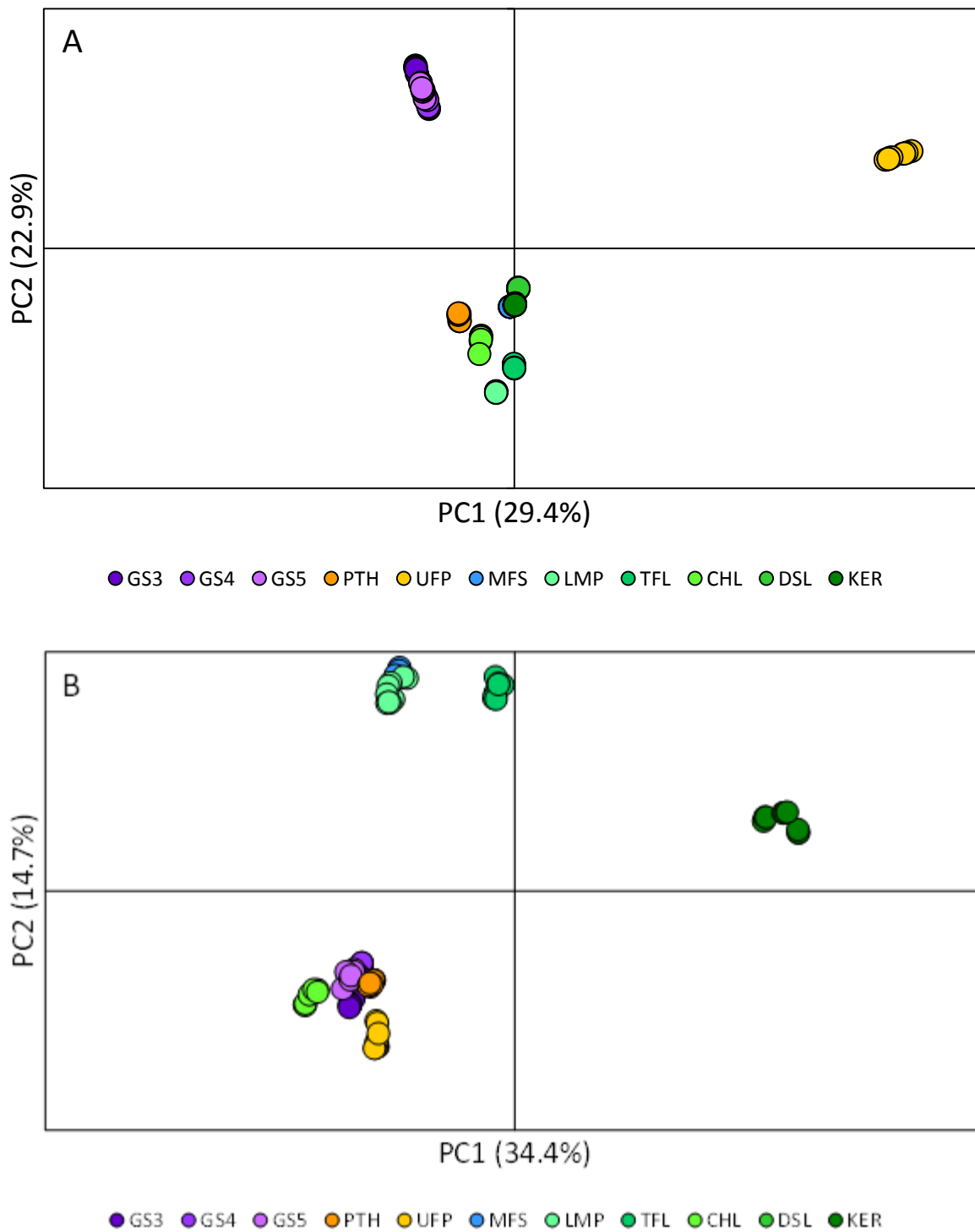


**Figure 10.** Scores plots for data set of reference standards after constant sum normalization and (A) no scaling, (B) autoscaling, (C) Pareto scaling. Abbreviations for each standard are defined in Table 1.

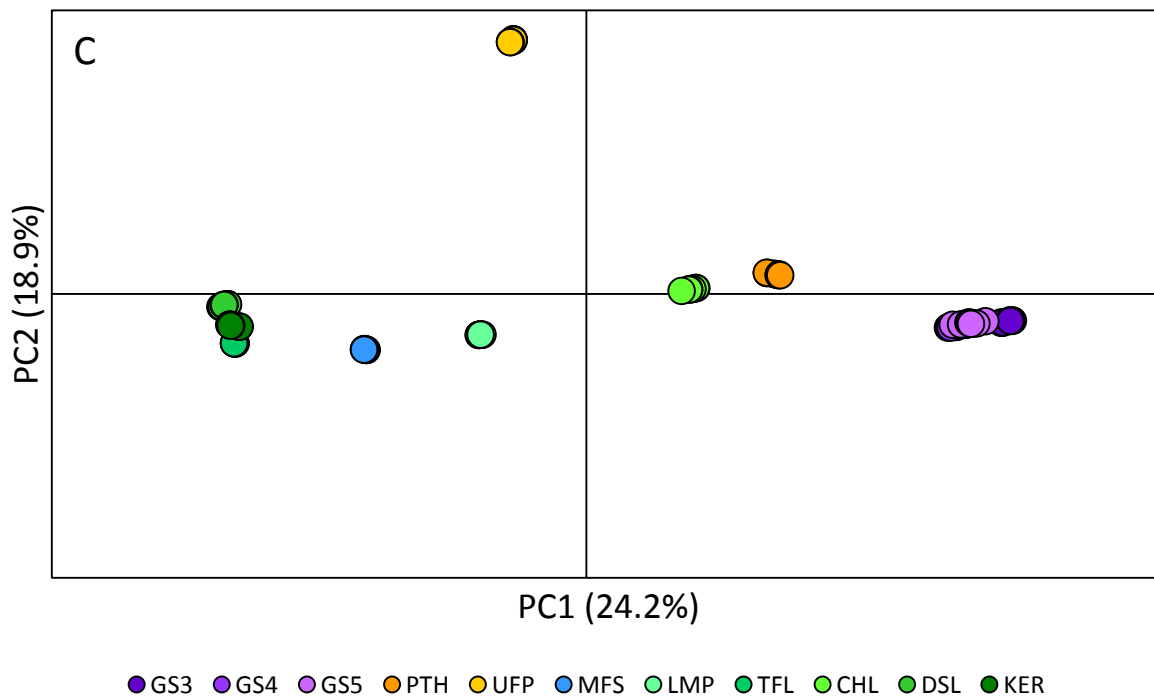


**Figure 10 contd.** Scores plots for data set of reference standards after constant sum normalization and (A) no scaling, (B) autoscaling, (C) Pareto scaling. Abbreviations for each standard are defined in Table 1.

**Table 9.** Relative standard deviation of scores on the first two principal components (PC1 and PC2) for constant sum normalized non-scaled and scaled ignitable liquid reference standards.

Reference standard	Relative standard deviation on PC1			Relative standard deviation on PC2		
	Non-scaled	Autoscaled	Pareto scaled	Non-scaled	Autoscaled	Pareto scaled
GS3	0.8	1.2	1.1	2.0	3.6	3.5
GS4	1.3	1.0	1.9	2.9	7.4	3.8
GS5	1.5	2.4	2.5	3.0	7.0	3.9
PTH	1.1	1.5	2.9	4.7	2.7	5.0
UFP	2.5	0.9	2.2	3.4	7.2	0.5
MFS	2.2	1.8	0.5	0.2	2.1	0.5
LMP	0.9	6.0	1.1	0.4	5.4	0.3
TFL	61.8	15.4	0.2	1.4	3.9	0.3
CHL	1.8	2.5	4.4	6.2	6.3	19.2
DSL	1.9	12.1	0.8	1.4	14.1	9.9
KER	53.8	5.4	1.3	1.5	12.3	2.8

Abbreviations for each reference standard are listed in Table 1.

#### 4.1.3 Pearson Product-Moment Correlation Coefficients

PPMC coefficients were firstly calculated for pairwise comparisons of TICs of the reference standards (Table 10). Mean PPMC coefficients indicate strong correlation for replicates of each reference standard, with  $r \geq 0.97$ . Theoretically, coefficients for replicates should equal 1.0; however, in this study, the calculated coefficients take into account extraction and instrument replicates. The strong correlation among replicates indicates acceptable precision in both the extraction and analysis procedures.

Within the gasoline class, there is strong correlation among the reference standards, as expected due to the high similarity in chemical composition. There is no correlation between the two isoparaffinic reference standards ( $r = -0.017$ ). Liquids in this class contain branched alkanes; however, the paint thinner and upholstery & fabric protector included here contain branched alkanes with different carbon number ranges. For the petroleum distillate class, there is moderate correlation between torch fuel and kerosene ( $r = 0.539$ ) and between diesel and kerosene ( $r = 0.726$ ), which is primarily due to an overlap in the range of normal alkanes present. There is weak to no correlation for all other comparisons (*i.e.*, between reference standards from different classes), as expected due to the differences in chemical composition.

PPMC coefficients were also calculated among replicates of both the 50% evaporated standards and the 90% evaporated standards (Tables 11 and 12). Strong correlation is observed for all comparisons, again indicating the acceptable precision in the extraction and analysis procedures. The evaporated standards were also compared to the unevaporated standards and the calculated PPMC coefficients are summarized in Tables 13 and 14.

**Table 10.** Mean PPMC coefficient  $\pm$  standard deviation for pairwise comparisons of reference standards within and between ASTM classes.

Class	Mean PPMC coefficient $\pm$ standard deviation										
	Gasoline			Isoparaffinic		NapPar	Petroleum Distillate				
Reference standard	GS3	GS4	GS5	PTH	UFP	MFS	LMP	TFL	CHL	DSL	KER
<b>GS3</b>	0.998 $\pm$ 0.002										
<b>GS4</b>	0.938 $\pm$ 0.020	0.996 $\pm$ 0.004									
<b>GS5</b>	0.944 $\pm$ 0.013	0.957 $\pm$ 0.010	0.993 $\pm$ 0.006								
<b>PTH</b>	0.098 $\pm$ 0.010	0.015 $\pm$ 0.013	0.119 $\pm$ 0.013	0.984 $\pm$ 0.016							
<b>UFP</b>	-0.016 $\pm$ 0.002	-0.002 $\pm$ 0.002	-0.016 $\pm$ 0.002	-0.017 $\pm$ 0.001	0.991 $\pm$ 0.008						
<b>MFS</b>	0.014 $\pm$ 0.004	0.061 $\pm$ 0.007	0.044 $\pm$ 0.009	0.068 $\pm$ 0.005	-0.041 $\pm$ 0.001	0.999 $\pm$ 0.001					
<b>LMP</b>	0.017 $\pm$ 0.003	0.039 $\pm$ 0.005	0.039 $\pm$ 0.005	0.083 $\pm$ 0.005	-0.020 $\pm$ 0.001	0.337 $\pm$ 0.003	0.999 $\pm$ 0.001				
<b>TFL</b>	-0.019 $\pm$ 0.001	-0.008 $\pm$ 0.002	-0.007 $\pm$ 0.003	-0.014 $\pm$ 0.000	-0.021 $\pm$ 0.001	0.343 $\pm$ 0.006	0.251 $\pm$ 0.004	0.997 $\pm$ 0.003			
<b>CHL</b>	0.091 $\pm$ 0.005	0.113 $\pm$ 0.003	0.120 $\pm$ 0.006	0.158 $\pm$ 0.009	-0.018 $\pm$ 0.001	0.078 $\pm$ 0.003	0.312 $\pm$ 0.053	0.025 $\pm$ 0.005	0.969 $\pm$ 0.057		
<b>DSL</b>	-0.093 $\pm$ 0.002	-0.091 $\pm$ 0.003	-0.086 $\pm$ 0.003	-0.076 $\pm$ 0.002	-0.074 $\pm$ 0.001	0.024 $\pm$ 0.014	-0.017 $\pm$ 0.004	0.265 $\pm$ 0.016	-0.081 $\pm$ 0.004	0.996 $\pm$ 0.004	
<b>KER</b>	-0.028 $\pm$ 0.004	-0.008 $\pm$ 0.007	-0.004 $\pm$ 0.008	-0.027 $\pm$ 0.003	-0.052 $\pm$ 0.001	0.283 $\pm$ 0.016	0.189 $\pm$ 0.018	0.539 $\pm$ 0.023	-0.032 $\pm$ 0.016	0.726 $\pm$ 0.034	0.995 $\pm$ 0.004

Abbreviations for each reference standard are listed in Table 1.

NapPar indicates naphthenic paraffinic.

For comparisons of the same reference standard, mean PPMC coefficient calculated based on 36 pairwise comparisons.

For comparisons of different reference standards, mean PPMC coefficient calculated based on 81 pairwise comparisons.

Light grey shading indicates mean PPMC coefficients for extraction replicates of the same reference standard.

Dark grey shading indicates mean PPMC coefficients for reference standards in the same ASTM class.

**Table 11.** Mean PPMC coefficient  $\pm$  standard deviation for pairwise comparisons of replicates of 50% evaporated standards.

<b>Reference standard</b>	<b>Mean PPMC coefficient <math>\pm</math> standard deviation</b>
50GS3	0.995 $\pm$ 0.005
50GS4	0.993 $\pm$ 0.006
50GS5	0.989 $\pm$ 0.009
50PTH	0.991 $\pm$ 0.009
50UFP	0.987 $\pm$ 0.014
50MFS	0.999 $\pm$ 0.001
50LMP	0.998 $\pm$ 0.001
50TFL	0.996 $\pm$ 0.003
50CHL	0.995 $\pm$ 0.003
50DSL	0.981 $\pm$ 0.018
50KER	0.992 $\pm$ 0.008

Abbreviations for each reference standard are listed in Table 1.

Mean PPMC coefficient calculated based on 36 replicates of each standard.

**Table 12.** Mean PPMC coefficient  $\pm$  standard deviation for pairwise comparisons of replicates of 90% evaporated standards.

<b>Reference standard</b>	<b>Mean PPMC coefficient <math>\pm</math> standard deviation</b>
90GS3	0.997 $\pm$ 0.002
90GS4	0.983 $\pm$ 0.027
90GS5	0.998 $\pm$ 0.001
90PTH	0.970 $\pm$ 0.026
90UFP	0.996 $\pm$ 0.002
90CHL	0.987 $\pm$ 0.014
90DSL	0.993 $\pm$ 0.006
90KER	0.993 $\pm$ 0.006

Abbreviations for each reference standard are listed in Table 1.

Mean PPMC coefficient calculated based on 36 replicates of each standard.

**Table 13.** Mean PPMC coefficient  $\pm$  standard deviation for pairwise comparisons of 50% evaporated standards to the unevaporated standards.

Class	Mean PPMC coefficient $\pm$ standard deviation										
	Gasoline			Isoparaffinic		NapPar <sup>a</sup>	Petroleum Distillate				
Reference standard	GS3	GS4	GS5	PTH	UFP	MFS	LMP	TFL	CHL	DSL	KER
<b>50GS3</b>	<b>0.963</b> $\pm$ <b>0.010</b>	<b>0.983</b> $\pm$ <b>0.013</b>	<b>0.939</b> $\pm$ <b>0.013</b>	0.123 $\pm$ 0.011	-0.021 $\pm$ 0.001	0.041 $\pm$ 0.005	0.033 $\pm$ 0.003	-0.012 $\pm$ 0.001	0.111 $\pm$ 0.004	-0.095 $\pm$ 0.003	-0.018 $\pm$ 0.006
<b>50GS4</b>	<b>0.802</b> $\pm$ <b>0.032</b>	<b>0.948</b> $\pm$ <b>0.020</b>	<b>0.880</b> $\pm$ <b>0.023</b>	0.179 $\pm$ 0.013	-0.027 $\pm$ 0.001	0.117 $\pm$ 0.011	0.067 $\pm$ 0.004	0.008 $\pm$ 0.004	0.123 $\pm$ 0.004	-0.083 $\pm$ 0.006	0.020 $\pm$ 0.010
<b>50GS5</b>	<b>0.821</b> $\pm$ <b>0.036</b>	<b>0.953</b> $\pm$ <b>0.021</b>	<b>0.915</b> $\pm$ <b>0.025</b>	0.151 $\pm$ 0.014	-0.025 $\pm$ 0.001	0.100 $\pm$ 0.010	0.069 $\pm$ 0.006	0.011 $\pm$ 0.004	0.141 $\pm$ 0.003	-0.075 $\pm$ 0.005	0.026 $\pm$ 0.010
<b>50PTH</b>	0.080 $\pm$ 0.007	0.128 $\pm$ 0.009	0.098 $\pm$ 0.009	<b>0.951</b> $\pm$ <b>0.018</b>	-0.017 $\pm$ 0.000	0.091 $\pm$ 0.003	0.120 $\pm$ 0.004	-0.007 $\pm$ 0.001	0.130 $\pm$ 0.006	-0.073 $\pm$ 0.002	-0.016 $\pm$ 0.004
<b>50UFP</b>	-0.017 $\pm$ 0.002	-0.022 $\pm$ 0.002	-0.018 $\pm$ 0.002	-0.019 $\pm$ 0.001	<b>0.962</b> $\pm$ <b>0.028</b>	-0.045 $\pm$ 0.002	-0.022 $\pm$ 0.000	-0.023 $\pm$ 0.001	-0.020 $\pm$ 0.001	-0.082 $\pm$ 0.002	-0.057 $\pm$ 0.002
<b>50MFS</b>	-0.017 $\pm$ 0.002	0.010 $\pm$ 0.005	0.003 $\pm$ 0.006	-0.019 $\pm$ 0.001	-0.029 $\pm$ 0.003	<b>0.928</b> $\pm$ <b>0.005</b>	0.204 $\pm$ 0.004	0.372 $\pm$ 0.004	0.006 $\pm$ 0.002	0.087 $\pm$ 0.013	0.312 $\pm$ 0.014
<b>50LMP</b>	0.007 $\pm$ 0.002	0.028 $\pm$ 0.004	0.029 $\pm$ 0.005	0.050 $\pm$ 0.003	-0.021 $\pm$ 0.001	0.382 $\pm$ 0.004	<b>0.976</b> $\pm$ <b>0.002</b>	0.316 $\pm$ 0.004	0.271 $\pm$ 0.048	0.018 $\pm$ 0.005	0.238 $\pm$ 0.018
<b>50TFL</b>	-0.022 $\pm$ 0.001	-0.017 $\pm$ 0.001	-0.014 $\pm$ 0.002	-0.024 $\pm$ 0.001	-0.019 $\pm$ 0.001	0.242 $\pm$ 0.008	0.109 $\pm$ 0.002	<b>0.930</b> $\pm$ <b>0.015</b>	-0.005 $\pm$ 0.002	0.318 $\pm$ 0.018	0.606 $\pm$ 0.020
<b>50CHL</b>	0.058 $\pm$ 0.006	0.077 $\pm$ 0.007	0.084 $\pm$ 0.008	0.118 $\pm$ 0.010	-0.017 $\pm$ 0.001	0.124 $\pm$ 0.004	0.313 $\pm$ 0.015	0.048 $\pm$ 0.004	<b>0.902</b> $\pm$ <b>0.052</b>	-0.058 $\pm$ 0.005	0.068 $\pm$ 0.016
<b>50DSL</b>	-0.085 $\pm$ 0.003	-0.097 $\pm$ 0.003	-0.091 $\pm$ 0.003	-0.066 $\pm$ 0.002	-0.053 $\pm$ 0.002	-0.161 $\pm$ 0.009	-0.066 $\pm$ 0.001	0.011 $\pm$ 0.033	-0.078 $\pm$ 0.003	0.779 $\pm$ 0.026	0.348 $\pm$ 0.067
<b>50KER</b>	-0.073 $\pm$ 0.001	-0.077 $\pm$ 0.002	-0.072 $\pm$ 0.002	-0.060 $\pm$ 0.002	-0.049 $\pm$ 0.001	0.016 $\pm$ 0.027	-0.018 $\pm$ 0.013	0.401 $\pm$ 0.043	-0.062 $\pm$ 0.004	0.831 $\pm$ 0.021	<b>0.831</b> $\pm$ <b>0.041</b>

Abbreviations for each reference standard are listed in Table 1.

NapPar indicates naphthenic paraffinic.

Mean PPMC coefficient calculated based on 81 pairwise comparisons.

**Table 14.** Mean PPMC coefficient  $\pm$  standard deviation for pairwise comparisons of 90% evaporated standards to the unevaporated standards.

Class	Mean PPMC coefficient $\pm$ standard deviation										
	Gasoline			Isoparaffinic		NapPar <sup>a</sup>	Petroleum Distillate				
Reference standard	GS3	GS4	GS5	PTH	UFP	MFS	LMP	TFL	CHL	DSL	KER
<b>90GS3</b>	0.588 $\pm$ 0.027	0.777 $\pm$ 0.030	0.682 $\pm$ 0.033	0.167 $\pm$ 0.011	-0.032 $\pm$ 0.001	0.219 $\pm$ 0.011	0.109 $\pm$ 0.002	0.053 $\pm$ 0.006	0.116 $\pm$ 0.005	-0.053 $\pm$ 0.008	0.088 $\pm$ 0.012
<b>90GS4</b>	0.227 $\pm$ 0.016	0.357 $\pm$ 0.025	0.301 $\pm$ 0.026	0.074 $\pm$ 0.006	-0.036 $\pm$ 0.002	0.357 $\pm$ 0.008	0.097 $\pm$ 0.005	0.144 $\pm$ 0.008	0.020 $\pm$ 0.003	0.064 $\pm$ 0.015	0.245 $\pm$ 0.014
<b>90GS5</b>	0.219 $\pm$ 0.016	0.338 $\pm$ 0.024	0.300 $\pm$ 0.027	0.063 $\pm$ 0.005	-0.035 $\pm$ 0.001	0.362 $\pm$ 0.004	0.102 $\pm$ 0.004	0.168 $\pm$ 0.006	0.035 $\pm$ 0.004	0.084 $\pm$ 0.013	0.289 $\pm$ 0.012
<b>90PTH</b>	0.062 $\pm$ 0.009	0.113 $\pm$ 0.014	0.080 $\pm$ 0.012	0.734 $\pm$ 0.047	-0.019 $\pm$ 0.003	0.152 $\pm$ 0.028	0.180 $\pm$ 0.032	0.016 $\pm$ 0.009	0.120 $\pm$ 0.015	-0.062 $\pm$ 0.007	0.018 $\pm$ 0.009
<b>90UFP</b>	-0.022 $\pm$ 0.001	-0.021 $\pm$ 0.001	-0.022 $\pm$ 0.000	-0.020 $\pm$ 0.001	0.453 $\pm$ 0.036	-0.044 $\pm$ 0.001	-0.024 $\pm$ 0.000	-0.025 $\pm$ 0.001	-0.004 $\pm$ 0.001	-0.089 $\pm$ 0.001	-0.061 $\pm$ 0.001
<b>90CHL</b>	0.017 $\pm$ 0.003	0.034 $\pm$ 0.003	0.039 $\pm$ 0.006	0.039 $\pm$ 0.003	-0.016 $\pm$ 0.000	0.199 $\pm$ 0.003	0.278 $\pm$ 0.023	0.079 $\pm$ 0.006	0.542 $\pm$ 0.051	-0.019 $\pm$ 0.005	0.123 $\pm$ 0.020
<b>90DSL</b>	-0.051 $\pm$ 0.003	-0.059 $\pm$ 0.004	-0.055 $\pm$ 0.004	-0.040 $\pm$ 0.002	-0.031 $\pm$ 0.002	-0.109 $\pm$ 0.005	-0.029 $\pm$ 0.003	-0.055 $\pm$ 0.003	-0.047 $\pm$ 0.003	0.367 $\pm$ 0.042	-0.045 $\pm$ 0.013
<b>90KER</b>	-0.062 $\pm$ 0.001	-0.071 $\pm$ 0.001	-0.066 $\pm$ 0.001	-0.047 $\pm$ 0.001	-0.039 $\pm$ 0.001	-0.118 $\pm$ 0.003	-0.049 $\pm$ 0.001	-0.025 $\pm$ 0.005	-0.056 $\pm$ 0.002	0.724 $\pm$ 0.007	0.400 $\pm$ 0.035

Abbreviations for each reference standard are listed in Table 1.

NapPar indicates naphthenic paraffinic.

Mean PPMC coefficient calculated based on 81 pairwise comparisons.

In Tables 13 and 14, strong correlations are highlighted in bold. The 50% evaporated standards are strongly correlated to the corresponding unevaporated standard and only weakly correlated (at most) to all other standards. There are some exceptions to this generalization. Firstly, each 50% evaporated gasoline standard is also strongly correlated to the other two unevaporated gasoline standards. This is expected due to the highly similar chemical composition among the three gasoline standards. Secondly, the 50% evaporated diesel standard is only moderately correlated to the unevaporated diesel reference standard. This lower than expected correlation is primarily due to the loss of the early eluting aromatic compounds as a result of evaporation. However, when the standard deviation is also taken into account, the 50% evaporated diesel standards are strongly correlated to the unevaporated standard. And thirdly, the 50% evaporated kerosene standard is moderately correlated to the unevaporated diesel reference standard. These two liquids have a similar distribution of normal alkanes and, even with evaporation, sufficient overlap remains to indicate a moderate correlation between these two liquids.

The 90% evaporated standards are generally only moderately to weakly correlated to the corresponding unevaporated standard, primarily due to the substantial difference in chemical composition at this advanced stage of evaporation. Chromatograms of the paint thinner standards are shown in Figure 11 as an example. In the unevaporated standard (Figure 11A), C<sub>7</sub>- and C<sub>8</sub>-branched alkanes are present, eluting between 8.5 and 9.4 minutes; however, at the 90% evaporation level, these compounds are no longer present (Figure 11B). As correlation coefficients are calculated on a point-by-point basis, the presence of compounds in one chromatogram but not the other, as is the case here, lowers the coefficient.

Finally, the utility of PPMC coefficients to indicate correlation between fire debris samples and the corresponding reference standards was investigated using Set 1 of the simulated fire debris samples. This set consisted of eight ignitable liquids spiked onto a carpet and carpet padding substrate, then burned. Coefficients were calculated for pairwise comparisons of each fire debris sample to the unevaporated, 50% evaporated, and 90% evaporated standards (Table 15).

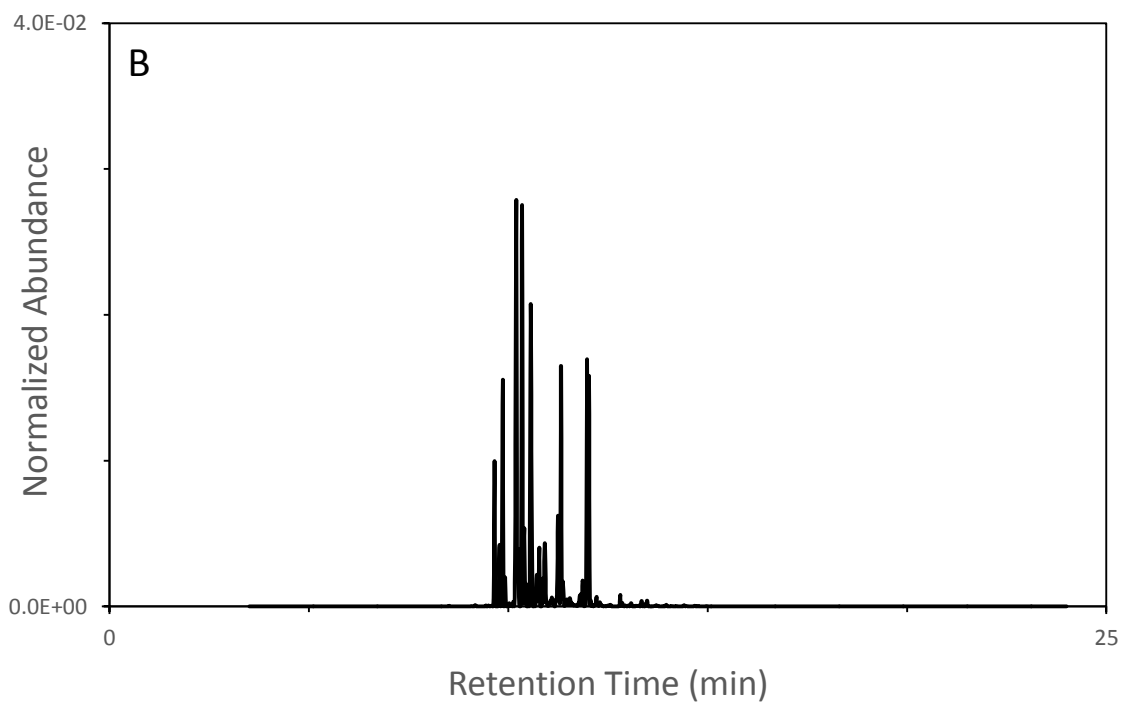
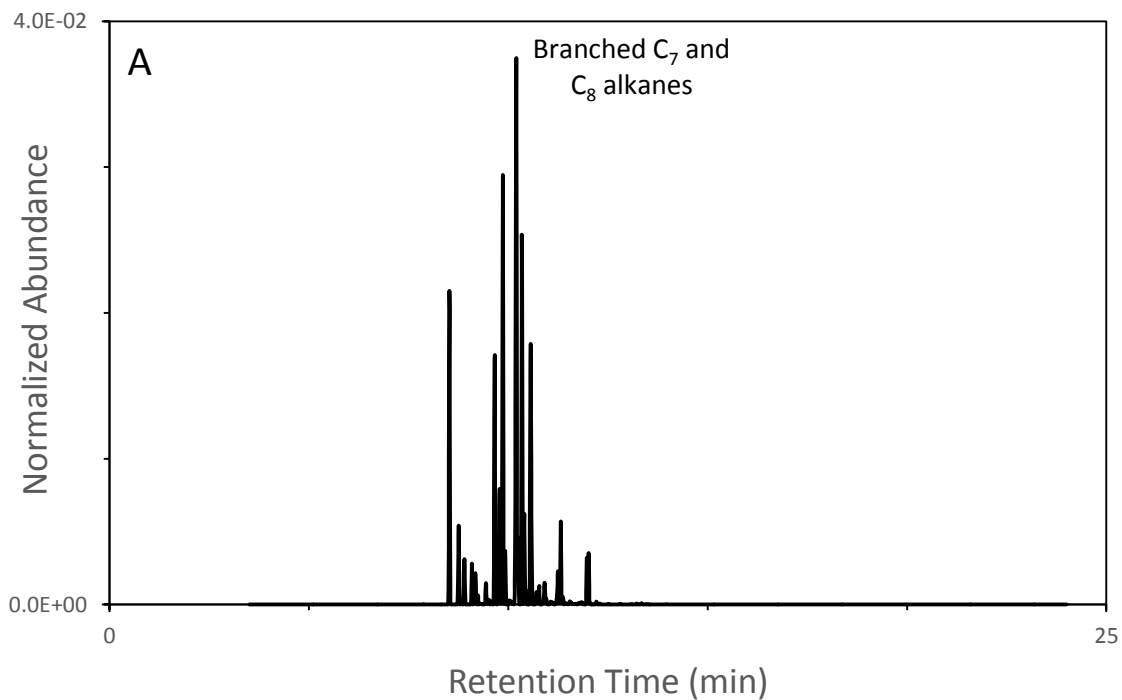


**Figure 11.** Representative chromatograms of paint thinner reference standard (A) unevaporated and (B) evaporated 90% by volume.

**Table 15.** Mean PPMC coefficient  $\pm$  standard deviation for pairwise comparisons of simulated fire debris (carpet and carpet padding substrate) to corresponding reference standard.

Reference standard	Mean PPMC coefficient for comparison of standards and simulated fire debris on carpet and carpet padding (CPT) substrate							
	PTH CPT	UFP CPT	MFS CPT	LMP CPT	TFL CPT	CHL CPT	DSL CPT	KER CPT
GS3	0.060 $\pm$ 0.013	-0.008 $\pm$ 0.002	0.015 $\pm$ 0.005	0.022 $\pm$ 0.010	-0.003 $\pm$ 0.002	0.062 $\pm$ 0.021	0.030 $\pm$ 0.005	0.063 $\pm$ 0.008
50GS3	0.073 $\pm$ 0.016	-0.015 $\pm$ 0.002	0.030 $\pm$ 0.005	0.032 $\pm$ 0.011	0.006 $\pm$ 0.002	0.076 $\pm$ 0.023	0.037 $\pm$ 0.006	0.072 $\pm$ 0.009
90GS3	0.093 $\pm$ 0.015	-0.029 $\pm$ 0.002	0.136 $\pm$ 0.018	0.077 $\pm$ 0.009	0.094 $\pm$ 0.007	0.081 $\pm$ 0.013	0.085 $\pm$ 0.015	0.151 $\pm$ 0.014
GS4	0.085 $\pm$ 0.020	-0.016 $\pm$ 0.002	0.041 $\pm$ 0.007	0.033 $\pm$ 0.011	0.008 $\pm$ 0.003	0.078 $\pm$ 0.022	0.045 $\pm$ 0.007	0.083 $\pm$ 0.009
50GS4	0.101 $\pm$ 0.021	-0.022 $\pm$ 0.002	0.075 $\pm$ 0.011	0.050 $\pm$ 0.012	0.031 $\pm$ 0.004	0.087 $\pm$ 0.020	0.061 $\pm$ 0.010	0.108 $\pm$ 0.012
90GS4	0.035 $\pm$ 0.005	-0.029 $\pm$ 0.005	0.232 $\pm$ 0.029	0.059 $\pm$ 0.012	0.190 $\pm$ 0.007	0.028 $\pm$ 0.009	0.142 $\pm$ 0.024	0.217 $\pm$ 0.015
GS5	0.072 $\pm$ 0.016	-0.009 $\pm$ 0.003	0.035 $\pm$ 0.007	0.041 $\pm$ 0.008	0.017 $\pm$ 0.005	0.085 $\pm$ 0.025	0.047 $\pm$ 0.008	0.093 $\pm$ 0.011
50GS5	0.087 $\pm$ 0.019	-0.020 $\pm$ 0.001	0.068 $\pm$ 0.010	0.062 $\pm$ 0.009	0.043 $\pm$ 0.006	0.098 $\pm$ 0.024	0.060 $\pm$ 0.010	0.114 $\pm$ 0.013
90GS5	0.035 $\pm$ 0.004	-0.019 $\pm$ 0.002	0.248 $\pm$ 0.030	0.080 $\pm$ 0.017	0.244 $\pm$ 0.006	0.040 $\pm$ 0.008	0.161 $\pm$ 0.026	0.254 $\pm$ 0.018
PTH	<b>0.597 <math>\pm</math> 0.184</b>	-0.015 $\pm$ 0.001	0.012 $\pm$ 0.005	0.035 $\pm$ 0.007	-0.007 $\pm$ 0.001	0.108 $\pm$ 0.028	0.018 $\pm$ 0.005	0.034 $\pm$ 0.005
50PTH	<b>0.596 <math>\pm</math> 0.170</b>	-0.016 $\pm$ 0.001	0.024 $\pm$ 0.006	0.058 $\pm$ 0.010	0.004 $\pm$ 0.002	0.101 $\pm$ 0.018	0.021 $\pm$ 0.005	0.044 $\pm$ 0.005
90PTH	<b>0.513 <math>\pm</math> 0.125</b>	-0.020 $\pm$ 0.002	0.072 $\pm$ 0.019	0.101 $\pm$ 0.028	0.036 $\pm$ 0.013	0.091 $\pm$ 0.015	0.034 $\pm$ 0.011	0.076 $\pm$ 0.015
UFP	-0.021 $\pm$ 0.001	<b>0.735 <math>\pm</math> 0.046</b>	-0.034 $\pm$ 0.001	-0.022 $\pm$ 0.001	-0.028 $\pm$ 0.001	-0.023 $\pm$ 0.001	-0.031 $\pm$ 0.002	-0.035 $\pm$ 0.001
50UFP	-0.023 $\pm$ 0.001	<b>0.773 <math>\pm</math> 0.041</b>	-0.037 $\pm$ 0.002	-0.024 $\pm$ 0.001	-0.030 $\pm$ 0.001	-0.025 $\pm$ 0.001	-0.033 $\pm$ 0.003	-0.037 $\pm$ 0.001
90UFP	-0.002 $\pm$ 0.001	<b>0.388 <math>\pm</math> 0.032</b>	-0.034 $\pm$ 0.002	-0.024 $\pm$ 0.002	-0.030 $\pm$ 0.001	-0.017 $\pm$ 0.002	-0.031 $\pm$ 0.002	-0.036 $\pm$ 0.001
MFS	0.032 $\pm$ 0.002	-0.038 $\pm$ 0.003	<b>0.514 <math>\pm</math> 0.049</b>	0.195 $\pm$ 0.045	0.355 $\pm$ 0.008	0.092 $\pm$ 0.005	0.179 $\pm$ 0.032	0.281 $\pm$ 0.019
50MFS	-0.022 $\pm$ 0.005	-0.037 $\pm$ 0.001	<b>0.441 <math>\pm</math> 0.043</b>	0.110 $\pm$ 0.033	0.341 $\pm$ 0.007	0.018 $\pm$ 0.010	0.160 $\pm$ 0.028	0.244 $\pm$ 0.016
LMP	0.047 $\pm$ 0.003	-0.014 $\pm$ 0.003	0.169 $\pm$ 0.019	<b>0.660 <math>\pm</math> 0.095</b>	0.304 $\pm$ 0.018	0.460 $\pm$ 0.023	0.115 $\pm$ 0.020	0.341 $\pm$ 0.029
50LMP	0.029 $\pm$ 0.004	-0.015 $\pm$ 0.003	0.192 $\pm$ 0.021	<b>0.637 <math>\pm</math> 0.096</b>	0.353 $\pm$ 0.017	0.424 $\pm$ 0.016	0.135 $\pm$ 0.023	0.365 $\pm$ 0.029
TFL	-0.020 $\pm$ 0.001	-0.028 $\pm$ 0.001	0.133 $\pm$ 0.016	0.137 $\pm$ 0.030	<b>0.536 <math>\pm</math> 0.024</b>	0.053 $\pm$ 0.006	0.198 $\pm$ 0.032	0.338 $\pm$ 0.023
50TFL	-0.028 $\pm$ 0.001	-0.028 $\pm$ 0.001	0.074 $\pm$ 0.012	0.053 $\pm$ 0.016	<b>0.578 <math>\pm</math> 0.028</b>	0.000 $\pm$ 0.005	0.191 $\pm$ 0.031	0.325 $\pm$ 0.022

<b>CHL</b>	0.117 ± 0.025	-0.014 ± 0.002	0.051 ± 0.009	0.335 ± 0.072	0.128 ± 0.017	<b>0.396 ±</b> <b>0.142</b>	0.042 ± 0.010	0.179 ± 0.031
<b>50CHL</b>	0.088 ± 0.018	-0.017 ± 0.001	0.084 ± 0.013	0.340 ± 0.065	0.185 ± 0.017	<b>0.334 ±</b> <b>0.102</b>	0.053 ± 0.011	0.203 ± 0.025
<b>90CHL</b>	0.029 ± 0.004	-0.018 ± 0.000	0.159 ± 0.023	0.159 ± 0.023	0.265 ± 0.028	<b>0.194 ±</b> <b>0.040</b>	0.077 ± 0.013	0.230 ± 0.029
<b>DSL</b>	-0.089 ± 0.003	-0.088 ± 0.003	-0.009 ± 0.015	-0.034 ± 0.013	0.181 ± 0.021	-0.077 ± 0.016	<b>0.094 ±</b> <b>0.028</b>	0.125 ± 0.017
<b>50DSL</b>	-0.080 ± 0.004	-0.073 ± 0.004	-0.122 ± 0.008	-0.079 ± 0.004	-0.071 ± 0.017	-0.092 ± 0.007	<b>-0.043 ±</b> <b>0.021</b>	-0.066 ± 0.019
<b>90DSL</b>	-0.049 ± 0.004	-0.044 ± 0.004	-0.081 ± 0.006	-0.081 ± 0.006	-0.070 ± 0.004	-0.059 ± 0.005	<b>-0.066 ±</b> <b>0.010</b>	-0.082 ± 0.006
<b>KER</b>	-0.035 ± 0.004	-0.053 ± 0.002	0.168 ± 0.026	0.155 ± 0.045	0.562 ± 0.033	0.062 ± 0.018	0.250 ± 0.043	<b>0.417 ±</b> <b>0.033</b>
<b>50KER</b>	-0.061 ± 0.004	-0.052 ± 0.002	-0.021 ± 0.016	-0.025 ± 0.012	0.228 ± 0.048	-0.051 ± 0.015	0.127 ± 0.033	<b>0.165 ±</b> <b>0.029</b>
<b>90KER</b>	-0.059 ± 0.002	-0.055 ± 0.001	-0.090 ± 0.004	-0.090 ± 0.004	-0.058 ± 0.005	-0.068 ± 0.004	-0.024 ± 0.014	<b>-0.042 ±</b> <b>0.007</b>

Abbreviations for each reference standard are listed in Table 1.

Mean PPMC coefficient calculated based on 81 pairwise comparisons.

In Table 15, mean PPMC coefficients representing correlation between the simulated fire debris samples and the corresponding reference standards are highlighted in bold. For each fire debris sample, the highest correlation is observed between the sample and corresponding standard although in most cases, only a weak to moderate correlation is observed. For the majority of the fire debris samples, the chromatograms contain some characteristic compounds from the ignitable liquid, along with additional compounds (styrene, trichloropropane, and biphenyl) from the carpet and carpet padding substrate. The presence of compounds from the liquids enables some degree of correlation with the appropriate standard. However, as PPMC coefficients are calculated on a point-by-point basis, the presence of the additional compounds from the substrate lowers the coefficient.

For the fire debris sample containing diesel, there is no correlation to any of the corresponding standards. Chromatograms of this particular sample show none of the characteristic diesel compounds, namely the Gaussian shaped distribution of normal alkanes (Figure 12) that would be expected. As a result, there is little to no correlation between this fire debris sample and the corresponding standards.

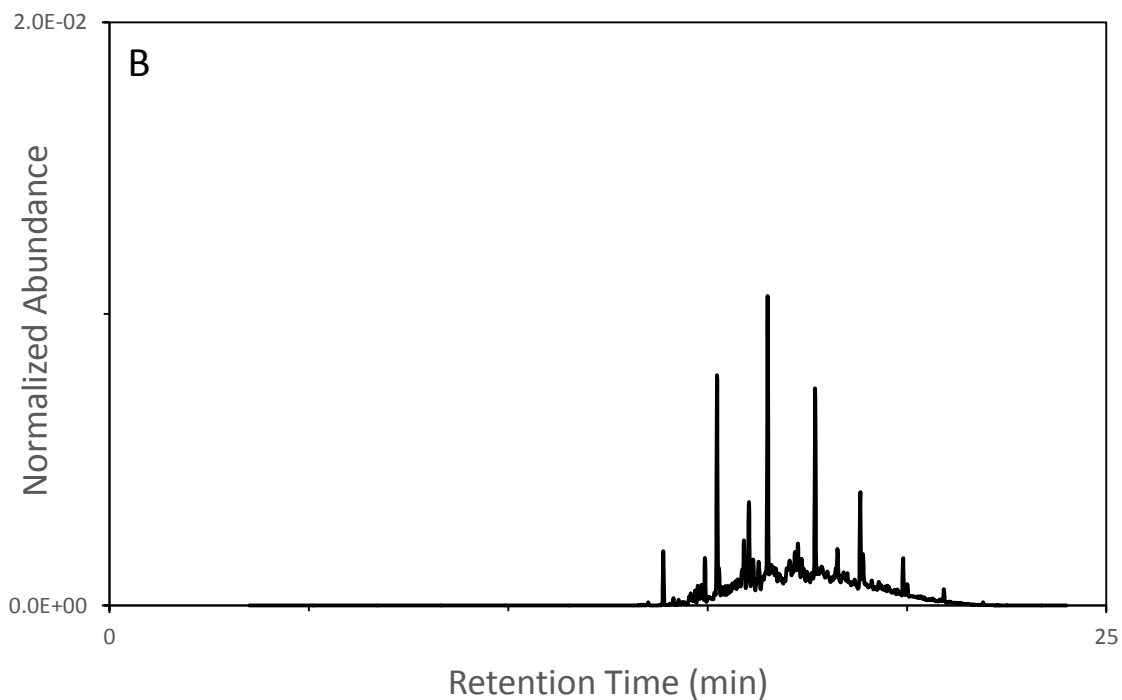
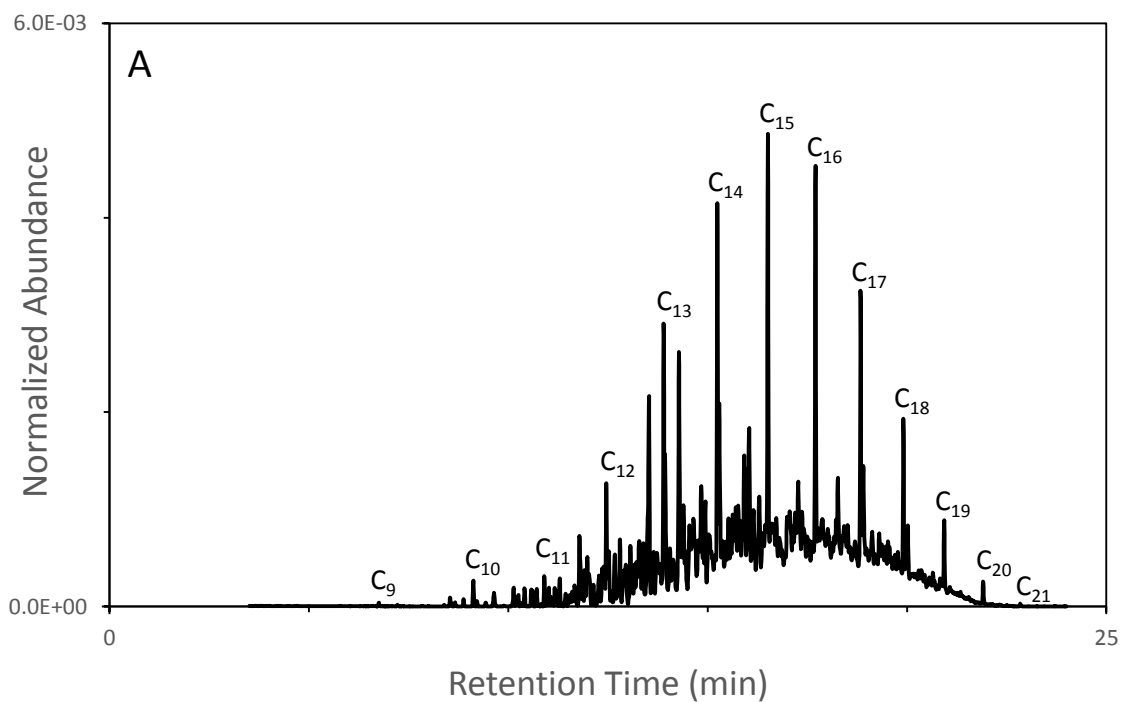


**Figure 12.** Representative chromatograms of diesel reference standard (A) unevaporated, (B) 50% evaporated, and (C) simulated fire debris containing diesel on a carpet and carpet padding substrate.

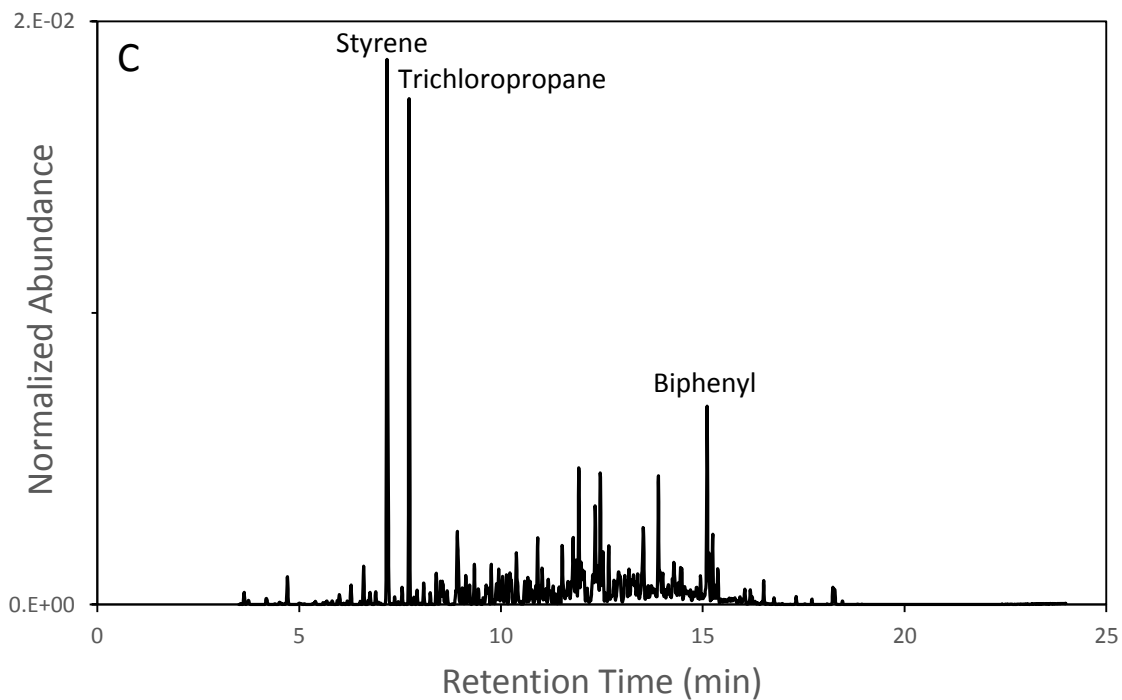


**Figure 12 contd.** Representative chromatograms of diesel reference standard (A) unevaporated, (B) 50% evaporated, and (C) simulated fire debris containing diesel on a carpet and carpet padding substrate.

Pearson product-moment correlation coefficients were also calculated for pairwise comparisons of the reference standards with simulated fire debris samples containing the oil-finished wood flooring substrate (Set 2, coefficients summarized in Table 16).

**Table 16.** Mean PPMC coefficient  $\pm$  standard deviation for pairwise comparisons of simulated fire debris (oil-finished wood flooring substrate) to corresponding reference standard.

Reference standard	Mean PPMC coefficient $\pm$ standard deviation for comparison of standards and simulated fire debris on oil-finished wood (OWD) substrate		
	PTH OWD	TFL OWD	DSL OWD
<b>GS3</b>	0.116 $\pm$ 0.013	0.058 $\pm$ 0.009	0.066 $\pm$ 0.013
<b>50GS3</b>	0.151 $\pm$ 0.012	0.081 $\pm$ 0.009	0.100 $\pm$ 0.015
<b>90GS3</b>	0.227 $\pm$ 0.004	0.137 $\pm$ 0.010	0.213 $\pm$ 0.007
<b>GS4</b>	0.170 $\pm$ 0.013	0.093 $\pm$ 0.009	0.118 $\pm$ 0.015
<b>50GS4</b>	0.211 $\pm$ 0.010	0.120 $\pm$ 0.006	0.164 $\pm$ 0.013
<b>90GS4</b>	0.103 $\pm$ 0.013	0.115 $\pm$ 0.030	0.199 $\pm$ 0.012
<b>GS5</b>	0.153 $\pm$ 0.016	0.082 $\pm$ 0.008	0.102 $\pm$ 0.017
<b>50GS5</b>	0.198 $\pm$ 0.012	0.113 $\pm$ 0.005	0.152 $\pm$ 0.016
<b>90GS5</b>	0.094 $\pm$ 0.011	0.111 $\pm$ 0.043	0.200 $\pm$ 0.012
<b>PTH</b>	0.332 $\pm$ 0.008	0.188 $\pm$ 0.020	0.253 $\pm$ 0.013
<b>50PTH</b>	0.348 $\pm$ 0.006	0.188 $\pm$ 0.016	0.263 $\pm$ 0.012
<b>90PTH</b>	0.333 $\pm$ 0.032	0.161 $\pm$ 0.019	0.252 $\pm$ 0.029
<b>UFP</b>	-0.035 $\pm$ 0.001	-0.032 $\pm$ 0.003	-0.050 $\pm$ 0.004
<b>50UFP</b>	-0.039 $\pm$ 0.001	-0.035 $\pm$ 0.004	-0.055 $\pm$ 0.004
<b>90UFP</b>	-0.022 $\pm$ 0.002	-0.023 $\pm$ 0.006	-0.043 $\pm$ 0.003
<b>MFS</b>	0.240 $\pm$ 0.025	0.276 $\pm$ 0.101	0.467 $\pm$ 0.020
<b>50MFS</b>	0.057 $\pm$ 0.018	0.179 $\pm$ 0.112	0.327 $\pm$ 0.023
<b>LMP</b>	0.609 $\pm$ 0.061	0.437 $\pm$ 0.105	0.584 $\pm$ 0.031
<b>50LMP</b>	0.559 $\pm$ 0.056	0.442 $\pm$ 0.125	0.592 $\pm$ 0.032
<b>TFL</b>	0.086 $\pm$ 0.014	0.445 $\pm$ 0.233	0.412 $\pm$ 0.027
<b>50TFL</b>	-0.012 $\pm$ 0.007	0.345 $\pm$ 0.215	0.300 $\pm$ 0.021
<b>CHL</b>	0.368 $\pm$ 0.053	0.216 $\pm$ 0.024	0.249 $\pm$ 0.037
<b>50CHL</b>	0.323 $\pm$ 0.036	0.196 $\pm$ 0.024	0.239 $\pm$ 0.021
<b>90CHL</b>	0.195 $\pm$ 0.029	0.128 $\pm$ 0.037	0.187 $\pm$ 0.010
<b>DSL</b>	-0.151 $\pm$ 0.007	0.015 $\pm$ 0.067	0.082 $\pm$ 0.036
<b>50DSL</b>	-0.148 $\pm$ 0.004	-0.098 $\pm$ 0.018	-0.061 $\pm$ 0.049
<b>90DSL</b>	-0.091 $\pm$ 0.005	-0.080 $\pm$ 0.010	-0.133 $\pm$ 0.013
<b>KER</b>	0.034 $\pm$ 0.018	0.231 $\pm$ 0.140	0.342 $\pm$ 0.026
<b>50KER</b>	-0.119 $\pm$ 0.006	0.088 $\pm$ 0.096	0.176 $\pm$ 0.041
<b>90KER</b>	-0.106 $\pm$ 0.002	-0.082 $\pm$ 0.004	-0.035 $\pm$ 0.034

Abbreviations for each reference standard are listed in Table 1.

Mean PPMC coefficient calculated based on 81 pairwise comparisons.

For fire debris samples containing paint thinner and diesel, the highest correlation is observed for pairwise comparison to the lamp oil reference standard, albeit only a moderate correlation in both cases. Debris samples containing paint thinner are only weakly correlated to the corresponding reference standard while there is no correlation between the diesel-containing debris samples and the appropriate reference standards. For the torch fuel-containing debris samples, weak correlation (0.445) is observed for comparison to the torch fuel reference standard, although a similar correlation (0.442) is also observed for the 50% evaporated lamp oil standard. Similarity of the debris samples to lamp oil is based on the substrate interference compounds from the oil-finished wood; that is, the range of normal alkanes from the substrate (C<sub>9</sub>-C<sub>12</sub>) is similar to that observed in the lamp oil standard. As a consequence, the presence of interference compounds from the debris results in apparent similarity of the fire debris samples to one particular reference standard.

These results indicate that PPMC coefficients are of limited utility in assessing similarity between reference standards and simulated fire debris samples as coefficients are calculated on a point-by-point basis. For the carpet and carpet padding substrate, interference compounds do not correspond to any compounds present in the liquids and hence, the presence of such compounds lowers the coefficient. For the oil-finished wood substrate, interference compounds correspond to those present in some of the reference standards and hence, their presence increases similarity to those standards. Additionally, and irrespective of substrate, the greater the extent of burning, fewer compounds characteristic of the liquid remain in the debris, further lowering the coefficient when compared to the reference standard.

#### 4.1.4 Principal Components Analysis

Principal components analysis was initially performed on the pretreated reference standards and the scores plot of PC1 and PC2 is shown in Figure 13.

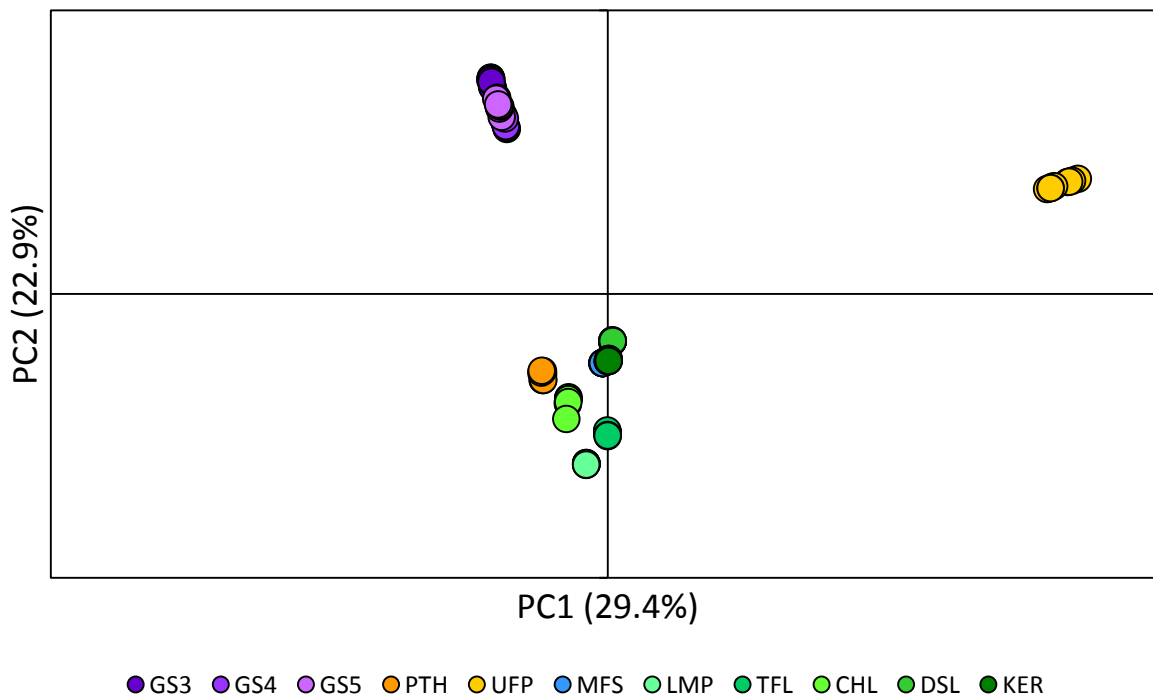


**Figure 13.** Scores plot of PC1 versus PC2 for ignitable liquid reference standards. Each reference standard was analyzed in replicate (n=9) and each standard is represented by a different color in the plot. Abbreviations for each standard are defined in Table 1.

The first two PCs account for 52% of the variance among the reference standards. Replicates of each standard are closely positioned in the scores plot and three groups of the standards are apparent. The first contains the three gasoline standards, the second contains the upholstery and fabric protector standard, and the third group contains the remaining standards. This positioning can be explained with reference to the loadings plots, which are shown in Figure 14 for the first two principal components.

The loadings plot for PC1 (Figure 14A) is dominated by the branched C<sub>5</sub>- and C<sub>7</sub>-alkanes that are present in the upholstery protector standard. This is an artifact of the normalization procedure, which results in a substantial increase in abundance of these compounds. These compounds are weighted positively in the loadings plot for both PC1 and PC2, which results in the positive positioning of this standard on these two PCs. The C<sub>3</sub>- and C<sub>4</sub>-alkylbenzenes that are present in gasoline are weighted negatively in the loadings plot for PC1 and positively in the loadings plot for PC2. As a result, the gasoline standards are positioned negatively on PC1 and positively on PC2 in the scores plot.

The remaining standards are positioned negatively on both PC1 and PC2 in the scores plot, albeit close to zero in both cases. The normal alkanes C<sub>11</sub>-C<sub>14</sub> are weighted negatively in the loadings for PC2 (Figure 14B). The petroleum distillate standards all contain these four normal alkanes, resulting in the negative positioning of these standards on PC2 in the scores plot. Paint thinner and marine fuel stabilizer are also positioned negatively on PC2 in the scores plot, which is due to some of the compounds present in these standards being weighted negatively on PC2 in the loadings plot.

For further discrimination of the reference standards, it is necessary to consider additional principal components, particularly as the first two account for only 52% of the variance in the data set. The third and fourth principal components account for an additional 30.3% of the variance, resulting in 82.6% of the total variance described by the first four PCs. The scores plot of PC3 versus PC4 is shown in Figure 15, with the loadings plots for each of these PCs shown in Figure 16.

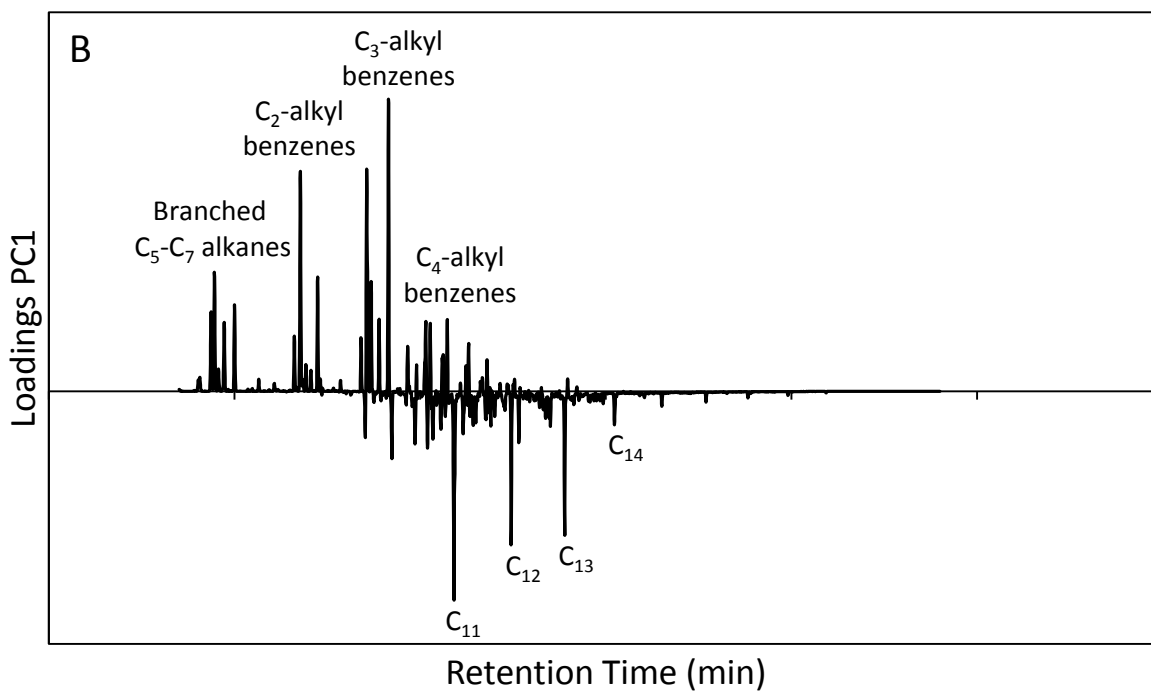
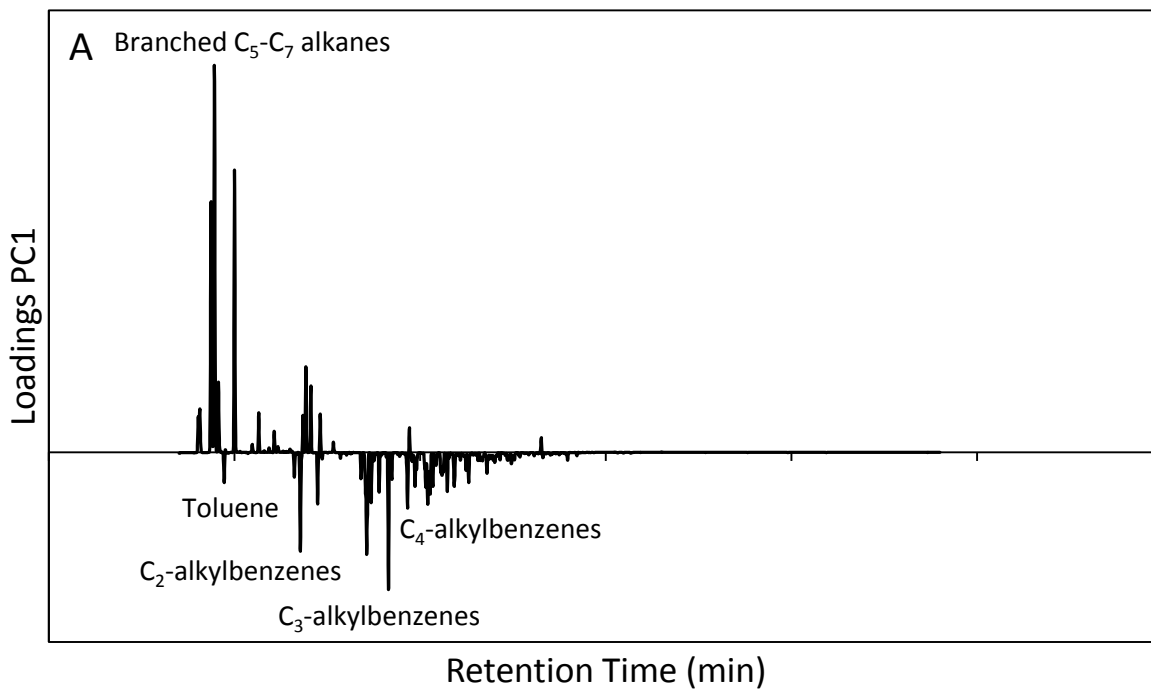


**Figure 14.** Loadings plot of (A) PC1 and (B) PC2 for ignitable liquid reference standards.

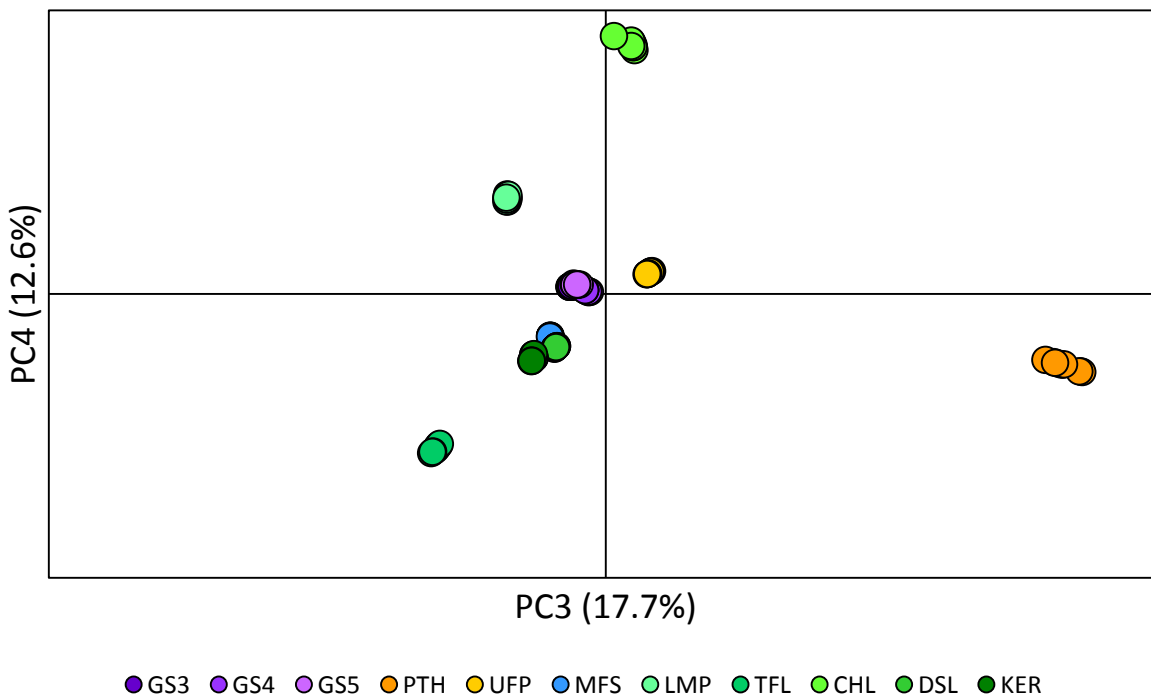


**Figure 15.** Scores plot of PC3 versus PC4 for ignitable liquid reference standards. Each reference standard was analyzed in replicate (n=9) and each standard is represented by a different color in the plot. Abbreviations for each standard are defined in Table 1.

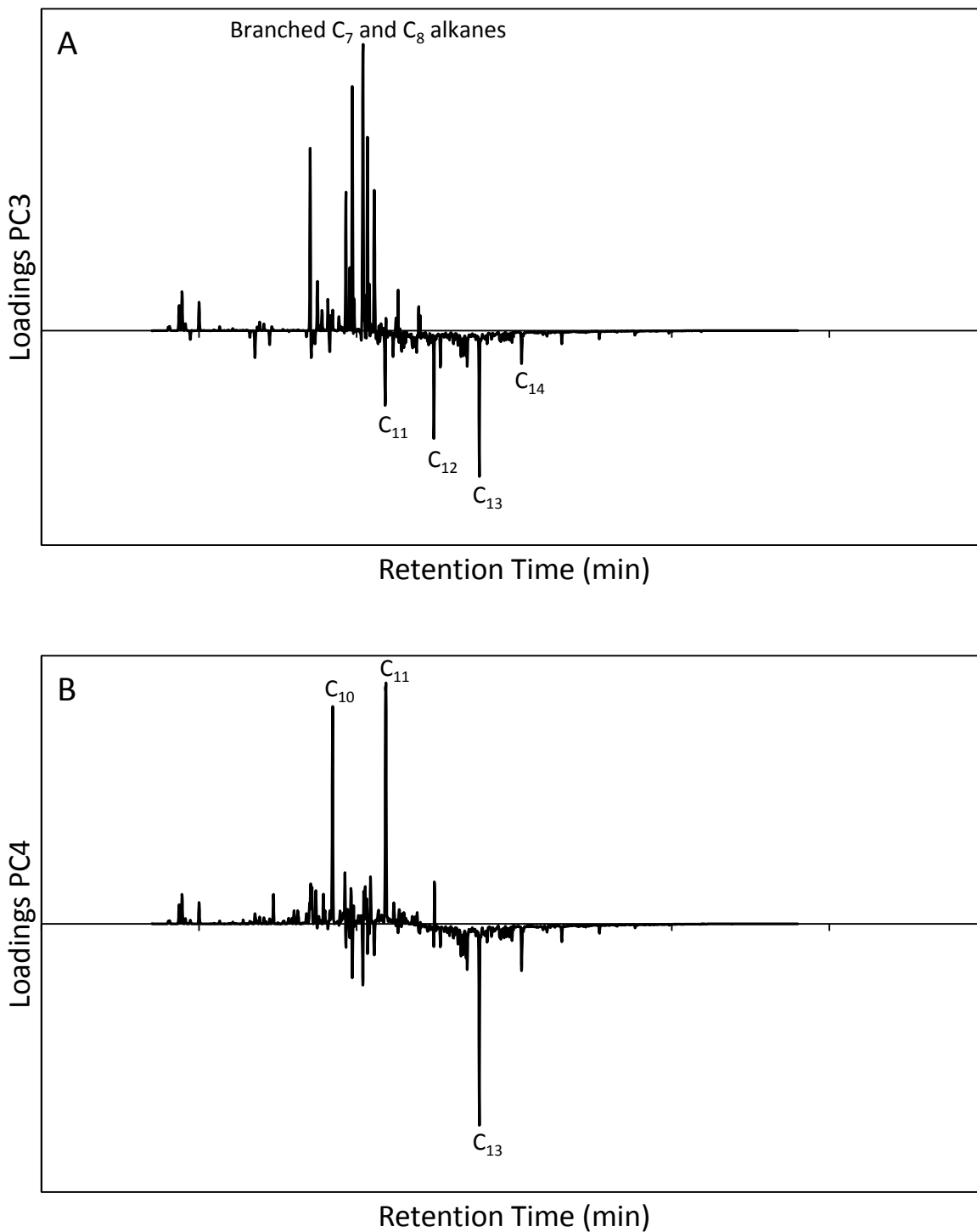


**Figure 16.** Loadings plot of (A) PC3 and (B) PC4 for ignitable liquid reference standards.

The loadings plot for PC3 (Figure 16A) is dominated by branched C<sub>7</sub>- and C<sub>8</sub>-alkanes, which are weighted positively, and C<sub>11</sub>-C<sub>14</sub> normal alkanes that are weighted negatively. The branched alkanes are the major compounds present in the paint thinner reference standard while the C<sub>11</sub>-C<sub>14</sub> normal alkanes are the major compounds in the torch fuel reference standard. As a result, the third principal component further distinguishes these two standards from the others, with paint thinner positioned positively, and torch fuel positioned negatively, on PC3 (Figure 15).

The loadings plot for PC4 (Figure 16B) is dominated by C<sub>10</sub> and C<sub>11</sub> normal alkanes, which are weighted positively, and C<sub>13</sub>, which is weighted negatively. While all three of these normal alkanes are present in the petroleum distillate standards, the C<sub>10</sub> and C<sub>11</sub> normal alkanes are the major compounds in charcoal lighter, resulting in the very positive positioning of this standard on PC4 and facilitating distinction of this standard from the other petroleum distillates. Similarly, C<sub>13</sub> is the dominant compound in torch fuel, resulting in the very negative positioning of this standard on PC4 and again, enabling distinction from the other petroleum distillate standards.

Therefore, the variance described by the first principal component distinguishes the upholstery protector reference standard from the remaining standards. The second principal component distinguishes gasoline, while the third distinguishes paint thinner and torch fuel, and the fourth further distinguishes the petroleum distillate reference standards. Hence, while the variance described by each PC progressively decreases, important information is still contained and PCA of a diverse data set should not be limited to consideration of only the first two principal components.

Principal components analysis was repeated, including the 50% and 90% evaporated reference standards in the data set to investigate association of these standards to the corresponding unevaporated standard. The resulting scores plot for the first two principal components is shown in Figure 17 and the corresponding loadings plots are shown in Figure 18.

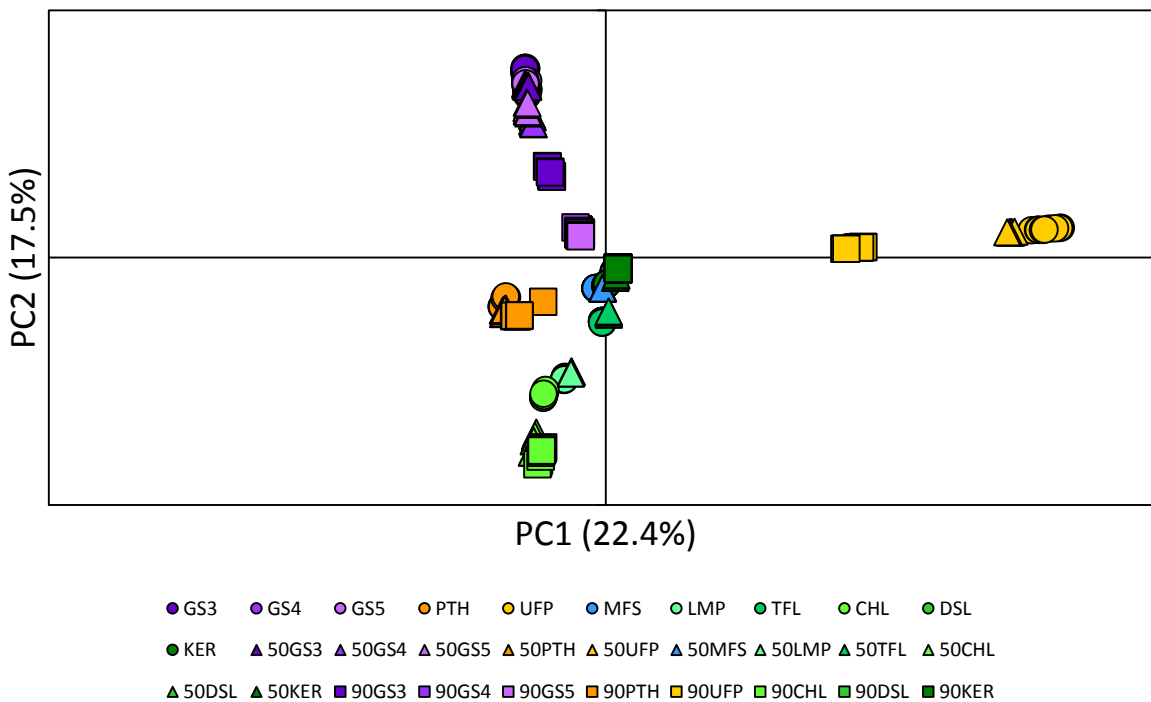


**Figure 17.** Scores plot of PC1 versus PC2 for unevaporated and evaporated ignitable liquid reference standards. Each reference standard was analyzed in replicate (n=9) and each standard is represented by a different color in the plot. Unevaporated standards are shown as circles, 50% evaporated as triangles, and 90% evaporated as squares. Abbreviations for each standard are defined in Table 1.

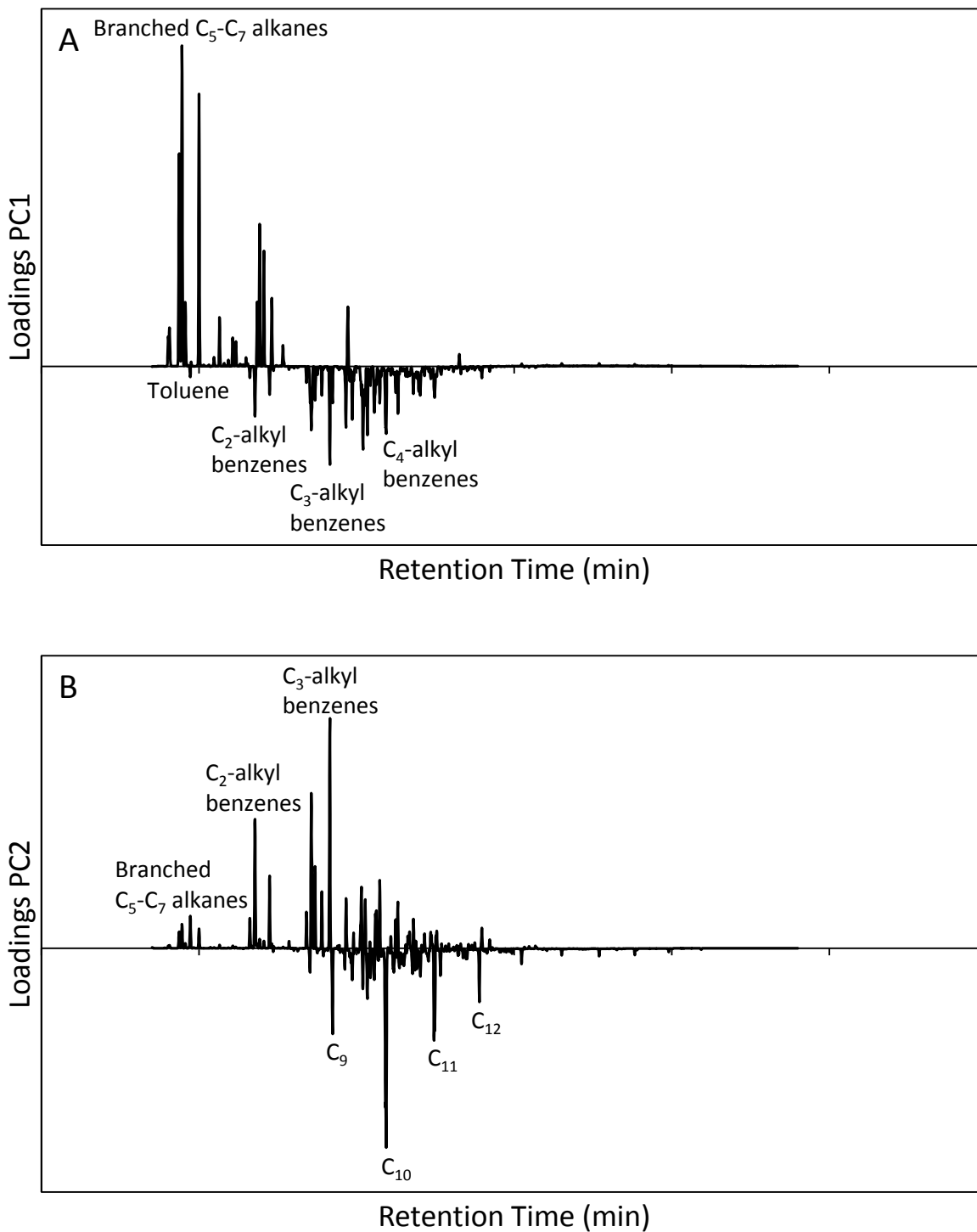


**Figure 18.** Loadings plot for (A) PC1 and (B) PC2 for unevaporated and evaporated ignitable liquid reference standards.

The general positioning of standards on the scores plot is similar to that observed previously for PCA of the unevaporated standards only (compare Figure 17 to Figure 13); that is, the first principal component distinguishes the upholstery protector standards from the others. It is important to note that in general, the evaporated standards are positioned closely to the unevaporated counterparts on PC1, while the second principal component distinguishes the standards based on evaporation level. However, some exceptions do exist, including the 90% evaporated upholstery protector standard and the 90% evaporated gasoline standards.

Replicates of the 90% evaporated upholstery protector standard are positioned less positively on PC1 than the corresponding 50% evaporated and unevaporated standards. The branched alkanes present in this liquid are weighted positively in the PC1 loadings plot (Figure 18A). However, due to their volatility, these compounds are no longer present in the 90% evaporated standard. As a result, there are fewer compounds with a positive weighting on PC1 and consequently, a less positive score on this PC for the 90% evaporated standard compared to the 50% evaporated and unevaporated standards.

Replicates of the 90% evaporated gasoline are positioned more negatively on PC2 than the 50% and unevaporated counterparts. Toluene and the C<sub>2</sub>-alkylbenzenes, which are the more volatile compounds present in gasoline, are weighted positively in the PC2 loadings plot (Figure 18B). As evaporation progresses, the abundance of these volatile compounds decreases (Figure 19) and at the 90% evaporation level, toluene and ethylbenzene (the first eluting C<sub>2</sub>-alkylbenzene) are no longer present, while the xylenes (the remaining C<sub>2</sub>-alkylbenzenes) are present at very low abundance. Hence, there are fewer compounds with a positive contribution, which results in a less positive score for the 90% evaporated standards on PC2.

The 90% evaporated Gasoline 3 standard is positioned more positively on PC2 than the 90% evaporated standards of Gasolines 4 and 5. This effect is due to the higher abundance of 1,2,4-trimethylbenzene in Gasoline 3 compared to the other two gasolines (Figure 20). This compound is weighted positively in the PC2 loadings plot and hence, the higher abundance in Gasoline 3 results in a more positive score on PC2 for this standard compared to the other two 90% evaporated gasoline standards.

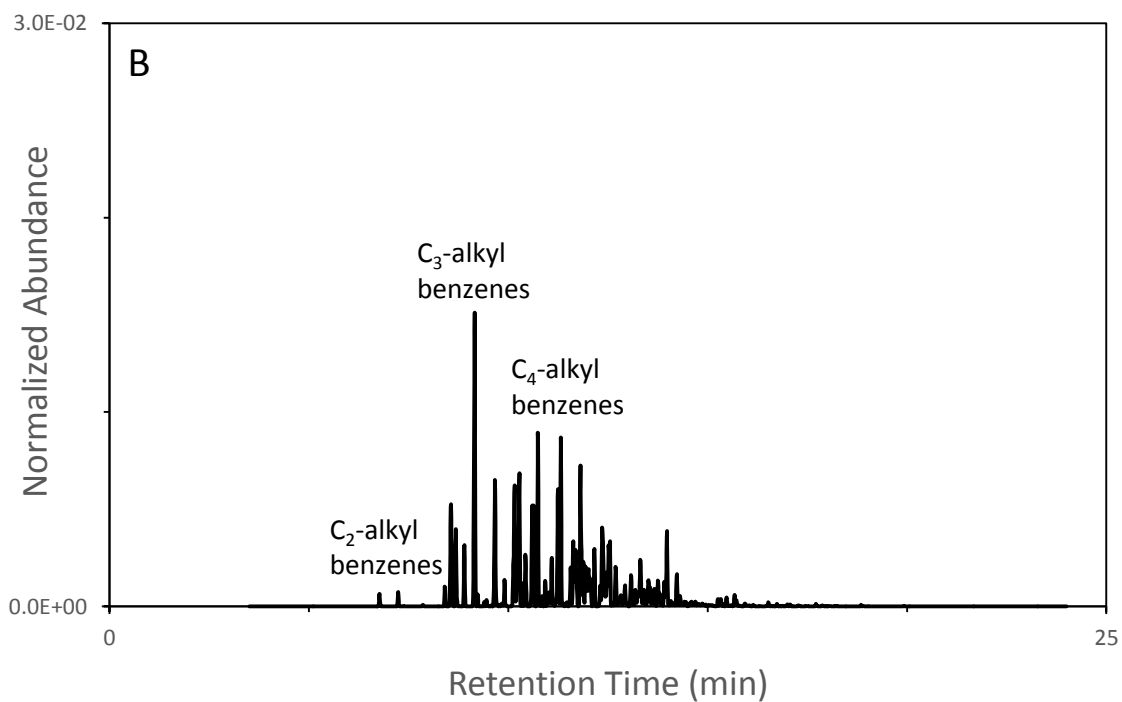
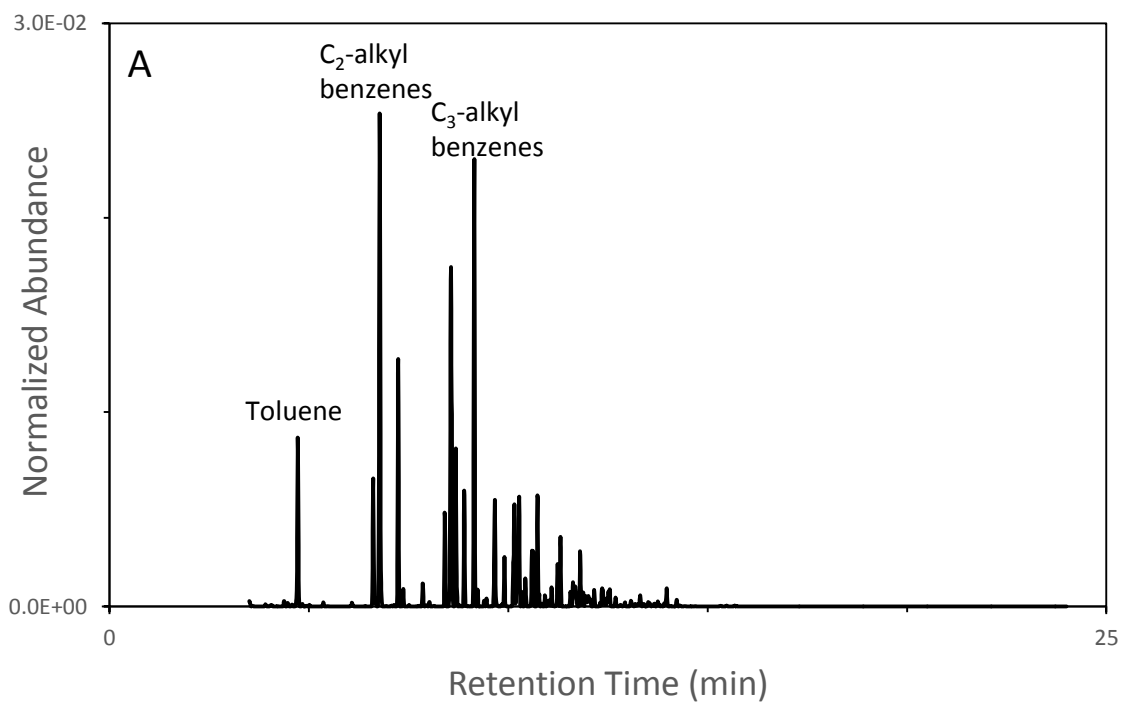


**Figure 19.** Representative chromatograms of Gasoline 3 reference standards (A) unevaporated and (B) 90% evaporated by volume.

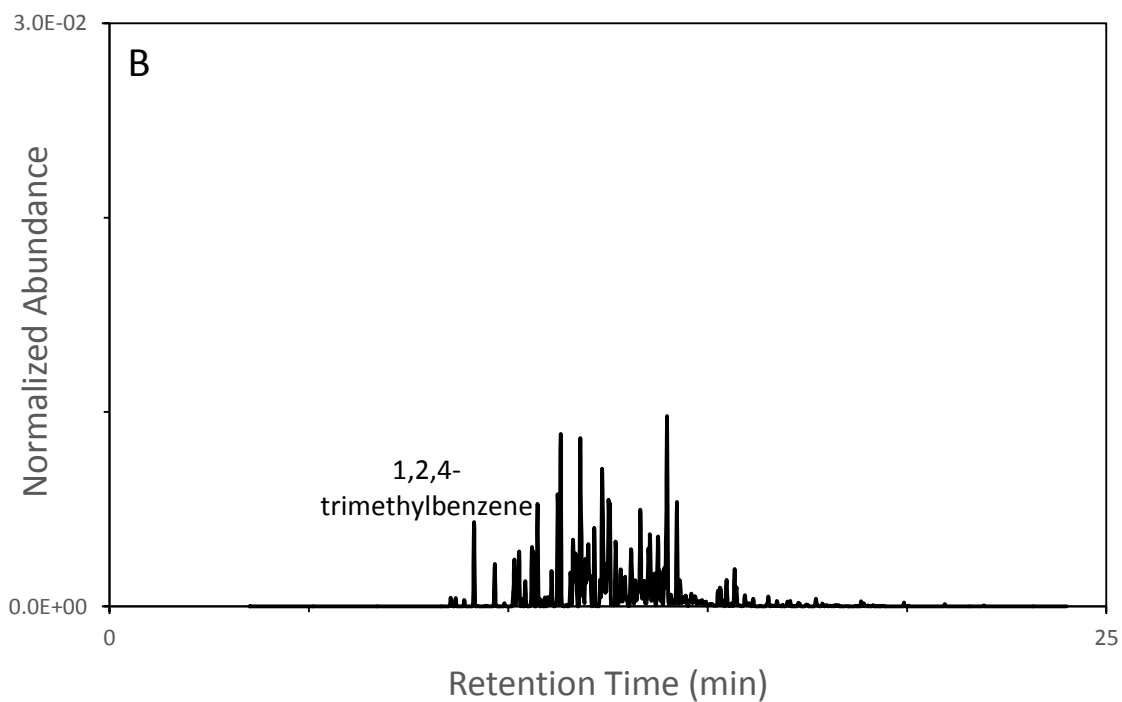
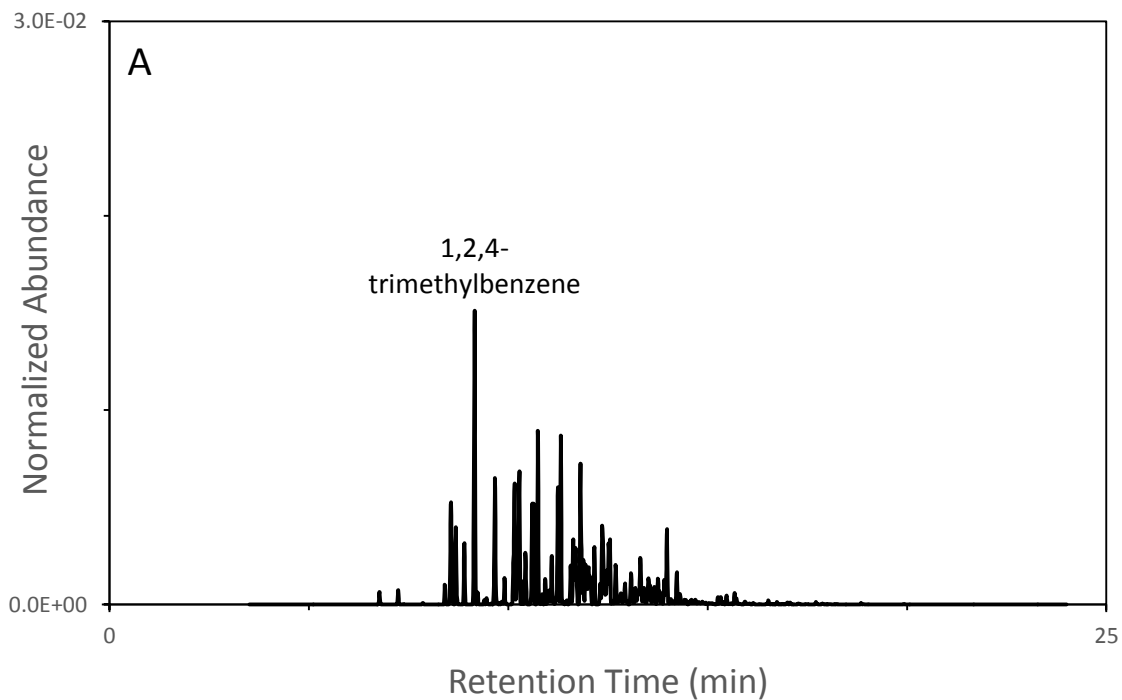


**Figure 20.** Representative chromatograms of 90% evaporated by volume gasoline reference standards (A) Gasoline 3 and (B) Gasoline 4.

The evaporated charcoal lighter standards have more negative scores on PC2 than the unevaporated standard (Figure 17). Charcoal lighter contains the normal alkanes C<sub>9</sub>-C<sub>12</sub>, which are all weighted negatively in the PC2 loadings plot (Figure 18B). As evaporation progresses, the abundance of C<sub>9</sub> and C<sub>10</sub> decreases and in fact, C<sub>9</sub> is no longer present in the 90% evaporated standard (Figure 21). However, C<sub>11</sub> and C<sub>12</sub> become more concentrated as evaporation progresses. The higher abundance of C<sub>11</sub> and C<sub>12</sub> in the evaporated standards increases the negative contribution of these compounds on PC2 with the result that the evaporated standards have a more negative score on PC2 than the unevaporated counterparts.

Association of simulated fire debris samples to the appropriate reference standard was also assessed using PCA. Again, this was initially assessed using Set 1 of the simulated fire debris samples (carpet and carpet padding substrate). PCA was performed on only the reference standards and the resulting eigenvectors were used to calculate scores for the fire debris samples, which were then projected onto the scores plot. To calculate scores, the mean-centered data for the sample is multiplied by the eigenvector for PC1 and the product is summed across all variables to generate the score for the sample on PC1. The procedure is repeated, multiplying the mean-centered data by the eigenvector for subsequent PCs (generating the loadings for the sample) and summing the product to generate the score for the sample on those PCs.

Performing PCA in this manner theoretically eliminates contributions from the substrate (*i.e.*, interference compounds inherent to the substrate and/or produced during burning) as the eigenvectors are generated based on the reference standards. This means that the positioning of the fire debris samples on the scores plot is affected only by compounds present in the liquid as these compounds are also present in the reference standards. As a result, association and discrimination of the fire debris samples are due to compounds from the ignitable liquids remaining in the sample, rather than any contributions from the substrate.

To be more representative of the way in which forensic laboratories may implement this procedure, replicates of one simulated sample at a time were projected onto the scores plot. Examples of the resulting scores plots are shown in Figure 22 for the simulated fire debris samples containing paint thinner, torch fuel and diesel.

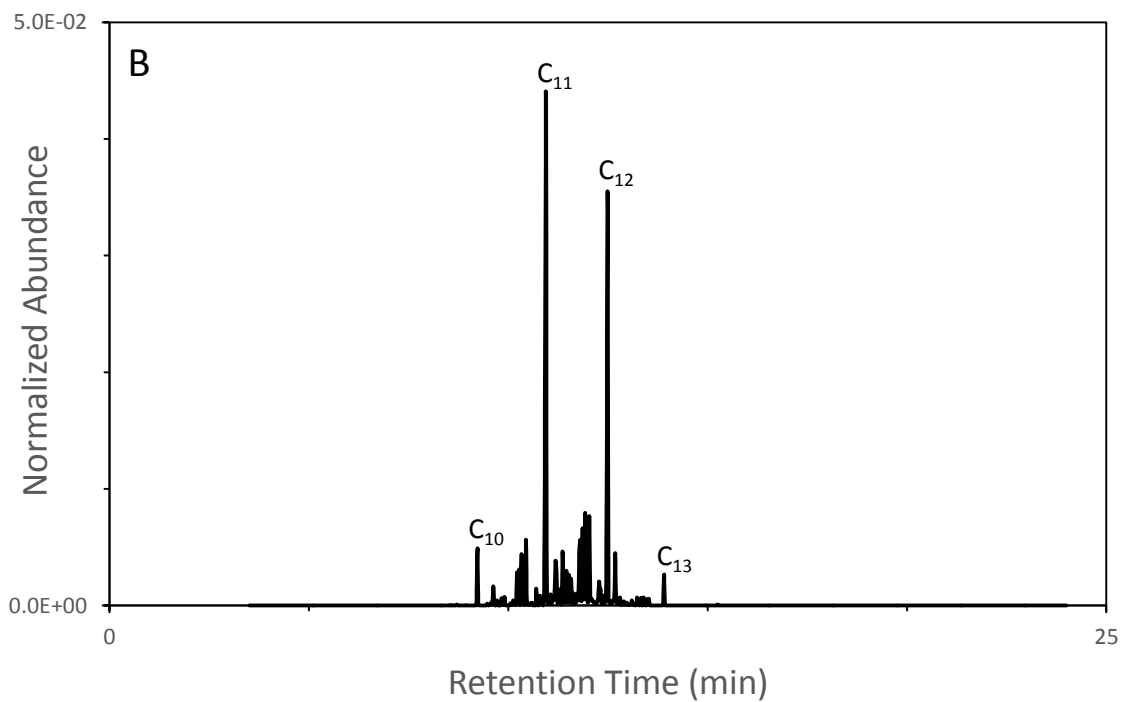
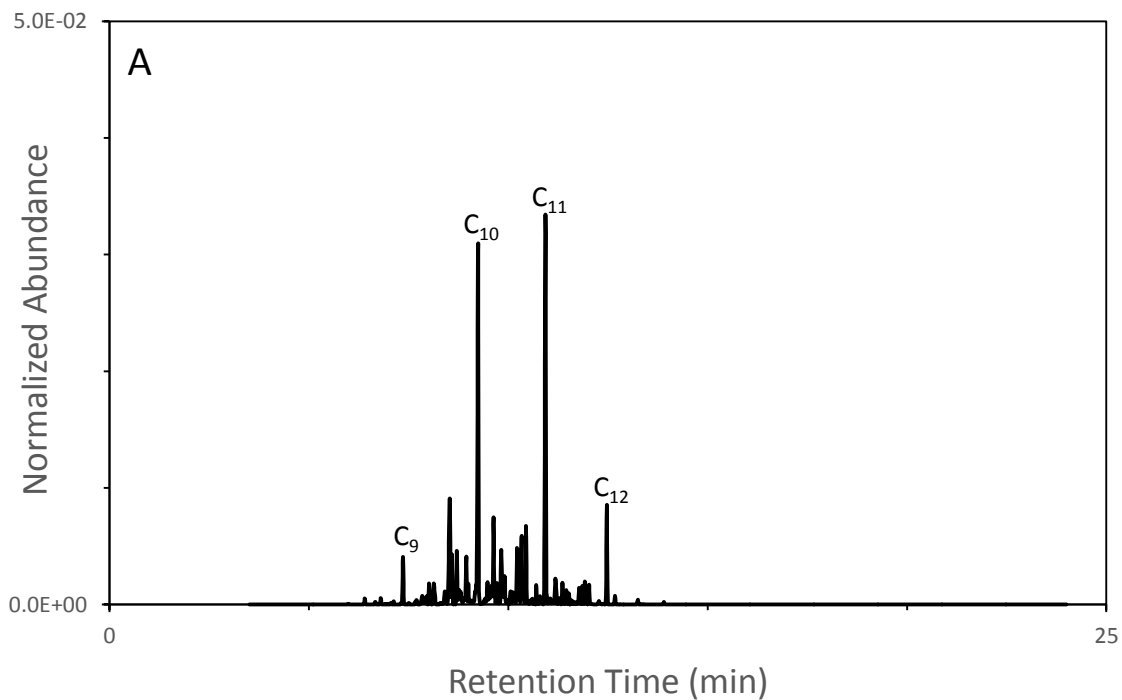


**Figure 21.** Representative chromatograms of charcoal lighter reference standards (A) unevaporated and (B) 90% evaporated by volume.

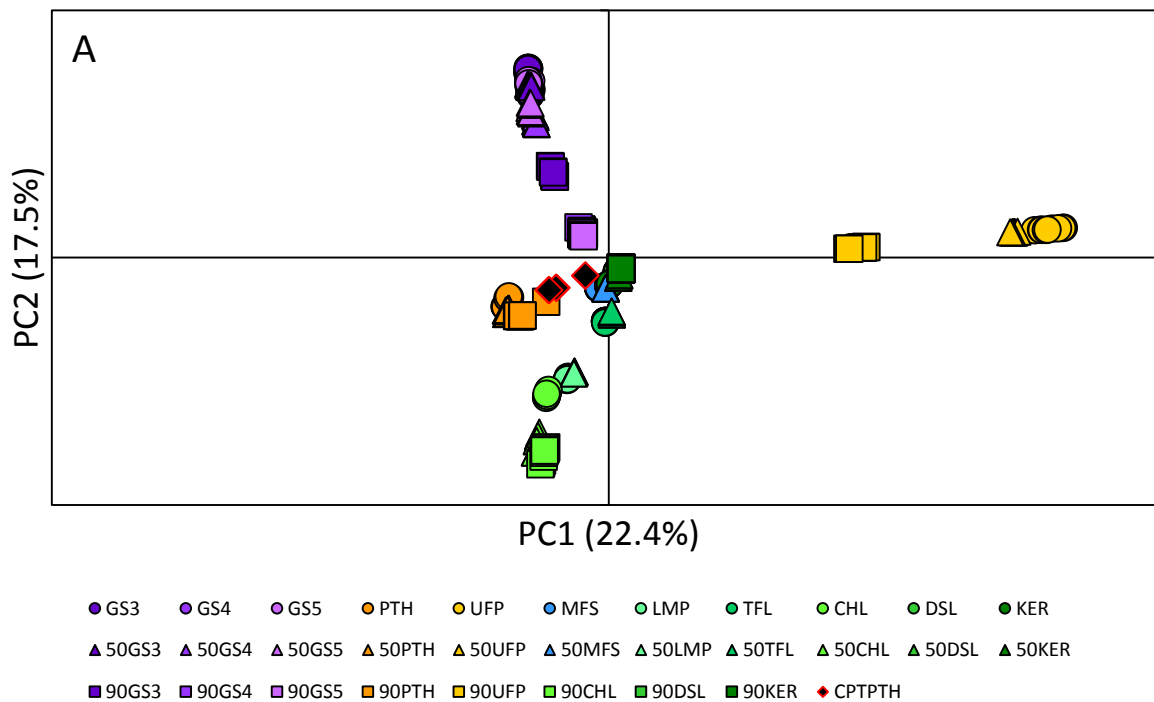


**Figure 22.** Scores plot of PC1 versus PC2 for the ignitable liquid reference standards and simulated fire debris sample containing carpet and carpet padding and (A) paint thinner, (B) torch fuel, and (C) diesel. Each reference standard was analyzed in replicate (n=9) and each standard is represented by a different color in the plot. Unevaporated standards are shown as circles, 50% evaporated as triangles, and 90% evaporated as squares. Simulated fire debris samples were analyzed in triplicate and are shown as black diamonds with red outlines. Abbreviations for each standard are defined in Table 1.

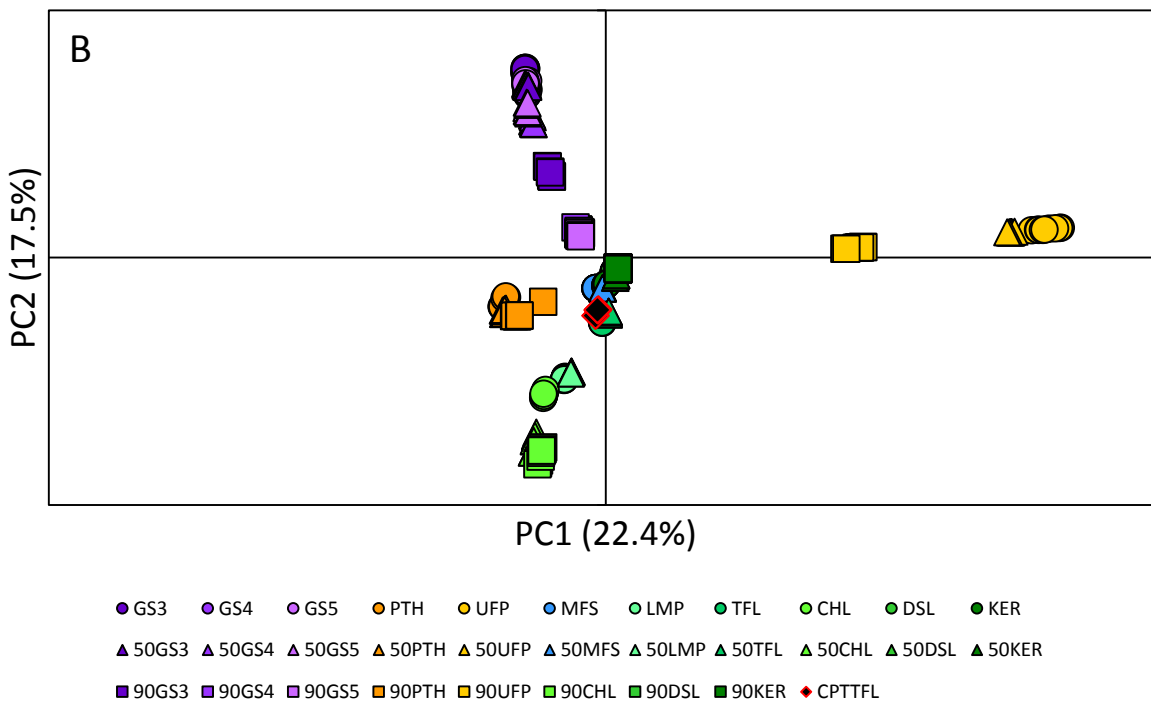


**Figure 22.** Scores plot of PC1 versus PC2 for the ignitable liquid reference standards and simulated fire debris sample containing carpet and carpet padding and (A) paint thinner, (B) torch fuel, and (C) diesel. Each reference standard was analyzed in replicate (n=9) and each standard is represented by a different color in the plot. Unevaporated standards are shown as circles, 50% evaporated as triangles, and 90% evaporated as squares. Simulated fire debris samples were analyzed in triplicate and are shown as black diamonds with red outlines. Abbreviations for each standard are defined in Table 1.

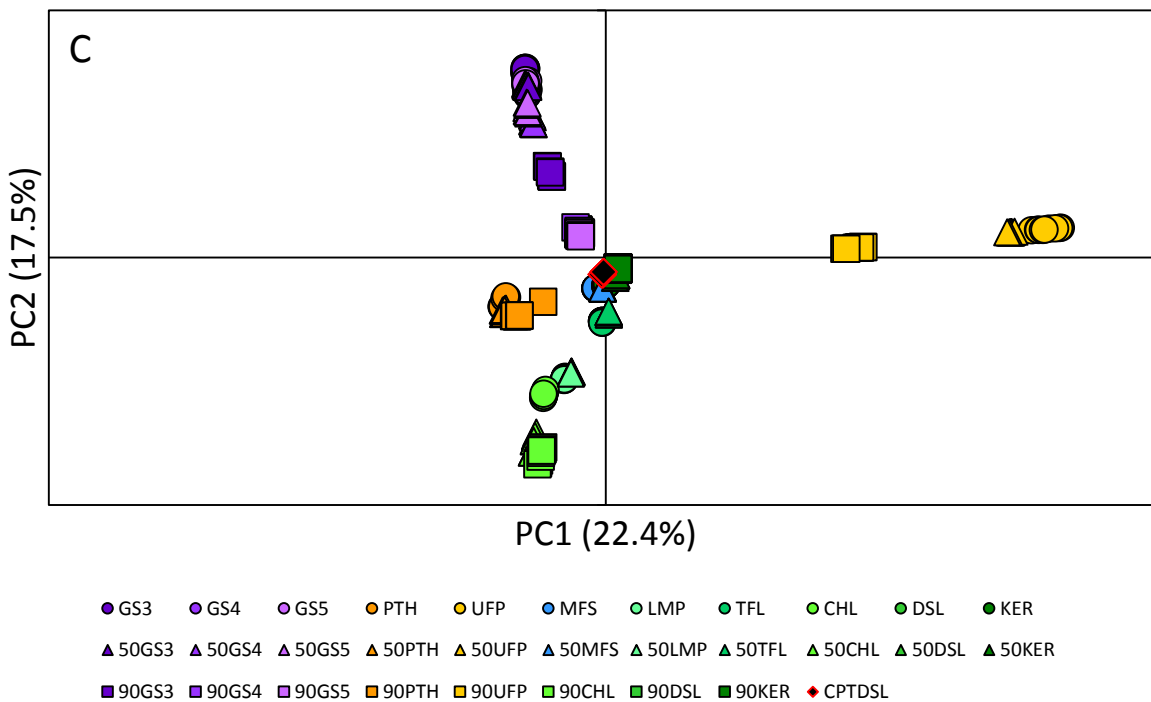


**Figure 22.** Scores plot of PC1 versus PC2 for the ignitable liquid reference standards and simulated fire debris sample containing carpet and carpet padding and (A) paint thinner, (B) torch fuel, and (C) diesel. Each reference standard was analyzed in replicate (n=9) and each standard is represented by a different color in the plot. Unevaporated standards are shown as circles, 50% evaporated as triangles, and 90% evaporated as squares. Simulated fire debris samples were analyzed in triplicate and are shown as black diamonds with red outlines. Abbreviations for each standard are defined in Table 1.

In terms of associating the fire debris samples to the corresponding standard, visual assessment of the scores plots is limited. The success of association is dependent on the extent of burning and hence, the compounds characteristic of the liquid that remain in the fire debris samples. For this particular data set, some fire debris samples associate well to the corresponding standard (*e.g.*, upholstery protector, torch fuel, paint thinner, etc.) as reference standards of these liquids are already well discriminated from the others. However, in other cases, association to the corresponding standard is not possible, particularly for the debris samples containing marine fuel stabilizer, diesel, and kerosene. Each of these samples is positioned closely to a group containing the marine fuel stabilizer, diesel, and kerosene reference standards although clear association to one liquid over the other two is not possible, even with the consideration of additional principal components. This is likely due to the overlap in compounds present in the unresolved section of the chromatogram between approximately 10 and 13 min.

To further assess positioning of the simulated fire debris samples on the scores plots, two additional metrics were used: Euclidean distance measurement and PPMC coefficients, which were calculated using the eigenvectors and mean-centered data (see section 2.2.2 for more details). For the simulated fire debris samples containing paint thinner, upholstery and fabric protector, marine fuel stabilizer, and lamp oil, the shortest Euclidean distance was to the corresponding standard. However, for fire debris samples containing torch fuel, charcoal lighter, diesel, and kerosene, the shortest distance was to the marine fuel stabilizer standard.

For the second metric, the absolute mean PPMC coefficient for the first four principal components was calculated for pairwise comparisons of each simulated fire debris sample to all reference standards (Table 17).

**Table 17.** Absolute mean PPMC coefficient calculated using the first four principal components to assess association of simulated fire debris (carpet and carpet padding substrate) to reference standards.

Reference standard	Absolute mean PPMC coefficient based on first four principal components							
	PTH CPT	UFP CPT	MFS CPT	LMP CPT	TFL CPT	CHL CPT	DSL CPT	KER CPT
GS3	0.290	0.356	0.374	0.239	0.306	0.270	0.354	0.365
50 GS3	0.305	0.367	0.389	0.248	0.318	0.277	0.367	0.379
90 GS3	0.387	0.403	0.504	0.309	0.357	0.350	0.474	0.415
GS4	0.304	0.364	0.383	0.242	0.309	0.273	0.361	0.369
50 GS4	0.328	0.372	0.411	0.254	0.317	0.277	0.385	0.371
90 GS4	0.641	0.625	0.871	0.325	0.478	0.395	0.837	0.641
GS5	0.285	0.359	0.362	0.232	0.304	0.266	0.343	0.364
50 GS5	0.294	0.364	0.364	0.232	0.308	0.264	0.343	0.370
90 GS5	0.630	0.615	0.867	0.319	0.540	0.392	0.848	0.688
PTH	<b>0.760</b>	0.468	0.556	0.200	0.267	0.308	0.535	0.405
50 PTH	<b>0.763</b>	0.475	0.574	0.217	0.285	0.359	0.549	0.440
90 PTH	<b>0.747</b>	0.474	0.586	0.322	0.337	0.435	0.554	0.480
UFP	0.423	<b>0.914</b>	0.510	0.246	0.368	0.272	0.489	0.402
50 UFP	0.450	<b>0.945</b>	0.547	0.255	0.381	0.280	0.524	0.415
90 UFP	0.552	<b>0.759</b>	0.698	0.245	0.367	0.330	0.668	0.495
MFS	0.674	0.662	<b>0.971</b>	0.297	0.568	0.490	0.916	0.732
50 MFS	0.639	0.652	<b>0.950</b>	0.306	0.596	0.460	0.908	0.738
LMP	0.202	0.216	0.203	<b>0.871</b>	0.311	0.721	0.211	0.436
50 LMP	0.199	0.221	0.243	<b>0.850</b>	0.399	0.718	0.255	0.520
TFL	0.361	0.362	0.463	0.288	<b>0.747</b>	0.335	0.571	0.637
50 TFL	0.371	0.373	0.474	0.250	<b>0.784</b>	0.300	0.582	0.644
CHL	0.345	0.343	0.340	0.417	0.234	<b>0.270</b>	0.372	0.287
50 CHL	0.354	0.368	0.368	0.274	0.222	<b>0.182</b>	0.411	0.303
90 CHL	0.351	0.335	0.326	0.247	0.214	<b>0.190</b>	0.370	0.292
DSL	0.679	0.688	0.954	0.328	0.641	0.472	<b>0.979</b>	0.794
50 DSL	0.676	0.697	0.951	0.315	0.539	0.481	<b>0.936</b>	0.721
90 DSL	0.674	0.698	0.950	0.308	0.520	0.488	<b>0.917</b>	0.702
KER	0.582	0.594	0.836	0.363	0.857	0.464	0.955	<b>0.914</b>
50 KER	0.605	0.627	0.858	0.340	0.716	0.402	0.950	<b>0.809</b>
90 KER	0.668	0.693	0.943	0.310	0.522	0.481	0.920	<b>0.706</b>

Abbreviations for each reference standard are listed in Table 1. Mean PPMC coefficient calculated based on 81 pairwise comparisons. CPT indicates carpet and carpet padding substrate.

In Table 17, coefficients indicating correlation to corresponding standards are shown in bold. For fire debris samples containing upholstery and fabric protector, lamp oil, and kerosene, the highest coefficient, indicating strong correlation, is obtained for comparisons to the corresponding standards. For the paint thinner fire debris sample, the highest coefficient is also obtained for comparison to the corresponding standard but in this case, a moderate rather than

strong correlation is indicated. The debris sample containing torch fuel is strongly correlated to the kerosene reference standards but only moderately correlated to the appropriate reference standard. Debris samples containing marine fuel stabilizer and diesel are each strongly correlated to both the marine fuel stabilizer and diesel reference standards. However, the higher coefficient is observed between the fire debris and the corresponding standard indicating greater similarity. Finally, the debris sample containing charcoal lighter is not strongly correlated to any reference standard.

Principal components analysis was also performed on fire debris samples in Set 2 which contained an oil-finished hardwood flooring substrate (Figure 23). Separate samples of the substrate were spiked with paint thinner, torch fuel, and diesel, then burned, extracted and analyzed following procedures described previously. For this particular substrate, dominant interference compounds are the normal alkanes C<sub>9</sub>-C<sub>12</sub>. These compounds are also present in the petroleum distillate standards and hence, for this particular substrate, the substrate compounds do contribute to positioning of the fire debris samples on the scores plot.

In each of the scores plots, the fire debris samples are positioned most closely to the marine fuel stabilizer reference standard (Figure 23). This was verified with Euclidean distance calculations using the first four principal components: in each case, the shortest Euclidean distance is between the fire debris sample and the marine fuel stabilizer standard (0.022, 0.006, and 0.006 for debris containing paint thinner, torch fuel, and diesel, respectively).

To further assess positioning on the scores plots, PPMC coefficients were calculated using the eigenvectors for each PC (Table 18). The paint thinner fire debris samples are only weakly correlated to the corresponding standards while the torch fuel fire debris samples are moderately correlated to the corresponding standard. However, torch fuel fire debris samples are more strongly correlated to the diesel and kerosene reference standards, most likely due to the normal alkane substrate interference compounds. Fire debris containing diesel is strongly correlated to the corresponding standards although these samples are also strongly correlated to marine fuel stabilizer and kerosene reference standards, primarily due to the substrate interference compounds.

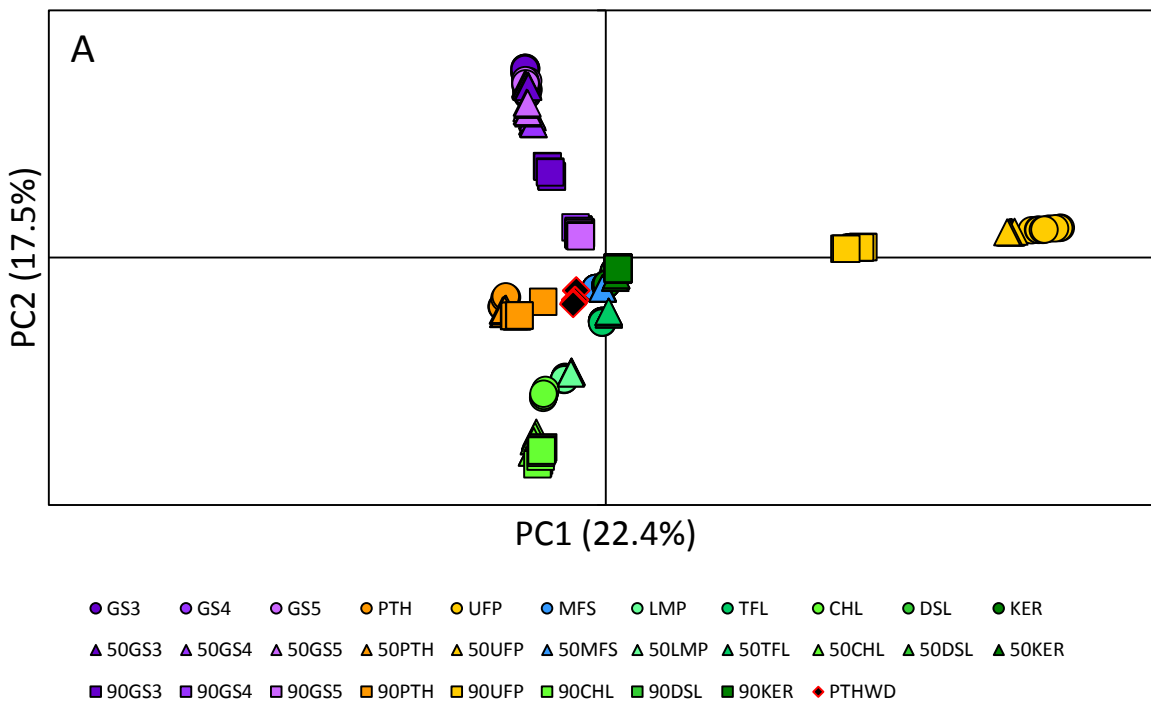


**Figure 23.** Scores plot of PC1 versus PC2 for the ignitable liquid reference standards and simulated fire debris sample containing oil-finished hardwood flooring (A) paint thinner, (B) torch fuel, and (C) diesel. Each reference standard was analyzed in replicate (n=9) and each standard is represented by a different color in the plot. Unevaporated standards are shown as circles, 50% evaporated as triangles, and 90% evaporated as squares. Simulated fire debris samples were analyzed in triplicate and are shown as black diamonds with red outlines. Abbreviations for each standard are defined in Table 1.

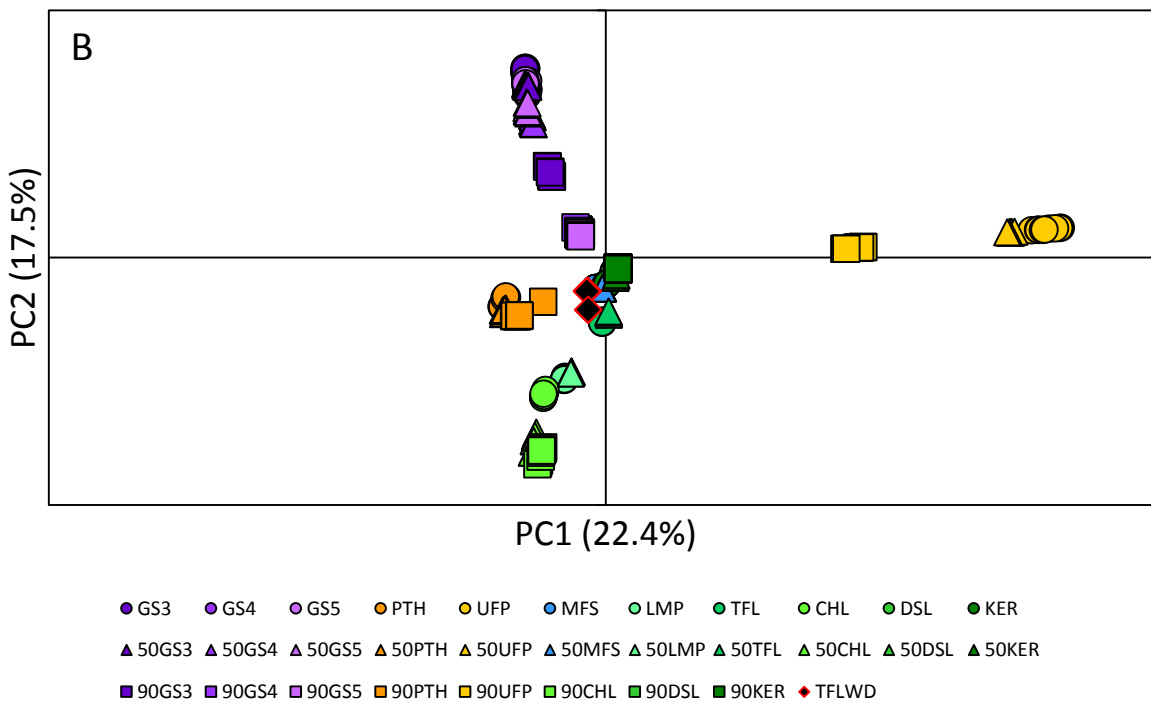


**Figure 23 contd.** Scores plot of PC1 versus PC2 for the ignitable liquid reference standards and simulated fire debris sample containing oil-finished hardwood flooring (A) paint thinner, (B) torch fuel, and (C) diesel. Each reference standard was analyzed in replicate (n=9) and each standard is represented by a different color in the plot. Unevaporated standards are shown as circles, 50% evaporated as triangles, and 90% evaporated as squares. Simulated fire debris samples were analyzed in triplicate and are shown as black diamonds with red outlines. Abbreviations for each standard are defined in Table 1.

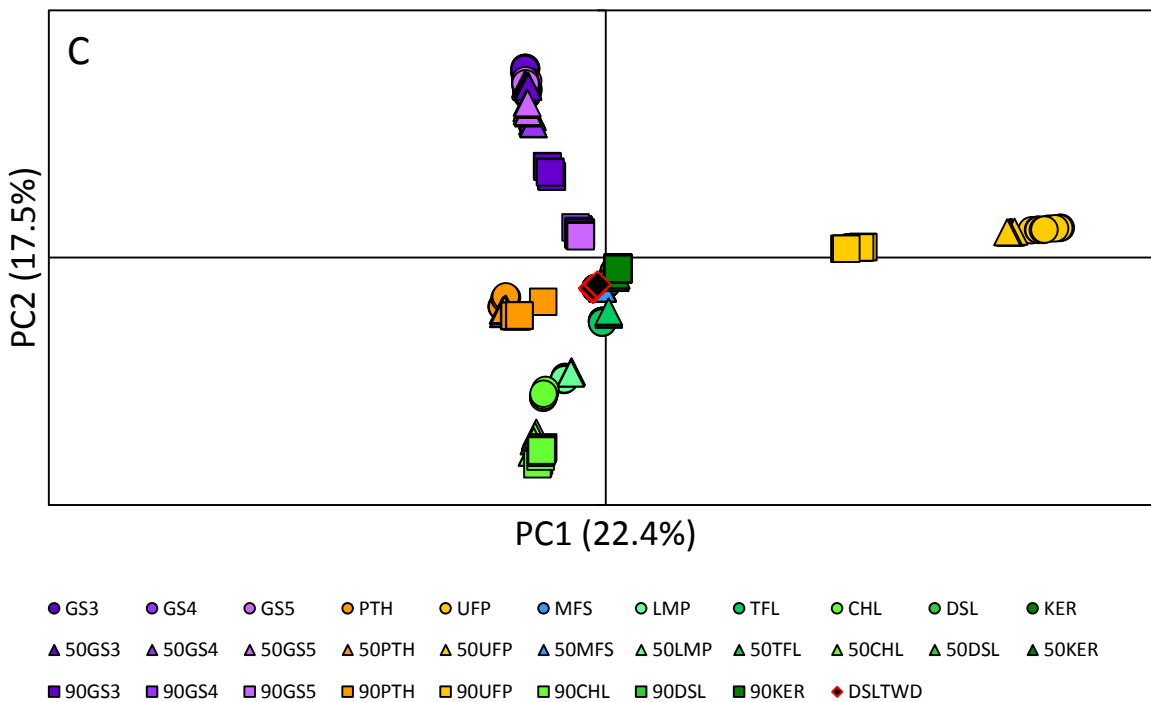


**Figure 23 contd.** Scores plot of PC1 versus PC2 for the ignitable liquid reference standards and simulated fire debris sample containing oil-finished hardwood flooring (A) paint thinner, (B) torch fuel, and (C) diesel. Each reference standard was analyzed in replicate (n=9) and each standard is represented by a different color in the plot. Unevaporated standards are shown as circles, 50% evaporated as triangles, and 90% evaporated as squares. Simulated fire debris samples were analyzed in triplicate and are shown as black diamonds with red outlines. Abbreviations for each standard are defined in Table 1.

**Table 18.** Absolute mean PPMC coefficient calculated using the first four principal components to assess association of simulated fire debris (oil-finished wood substrate) to reference standards.

Reference standard	Absolute mean PPMC coefficient based on first four principal components		
	PTH OWD	TFL OWD	DSL OWD
GS3	0.211	0.276	0.331
50 GS3	0.230	0.283	0.344
90 GS3	0.333	0.307	0.456
GS4	0.231	0.276	0.340
50 GS4	0.261	0.273	0.367
90 GS4	0.442	0.519	0.767
GS5	0.206	0.278	0.324
50 GS5	0.225	0.276	0.321
90 GS5	0.430	0.522	0.759
PTH	<b>0.350</b>	0.349	0.524
50 PTH	<b>0.388</b>	0.371	0.550
90 PTH	<b>0.431</b>	0.400	0.570
UFP	0.349	0.365	0.442
50 UFP	0.361	0.363	0.476
90 UFP	0.353	0.428	0.627
MFS	0.565	0.662	0.901
50 MFS	0.497	0.642	0.867
LMP	0.534	0.312	0.263
50 LMP	0.542	0.397	0.357
TFL	0.452	<b>0.688</b>	0.461
50 TFL	0.431	<b>0.621</b>	0.441
CHL	0.218	0.309	0.345
50 CHL	0.274	0.337	0.387
90 CHL	0.291	0.326	0.359
DSL	0.509	0.704	<b>0.904</b>
50 DSL	0.529	0.648	<b>0.893</b>
90 DSL	0.540	0.625	<b>0.879</b>
KER	0.432	0.741	0.823
50 KER	0.405	0.740	0.843
90 KER	0.530	0.622	0.879

Abbreviations for each reference standard are listed in Table 1.  
Mean PPMC coefficient calculated based on 81 pairwise comparisons.  
OWD indicates oil-finished wood substrate.

In Table 18, coefficients indicating correlation to corresponding standards shown in bold font. Irrespective of the substrate (carpet and carpet padding or oil-finished wood), PCA is limited for this particular application. These limitations remain despite performing PCA in a manner that theoretically eliminates or minimizes contributions from the substrate interference

compounds and despite taking into account additional PCs that explain more of the variance in the data set.

#### 4.1.5 Hierarchical Cluster Analysis

Initially, HCA was performed on only the ignitable liquid reference standards to assess the ability to cluster according to ASTM class, using the Euclidean distance measurement and three common linkage methods (single, complete, and average). The resulting dendrograms are shown in Figure 24 and a summary of the clustering is given in Table 19.

**Table 19.** Similarity level at which replicates and liquids within each ASTM class cluster.

Reference standard	Similarity level (%) of clusters		
	Euclidean distance Single linkage	Euclidean distance Complete linkage	Euclidean distance Average linkage
GS3	96.4	95.6	95.9
GS4	96.5	94.4	95.2
GS5	90.3	89.9	90.7
<b>Gasoline</b>	88.3	79.9	83.0
PTH	95.4	93.0	94.0
UFP	92.7	90.9	92.0
<b>Isoparaffinic</b>	30.7	0.0	0.0
MFS	98.6	98.5	98.5
LMP	99.2	98.4	98.9
TFL	98.1	96.8	97.3
CHL	89.2	90.0	89.4
DSL	98.1	97.4	97.7
KER	97.9	97.8	97.8
<b>Petroleum distillate</b>	41.5	32.4	35.0

Abbreviations for each liquid are listed in Table 1.

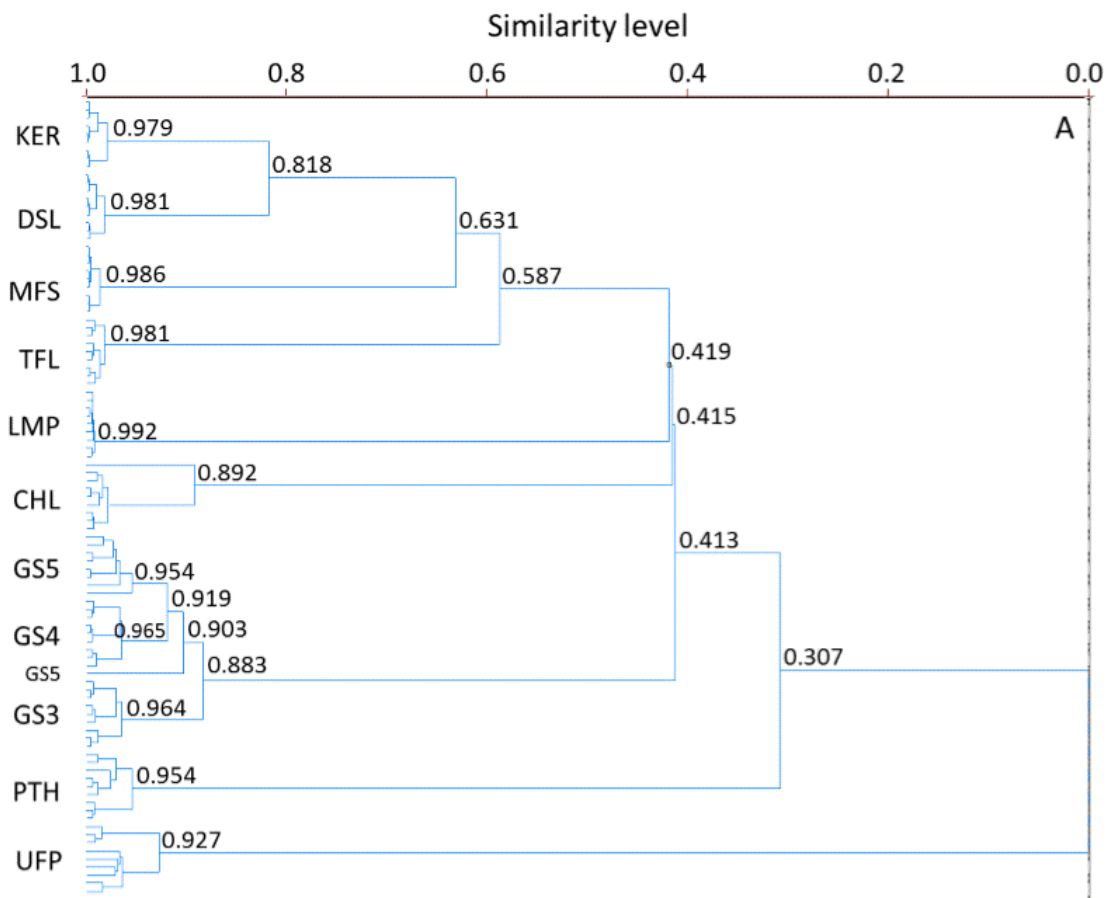


**Figure 24.** Hierarchical cluster analysis of ignitable liquid reference standards using Euclidean distance and (A) single linkage, (B) complete linkage, and (C) average linkage. Abbreviations for each standard are defined in Table 1.

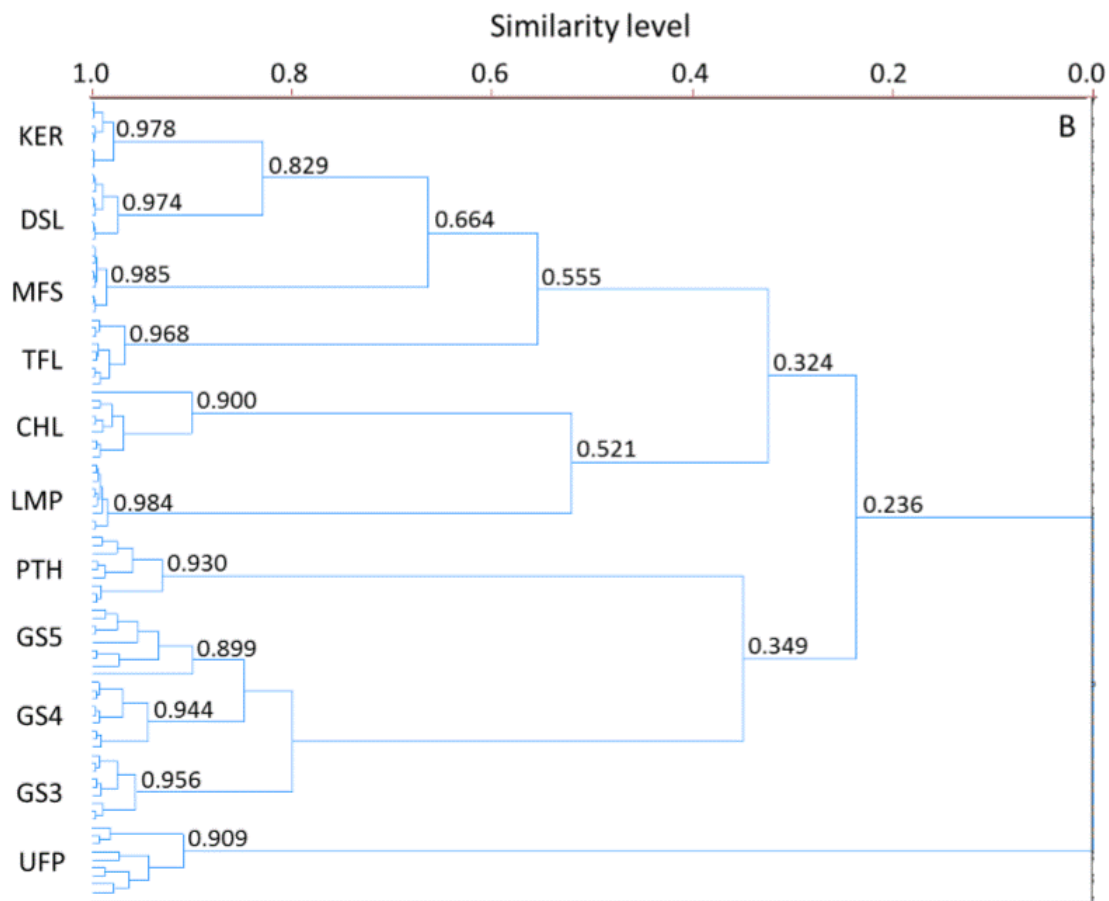


**Figure 24 contd.** Hierarchical cluster analysis of ignitable liquid reference standards using Euclidean distance and (A) single linkage, (B) complete linkage, and (C) average linkage. Abbreviations for each standard are defined in Table 1.

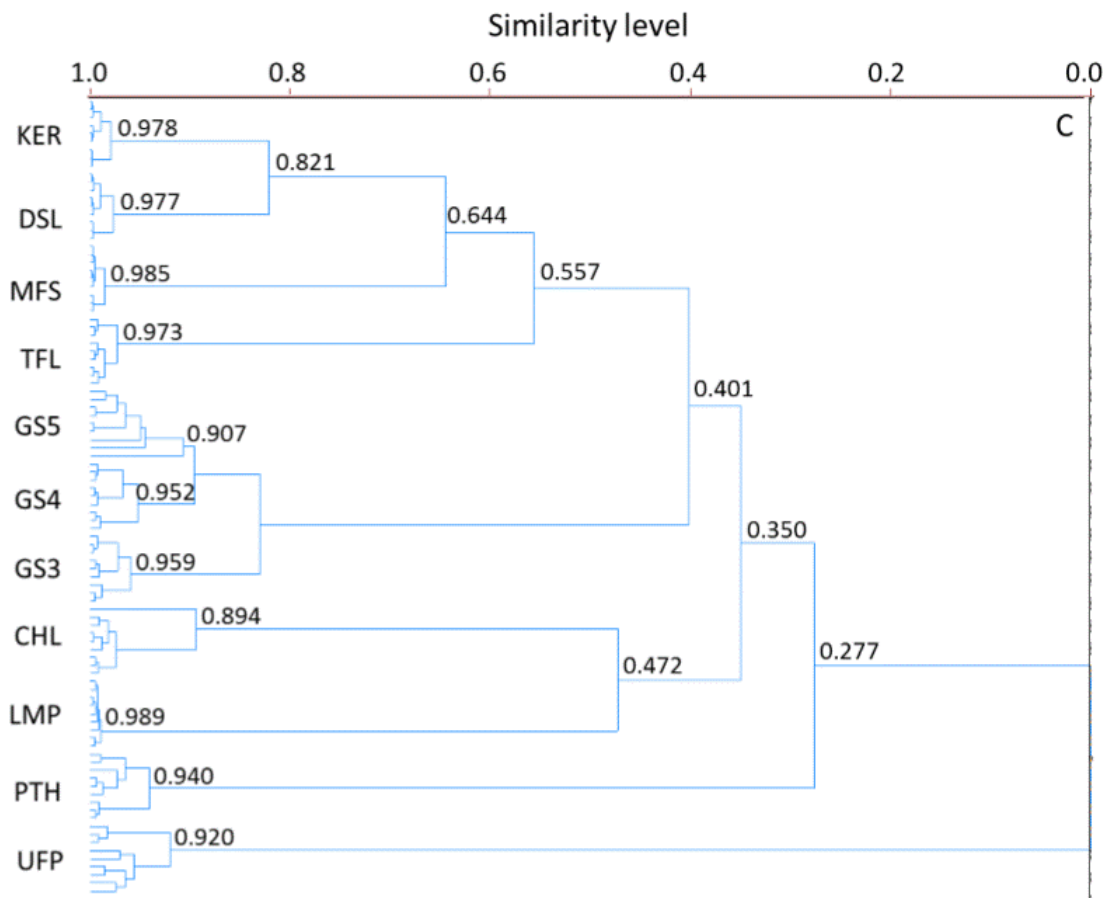


**Figure 24 contd.** Hierarchical cluster analysis of ignitable liquid reference standards using Euclidean distance and (A) single linkage, (B) complete linkage, and (C) average linkage. Abbreviations for each standard are defined in Table 1.

In general, the linkage method used does not drastically influence the clusters formed for this data set. For all three methods, replicates of each ignitable liquid reference standard form distinct clusters at similarity levels greater than 90%. Further, replicates are clustered before forming clusters with other standards, indicating that replicates are more similar to each other than to those of other standards, as expected.

The linkage method also does not greatly influence the similarity level at which standards in the same ASTM class are clustered, with the exception of the isoparaffinic class. In this instance, there is 31% similarity between upholstery protector and paint thinner using the single linkage method but 0% similarity using the complete linkage and average linkage methods. Despite being in the same class, these two standards are very different in chemical composition, containing branched alkanes with a different carbon number range. In cluster analysis, the similarity levels are calculated relative to the data set under consideration: as a result, there will always be two samples that have 0% similarity. Given the prior knowledge of this particular data set, upholstery protector is the most dissimilar and therefore, the clustering afforded by the complete and average linkage methods is not unexpected.

For all three linkage methods, the petroleum distillate reference standards are clustered at relatively low similarity levels (ranging from 32-42%). Again, given the prior knowledge of this data set, the lower similarity levels are not unexpected. The five reference standards in this class all contain normal alkanes although the identity and number of the alkanes varies. Among the petroleum distillates, diesel and kerosene are the most similar, both containing a similar range of unresolved compounds and with a wide range of normal alkanes ( $C_{10}$ - $C_{20}$  in diesel and  $C_{10}$ - $C_{17}$  in kerosene). These two standards are clustered at similarity levels of 81.8%, 82.9%, and 82.1% using single, complete, and average linkage methods, respectively.

The cluster analysis results indicate that, in a chemically diverse data set such as this, the choice of linkage method does not greatly influence the clusters obtained. While all three methods could easily be used in subsequent data analysis, for simplicity and clarity, only one linkage method was selected for further consideration. The single linkage method is analogous to the  $k$ -nearest neighbors classification procedure, with  $k$  (*i.e.*, the number of neighbors for classification) equal to 1. As these data were also subjected to  $k$ -nearest neighbors, the single linkage method was selected.

Cluster analysis was repeated, including the evaporated standards in the data set. The similarity level at which replicates of each reference standard are clustered is summarized in Table 20. The similarity levels at which the evaporated standards cluster with the corresponding non-evaporated standard are summarized in Table 21.

**Table 20.** Similarity level of replicates of each reference standard.

Reference standard	Similarity level (%) of replicates	Reference standard	Similarity level (%) of replicates
GS3	95.2	LMP	96.7
50 GS3	92.4	50 LMP	97.5
90 GS3	96.3		
		TFL	96.0
GS4	95.4	50 TFL	94.2
50 GS4	92.6		
90 GS4	96.6	CHL	59.3
		50 CHL	91.1
GS5	88.7	90 CHL	87.9
50 GS5	91.7		
90 GS5	97.0	DSL	98.1
		50 DSL	94.8
PTH	89.1	90 DSL	93.4
50 PTH	89.2		
		KER	96.9
UFP	87.4	50 KER	95.7
50 UFP	90.3	90 KER	93.6
MFS	98.0		
50 MFS	97.2		

Abbreviations for each liquid are listed in Table 1.

Replicates of each standard cluster at high similarity irrespective of evaporation level, with the exception of unevaporated charcoal lighter for which replicates only cluster at 59.3% similarity. For this liquid, one replicate was slightly misaligned compared to the other eight replicates. As a result, this replicate clustered to the others at the slightly lower similarity level. When this replicate is excluded, the remaining replicates of the unevaporated charcoal lighter reference standard cluster at a similarity level of 96.3%.

**Table 21.** Similarity level at which evaporated standards cluster with corresponding unevaporated standard.

Unevaporated reference standard	Similarity level (%) of cluster formation with corresponding evaporated standard	
	50% evaporated standard	90% evaporated standard
GS3	85.3	81.0
GS4	90.9	67.3
GS5	85.3	67.3
PTH	76.1	--
UFP	80.1	--
MFS	82.5	--
LMP	84.6	--
TFL	74.9	--
CHL	59.3	44.7
DSL	82.5	65.3
KER	85.8	77.9

Abbreviations for each liquid are listed in Table 1.

For those standards for which there are only two levels of evaporation (unevaporated and 50% evaporated), the unevaporated and evaporated standards cluster at high similarity levels (75% and higher). Additionally, these clusters are formed first, prior to forming clusters with any other standard. For those standards for which there are three evaporation levels, the 50% evaporated standard clusters with the unevaporated standard first, and then to the 90% evaporated standard. However, these clusters tend to include reference standards of other liquids. For example, the unevaporated and 50% evaporated diesel standards cluster at 82.5% similarity. These standards then cluster not with the 90% evaporated diesel but instead, with a cluster containing the unevaporated and 50% evaporated kerosene standards. Similarly, unevaporated gasoline 5 clusters with a group containing the corresponding 50% evaporated standard along with the unevaporated and 50% evaporated standards of gasolines 3 and 4.

To assess association of simulated fire debris samples to the corresponding reference standards, cluster analysis was repeated using Set 1 of the fire debris samples. As before, replicates of one fire debris sample at a time were included with the reference standards for analysis. This method of conducting HCA was deemed more relevant to the way in which forensic laboratories could perform similar analyses in the future. In all cases, HCA was performed using Euclidean distance and single linkage. All dendrograms are shown in Appendix 5 and the results of cluster analysis are summarized in Table 22.

**Table 22.** Similarity level at which simulated fire debris samples (carpet and carpet padding substrate) cluster with corresponding reference standards.

<b>Simulated fire debris</b>	<b>Similarity level (%) of cluster formation with corresponding standard</b>
PTH CPT	42.2
UFP CPT	32.1
MFS CPT	64.4
LMP CPT	50.4
TFL CPT	43.8
CHL CPT	43.9
DSL CPT	56.0
KER CPT	63.4

Abbreviations for each liquid are listed in Table 1. CPT indicates carpet and carpet padding substrate.

Debris samples containing paint thinner, upholstery protector, marine fuel stabilizer, lamp oil, and charcoal lighter cluster first with the corresponding standards, forming an exclusive cluster. Thus, despite the relatively low similarity levels, these debris samples are most similar to the corresponding standards than to any other standard in the data set.

In contrast, debris samples containing torch fuel first form a cluster (60.6% similarity) with the marine fuel stabilizer, diesel, and kerosene reference standards. This is likely due to the overlap and similarity in abundance of compounds in the unresolved section of the chromatograms (approximately between 10 and 13 min) for the fire debris sample and each of the afore-mentioned reference standards. The debris sample containing torch fuel only clusters with the appropriate standards at a similarity level of 43.8%. While both the torch fuel debris samples and reference standards contain the unresolved section or peaks, the abundance of these peaks is greater in the debris sample as a result of evaporation (*i.e.*, evaporation of earlier eluting compounds resulting in concentration effects), leading to the lower similarity.

The debris samples containing diesel and kerosene cluster with the appropriate standards at relatively high similarity levels (56.0 and 63.4% for diesel and kerosene, respectively). However, these debris samples do not form exclusive clusters with the corresponding standard; instead, the diesel debris samples cluster with diesel, kerosene, and marine fuel stabilizer reference standards while the kerosene debris samples cluster with the diesel and kerosene reference standards. Again, for these reference standards, there is overlap in the compounds present in the unresolved section of the chromatogram in the debris samples and reference standards. Nonetheless, the class of ignitable liquid can be ascertained from this cluster pattern.

Set 2 of the simulated fire debris samples (paint thinner, torch fuel, and diesel on an oil-finished wood flooring) was also subjected to HCA. As before, replicates of one fire debris sample at a time were included with the reference standards for analysis and in all cases, HCA was performed using Euclidean distance and single linkage. The three simulated fire debris samples all first form clusters with a larger group that contains the diesel and kerosene reference standards, albeit at different similarity levels (52.3% for simulated fire debris containing paint thinner, 44.2% for fire debris containing torch fuel, and 61.8% for fire debris containing diesel). In all cases, the presence of the normal alkanes in the substrate (from the oil finish) increases similarity to the petroleum distillate standards, resulting in the clustering observed. As noted previously, the diesel simulated fire debris sample does not resemble the diesel reference standard and hence, the apparent high similarity observed in clustering is due to the presence of the interference compounds from the substrate (C<sub>9</sub>-C<sub>12</sub>).

For the oil-finished wood substrate, the use of HCA is more limited than observed previously for the carpet and carpet padding substrate. Samples and reference standards are clustered based on similarities in chemical composition. For the carpet and carpet padding substrate, the interference compounds (styrene, trichloropropane, and biphenyl) are not present in the reference standards. Hence, clustering of these samples is based on the compounds present in the liquid, resulting in successful association of the debris samples and reference standards. In contrast, the substrate interference compounds (C<sub>9</sub>-C<sub>12</sub>) in the oil-finished wood are also present in the petroleum distillate reference standards. As a result, clustering of these debris samples is based on similarity of the interference compounds, resulting in association of the fire debris samples to the kerosene and diesel standards first.

It is interesting to note the agreement between cluster analysis and principal components analysis: that is, positioning of simulated samples in the PCA scores plot corresponds to clustering observed in the HCA dendrogram. Cluster analysis is often considered to assess similarity while, in contrast, PCA is considered to assess differences (*i.e.*, variance) among samples in a data set. However, both procedures are based on distance measurements in multidimensional space. In fact, the dendrogram output from HCA includes all dimensions whereas, scores plots from PCA typically include only a few dimensions that account for the majority of the variance. Thus, in comparing the outputs from both procedures, the dendrogram is actually more representative of the full data set. The implication of this difference becomes

apparent in the classification procedures which are discussed in the following sections (4.1.6 and 4.1.7).

#### 4.1.6 Soft Independent Modeling of Class Analogy

To begin investigating the SIMCA approach, Set 1 of the simulated fire debris samples (carpet and carpet padding substrate) was again used. In the first iteration, statistical models were developed based on the isoparaffinic and petroleum distillate ignitable liquid classes as these were the two classes represented in the fire debris samples in this data set. The isoparaffinic model contained the two isoparaffinic reference standards at all three evaporation levels (*i.e.*, unevaporated, 50%, and 90% evaporated) while the petroleum distillate model contained all evaporation levels available for these reference standards. Both models were generated by PCA of the appropriate data set. For the isoparaffinic class, four principal components were included in the model, accounting for 98.2% of the variance, while for the petroleum distillate model, six principal components were included, accounting for 97.0% of the variance. This highlights one of the advantages of the SIMCA method: the number of principal components included in a model does not have to be the same for all models in the data set. As a result, the number of PCs selected is tailored to adequately describe the variance in that model.

Classification of the simulated fire debris samples was subsequently performed using the generated models. However, with these two models, none of the fire debris samples were classified at any of the confidence levels investigated (95, 99, 99.5, and 99.9%). The lack of classification is primarily a result of the models not adequately describing the data to be classified; that is, the simulated fire debris samples contain interference compounds (*i.e.*, styrene, trichloropropane, and biphenyl) from the substrate that are not described by the models.

In the second SIMCA iteration, the burned substrate with no ignitable liquid present was included in the PCA models. For the isoparaffinic class, five principal components were included in the model, accounting for 98.2% of the variance, while for the petroleum distillate model, seven principal components were included, accounting for 97.4% of the variance. In both cases, the contributions of the substrate compounds were taken into account as compounds from the substrate contributed to the principal components included in the model.

Using these two models, some degree of classification of the simulated fire debris samples was possible. At the 95% confidence level ( $\alpha = 0.05$ ), only two extracts of the fire debris

containing upholstery protector are correctly classified. At the 99.9% confidence level (representing  $\alpha = 0.001$ ), there is greater success in classification. Fire debris samples containing paint thinner and upholstery protector are correctly classified in the isoparaffinic class while samples containing lamp oil and torch fuel are correctly classified in the petroleum distillate class. Thus, the rate of successful classification increases as confidence level increases. At first, this may seem counter-intuitive but in fact, higher confidence levels are less rigorous for association. To illustrate, the area under a normal distribution density curve is shown in Figure 25 for two sample populations, *A* and *B*. At lower confidence levels (*e.g.*, 95%), the distribution is narrow but broadens as confidence level increases. Therefore, there is greater chance of association as confidence level increases due to broadening of the distribution.

While there is greater success in classification at higher confidence levels, there is also an increase in the rate of multiple classifications. At the 99.9% confidence level, simulated fire debris samples containing charcoal lighter, diesel, and kerosene, are correctly classified as petroleum distillates but are also misclassified as isoparaffinics. Upon closer inspection, the chromatograms of these samples are all dominated by the substrate interference compounds, with less contribution from the compounds contained in the liquid (Appendix 1). As both class models now contain the substrate, the high contribution of substrate compounds in these fire debris samples means that classification to both models occurs. In contrast, chromatograms of the fire debris samples that are correctly classified (*i.e.*, paint thinner, upholstery protector, lamp fuel, and torch fuel) are dominated by compounds from the liquid itself, with less contribution from the substrate compounds.

A final iteration of SIMCA was performed in which replicates of one simulated fire debris sample were also included in the model, along with the reference standards and burned substrate. For the isoparaffinic class, six principal components were included in the model, accounting for 98.7% of the variance, while for the petroleum distillate model, seven principal components were included, accounting for 95.9% of the variance. Classification success is enhanced with this addition to the models, as summarized in Table 23.

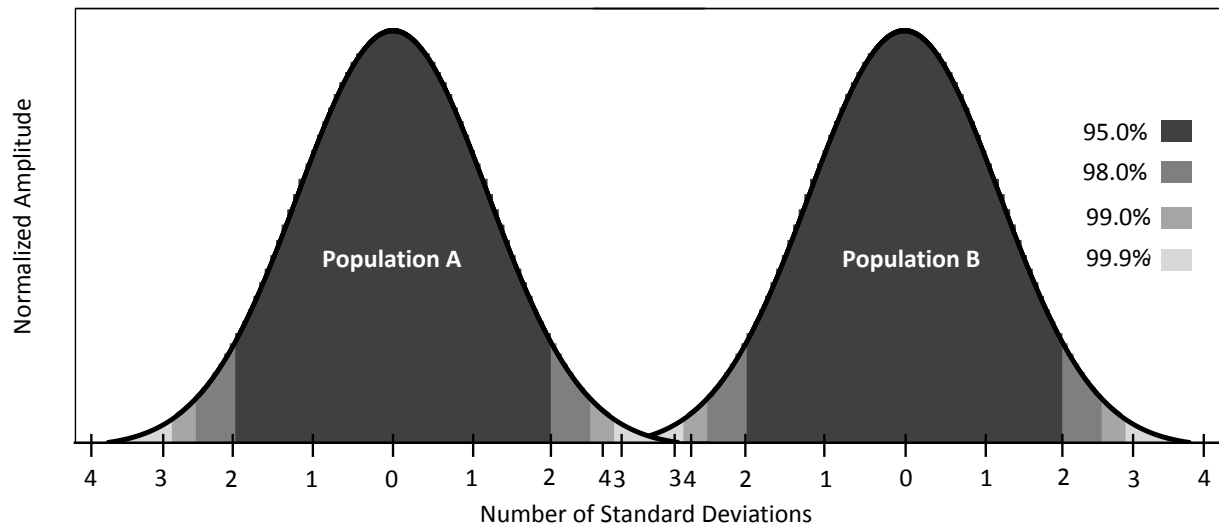


**Figure 25.** Normal distribution density curves for two sample populations for confidence levels from 95% to 99.9%.

**Table 23.** Summary of classification of simulated fire debris samples (carpet and carpet padding substrate) with inclusion of reference standards, substrate, and simulated fire debris in model.

Simulated fire debris	Classification at the following confidence levels		
	95%	99%	99.9%
PTH CPT Extract 2	NC	NC	ISO
PTH CPT Extract 3	ISO	ISO	ISO
UFP CPT Extract 2	ISO	ISO	ISO
UFP CPT Extract 3	NC	ISO	ISO
MFS CPT Extract 1	NC	PET	PET
MFS CPT Extract 2	NC	PET	PET
MFS CPT Extract 3	NC	PET	PET
LMP CPT Extract 1	PET	PET	PET
LMP CPT Extract 2	PET	PET	PET
TFL CPT Extract 2	PET	PET	PET
TFL CPT Extract 3	PET	PET	PET
CHL CPT Extract 2	PET	PET	PET
CHL CPT Extract 3	NC	PET	PET
DSL CPT Extract 1	PET	PET	PET
DSL CPT Extract 3	PET	PET	PET
KER CPT Extract 1	PET	PET	PET
KER CPT Extract 2	PET	PET	PET

Abbreviations for each liquid are listed in Table 1.

CPT indicates carpet and carpet padding substrate.

NC indicates Not classified.

ISO indicates Isoparaffinic.

PET indicates Petroleum distillate.

At the 95% confidence level, all samples are correctly classified, with the exception of one extract each of fire debris containing paint thinner, upholstery protector, and charcoal lighter. Upon further inspection of the chromatograms for these samples, all have a high abundance of the interference compounds, particularly trichloropropane, compared to the other extracts. At the highest confidence level (99.9%), all simulated fire debris samples are correctly classified although at this level, the sample containing marine fuel stabilizer (a naphthenic paraffinic liquid) is also classified as a petroleum distillate. However, this liquid is chemically similar to the petroleum distillates in the common unresolved portion of the chromatogram, as discussed previously.

With models that include fire debris samples, classification is more successful. However, the models are now so specific that even differences in abundance of the compounds from the liquid can prevent correct classification. In model building, a compromise must be reached between models that do not adequately describe the data (*e.g.*, the first models here that include

the standards only) and models that are too specific (*e.g.*, the final models that include simulated fire debris samples). For fire debris analysis, appropriate model generation is challenging as the nature of the substrate will change, as will the abundance of compounds in any liquid present. Thus, from a practical aspect, SIMCA may be limited for the classification of ignitable liquids present in fire debris samples.

Simulated fire debris samples prepared using the oil-finished wood substrate were also subjected to SIMCA in a similar manner. That is, in the first iteration, PCA models were generated for the isoparaffinic and petroleum distillate classes including only the appropriate reference standards in each model. With these models, classification was limited with only three of the nine fire debris samples correctly classified at the 99% confidence level and higher.

For the second iteration of SIMCA, PCA models for each class also included the burned oil-finished wood substrate (Table 24). While a greater number of fire debris samples are classified using these models, there is also an increase in the number of double classifications.

**Table 24.** Summary of classification of simulated fire debris samples (oil-finished wood flooring substrate) with inclusion of reference standards and burned substrate in model.

Simulated fire debris	Classification at the following confidence levels			
	95%	99%	99.5%	99.9%
PTH OWD Extract 1	ISO; PET	ISO; PET	ISO; PET	ISO; PET
PTH OWD Extract 2	NC	ISO; PET	ISO; PET	ISO; PET
PTH OWD Extract 3	ISO; PET	ISO; PET	ISO; PET	ISO; PET
TFL OWD Extract 1	NC	NC	NC	NC
TFL OWD Extract 2	NC	NC	NC	NC
TFL OWD Extract 3	PET	PET	PET	PET
DSL OWD Extract 1	PET	PET	ISO; PET	ISO; PET
DSL OWD Extract 2	PET	ISO; PET	ISO; PET	ISO; PET
DSL OWD Extract 3	PET	PET	PET	ISO; PET

Abbreviations for each liquid are listed in Table 1.

OWD indicates oil-finished wood substrate.

NC indicates Not classified.

ISO indicates Isoparaffinic; PET indicates Petroleum distillate.

ISO; PET indicates sample classified as both isoparaffinic and petroleum distillate.

All fire debris samples containing paint thinner are classified as members of both the isoparaffinic and petroleum distillate classes (Table 24) at confidence levels of 99% and greater. This double classification is due to the inclusion of the substrate in the models—the fire debris samples contain the normal alkanes from the substrate which are represented in both models. Similarly, fire debris samples containing diesel are correctly classified as petroleum distillates at confidence levels of 95% and greater. However, at higher confidence levels, fire debris samples are also considered to be members of the isoparaffinic class. Again, this is due to the inclusion of the substrate in the model.

Of the torch fuel-containing debris samples, only one extract (Extract 3) is classified at any of the confidence levels investigated. From assessment of relevant chromatograms, this lack of classification is due to differences in the abundance of two compounds present in the chromatograms: a substituted cycloketone ( $t_R$  13.7 min) that is an interference compound from the burned wood substrate and tridecane ( $t_R$  13.9 min) that is from the torch fuel. Extracts 1 and 2 contain a high abundance of the interference compound compared to the alkane whereas, Extract 3 contains a lower abundance of the interference compound. Extract 3, therefore, is more similar to the torch fuel reference standards (that contain no substrate interference compounds), resulting in appropriate classification.

In the final SIMCA iteration, replicates of one simulated fire debris sample for each liquid were included in the appropriate model. The models were then used to classify the remaining two fire debris samples for each liquid (Table 25). Classification was similar to that obtained previously when only the substrate was included in the model (previously shown in Table 24). However, with the inclusion of simulated fire debris samples, it is now possible to correctly classify a second fire debris sample containing torch fuel at the 99.5 and 99.9% confidence levels. In the previous model, this extract (Extract 2) was not classified primarily due to a high abundance of an interference compound from the substrate (discussed above). However, in this iteration of SIMCA, the fire debris extract included in the model (Extract 1) also contains a high abundance of this interference compound such that appropriate classification is now possible.

**Table 25.** Summary of classification of simulated fire debris samples (oil-finished wood substrate) with inclusion of reference standards, burned substrate, and simulated fire debris in model.

Simulated fire debris	Classification at the following confidence levels			
	95%	99%	99.5%	99.9%
PTH OWD Extract 2	ISO; PET	ISO; PET	ISO; PET	ISO; PET
PTH OWD Extract 3	ISO; PET	ISO; PET	ISO; PET	ISO; PET
TFL OWD Extract 2	NC	NC	PET	PET
TFL OWD Extract 3	PET	PET	PET	PET
DSL OWD Extract 1	PET	PET	ISO; PET	ISO; PET
DSL OWD Extract 2	PET	ISO; PET	ISO; PET	ISO; PET

Abbreviations for each liquid are listed in Table 1.

OWD indicates oil-finished wood substrate.

NC indicates Not classified.

ISO indicates Isoparaffinic; PET indicates Petroleum distillate.

ISO; PET indicates sample classified as both isoparaffinic and petroleum distillate.

For both substrates, some degree of classification of simulated fire debris samples is possible. However, development of representative models is challenging, requiring models that are sufficiently representative without being too specific. In this research, classification to any extent was only possible with inclusion of at least the burned substrate in the models. For practical applications in a forensic laboratory, this is a major limitation, particularly for fire debris analysis as, in many cases, the identity of the substrate will not be known or easily identifiable.

#### 4.1.7 *k*-Nearest Neighbors

The *k*-nearest neighbors (*k*-NN) classification procedure differs from SIMCA in a number of ways. Firstly, *k*-NN is a ‘hard’ classification, meaning that each sample will be classified into one, and only one, class. While this prevents samples being classified into more than one class (previously observed using SIMCA, section 4.1.6), the risk of misclassification remains as all samples are forced to be members of a class. Secondly, the SIMCA procedure is based on statistical models that must be representative of the samples to be classified for the actual classification to be accurate. However, as discussed in the previous section, this requirement is a

limitation for classification of ignitable liquids in fire debris. In contrast,  $k$ -NN does not require model development; instead, the full data set is considered and classification is based on distance of the samples to the standards in multidimensional space.

All reference standards were used in the training set to investigate the appropriate number of nearest neighbors ( $k$ ) to use for classification. For  $k = 1$  through to  $k = 10$  (all integer values investigated), every reference standard was classified correctly, indicating that any value  $k$  could be used for the subsequent classification. However, lower  $k$  values are more prone to misclassification if outliers are present in the data set and/or the classes are not sufficiently distinct. To avoid any potential problems,  $k = 5$  was initially used for classification.

Using this number of neighbors, the simulated samples in Set 1 (carpet and carpet padding substrate) are correctly classified according to ASTM class, with only one exception: one extract of simulated fire debris containing paint thinner is classified as a petroleum distillate. This particular extract was consistently misclassified using SIMCA primarily due to the high abundance of substrate interference compounds and low abundance of compounds characteristic of the liquid. It is interesting to note that simulated fire debris containing diesel is correctly classified using  $k$ -NN whereas, these samples were not exclusively classified using SIMCA due to the high abundance of substrate compounds coupled with the low abundance of compounds from diesel itself. It should also be noted that the  $k$ -NN classification of the simulated samples was repeated using  $k = 1, 3, 7,$  and  $9$ , with the same classification results being returned irrespective of the number of neighbors used for classification.

Set 2 of the simulated fire debris samples (oil-finished wood substrate) was also subjected to  $k$ -NN. Classification was performed using  $k = 1, 3, 5, 7,$  and  $9$  and in each case, the same classification was obtained. That is, the simulated fire debris samples containing paint thinner are misclassified as naphthenic paraffinic while the debris samples containing torch fuel and diesel are correctly classified as petroleum distillates. Misclassification of the paint thinner is likely due to the unresolved region in the chromatogram that occurs over a similar retention time range, along with the presence of later-eluting compounds in the same range, as observed in the marine fuel stabilizer (the only naphthenic paraffinic in the data set) reference standard.

Despite the afore-mentioned misclassifications,  $k$ -NN was demonstrated to be more successful and hence, have greater potential, for the analysis of fire debris. As discussed previously, generating the necessary SIMCA models that are sufficiently representative without

being too specific is challenging, especially for fire debris applications. As the  $k$ -NN approach is not model-based, these limitations are not a factor and hence, this approach is worthy of further investigation and validation.

## 4.2 Spectral Data

Exemplar spectra of the controlled substance reference standards and simulated street samples are included in Appendix 3.

### 4.2.1 Normalization

The spectral data for the controlled substance reference standards were normalized using three different procedures: constant sum, constant vector length, and SNV normalization. The non-normalized and normalized data sets were individually subjected to PCA to assess the effect of normalization on the association of replicates of each standard and the distinction of different standards. The resulting scores plots are shown in Figure 26.

For the non-normalized data, there is substantial spread among replicates of each standard on both PC1 and PC2 (Figure 26A). As a result of the spread, there are no distinct clusters of any of the standards such that association and discrimination is not possible. Similar trends are observed for the data after normalization to constant sum (Figure 26B) and after normalization to constant vector length (Figure 26C). In contrast, for the SNV-normalized data, replicates of each standard are closely positioned in the scores plot (Figure 26D) and clear differentiation among the three classes of controlled substances (amphetamines, opiates, and barbiturates) is possible.

To quantify the improvement in clustering of the replicates, the relative standard deviation of the scores on both PC1 and PC2 was calculated for each reference standard (Tables 26 and 27). On PC1, there is improved precision among replicates of all reference standards as indicated by the low relative standard deviations. This trend is also true for PC2, with the exception of replicates of MDEA, MDMA, methamphetamine, and phenobarbital. For these standards, precision of replicates is improved using the other normalization procedures. However, in general, the RSDs obtained for these standards after SNV normalization are

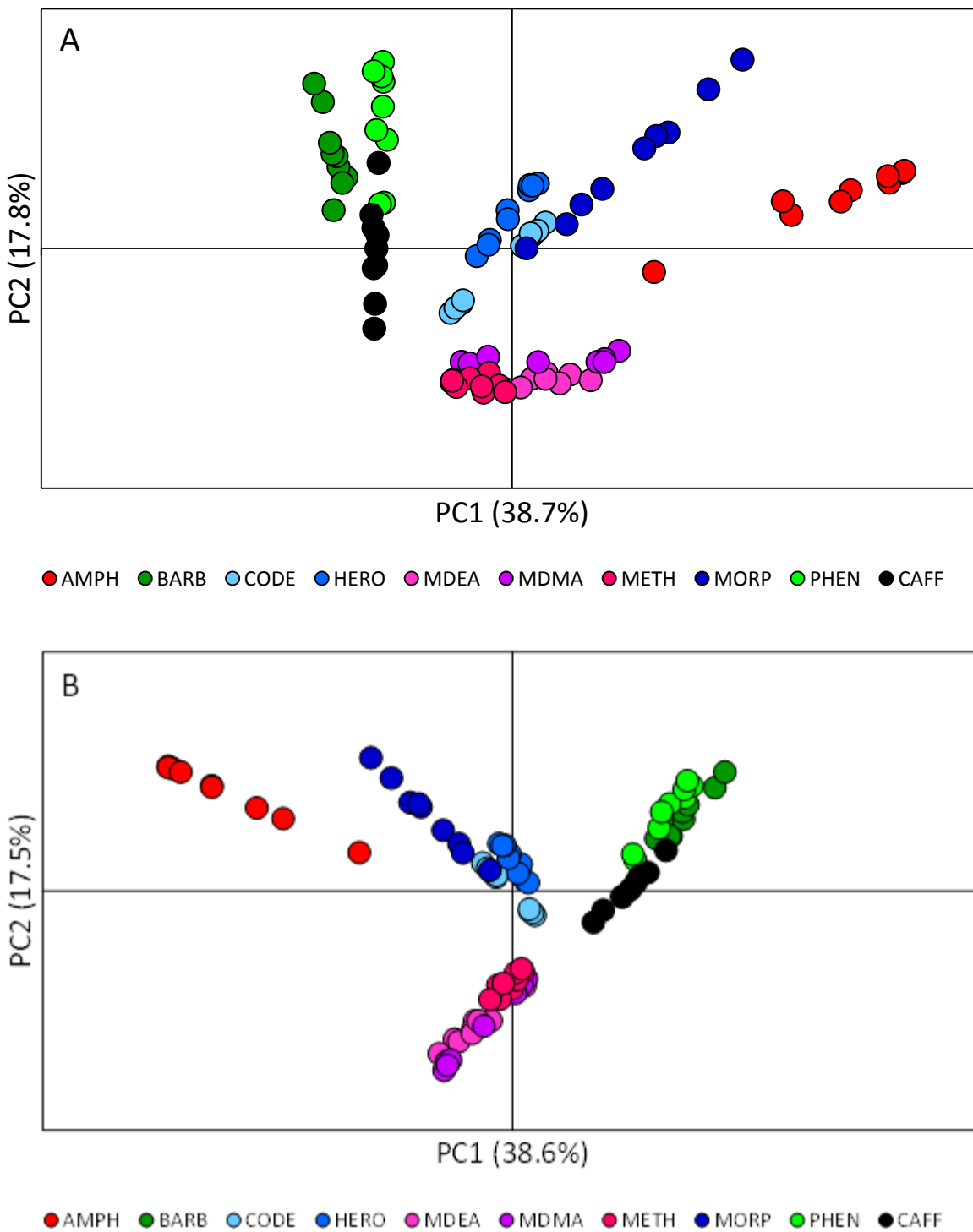


**Figure 26.** Scores plot for controlled substance reference standards with (A) no normalization, (B) constant sum normalization, (C) constant vector length normalization and (D) standard normal variate normalization. Abbreviations for each standard are defined in Table 3.

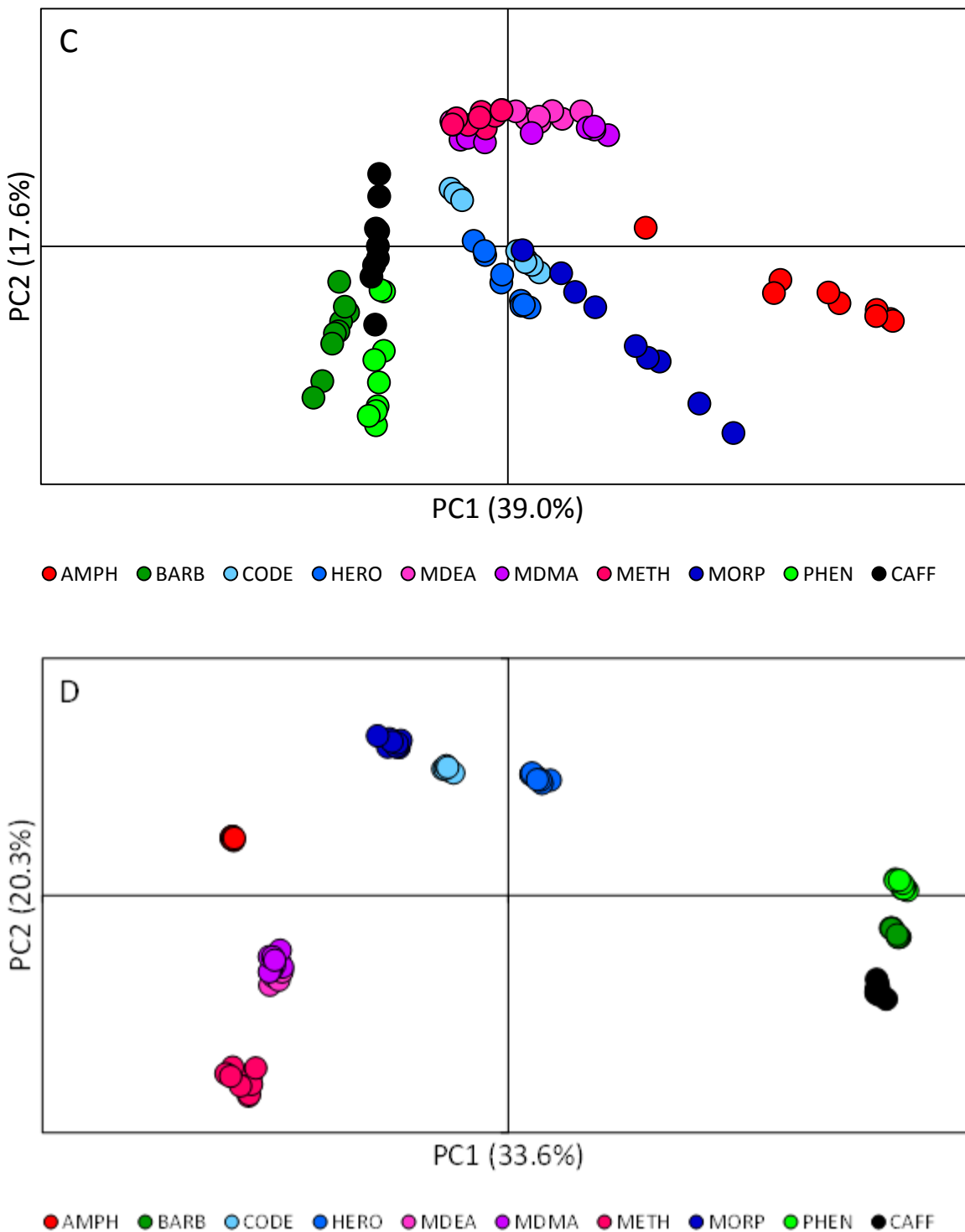


**Figure 26 contd.** Scores plot for controlled substance reference standards with (A) no normalization, (B) constant sum normalization, (C) constant vector length normalization and (D) standard normal variate normalization. Abbreviations for each standard are defined in Table 3.

comparable to those RSDs obtained using the other normalization procedures. Hence, for all subsequent data analysis, the reference standards were normalized using the SNV procedure.

**Table 26.** Relative standard deviation of scores on the first principal component (PC1) for non-normalized and normalized controlled substance reference standards.

Reference standard	Relative standard deviation on PC1			
	Non-normalized	Constant sum	Constant vector length	Standard normal variate
Amphetamine	25.2	0.4	0.4	0.4
Barbital	5.5	12.8	6.4	0.9
Codeine	336.5	660.8	342.8	4.8
Heroin	3076.0	1588.1	672.1	20.8
MDEA	169.1	63.4	170.2	1.7
MDMA	245.4	130.7	247.5	2.1
Methamphetamine	56.1	341.1	55.6	4.1
Morphine	57.6	45.4	57.7	6.5
Phenobarbital	3.1	14.3	3.7	1.1
Caffeine	1.6	19.0	2.0	0.9

**Table 27.** Relative standard deviation of scores on the second principal component (PC2) for non-normalized and normalized controlled substance reference standards.

Reference standard	Relative standard deviation on PC2			
	Non-normalized	Constant sum	Constant vector length	Standard normal variate
Amphetamine	62.4	29.6	58.6	2.3
Barbital	41.3	29.8	41.0	11.0
Codeine	221.8	1349.8	255.6	1.6
Heroin	80.3	50.6	77.2	2.9
MDEA	4.1	14.0	3.7	6.5
MDMA	3.9	29.5	4.9	10.6
Methamphetamine	4.8	12.3	5.0	5.8
Morphine	70.1	48.6	67.4	2.7
Phenobarbital	42.2	36.9	41.6	40.3
Caffeine	2225.2	988.3	2448.2	6.2

#### 4.2.2 Principal Components Analysis

Principal components analysis was initially performed on the SNV-normalized reference standards and the scores plot of PC1 and PC2 is shown in Figure 27.

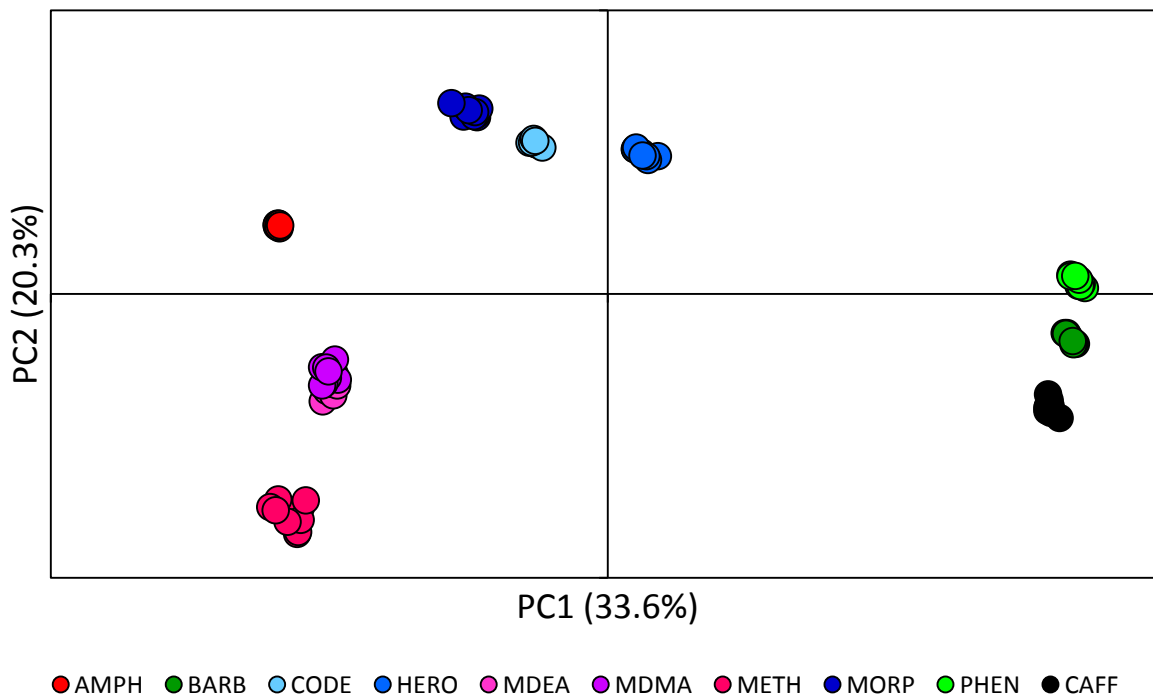


**Figure 27.** Scores plot of PC1 versus PC2 for controlled substance reference standards. Each reference standard was analyzed in replicate (n=9) and each standard is represented by a different color in the plot. Abbreviations for each standard are defined in Table 3.

The first two PCs account for 54% of the variance among the reference standards. Replicates of each standard are closely positioned and three groups of the standards are apparent. The first contains standards in the amphetamine class, the second contains standards in the opiates class, and the third contains the two barbiturate standards. The caffeine standard is positioned closely to the barbiturate standards, most notably on PC1. Hence, although the first two principal components only describe 54% of the variance in the data set, this is sufficient to distinguish the reference standards.

The majority of the positively-weighted contributions in the PC1 loadings plot (Figure 28A) result from the barbital, phenobarbital, and caffeine reference standards and hence, these three standards are positioned positively on PC1 in the scores plot (Figure 27). The majority of the negatively-weighted contributions result from the amphetamine, MDEA, MDMA, and methamphetamine reference standards. As a result, the amphetamine class of standards is positioned negatively on PC1 in the scores plot (Figure 27). Thus, the first principal component essentially distinguishes the barbiturate and amphetamine classes.

The majority of the positively-weighted contributions in the PC2 loadings plot (Figure 28B) result from the opiate class of standards and hence, this class is positioned positively on PC2 in the scores plot (Figure 27). The majority of the negatively-weighted contributions result from the MDEA, MDMA, methamphetamine, and caffeine standards. As a result, these four standards are positioned negatively on PC2 in the scores plot (Figure 27).

The two barbiturate standards have an equal number of positive and negative contributions on PC2 but barbital is positioned negatively while phenobarbital is positioned positively on this PC. This is explained with reference to the loadings (the product of the mean-centered data and the PC2 eigenvector). For barbital, there are more negative loadings than positive across all variables with the result that the score (the sum of the loadings) is negative. In contrast, for phenobarbital, there are more positive loadings than negative, resulting in a positive score on this PC.

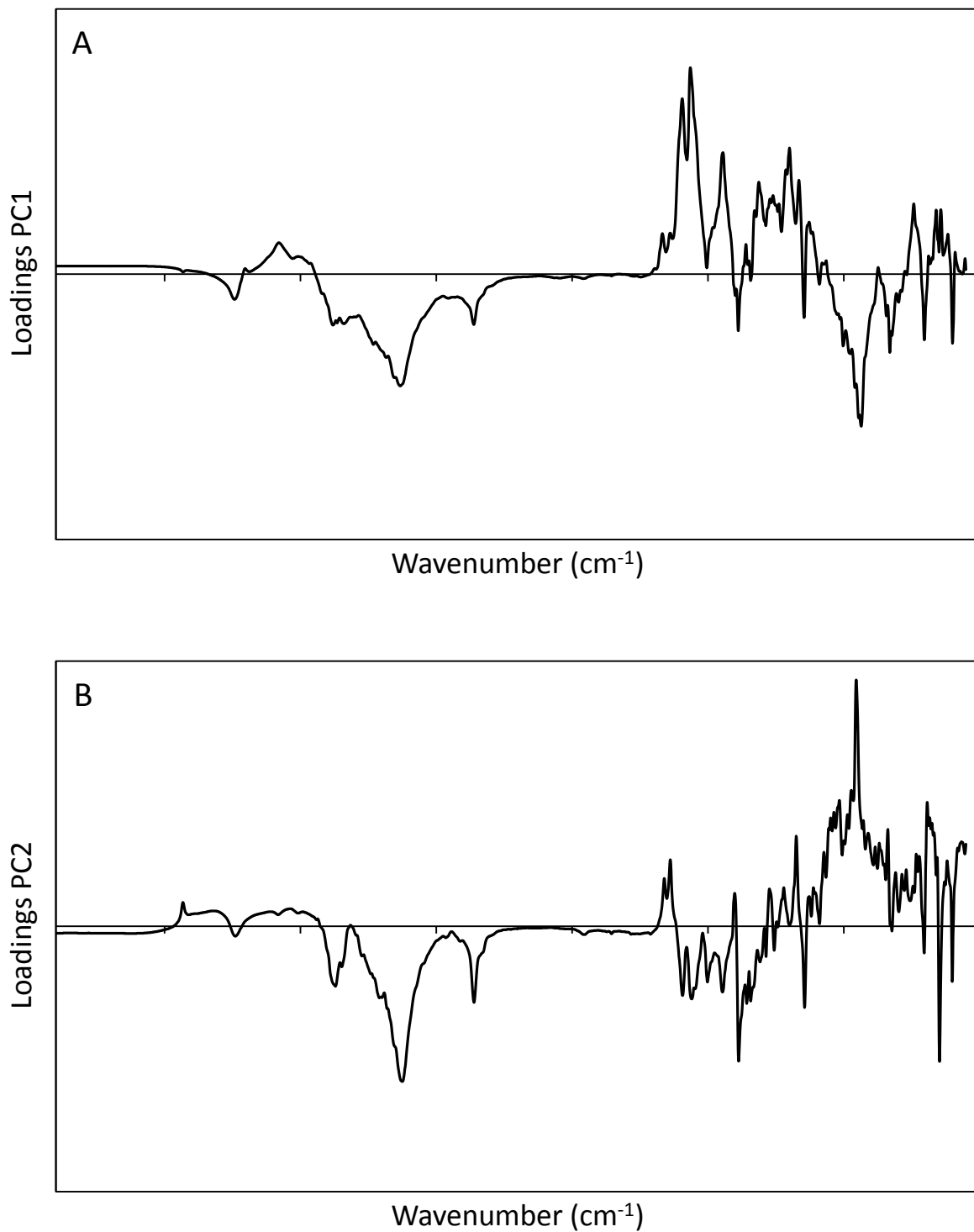


**Figure 28.** Loadings plot of (A) PC1 and (B) PC2 for controlled substance reference standards.

To investigate association of simulated street samples to the corresponding controlled substance reference standard, scores were calculated for the samples and then projected onto the scores plot, following the procedure described previously (section 4.1.4). The scores plot with the 80/20 samples (80 parts controlled substance/20 parts caffeine, by mass) projected is shown in Figure 29 while the plot with the 50/50 samples (50 parts controlled substance/50 parts caffeine, by mass) projected is shown in Figure 30. Within a forensic laboratory, it is more likely that a single case sample would be included with the reference standards for PCA rather than multiple samples as shown here. However, as scores for each sample are calculated using the relevant mean-centered data and the eigenvectors generated for the standards, the positioning of individual samples does not change if only one sample is included in the data set. For these reasons, additional scores plots showing the reference standards with the inclusion of one simulated sample at a time are not shown here.

The 80/20 samples are positioned more positively on PC1 than the reference standards, with a shift toward the caffeine standard. This shift is primarily due to the additional presence of two absorptions ( $1694$  and  $1649\text{ cm}^{-1}$ ) from caffeine that are present in the simulated samples. These two absorptions have positive contributions to the PC1 eigenvector, resulting in the positive shift observed.

The 80/20 samples are positioned more closely to the respective standard on PC2, albeit slightly more negatively. This is also primarily due to the presence of the two absorbance bands resulting from caffeine, which have a negative contribution on PC2. The exceptions to this are the samples containing codeine for which there is a greater negative shift on PC2 compared to the standard. For these particular samples, the absorptions from caffeine mask two of the absorptions from codeine. Accordingly, there is less contribution from the controlled substance and a greater shift toward caffeine. Despite the shifts observed on PC2, association of the 80/20 samples to the respective standards is possible on this principal component.

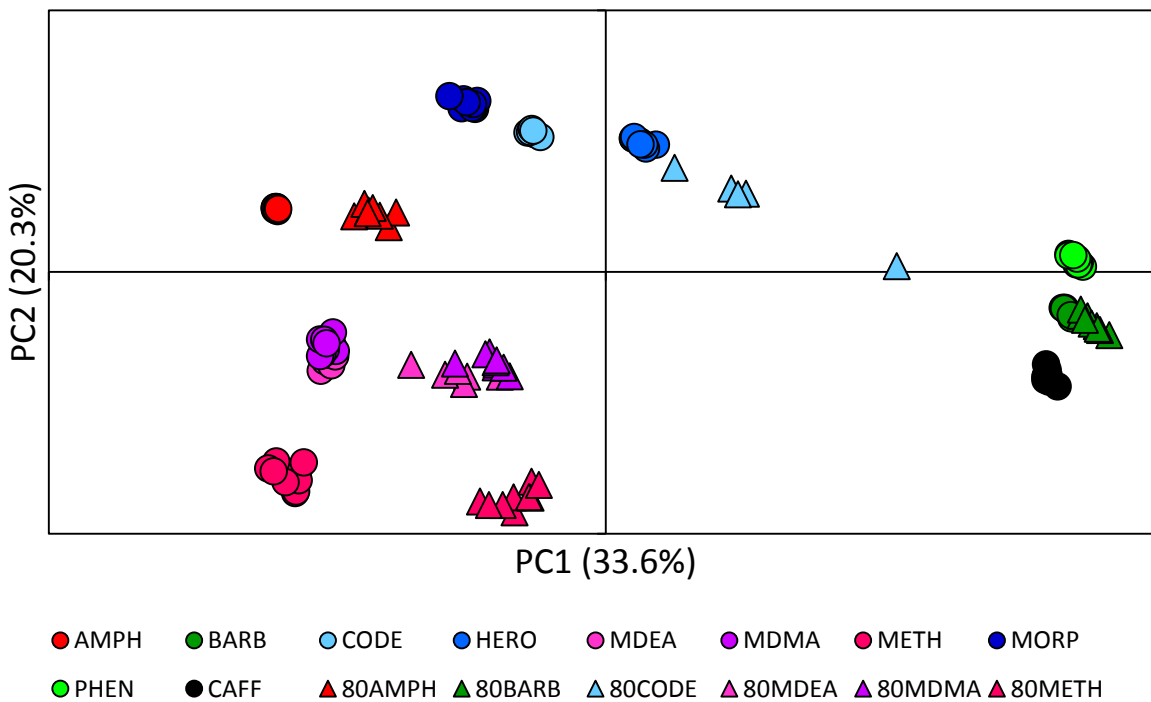


**Figure 29.** Scores plot of PC1 versus PC2 for the controlled substance reference standards and simulated street samples containing 80 parts controlled substance/20 parts caffeine, by mass. Each reference standard was analyzed in replicate (n=9) and each standard is represented by a different color in the plot. Reference standards are shown as circles and simulated samples are shown as triangles, with the color corresponding to the controlled substance present. Abbreviations for each standard are defined in Table 3.

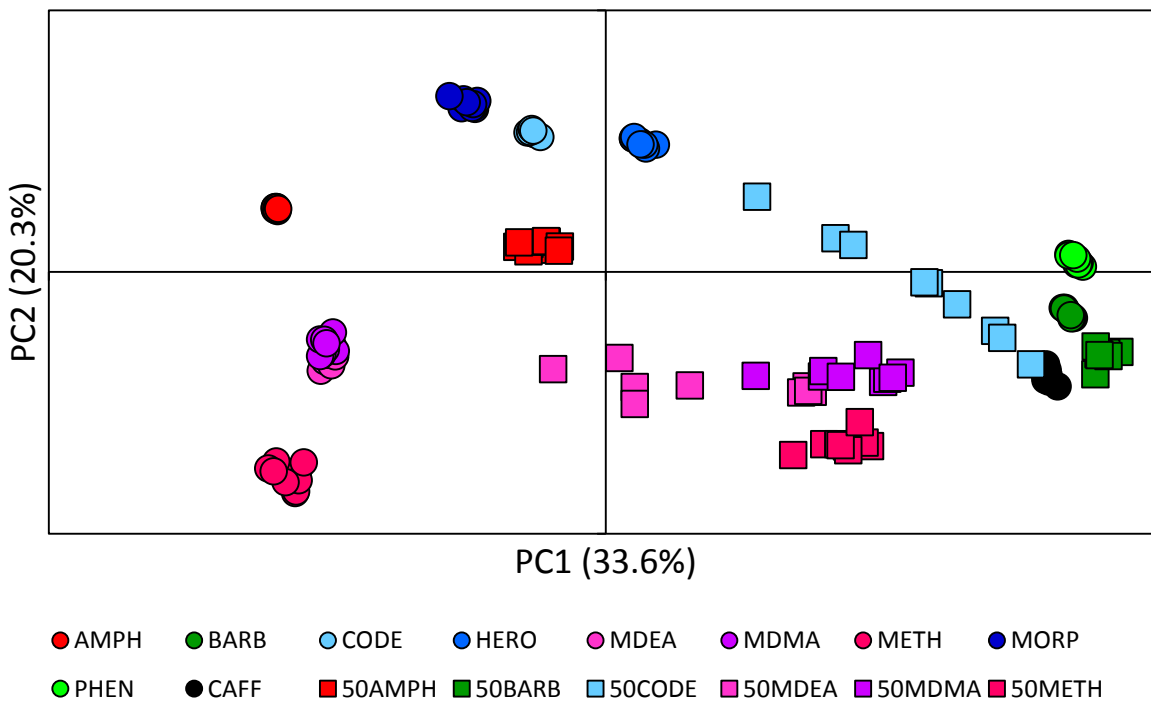


**Figure 30.** Scores plot of PC1 versus PC2 for the controlled substance reference standards and simulated street samples containing 50 parts controlled substance/50 parts caffeine, by mass. Each reference standard was analyzed in replicate (n=9) and each standard is represented by a different color in the plot. Reference standards are shown as circles and simulated samples are shown as squares with the color corresponding to the controlled substance present. Abbreviations for each standard are defined in Table 3.

Similar trends are observed for the 50/50 simulated samples; that is, the samples have similar scores on PC2 as the corresponding standards but have more positive scores on PC1 due to the contributions from caffeine. However, as the caffeine content of the 50/50 samples is greater, the shift on PC1 is more apparent than for the 80/20 samples. This greater shift prevents confident association of the 50/50 samples to the corresponding reference standard.

To provide a more quantitative assessment of the scores plot, Euclidean distances and PPMC coefficients were calculated between each simulated sample and all reference standards (Tables 28 and 29). Quantitative assessment of both scores plots was performed; however, due to the large shifts observed in the scores plot for the 50/50 samples, quantitative assessment provided no additional information. Hence, only quantitative assessment of association of the 80/20 samples and reference standards is discussed below. Additionally, as discrimination was possible based on the first two principal components, Euclidean distances and PPMC coefficients were calculated using only these two PCs.

**Table 28.** Euclidean distance between simulated street samples and reference standards calculated based on scores for first two principal components.

Reference standard	Euclidean distance between reference standard and simulated sample containing					
	Amphetamine	Barbital	Codeine	MDEA	MDMA	Methamphetamine
Amphetamine	<b>7.86</b>	68.78	38.88	32.05	31.76	53.33
Barbital	58.81	<b>2.46</b>	31.63	50.51	47.39	54.91
Codeine	18.93	55.73	21.67	42.02	39.75	62.82
Heroin	24.83	47.83	<b>13.89</b>	42.56	39.80	61.97
MDEA	25.52	61.96	43.97	<b>10.62</b>	<b>13.13</b>	28.01
MDMA	23.12	61.97	42.67	<b>11.66</b>	<b>13.67</b>	30.24
Methamphetamine	45.65	70.06	60.39	22.10	25.31	<b>18.64</b>
Morphine	20.28	62.90	28.81	46.53	44.60	67.85
Phenobarbital	57.30	10.90	27.54	53.68	50.37	61.09
Caffeine	61.41	9.97	38.18	47.76	45.03	47.92

In Table 28, the shortest Euclidean distance for each comparison is highlighted in bold. In general, the shortest distance is observed between the sample and the corresponding reference standard and in each case, this distance is approximately half the next greatest distance. The exceptions are the samples containing codeine, MDEA, and MDMA. For codeine, the shortest distance is to the heroin reference standard, while the next shortest distance is to the codeine standard. For the simulated samples containing MDEA and MDMA, there is little difference in

the distance calculated between the sample and both the MDEA and MDMA reference standards. That is, it is not possible to associate the samples to the corresponding reference standard; rather, the samples are equally associated to both MDEA and MDMA.

**Table 29.** Absolute mean PPMC coefficient calculated using the first two principal components to assess association of simulated street samples to controlled substance reference standards.

Reference standard	Absolute mean PPMC coefficient based on first two principal components for comparison of reference standard and samples containing					
	Amphetamine	Barbital	Codeine	MDEA	MDMA	Methamphetamine
Amphetamine	<b>0.936</b>	0.636	0.152	0.129	0.260	0.299
Barbital	0.500	<b>0.955</b>	0.134	0.246	0.111	0.067
Codeine	0.349	0.460	<b>0.515</b>	0.300	0.523	0.547
Heroin	0.086	0.320	0.189	0.186	0.263	0.634
MDEA	0.112	0.510	0.494	<b>0.828</b>	0.545	0.195
MDMA	0.193	0.416	0.606	0.609	<b>0.694</b>	0.220
Methamphetamine	0.179	0.279	0.516	0.212	0.156	<b>0.810</b>
Morphine	0.675	0.517	0.234	0.247	0.341	0.629
Phenobarbital	0.565	0.705	0.232	0.252	0.044	0.141
Caffeine	0.333	0.782	0.320	0.031	0.237	0.311

In Table 29, coefficients indicating correlation between samples and corresponding standards are shown in bold. For each simulated sample, the highest coefficient is observed for comparison to the corresponding reference standard and in general, strong correlation is indicated. Exceptions are the simulated street samples containing MDMA and codeine. For MDMA, the highest coefficient is observed for comparison of the simulated sample to the reference standard; however, only a moderate correlation is indicated. For the simulated sample containing codeine, only a moderate correlation is observed between the simulated sample and reference standard. In addition, higher coefficients are observed for the codeine simulated sample and the MDMA and methamphetamine reference standards.

From the scores plot (Figure 29) and the Euclidean distances calculated (Table 28), clear association of the samples containing MDEA and MDMA to their respective standards is not possible, with each sample being equally associated to both standards. However, when calculating PPMC coefficients based on the first two principal components, association of these samples to the corresponding reference standard is indicated (Table 29), based on the highest coefficients. It should be noted that the sample containing MDEA is moderately correlated to the

MDMA standard while the sample containing MDMA is moderately correlated to the MDEA standard.

#### 4.2.3 Hierarchical Cluster Analysis

Cluster analysis was initially performed on the controlled substance reference standards only, using three different linkage methods (single, complete, and average linkage). The corresponding dendrograms are shown in Figure 31 and a summary of the clustering obtained using each linkage method is given in Table 30.

**Table 30.** Similarity level at which replicates and controlled substances within each class cluster.

Reference standard	Similarity level (%) of clusters		
	Euclidean distance Single linkage	Euclidean distance Complete linkage	Euclidean distance Average linkage
Amphetamine	95.4	92.6	94.6
MDEA	94.3	89.2	91.0
MDMA	91.2	87.3	88.8
Methamphetamine	91.9	89.1	
<b>Amphetamines</b>	9.8	2.6	12.7
Codeine	94.1	94.2	94.7
Heroin	95.4	94.0	95.2
Morphine	90.6	86.2	87.7
<b>Opiates</b>	16.2	20.6	21.3
Barbital	94.5	94.8	94.9
Phenobarbital	96.4	94.9	95.8
<b>Barbiturates</b>	14.3	37.1	30.2
Caffeine	91.1	83.8	87.7

There are no substantial differences in the clusters formed using the three linkage methods. In all cases, replicates of each reference standard form clusters at similarity levels greater than 87%. Furthermore, replicates form clusters before forming clusters with other reference standards. In general, controlled substances in the same class cluster first before clustering with standards in other classes. The exception to this is the amphetamine reference standard which, irrespective of linkage method, forms a cluster with morphine and codeine before clustering with the other amphetamine-type stimulants.

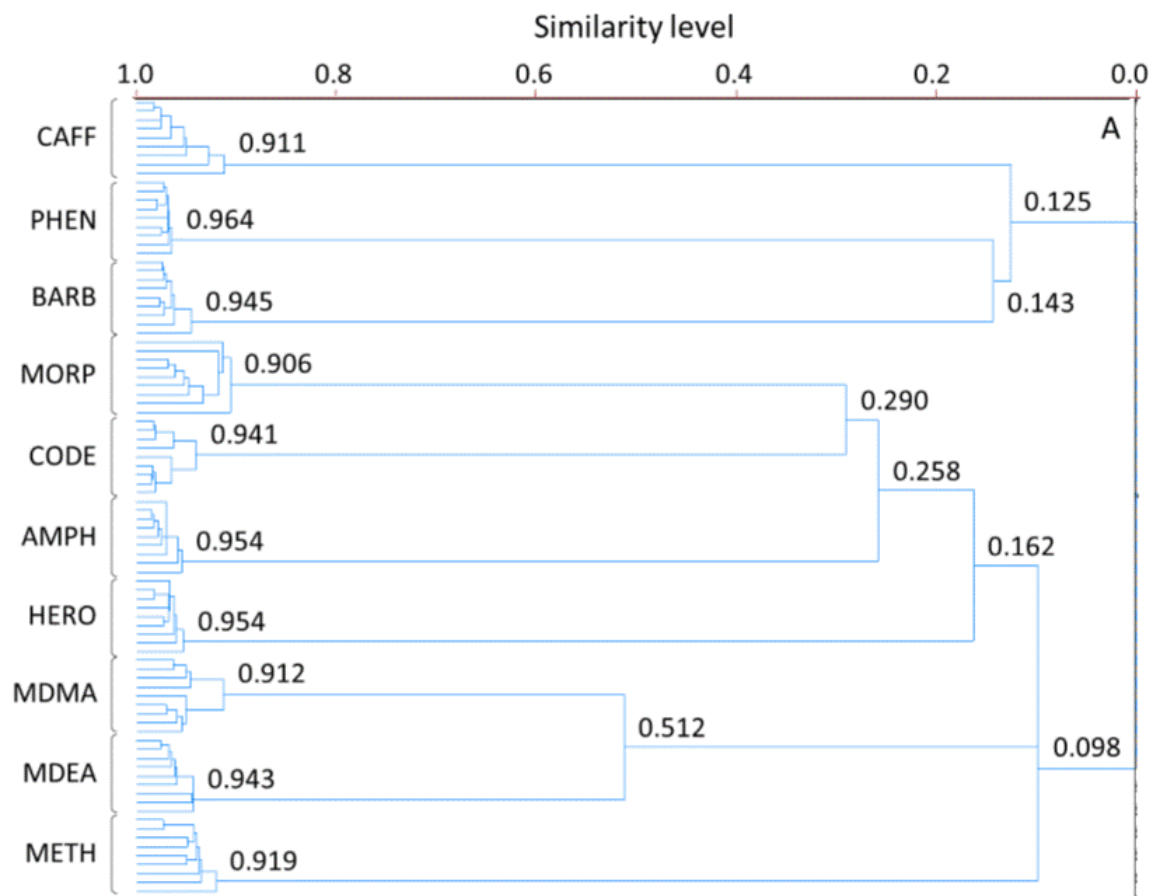


**Figure 31.** Hierarchical cluster analysis of controlled substance reference standards using Euclidean distance and (A) single linkage, (B) complete linkage, and (C) average linkage. Abbreviations for each standard are defined in Table 3.

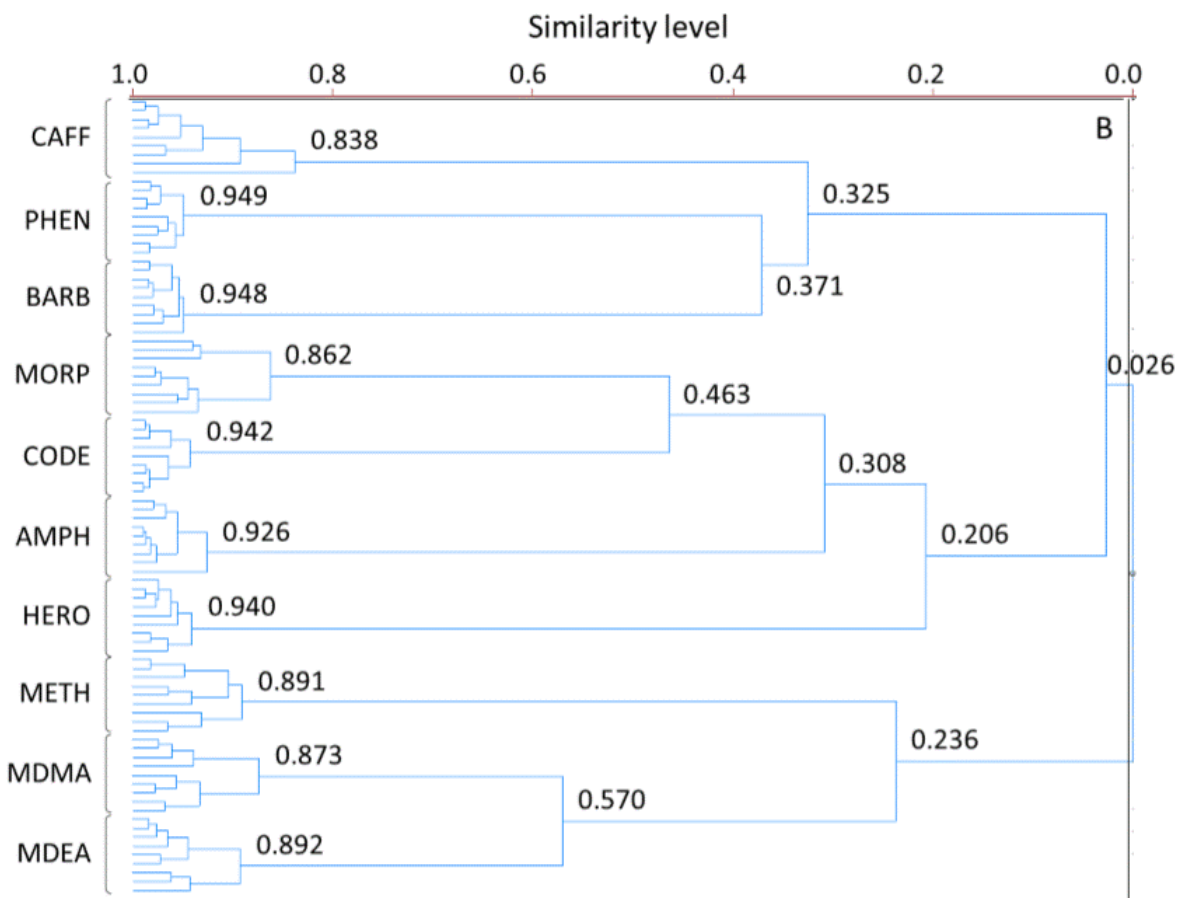


**Figure 31 contd.** Hierarchical cluster analysis of controlled substance reference standards using Euclidean distance and (A) single linkage, (B) complete linkage, and (C) average linkage. Abbreviations for each standard are defined in Table 3.

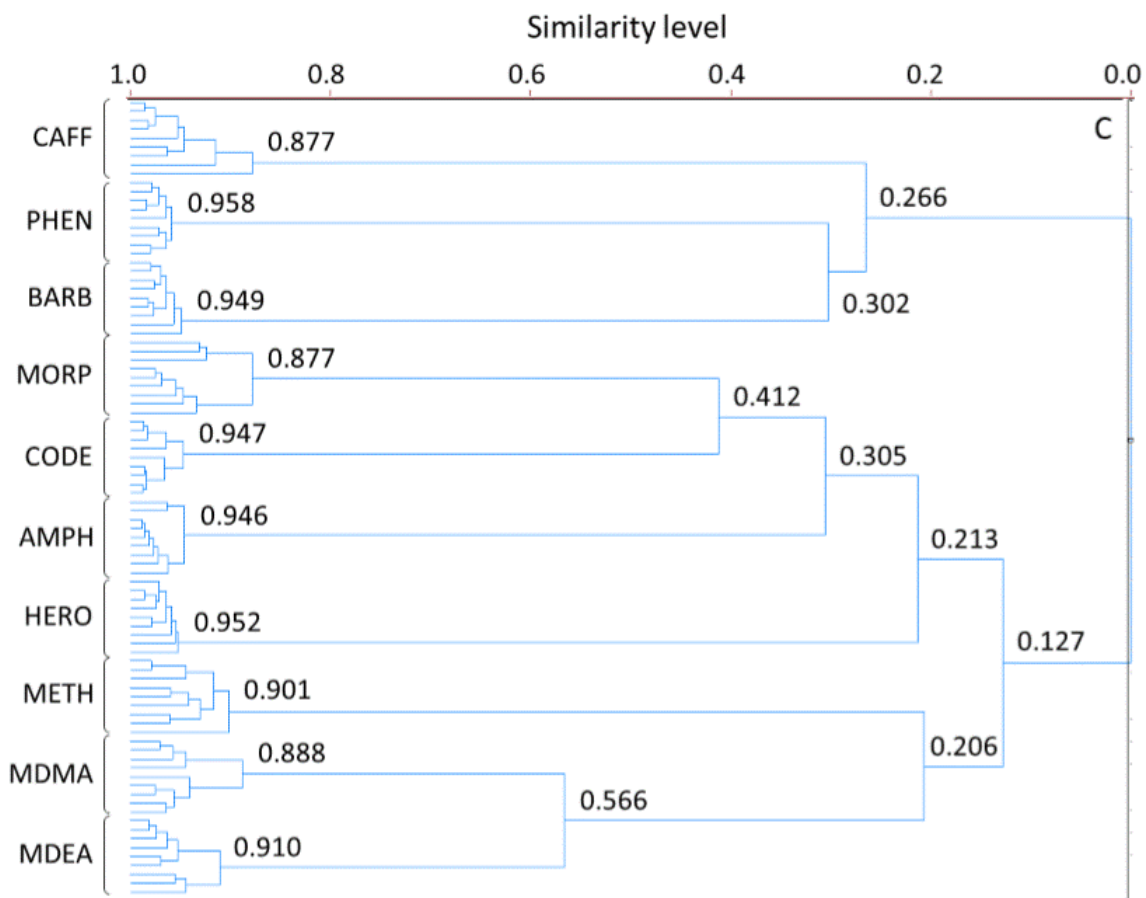


**Figure 31 contd.** Hierarchical cluster analysis of controlled substance reference standards using Euclidean distance and (A) single linkage, (B) complete linkage, and (C) average linkage. Abbreviations for each standard are defined in Table 3.

However, the similarity level at which amphetamine clusters with morphine and codeine is relatively low (25.8%, 30.8%, and 30.5% for single, complete, and average linkage methods, respectively). Due to the similarities in the clusters formed, any of the three linkage methods could be used in subsequent data analysis. For the purposes of this research, the single linkage method was again selected as this method is analogous to the *k*-NN classification method, as discussed previously.

To investigate association of simulated street samples to the appropriate reference standards, HCA was repeated including one simulated sample at a time with the reference standards. All dendrograms are shown in Appendix 6 and a summary of the results is given in Table 31.

**Table 31.** Similarity level at which simulated samples cluster with corresponding reference standard.

<b>Simulated street sample containing</b>	<b>Similarity level (%) of cluster formation with corresponding standard</b>
Amphetamine, 80/20	75.0
Amphetamine, 50/50	45.1
Barbital, 80/20	73.7
Barbital, 50/50	45.4
Codeine, 80/20	51.5
Codeine, 50/50	47.8
MDEA, 80/20	77.6
MDEA, 50/50	53.5
MDMA, 80/20	62.1
MDMA, 50/50	2.3
Methamphetamine, 80/20	58.2
Methamphetamine, 50/50	0.0

80/20 indicates samples containing 80 parts controlled substance and 20 parts caffeine.

50/50 indicates samples containing 50 parts controlled substance and 50 parts caffeine.

Using HCA, association of the 80/20 samples to the respective standard is possible. All samples form clusters with the standards first, before forming subsequent clusters. Hence, despite only 51.5% similarity between the 80/20 codeine sample and respective standard, this sample is most similar to the codeine reference standard than to any other standard in the data set. A similar general trend is observed for the 50/50 samples: although similarity levels are around 45%, the simulated samples are most similar to the respective standards than any other standard or sample in the data set. However, there are notable exceptions to this trend. The 50/50

simulated sample containing barbital first clusters with caffeine (at a similarity level of 59.3%) before clustering with the barbital standard (at a similarity level of 45.4%). Despite first clustering with the cutting agent, this simulated sample is still most similar to the barbital standard than to any other reference standard in the data set. The 50/50 samples containing MDMA and methamphetamine are also both most similar to caffeine (50.0% and 56.5%, respectively). However, in this instance, these samples first form clusters with other standards and only cluster to the appropriate standard at very low similarity levels (2.3% and 0.0% for MDMA and methamphetamine, respectively).

#### 4.2.4 Soft Independent Modeling of Class Analogy

Initially, PCA models were developed for each reference standard; however, when the optimal number of PCs (1) in each model are maintained, none of the 80/20 simulated samples are classified at any of the confidence levels investigated ( $\alpha = 0.25$  to 0.001). In each model, the first principal component accounts for 97-100% of the variance in the data set. As a result, the models are too specific which prevents classification of the simulated samples. In cases such as this, the next step would typically be to include more principal components in the models to better describe data. However, for these data, no advantage is gained in doing this as the subsequent PCs describe a negligible proportion of the variance.

To more adequately describe the data, simulated samples were included in the PCA models. Each model therefore contained the appropriate controlled substance reference standards, caffeine, and four of the nine corresponding simulated samples. Exceptions to this were the models for codeine and MDEA, for which three simulated samples were included in the model. All PCA models retained one PC (which accounted for 99.1-99.5% variance), except codeine for which the optimal number of PCs was three (which accounted for 99.9% variance). With these models, classification of the 80/20 simulated samples is possible at different confidence levels, as summarized in Table 32.

With the exception of simulated samples containing codeine and MDEA, classification ability improves as confidence level increases. However, and as discussed previously, higher confidence levels are less rigorous with regards to association and hence, the observed trend is not unexpected. All classified samples are exclusively classified; that is, none are also considered a member of additional classes, indicating sufficient discrimination among the defined classes.

However, for codeine, only one of the two samples is correctly classified while interestingly, no MDEA samples are classified at any confidence level.

**Table 32.** Summary of classification of 80/20 simulated samples with inclusion of reference standards and selected simulated samples in model.

Simulated samples containing	Samples classified (%) at the following confidence levels		
	95%	99%	99.9%
Amphetamine, 80/20	80	100	100
Barbital, 80/20	80	80	100
Codeine, 80/20	50	50	50
MDEA, 80/20	0	0	0
MDMA, 80/20	80	80	100
Methamphetamine, 80/20	60	100	100

80/20 indicates samples containing 80 parts controlled substance and 20 parts caffeine.

For each model, four corresponding simulated samples were also included, with the exception of codeine and MDEA, for which three simulated samples were included.

For classification, five simulated samples were available for each controlled substance, with the exception of codeine, for which two simulated samples were available, and MDEA, for which three simulated samples were available.

Spectra of the codeine and MDEA simulated samples were overlaid to highlight any substantial differences among the spectra that may explain the lack of classification. Slight differences in abundance are apparent, especially in the wavenumber range 1720-1620  $\text{cm}^{-1}$  (shown as inset in Figure 32) which corresponds to absorptions from caffeine. For codeine, the intensity of these absorptions in the classified sample (sample number 5) is within the range defined by the samples included in the model (sample numbers 1, 2, and 3). However, sample number 4, which is not classified, has the lowest absorption intensity, indicating that the codeine model is too specific such that differences in abundance prevent classification.

For MDEA, the intensity of the absorption in the three simulated samples that are classified (sample numbers 4, 5, and 6) lies within the range defined by the other three simulated samples that were included in the model (sample numbers 1, 2, and 3). Hence, the differences in intensity that are apparent are unlikely to contribute to the lack of classification of the MDEA simulated samples. However, the lack of classification indicates that the MDEA models is not sufficiently representative of the data. It should be noted that in models for the other controlled substances, four simulated samples are included, leaving five samples for classification.

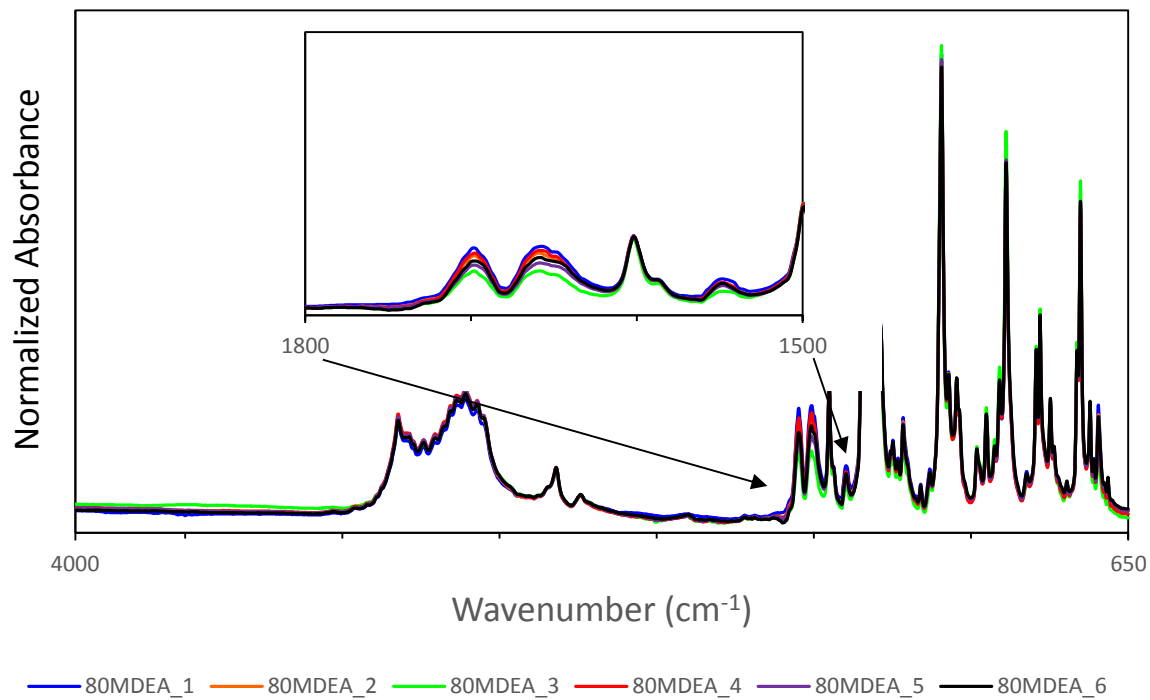


**Figure 32.** Overlay of spectra of simulated samples containing 80 parts MDEA/20 parts caffeine by mass.

Therefore, a new MDEA model was developed that included four simulated samples, leaving two samples for classification. In this model, one principal component was retained, which accounted for 99.3% variance. All other models were the same as before and SIMCA was repeated. The classification obtained using these models is summarized in Table 33.

**Table 33.** Summary of classification of 80/20 simulated samples using new MDEA model, with inclusion of reference standards and selected simulated samples in model.

Simulated samples containing	Samples classified (%) at the following confidence levels		
	95%	99%	99.9%
Amphetamine, 80/20	100	100	100
Barbital, 80/20	80	80	80
Codeine, 80/20	50	50	50
MDEA, 80/20	100	100	100
MDMA, 80/20	80	80	80
Methamphetamine, 80/20	100	100	100

80/20 indicates samples containing 80 parts controlled substance and 20 parts caffeine.

For each model, four corresponding simulated samples were also included, with the exception of codeine, for which three simulated samples were included.

For classification, five simulated samples were available for each controlled substance, with the exception of codeine and MDEA, for which two simulated samples were available.

With these models, both simulated samples containing MDEA were successfully classified at confidence levels of 95% and above and classification of all other controlled substance samples was the same as indicated in Table 28. This further highlights the limitation of SIMCA in the development of representative models.

The SIMCA procedure was somewhat successful in classifying simulated samples according to the controlled substance present. However, for some samples, classification was not possible due to limitations in the developed model. To some extent, this can be attributed to the small data set that was used in this research. Nonetheless, appropriate model development and optimization is time consuming and potentially limiting for practical applications in forensic laboratories.

#### 4.2.5 *k*-Nearest Neighbors

The *k*-NN classification procedure was initially performed on the reference standards alone to determine the appropriate number of neighbors (*k*) for optimal classification. All standards were correctly classified according to controlled substance for all integer values of *k*

from 1 to 10. Hence, any value  $k$  could be used for classification. With  $k = 5$ , all 80/20 samples are correctly classified to the appropriate reference standard, with one exception: one simulated sample containing codeine is classified as caffeine. Figure 33 shows the spectrum of this particular simulated sample, along with representative spectra of caffeine and the codeine reference standard. Absorptions from caffeine (*e.g.*,  $1692\text{ cm}^{-1}$ ,  $1643\text{ cm}^{-1}$  and the range  $1480\text{-}1430\text{ cm}^{-1}$ ) dominate the spectrum of this sample, resulting in the misclassification. The dominance of the caffeine absorptions in this spectrum indicate poor homogeneity of this simulated sample, most likely a result of inadequate mixing prior to collecting the spectrum.

The 50/50 simulated samples were also classified using the  $k$ -NN procedure. However, due to the increased proportion of cutting agent in these samples, classification is not as successful as previously, with a total of 38 misclassifications. In each case, the samples are misclassified as the cutting agent rather than the appropriate controlled substance.

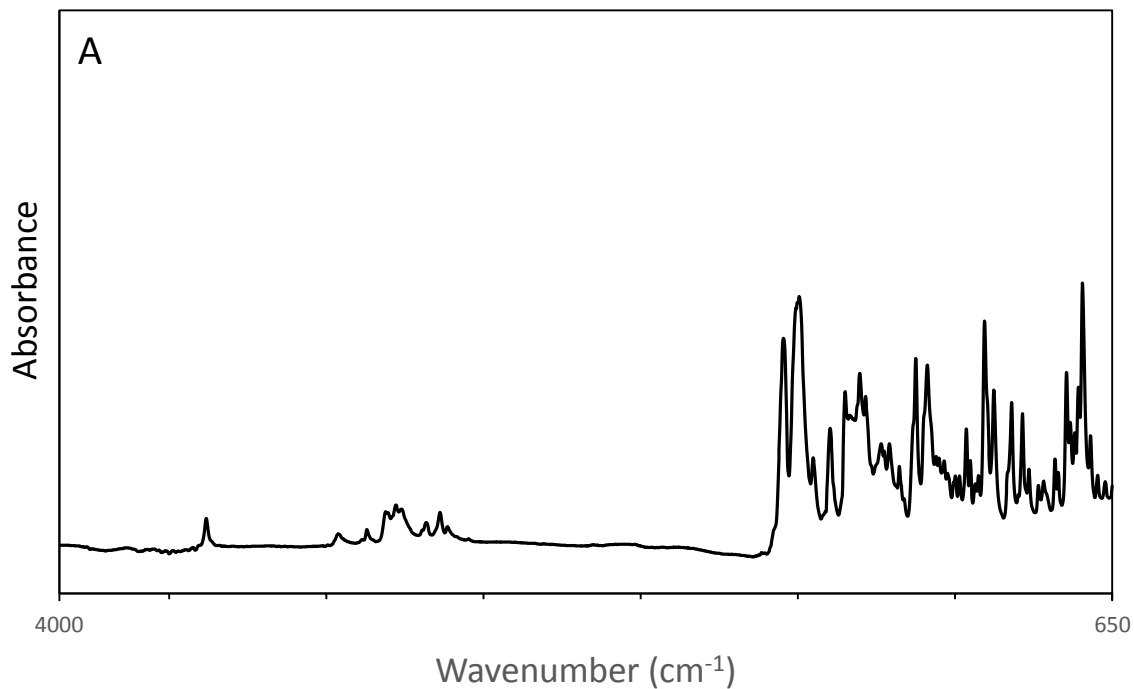


**Figure 33.** Representative spectra of (A) misclassified simulated sample containing 80 parts codeine/20 parts caffeine, by mass (B) caffeine reference standard, and (C) codeine reference standard.

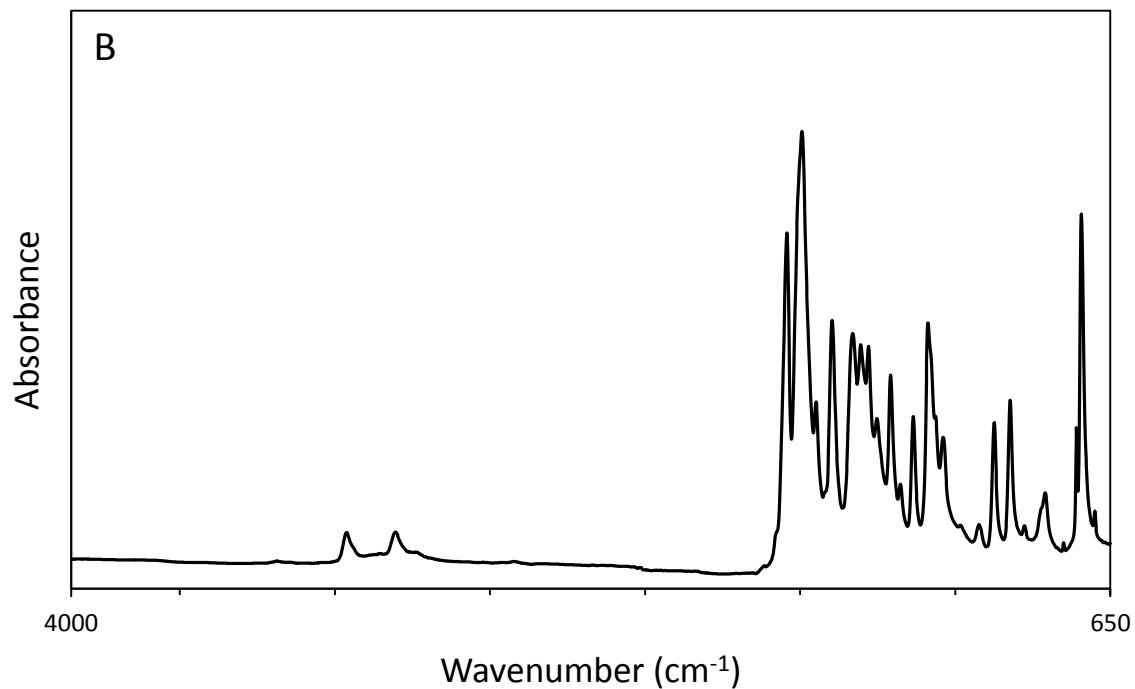


**Figure 33 contd.** Representative spectra of (A) misclassified simulated sample containing 80 parts codeine/20 parts caffeine, by mass (B) caffeine reference standard, and (C) codeine reference standard.

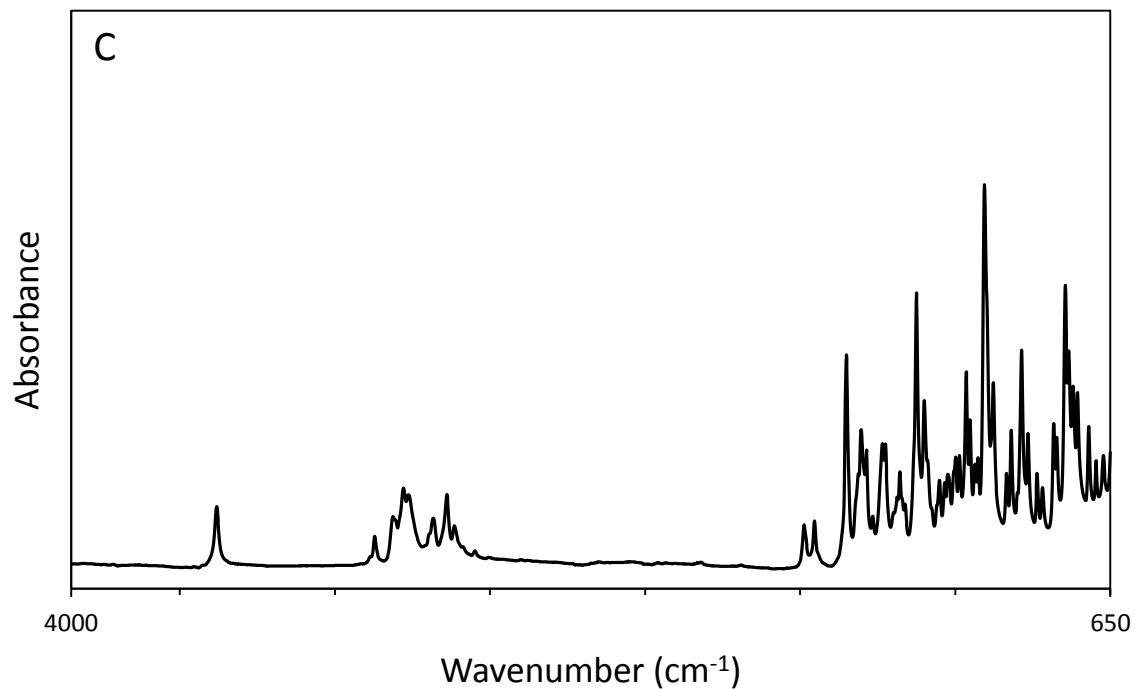


**Figure 33 contd.** Representative spectra of (A) misclassified simulated sample containing 80 parts codeine/20 parts caffeine, by mass (B) caffeine reference standard, and (C) codeine reference standard.

## 4.3 Gene Sequence Data

### 4.3.1 Amplification and Quantification

All samples exhibited strong amplification around 650 basepairs with minor product occasionally surrounding the brightest band and primer dimer (Figure 34). The exact length of the region amplified can vary based on the bacteria present in the soils and these minor products are likely species with either longer or shorter regions. Quantification revealed DNA concentrations ranging from 19.82 – 24.14 ng/mL with a standard curve  $R^2$  value of 0.9982.

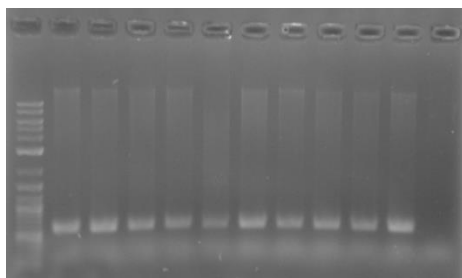


**Figure 34.** PCR amplicons compared against DNA ladder showing strong amplification at the appropriate size.

### 4.3.2 Mothur Processing

At the end of processing the sequencing data with the mother software, the number of sequences in each group ranged from 1843 – 3147 (Table 34) with an average of 2533 sequences per group. The number of sequences varied because the subsample command in mothur was not utilized, allowing all the data to be analyzed. Furthermore, the sequences were sorted into 11,853 OTUs at the unique cutoff level for PCA analysis. Mothur clusters sequences at a variety of cutoffs, or distances, with higher cutoffs sorting less similar sequences into the same OTU. The unique cutoff level was used as it gave the greatest degree of separation among the sequences. This cutoff maintains that each OTU has identical sequences, which allows for a direct count of that clade.

**Table 34.** Unique DNA sequences per soil extract after processing with mother software

<b>Sample</b>	<b>Number of unique sequences</b>
Marsh 1 (M1)	2921
Marsh 2 (M2)	3147
Marsh 3 (M3)	2486
Woodlot 1 (W1)	2266
Woodlot 2 (W2)	1843
Woodlot 3 (W3)	2607
Yard 1 (Y1)	2127
Yard 2 (Y2)	2713
Yard 3 (Y3)	2822
Yard Mixture (Ymix)	2424

#### 4.3.3 Bacterial Classification

Sequences were classified with mothur software using the SILVA bacterial reference file, allowing identification of each OTU. The 11,853 OTUs were first catalogued into 42 class level taxonomies and the abundance of each is shown in Figure 35. Over 90% of the total bacterial abundance is found within nine classes for most samples. Further, all of the samples have similar compositions of the seven most prevalent classes. Therefore, the vast majority of the variability of taxonomies exists in the last 5 – 10% of the total abundance, and 25 of the 42 classes identified exist in the remaining 5% of the total abundance (Figure 36). The large number of relatively rare bacterial classes demonstrates the diversity in each habitat even at low levels, and has the potential to act as the ‘fingerprint’ region of the data.

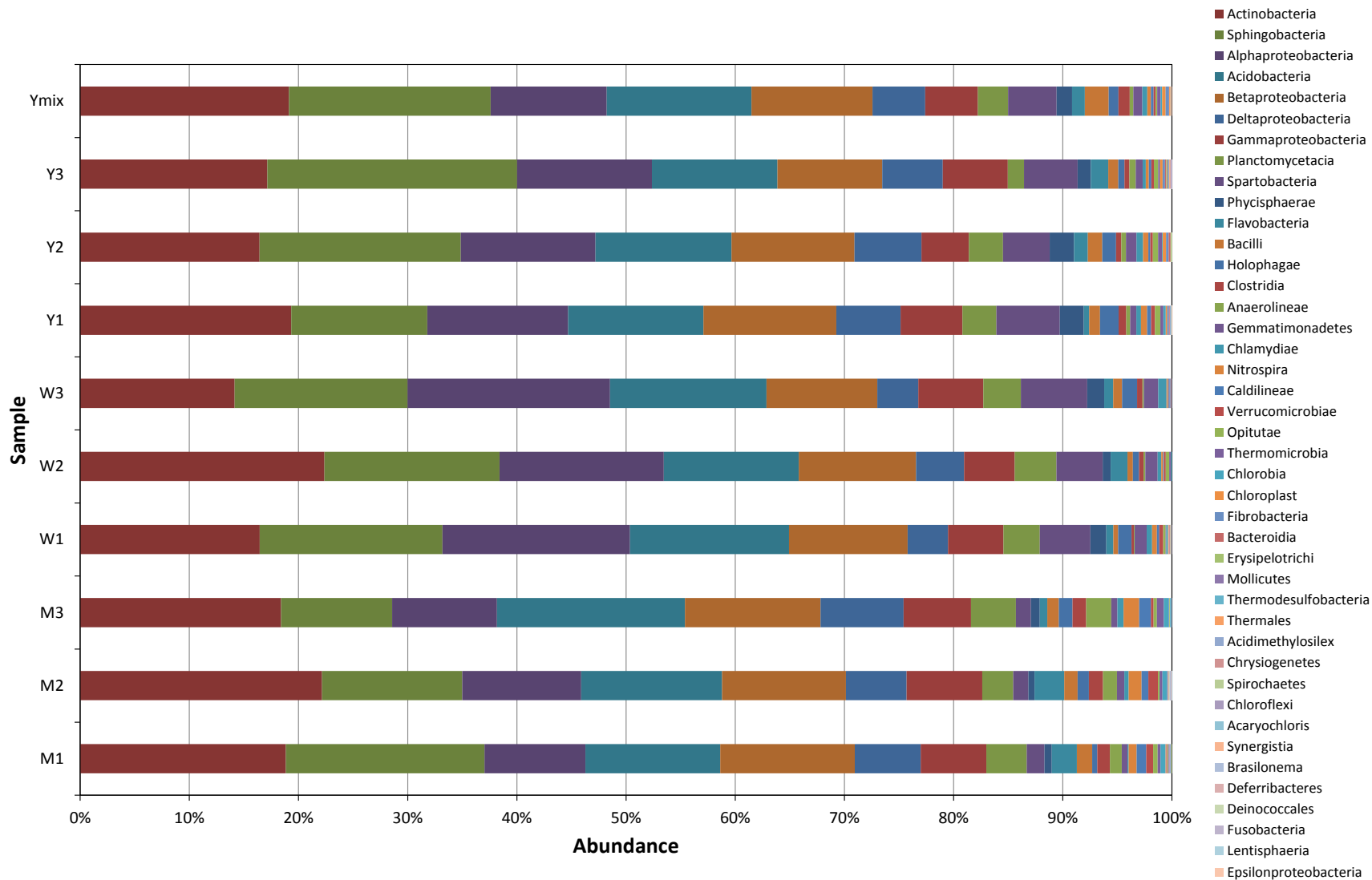


**Figure 35.** Bacterial classes found in each sample displayed as a percentage of total number of sequences found in that phylogeny.

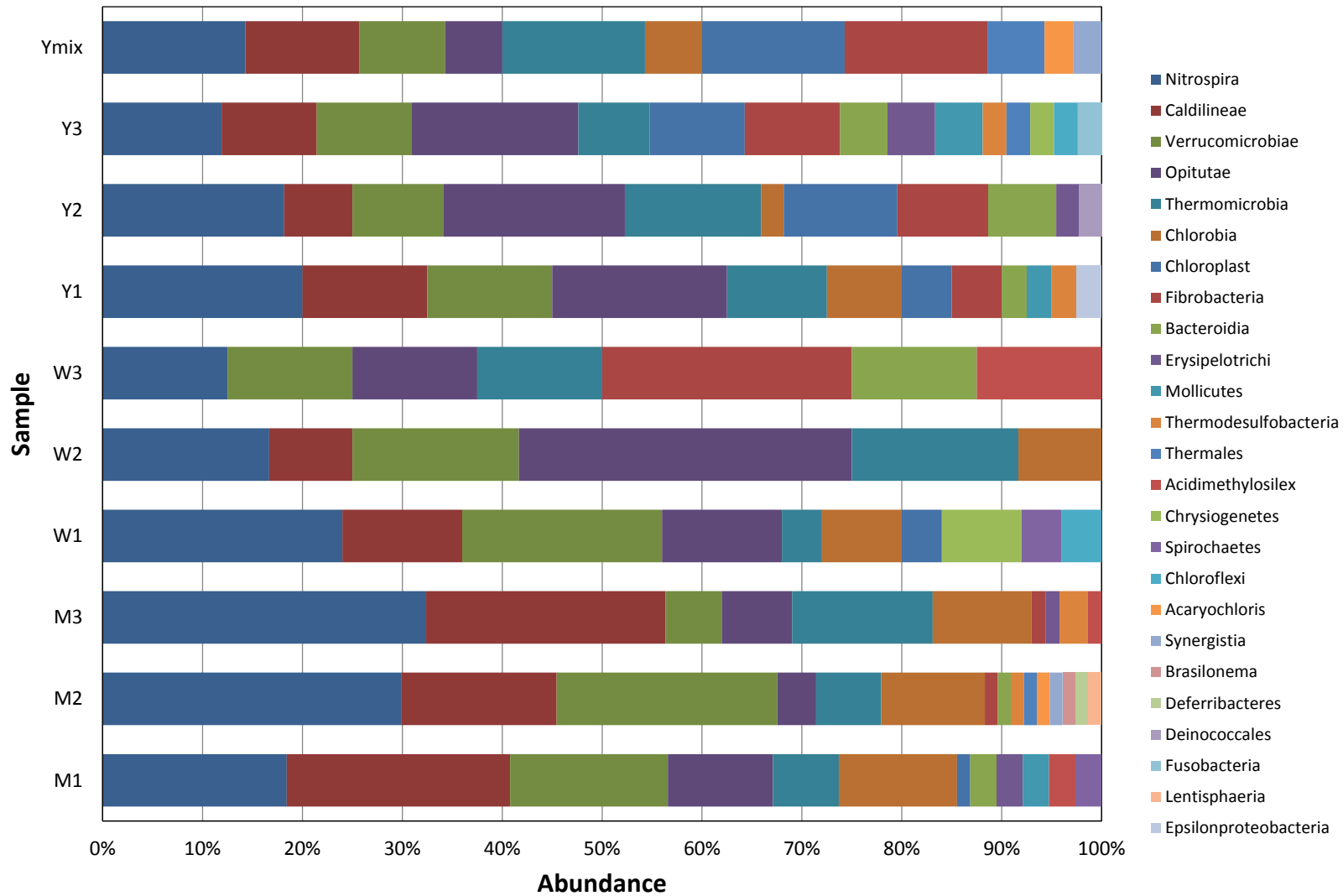


**Figure 36.** Subset of bacterial classes found in each sample displayed as a percentage of total number of sequences found in that phylogeny. These classes account for less than 5% of the total abundance shown in Figure 35.

#### 4.3.4 Principal Components Analysis

PCA was performed on the sequence data segregated into OTUs. The scores plot for the first two principal components, which account for 55% of the variance in the data set, is shown in Figure 37. Samples from different habitats are readily distinguished in the scores plot; however, there is some spread among replicates of each sample type. This is due to the nonparametric nature of these data, as well as the variable number of sequences in each OTU.

The corresponding loadings plot is shown in Figure 38, in which OTUs that contribute most to the variance in the data set are labeled. It should be noted that the majority of OTUs are positioned close to the origin, indicating that they contribute little to the variance. These OTUs generally only contain a few sequences with a majority containing only a single sequence. These singular sequences could result from sequencing error and belong to a larger group of sequences in a different OTU or be a rare sequence identifying a unique species in each habitat.

Generally OTUs with the greatest number of sequences contribute the most to the variance among samples, with the majority of sequences for that OTU found in one or two of the habitats sampled (Table 35). The marsh samples tend to have high levels of sequences in OTUs in which the yard and woodlot samples have few or no sequences (*e.g.*, OTUs 13, 40, 70, and 119) and *vice versa*. This variation in sequences indicates a microbiota difference between the marsh samples and the woodlot and yard sites. Additionally, while some sequences (*e.g.*, OTUs 1, 3, 6, 8, and 11) occur in both the woodlot and yard samples, there are also some instances where sequences exist in one or other of these habitats. For the OTUs where both habitats contain sequences, the number of sequences varies from being similar (*e.g.*, OTUs 1, 3, and 8) to being very different.

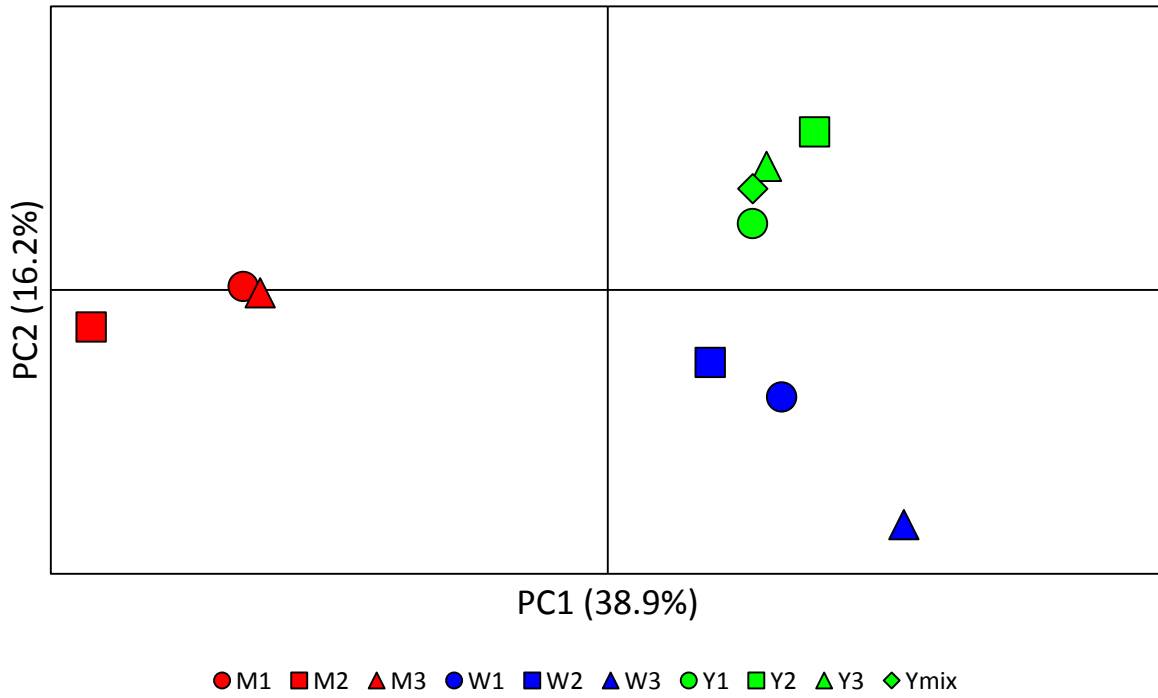


**Figure 37.** Scores plot of PC1 versus PC2 for gene sequence data from samples collected from three different habitats: marsh (M), woodlot (W), and yard (Y).

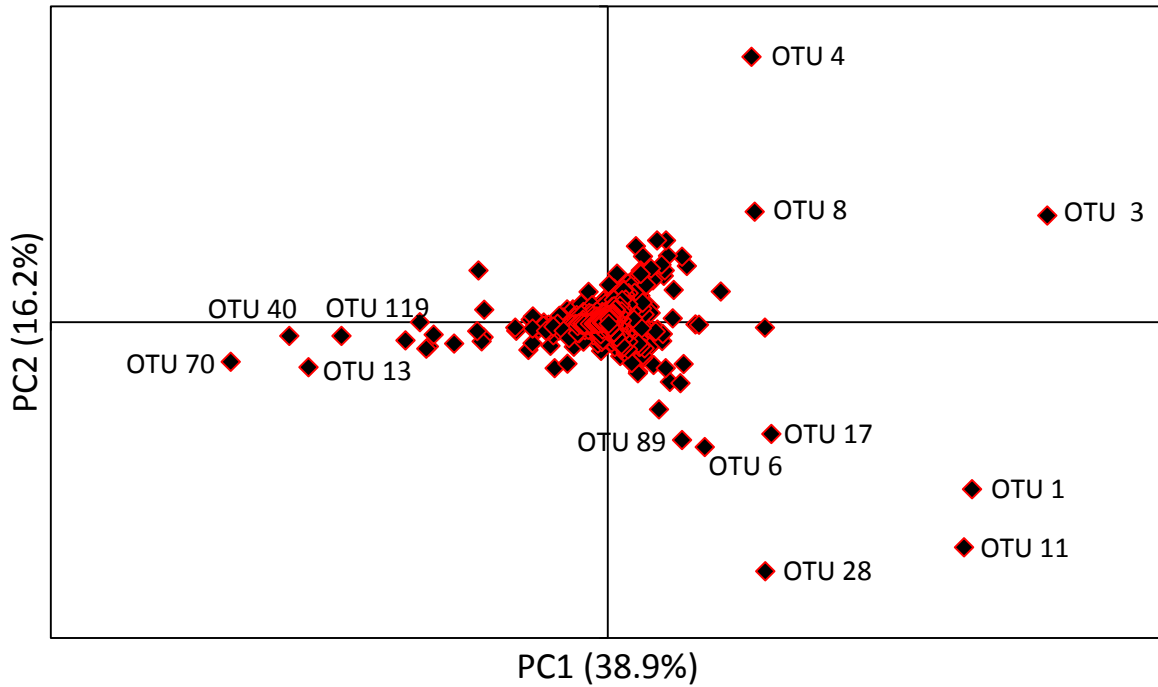


**Figure 38.** Loadings plot of PC1 versus PC2 for gene sequence data from samples collected from three different habitats. Each data point represents a different OTU that contains identical sequences. OTUs contributing most to the variance are labeled.

**Table 35.** Number of sequences and classification of each OTU for the seven bacterial classes that contributed the most variance in the scores plot.

OTU	M1	M2	M3	W1	W2	W3	Y1	Y2	Y3	Ymix	Classification: Class
1	6	8	8	41	37	53	36	37	15	20	Alphaproteobacteria
3	5	2	2	30	22	39	45	44	45	33	Spartobacteria
4	2	3	0	0	0	0	2	56	9	21	Actinobacteria
6	4	4	1	19	22	17	1	3	8	5	Actinobacteria
8	3	2	2	17	9	3	25	13	23	17	Actinobacteria
11	0	2	0	32	24	56	9	19	18	22	Alphaproteobacteria
13	1	56	0	0	0	0	0	0	0	0	Flavobacterium
17	0	2	0	16	21	23	9	10	4	9	Actinobacteria
28	0	0	0	16	0	42	0	1	0	0	Sphingobacteria
40	25	26	26	0	0	0	0	2	0	0	Deltaproteobacteria
70	38	30	25	3	3	1	0	0	0	0	Acidobacteria
89	0	0	0	4	2	21	0	0	0	1	Spartobacteria
119	25	18	22	0	0	0	0	0	0	0	Actinobacteria

The number and distribution of sequences in each OTU, and correspondingly the location of that OTU on the loadings plot (Figure 38), is indicative of the position of the samples on the scores plot (Figure 37). OTUs 13, 40, 70, and 119 are weighted negatively on PC1 and around zero for PC2. These OTUs contain sequences primarily found in samples from the marsh habitat, resulting in these samples being positioned negatively on PC1 and around zero on PC2 in the scores plot. Despite spread in the positioning of replicates, there are samples that cluster closely, most notably two replicates from the marsh habitat (M1 and M3), as well as three replicates from the yard habitat (Y1, Y3, and Ymix). These replicate samples from each habitat contain a similar number of sequences in each OTU. However, when OTU 13 and OTU 14 are considered, the afore-mentioned replicates contain a higher abundance of *Flavobacterium* and *Actinobacteria*, respectively, than the other replicates for that habitat. Finally, the spread observed among samples from the woodlot is due to the variation in sequence abundance among the replicates.

The sequences were identified to the class level. It is interesting to note that the majority of variance results from seven classes of bacteria, three of which almost exclusively exist in the marsh samples (*Flavobacterium*, *Deltaproteobacteria*, and *Acidobacteria*). The remaining classes were found in both the yard and woodlot samples, with little to no representation in the marsh samples. This sharing of bacterial classes between the yard and woodlot is not surprising

as they are only separated on PC2 (Figure 37) and are much more similar to each other than to the marsh samples.

As previously mentioned, these data do not meet the data linearity assumption PCA requires. The spread of the data points on the scores plot among replicate samples is evidence of this. Despite this, the three habitats can be satisfactorily distinguished from each other, although more appropriate and informative statistics may be available using a statistical procedure that does not make any assumptions regarding the linearity of the data.

#### 4.3.5 Nonmetric Multidimensional Scaling

Two 10 x 10 square matrices of pairwise comparisons were used as the starting point for NMDS analysis generated by the BCDI or SDC algorithms using the mother software. The stress plots of comparative stresses (Figure 39, and Appendix 7A) diagram the change in stress as dimensionality increases. For both indices, a single dimension plot fails to meet the requirements of the stress null hypothesis and is considered random noise; however, for dimensions greater than one, the stress for each NMDS plot is below random stress and is accepted as accurately fitting the data.<sup>65</sup> The ‘elbow’ in the stress plot at two dimensions indicates that the NMDS configuration can be interpreted in two dimensions with minimal additional information gained as the number of dimensions increases. Furthermore, the extremely low stress at two dimensions ( $3.634 \times 10^{-4}$  and  $5.197 \times 10^{-4}$  in Figure 39 and in Appendix 7A respectively) supports an accurate portrayal of these data in the NMDS plot.

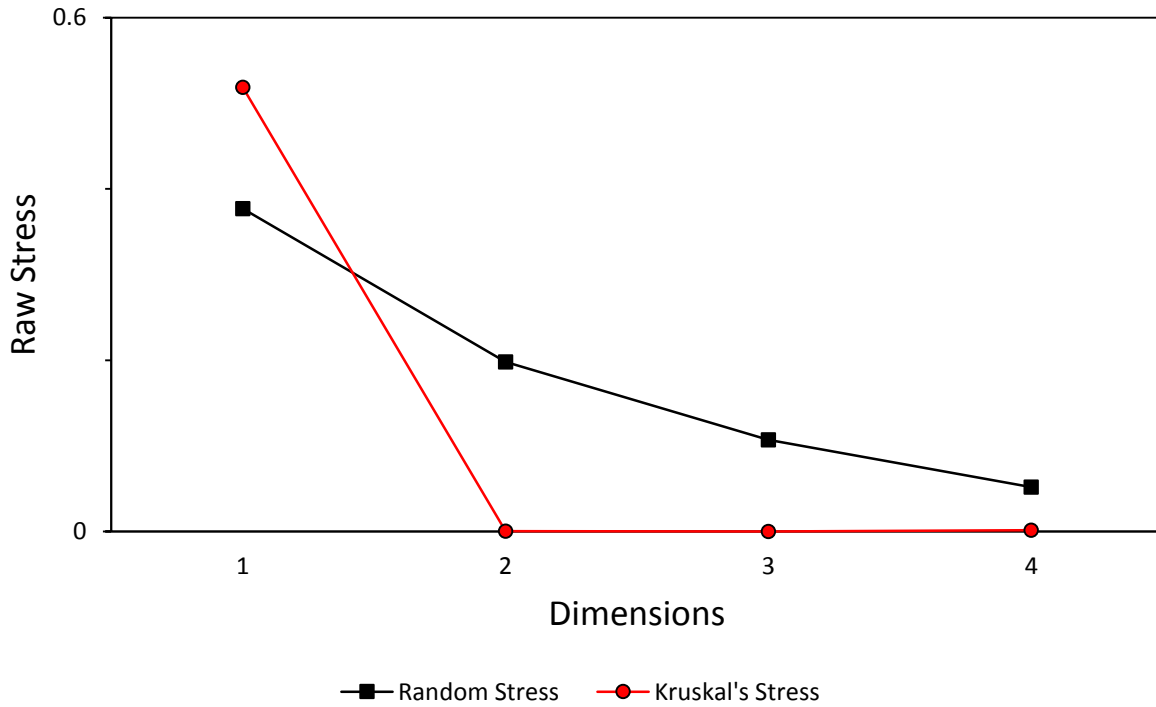


**Figure 39.** Plot of Kruskal’s stress (red line) vs. Spence’s random stress (black line) for Bray-Curtis dissimilarity data across four dimensions.

The Shepard diagrams (Figure 40 and Appendix 7B) demonstrate a very high correlation between disparity and distance, indicating an accurate representation of these data in the NMDS plots. For NMDS, the rank-order between the disparities and proximities must be maintained and are plotted in a monotonic function, positively if the inputted distances are dissimilarities.<sup>62</sup> The staircase shape of the function in the Shepard diagrams is typical of NMDS.

Soil extracts from each habitat were analyzed on a two dimensional NMDS plot (Figure 41 and Appendix 7C) with standard error bars applied. Both BCDI and SDC show complete separation of the three habitats, with clustering of replicate samples within standard error. The clusters of replicate samples appear to dissociate from each other equidistantly. The tight clustering of replicate samples in the final configurations is expected based on analysis of the stress plots and Shepard diagrams. As mentioned previously, the low stress and high correlation of distances to disparities provides confidence that the NMDS plot is accurately representing the data.

These results show that multidimensional scaling is capable of modeling complex nonparametric data. This is evident from the NMDS plots and low stress associated with them. The replicate samples for each site cluster closely and within standard error, with all three habitats differentiated for both diversity indices. Of the two procedures, NMDS is more powerful than PCA for describing these data and is the more appropriate statistical procedure for soil analysis.

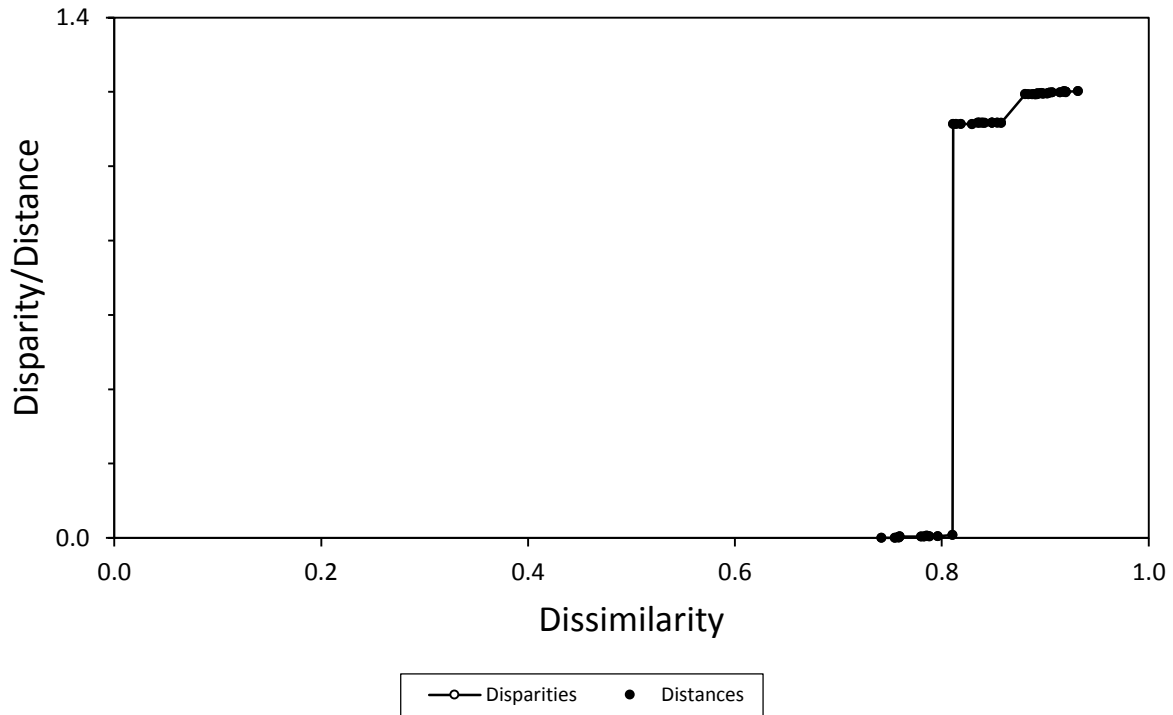


**Figure 40.** Shepard diagram plotting Bray-Curtis dissimilarities against the disparities/distances observed on the nonmetric multidimensional scaling (NMDS) plot. This strong correlation between the two indicates that NMDS has represented the rank-order of these data accurately.

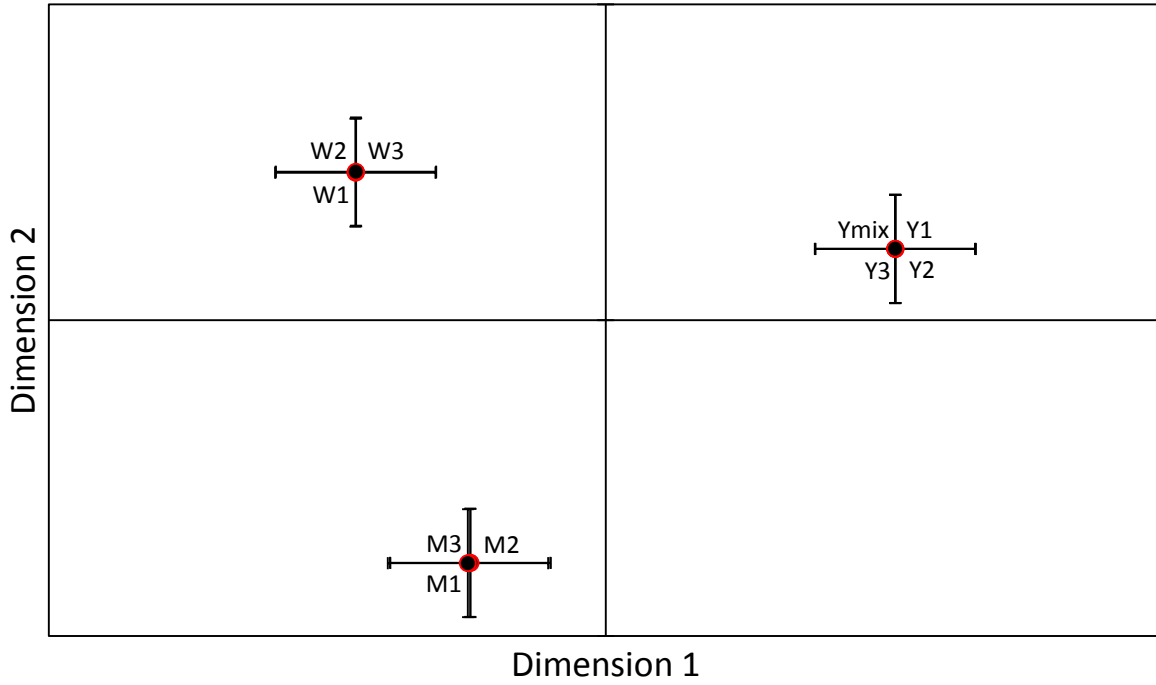


**Figure 41.** Nonmetric multidimensional scaling plot of ten samples in two dimensions with standard error bars for Bray-Curtis Index.

## 5. Conclusions

### 5.1 Summary of Findings

The purpose of this research was to investigate the utility of multivariate statistical procedures, specifically for forensic applications. While similar procedures are commonly used in different scientific disciplines, they are not widely used in forensic science. Therefore, this research aimed to further investigate the application of multivariate statistical procedures for forensic evidence comparisons to highlight both the potential of these procedures and the challenges associated with their implementation.

The first part of the research involved generating data sets to which the statistical procedures would subsequently be applied. Three different data sets were generated, each corresponding to different evidence types commonly generated by forensic laboratories. The chromatographic data set was composed of ignitable liquid reference standards and simulated fire debris samples that were prepared using different household substrates. This data set was chemically diverse and complex in nature, containing over 3,500 variables. The spectral data set was composed of controlled substance reference standards along with simulated street samples containing controlled substances cut with caffeine. Although this data set contained a similar number of variables (3,350 variables) as the chromatographic data set, the spectral data was less complex in nature. Finally, the biological data set was composed of soil bacteria sequence data from different habitat types. These data contained discrete variables, rather than the continuous variables that were present in the chromatographic and spectral data sets. Thus, the data sets in this work not only represented common types of data generated in forensic laboratories, they also ranged in complexity and included both continuous and discrete variables.

Chemical data sets were subjected to pretreatment procedures prior to data analysis. Such procedures are used to minimize or eliminate sources of variance that result from instrumental factors rather than from the samples themselves. It is important that these sources of variance are reduced before data analysis otherwise differences identified among samples will be a remnant of the analytical procedure rather than truly chemical in nature. For the chromatographic data, several pretreatment procedures were applied with normalization offering the greatest effect on improving replicate precision. For the spectral data, the commonly applied SNV normalization procedure was deemed optimal when compared to two other normalization procedures.

However, for the more chemically diverse chromatographic data, no one normalization procedure universally improved precision of all replicates.

Exploratory procedures were then investigated with the aim of associating the simulated chemical samples to the corresponding reference standard. Pearson product-moment correlation (PPMC) coefficients provide a single number that represents the correlation between two complex samples, which can simplify comparisons. While a single number representing the comparison of complex data containing thousands of variables is advantageous, the use of PPMC coefficients for this particular application is limited for a number of reasons. First, coefficients are calculated on a pairwise basis and hence, the number of coefficients calculated for a given data set increases with the square of the number of samples. Depending on the size of the data set under consideration, this can make the comparison of a large data set time-consuming. Second, the coefficient is calculated on a point-by-point basis for the two samples being compared. This means that peaks present in one sample but not the other (as is the case for the simulated samples and reference standards considered here) will result in a lower coefficient. And third, the range of coefficients representing each correlation strength is relatively wide (*e.g.*, any coefficient in the range  $\pm 0.8-1$  indicates strong correlation).

The chromatographic and spectral data sets were further analyzed using principal components analysis (PCA) and hierarchical cluster analysis (HCA), both of which offer several advantages over PPMC coefficients. Firstly, neither are limited to pairwise comparisons of samples; instead, all samples are considered simultaneously which makes analysis of a large data set substantially less time consuming. In contrast to PPMC coefficients, these procedures also provide a graphical representation of the similarities and differences in the data set in the form of the scores plot in PCA and the dendrogram in HCA.

Principal components analysis is used to identify sources of variance in a data set while HCA measures similarity among samples in the data set. However, it is important to note that despite this apparent difference in operation, both procedures are based on distance measurements among samples in multidimensional space. In PCA, though, typically only the first few dimensions (which account for the greatest variance) are retained and examined in the scores plots. In contrast, the dendrogram generated in HCA retains all dimensions rather than a select few. As a result, in this research, there was greater success in associating simulated samples to reference standards using HCA.

Nonetheless, PCA does offer an advantage in that the variables contributing to the association and differentiation in the data set can be identified through interrogation of the loadings plots. However, interpretation of the PCA scores plot is based on visual assessment and therefore, without additional evaluation metrics (such as Euclidean distance measurements or PPMC coefficients calculated using the principal component eigenvectors), it could be argued that there is some subjectivity in interpretation. In contrast, while HCA does not identify the variables contributing to the clustering, a numerical measure of the degree of association is inherent in the procedure.

Finally for the chemical data, the use of classification procedures was investigated, with the aim of classifying the simulated samples according to the appropriate reference standard with statistical confidence. Two such procedures were investigated: soft independent modeling of class analogy (SIMCA) and  $k$ -nearest neighbors ( $k$ -NN). These two procedures were selected for this initial investigation due to their relationship with the exploratory procedures previously investigated. That is, classification using SIMCA is based on the development of PCA models while  $k$ -NN is analogous to HCA.

Despite both procedures affording classification, again there are inherent differences in the manner in which the classification is performed. For SIMCA, classification is based on PCA models that are developed for pre-defined groups in the data set, which in this research meant performing PCA on the reference standards. However, the development of representative models is challenging. For both the chromatographic and spectral data sets, classification of the simulated samples was not possible when models were developed using only the reference standards. This is mainly because the models did not account for the substrate or cutting agent (for the chromatographic and spectral data sets, respectively). Limited classification was possible when simulated samples were included in the model; however, the models were now so specific that misclassifications arising from differences in abundance were apparent.

In contrast, the  $k$ -NN procedure is not based on true model development. Instead, for each classification to be performed, the reference standards and samples are re-subjected to the  $k$ -NN procedure. Samples are classified with the reference standards to which they are positioned most closely in the multidimensional space. While a perceived limitation is the forced classification of samples, the success rate of  $k$ -NN in this research was greater than for SIMCA.

This was attributed to the nature of operation in that classification is based on similarity of the sample to the set of reference standards rather than model development.

The gene sequence data were also subjected to data pretreatment to remove artificial sources of variation. For these data, erroneous and repetitive sequences were removed prior to statistical analysis using PCA and nonmetric multidimensional scaling (NMDS). Like PCA and HCA, NMDS reduces the complexity of the data, in this case over 100,000 sequences, into two or three dimensions. NMDS has advantages over PCA and HCA in that it is designed to accurately represent nonparametric data. However, NMDS is limited in its capability to identify the variables that are responsible for the variation observed in the final configuration of the data. Though NMDS is wanting in this respect, association of biological replicates was improved using this procedure compared to PCA. Although distinction of soil habitats was also possible using PCA, the natural variability within the bacterial populations hindered PCA from closely associating replicate samples together. All in all, NMDS was the more appropriate procedure to distinguish soil from the three different habitats, while closely associating the replicate samples.

## 5.2 Implications for policy and practice

This research indicates potential for the application of multivariate statistical procedures in the comparison of forensic evidence. It should be emphasized though that these procedures are not intended to replace analysts; instead, the statistical procedures should be viewed as an additional tool available to aid analysts in their comparisons. For the relatively small data sets considered here, greater success in association and classification of simulated samples was achieved using HCA and  $k$ -NN, indicating that these two procedures are worthy of further investigation, using larger data sets and incorporating real case samples rather than laboratory-simulated samples. For data that are nonparametric in nature, NMDS offers a suitable alternative to PCA as an exploratory procedure.

While further investigation is warranted, many challenges remain before such procedures could be routinely implemented in a forensic laboratory setting. Firstly, this research has demonstrated the need for data pretreatment procedures. At the same time, it also demonstrated that the actual procedures applied are not only dependent on the type of data in question, but also must be optimized for each data set. This poses some limitations for forensic laboratories as

optimization lengthens the time necessary for analysis and comparison of evidence and the final selection of the procedures applied can be subjective.

In terms of application of statistical procedures, there are again a number of considerations. Replicate measurements of samples and standards are necessary for statistical soundness although this may not be viable in forensic laboratories due to caseloads and sample backlogs. Application of the statistical procedures will also require substantial investment by the laboratory in the form of both hardware and software. Higher-end computers that are dedicated to statistical analysis, rather than also controlling instruments, are desirable. And, after purchasing the software package, there are costs associated with license renewals and technical support. Additional investment is also necessary to provide analysts with sufficient training for the implementation and interpretation of these procedures. Given the limited operating budgets most forensic laboratories are faced with, equipping the laboratory with such hardware and software is unlikely to be prioritized.

Presenting the results of these procedures in court yields additional challenges. Statistical procedures are often considered to be objective in nature; however, there is some degree of subjectivity in the selection of analysis parameters. For example, how many principal components should be considered in PCA? Which linkage and distance measurements should be used in HCA? How does the sample classification change if the SIMCA models are modified? How does the sample classification change if the number of nearest neighbors in the  $k$ -NN procedure is altered? How does the abundance estimator affect clustering in NMDS? While these questions can be answered, the answers depend on the data set in question again, necessitating additional steps and investigations during the analysis.

### 5.3 Future work

This research has generated three very rich data sets that will continue to be investigated and disseminated. For the chromatographic data, only the total ion chromatograms were used as the first stage in the statistical assessment. However, for each reference standard and simulated sample, extracted ion profiles of characteristic compound classes can be generated from the data that have already been collected. The next step in the continued investigation of statistical procedures will be to examine the effect of using extracted ion profiles rather than the total ion chromatogram for the association and classification of simulated fire debris samples.

As discussed previously, the two exploratory procedures considered are related in their mode of operation (based on distance measurements in the multidimensional space). Additionally, the classification procedures investigated can be considered an extension of the exploratory procedures. These relationships will be further investigated following the expansion of the chromatographic and spectral data sets through analysis of additional samples. According to the success of these investigations, contact will be made with the Michigan State Police Forensic Science Division in an attempt to procure similar chromatographic and spectral data from case samples to further investigate the statistical procedures.

The gene sequence data will continue to be investigated both through addition of new habitats, and with additional multivariate statistical procedures. As discussed earlier, a multitude of statistics have been used to analyze this type of data. Those commonly found within the literature (*e.g.*, NMDS, PCA, and HCA), as well as additional procedures that allow statistical classification will be investigated. Applying several statistical procedures to the sequence data will enable a more thorough understanding of the relationships among the three habitats, as well as a measure of the probative value of each statistical procedure.

In addition to the three manuscripts that are expected from this work (section 7.2), two tutorials that demonstrate the application of selected procedures are in preparation. The first tutorial focuses on chromatographic data while the second focuses on spectral data. Both present relevant statistical theory, as well as interpretation of the results. Graduate students in the Forensic Science Program at Michigan State University are currently working through the tutorials to identify and correct deficiencies. Once complete, these tutorials will be disseminated *via* a link on the Forensic Chemistry website ([www.forchem.msu.edu](http://www.forchem.msu.edu)). As our research in this area continues, additional tutorials will be prepared and disseminated in a similar manner.

## 6. References

1. *Strengthening Forensic Science in the United States: A Path Forward*. The National Academies Press: Washington DC, 2009.
2. Curran, J. M. Is forensic science the last bastion of resistance against statistics? *Science & Justice* **2013**, *53* (3), 251-252.
3. Morgan, S. L.; Bartick, E. G., Discrimination of forensic analytical chemical data using multivariate statistics. In *Forensic analysis on the cutting edge*, Blackledge, R. D., Ed.; John Wiley & Sons, Ltd.: Hoboken, NJ, 2007; pp. 333-74.
4. Brereton, R. G. *Chemometrics. Applications of Mathematics and Statistics to Laboratory Systems*. Ellis Horwood: Chichester, 1990.
5. Sandercock, P. M. L.; Du Pasquier, E. Chemical fingerprinting of unevaporated automotive gasoline samples. *Forensic Science International* **2003**, *134*, 1-10.
6. Sandercock, P. M. L.; Du Pasquier, E. Chemical fingerprinting of gasoline 2. Comparison of unevaporated and evaporated automotive gasoline samples. *Forensic Science International* **2004**, *140*, 43-59.
7. Tan, B.; Hardy, J. K.; Snavey, R. E. Accelerant classification by gas chromatography/mass spectrometry and multivariate pattern recognition. *Analytica Chimica Acta* **2000**, *422*, 37-46.
8. Baerncopf, J. M.; McGuffin, V. L.; Waddell Smith, R. Association of ignitable liquid residues to neat ignitable liquids in the presence of matrix interferences using chemometric procedures. *Journal of Forensic Sciences* **2011**, *56* (1), 70-81.
9. Prather, K. R.; McGuffin, V. L.; Waddell Smith, R. Effect of evaporation and matrix interferences on the association of simulated ignitable liquid residues to the corresponding liquid standard. *Forensic Science International* **2012**, *222* (1-3), 242-251.
10. Turner, D. A.; Goodpaster, J. V. The effects of season and soil type on microbial degradation of gasoline residues from incendiary devices. *Analytical and Bioanalytical Chemistry* **2013**, *405* (5), 1593-1599.
11. Waddell, E. E.; Song, E. T.; Rinke, C. N.; Williams, M. R.; Sigman, M. E. Progress toward the determination of correct classification rates in fire debris analysis. *Journal of Forensic Sciences* **2013**, *58* (4), 887-896.
12. Klemenc, S. In common batch searching of illicit heroin samples - evaluation of data by chemometrics methods. *Forensic Science International* **2001**, *115* (1-2), 43-52.
13. Chan, K. W.; Tan, G. H.; Wong, R. C. S. Investigation of trace inorganic elements in street doses of heroin. *Science & Justice* **2013**, *53* (1), 73-80.
14. Weyermann, C.; Marquis, R.; Delaporte, C.; Esseiva, P.; Lock, E.; Aalberg, L. et al. Drug intelligence based on MDMA tablets data I. Organic impurities profiling. *Forensic Science International* **2008**, *177*, 11-16.
15. Willard, M. A. B.; McGuffin, V. L.; Waddell Smith, R. Forensic analysis of *Salvia divinorum* using multivariate statistical procedures. Part I: discrimination from related *Salvia* species. *Analytical and Bioanalytical Chemistry* **2012**, *402* (2), 833-842.
16. Willard, M. A. B.; McGuffin, V. L.; Waddell Smith, R. Forensic analysis of *Salvia divinorum* using multivariate statistical procedures. Part II: association of adulterated samples to *S. divinorum*. *Analytical and Bioanalytical Chemistry* **2012**, *402* (2), 843-850.
17. NicDaeid, N.; Waddell, R. J. H. The analytical and chemoemtric procedures used to profile illicit drug seizures. *Talanta* **2005**, *67*, 280-5.

18. Trosvik, P.; Skanseng, B.; Jakobsen, K. S.; Stenseth, N. C.; Naes, T.; Rudi, K. Multivariate analysis of complex DNA sequence electropherograms for high-throughput quantitative analysis of mixed microbial populations. *Applied and Environmental Microbiology* **2007**, *73* (15), 4975-4983.
19. Abdo, Z.; Schuette, U. M. E.; Bent, S. J.; Williams, C. J.; Forney, L. J.; Joyce, P. Statistical methods for characterizing diversity of microbial communities by analysis of terminal restriction fragment length polymorphisms of 16S rRNA genes. *Environmental Microbiology* **2006**, *8* (5), 929-938.
20. Lenz, E. J.; Foran, D. R., Bacterial profiling of soil using genus-specific markers and multidimensional scaling. *Journal of Forensic Sciences* **2010**, *55* (6), 1437-1442.
21. Hedman, J.; Nordgaard, A.; Rasmusson, B.; Ansell, R.; Radstrom, P. Improved forensic DNA analysis through the use of alternative DNA polymerases and statistical modeling of DNA profiles. *Biotechniques* **2009**, *47* (5), 951-958.
22. Krane, D. E.; Bahn, V.; Balding, D.; Barlow, B.; Cash, H.; Desportes, B. L. et al. Time for DNA disclosure. *Science* **2009**, *326* (5960), 1631-1632.
23. Grayston S. J.; Wang S.; Cambell C. D.; Edwards A. C. Selective influence of plant species on microbial diversity in the rhizosphere. *Soil Biology and Biochemistry* **1998**, *30*, 369-378.
24. Marschner, P.; Yang, C.; Lieberei, R.; Crowley, D. E. Soil and plant specific effects on bacterial community composition in the rhizosphere. *Soil Biology and Biochemistry* **2001**, *33*, 1437-14445.
25. Boon, N.; Windt, W. D.; Verstaete, W.; Top, E. M. Evaluation of nested PCR-DGGE (denaturing gradient gel electrophoresis) with group-specific 16S rRNA primers for the analysis of bacterial communities from different wastewater treatment plants. *FEMS Microbiology Ecology* **2002**, *39*, 101-112.
26. Fantroussi, S. E.; Verschuere, L.; Verstraete, W.; Top, E. M. Effect of phenylurea herbicides on soil microbial communities estimated by analysis of 16S rRNA gene fingerprints and community-level physiological profiles. *Applied and Environmental Microbiology* **1999**, *65*, 982-988.
27. Legendre, P.; Legendre, L. *Numerical ecology*. Elsevier: Oxford, England, 2012.
28. Dollhopf, S. I.; Hashsham, S. A.; Tiedje, J. M. Interpreting 16S rDNA T-RFLP data: Application of self-organizing maps and principal component analysis to describe community dynamics and convergence. *Microbiology Ecology* **2001**, *42*, 495-505.
29. Girvan, M. S.; Bullimore, J.; Pretty, J. N.; Osborn, A. M.; Ball, A. S. Soil type is the primary determinant of the composition of the total active bacterial communities in arable soils. *Applied and Environmental Microbiology* **2003**, *69*, 1800-1809.
30. McCaig, A. E.; Glover, L. A.; Prosser, J. I. Numerical analysis of grassland bacterial community structure under different land management regimens by using 16S ribosomal DNA sequence data and denaturing gradient gel electrophoresis banding patterns. *Applied and Environmental Microbiology* **2001**, *67*, 4554-4559.
31. Fierer, N.; Jackson, R. B. The diversity and biogeography of soil bacterial communities. *Proceedings of the National Academy of Sciences* **2006**, *103*, 626-631.
32. Nagy, M. L.; Pérez, A.; Garcia-Pichel, F. The prokaryotic diversity of biological soil crusts in the Sonoran Desert (Organ Pipe Cactus National Monument, AZ). *FEMS Microbiology Ecology* **2004**, *54*, 233-245.

33. Philippot, L.; Bru, D.; Saby, N. P. A.; Čuhel, J.; Arrouays, D.; Šimek, M. et al. Spatial patterns of bacterial taxa in nature reflect ecological traits of deep branches of the 16S rRNA bacterial tree. *Environmental Microbiology* **2009**, *11*, 3096-3104.
34. Hughes, J. B.; Hellmann, J. J.; Ricketts, T. H. Counting the uncountable: Statistical approaches to estimating microbial diversity. *Applied and Environmental Microbiology* **2001**, *67*, 4399-4406.
35. Roesch, L. F. W.; Fulthorpe, R. R.; Riva, A.; Casella, F.; Hawdin, A. K. M.; Kent, A. D. et al. Pyrosequencing enumerates and contrasts soil microbial diversity. *ISME Journal* **2007**, *1*, 283-290.
36. Gans, J.; Wolinsky, M.; Dunbar, J. Computational improvements reveal great bacterial diversity and high metal toxicity in soil. *Science* **2005**, *309*, 1387-1390.
37. Chu, H.; Fierer, N.; Lauber, C. L.; Caporaso, J. G.; Knight, R.; Grogan, P. Soil bacterial diversity in the arctic is not fundamentally different from that found other biomes. *Environmental microbiology* **2010**, *12*, 2998-3006.
38. Dunbar, J.; Barns, S. M.; Ticknor, L. O. Empirical and theoretical bacterial diversity in four Arizona soils. *Applied and Environmental Microbiology* **2002**, *68*, 3035-3045.
39. Lauber, C. L.; Hamady, M.; Knight, R.; Fierer, N. Pyrosequencing-based assessment of soil pH as a predictor of soil bacterial community structure at the continental scale. *Applied and Environmental Microbiology* **2009**, *75*, 5111-5120.
40. Meyers, M. S.; Foran, D. R. Spatial and temporal influences on bacterial profiling of soil samples. *Journal of Forensic Sciences* **2008**, *53*, 652-660.
41. Petraco, N. D. K.; Gambino, C.; Kubic, T. A.; Olivio, D.; Petraco, N. Statistical discrimination of footwear: A method for the comparison of accidentals on shoe outsoles inspired by facial recognition techniques. *Journal of Forensic Sciences* **2010**, *55* (1), 34-41.
42. Sheets, H. D.; Gross, S.; Langenburg, G.; Bush, P. J.; Bush, M. A. Shape measurement tools in footwear analysis: A statistical investigation of accidental characteristics over time. *Forensic Science International* **2013**, *232* (1-3), 84-91.
43. Petraco, N. D. K.; Shenkin, P.; Speir, J.; Diaczuk, P.; Pizzola, P. A.; Gambino, C.; Petraco, N. Addressing the National Academy of Sciences' challenge: A method for statistical pattern comparison of striated tool marks. *Journal of Forensic Sciences* **2012**, *57* (4), 900-911.
44. Chumbley, L. S.; Morris, M. D.; Kreiser, M. J.; Fisher, C.; Craft, J.; Genalo, L. J. et al. Validation of tool mark comparisons obtained using a quantitative, comparative, statistical algorithm. *Journal of Forensic Sciences* **2010**, *55* (4), 953-961.
45. Gerules, G.; Bhatia, S. K.; Jackson, D. E. A survey of image processing techniques and statistics for ballistic specimens in forensic science. *Science & Justice* **2013**, *53* (2), 236-250.
46. Egan, W. J.; Morgan, S. L.; Bartick, E. G.; Merrill, R. A.; Taylor, H. J. Forensic discrimination of photocopy and printer toners. II. Discriminant analysis applied to infrared reflection-absorption spectroscopy. *Analytical and Bioanalytical Chemistry* **2003**, *376* (8), 1279-1285.
47. Egan, W. J.; Galipo, R. C.; Kochanowski, B. K.; Morgan, S. L.; Bartick, E. G.; Miller, M. L. et al. Forensic discrimination of photocopy and printer toners. III. Multivariate statistics applied to scanning electron microscopy and pyrolysis gas chromatography/mass spectrometry. *Analytical and Bioanalytical Chemistry* **2003**, *376* (8), 1286-1297.

48. Thanasoulis, N. C.; Parisis, N. A.; Evmiridis, N. P. Multivariate chemometrics for the forensic discrimination of blue ball-point pen inks based on their vis spectra. *Forensic Science International* **2003**, *138* (1-3), 75-84.
49. Savitzky, A.; Golay, M. J. E. Smoothing + differentiation of data by simplified least squares procedures. *Analytical Chemistry* **1964**, *36* (8), 1627-&.
50. Barak, P. Smoothing and differentiation by an adaptive-degree polynomial filter. *Analytical Chemistry* **1995**, *67* (17), 2758-2762.
51. Gorry, P. A. General least-squares smoothing and differentiation by the convolution (Savitzky-Golay) method. *Analytical Chemistry* **1990**, *62* (6), 570-573.
52. Johnson, K. J.; Wright, B. W.; Jarman, K. H.; Synovec, R. E. High-speed peak matching algorithm for retention time alignment of gas chromatographic data for chemometric analysis. *Journal of Chromatography A* **2003**, *996*, 141-155.
53. Nielsen, N. P. V.; Carstensen, J. M.; Smedsgaard, J. Aligning of single and multiple wavelength chromatographic profiles for chemometric data analysis using correlation optimised warping. *Journal of Chromatography A* **1998**, *805* (1-2), 17-35.
54. Tomasi, G.; van den Berg, F.; Andersson, C. Correlation optimized warping and dynamic time warping as preprocessing methods for chromatographic data. *Journal of Chemometrics* **2004**, *18*, 231-241.
55. Varmuza, K.; Filzmoser, P. *Introduction to multivariate statistical analysis in chemometrics*. CRC Press: Boca Raton, FL, 2009.
56. Moreda-Pineiro, A.; Marcos, A.; Fisher, A.; Hill, S. J. Evaluation of the effect of data pre-treatment procedures on classical pattern recognition and principal components analysis: A case study for the geographical classification of tea. *Journal of Environmental Monitoring* **2001**, *3* (4), 352-360.
57. van den Berg, R. A.; Hoefsloot, H. C. J.; Westerhuis, J. A.; Smilde, A. K.; van der Werf, M. J. Centering, scaling, and transformations: improving the biological information content of metabolomics data. *Bmc Genomics* **2006**, *7*.
58. Miller, C. E. Chemometrics in Process Analytical Technology (PAT). In *Process Analytical Technology: Spectroscopic Tools and Implementation Strategies for the Chemical and Pharmaceutical Industries*; Bakeev, K. A., Ed. John Wiley & Sons, Ltd.: Chichester, England, 2010; p 372.
59. Devore, J. L. *Probability and statistics for engineering and the sciences*. 3rd Ed.; Duxbury Press: Belmont, CA, 1991.
60. Miller, J. N.; Miller, J. C. *Statistics and chemometrics for analytical chemistry*. Pearson Prentice Hall: Harlow, England, 2000.
61. Brereton, R. G. *Applied chemometrics for scientists*. Wiley: Hoboken, New Jersey, 2007.
62. Borg, I.; Groenen, P. J. F. *Modern multidimensional scaling: Theory and applications*. Springer: New York., 2005.
63. Cox, T. F. *Multidimensional scaling*. Chapman & Hall: Boca Raton, Florida, 2001.
64. Kruskal, J. B. Multidimensional scaling by optimizing goodness of fit to a nonmetric hypothesis. *Psychometrika* **1964**, *29*, 1-27.
65. Spence, I. A simple approximation for random rankings stress values. *Multivariate Behavioral Research* **1979**, *14*, 355-365.
66. Whittaker, R. H. Vegetation of the Siskiyou mountains, Oregon and California. *Ecological Monographs* **1960**, *30*, 279-338.

67. Bray, J. R.; Curtis, J. T. An ordination of the upland forest communities of southern Wisconsin. *Ecological Monographs* **1957**, *4*, 325-349.
68. Sørensen, T. A method of establishing groups of equal amplitude in plant sociology base on similarity of species and its application to analyses of the vegetation on Danish common. *Biologiske Skrifter. K. Danske videnskabernes Selskab*, **1948**, *5*, 1-34.
69. Dice, L. R. Measures of the amount of ecologic association between species. *Ecology* **1945**, *26*, 297-302.
70. Lavine, B. K. Signal Processing and Data Analysis. In *Practical Guide to Chemometrics*; Haswell, S. J., Ed.; Marcel Dekker: New York, 1992; pp 225-227.
71. *Multivariate Data Analysis. Pirouette User Guide. Version 4.0*. Infometrix Inc.: Bothell, WA.
72. ASTM E 1618-11. Standard test method for ignitable liquid residues in extracts from fore debris samples by gas chromatography-mass spectrometry. ASTM International: West Conshohocken, PA, 2011.
73. Scloss, P. D.; Westcott, S. L.; Ryabin, T.; Hall, J.R.; Hartmann, M.; Hollister, E. B. et al. Introducing mothur: Open-source, platform-independent, community-supported software for describing and comparing microbial communities. *Applied and Environmental Microbiology* **2009**, *75*, 7537-7541.

## 7. Dissemination of Results

### 7.1 Presentations resulting from this work

DeJarnette AT, McGuffin VL, Waddell Smith R. Principal Components Analysis and Hierarchical Cluster Analysis for the Identification of Ignitable Liquids in Simulated Fire Debris. Oral presentation at the 65<sup>th</sup> Annual Meeting of the American Academy of Forensic Sciences, Washington DC. February 2013.

Hopkins JM, Foran DR. Multivariate Statistical Evaluation of Bacterial rRNA16S V4-V6 Sequencing to Identify Soil Evidence. Poster presentation at the 65<sup>th</sup> Annual Meeting of the American Academy of Forensic Sciences, Washington DC. February 2013. Winner of the Emerging Forensic Scientist Award.

McIlroy JW, McGuffin VL, Waddell Smith R. Applications of Multivariate Statistics in Forensic Science. Oral presentation at the Pittsburgh Conference on Analytical Chemistry and Applied Spectroscopy, Philadelphia PA. March 2013.

DeJarnette AT, McGuffin VL, Waddell Smith R. Investigation of Soft Independent Modeling of Class Analogy for the Classification of Ignitable Liquids in Simulated Fire Debris. Poster presentation at the Pittsburgh Conference on Analytical Chemistry and Applied Spectroscopy, Philadelphia PA. March 2013.

Geiger JL, McGuffin VL, Waddell Smith R. Classification Procedures for Identification of Ignitable Liquids in Fire Debris. Poster presentation at the 42<sup>nd</sup> Annual Meeting of the Midwestern Association of Forensic Scientists, Dayton OH. October 2013.

DeJarnette AT, Waddell Smith R. Multivariate Statistical Procedures for the Identification of Controlled Substances in Simulated Street Samples. Abstract accepted for oral presentation at the 66<sup>th</sup> Annual Meeting of the American Academy of Forensic Sciences, Seattle WA. February 2014.

## 7.2 Publications resulting from this work

### Planned

#### *Theses*

A Statistical Investigation of Bacterial Populations using the 16S rRNS Gene to Understand Habitat, Temporal, and Spatial Variability in a Forensic Context. James M. Hopkins, MS Thesis.

Comparison of Exploratory and Classification Procedures to Identify Ignitable Liquid Residues in Fire Debris Analysis. Andrew T. DeJarnette, MS Thesis.

#### *Manuscripts*

Next Generation Sequencing coupled with Multivariate Statistical Evaluation of Bacterial 16S rRNA to Identify Soil Evidence. J.M. Hopkins and D. R. Foran. In preparation for submission to *Journal of Forensic Sciences*.

Comparison of Multivariate Statistical Procedures for the Classification of Controlled Substance Samples. A.T. DeJarnette and R. Waddell Smith. In preparation for submission to *Journal of Forensic Sciences*.

Exploratory and Classification Data Analysis Procedures for the Identification of Ignitable Liquids in Simulated Fire Debris. A.T. DeJarnette, J.L. Geiger, V.L. McGuffin, and R. Waddell Smith. In preparation for submission to *Analytical and Bioanalytical Chemistry*.